WAR RESEARCH PROBLEMS

A. The Pro-knock Activity of Various Compounds.

B. The Dynamic Sorption of Ammonia and Butane on Charcoal.

C. The Reaction of Hydrogen Atoms with Propylene.

by

Stuart George Davis, B.Sc. in Chem. Eng., M.Sc.

from the

Physical Chemistry Laboratory,

McGill University,

Under the supervision of

Dr. C. A. Winkler.

Thesis submitted to the Faculty of Graduate Studies and Research of McGill University, in partial fulfillment of the requirements for the degree of Doctor of Philosophy.

Montreal, Quebec. April, 1942.

ACKNOWLEDGEMENTS

The author wishes to acknowledge the cooperation of the Organic Chemistry Department of McGill University, particularly B. K. Wasson and H. Orloff, and of A. L. Thompson for the synthesis of many of the compounds used as pro-knocks.

Acknowledgement is also made to the National Research Council for a studentship and for the loan of the knock testing engine used in the pro-knock investigations; and to the Canadian Industries Limited for a Fellowship.

Thanks are due J. A. Pearce for doing part of the solution work reported in table 21 of the pro-knock section.

TABLE OF CONTENTS

Ph. D. Physical Chemistry

Stuart George Davis

WAR RESEARCH PROBLEMS

A. The Pro-knock Activity of Various Compounds.

B. The Dynamic Sorption of Butane and Ammonia on Charcoal.

C. The Reaction of Hydrogen Atoms with Propylene.

A

Various compounds were investigated to determine their pro-knock activity, by adding them to the air stream of, or to the gasoline used in, an Ethyl Type 30-b Knock Rating Engine. The best compound tested was methyl dichloroarsine which required 3.8 parts per million parts of air by volume to cause a decrease of ten units in the octane rating of a leaded gasoline.

It was found that the best knock inducing elements were, in order of effectiveness, arsenic, antimony and phosphorous. Other elements that were very effective were mercury, vanadium and chromium. The halogens were the most effective group of radicals, the order of effectiveness being bromine, chlorine and iodine, and fluorine. The effectiveness of the halogen radicals appeared to be increased by the presence of a nitro group and a methyl radical on the same kernel.

The "ideal" pro-knock compound postulated was

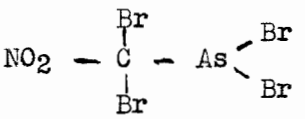

B

The dynamic sorption of ammonia and of butane was studied using an apparatus which followed the sorption by weight as a function of time, and permitted the temperature rise and analysis of effluent gases over a wide range of sorbate concentrations and flowrates.

The data obtained were applied to the theories of Danby et al and of Mecklenberg and were found to be essentially in good agreement.

C

The reaction of propylene with hydrogen atoms was studied for the temperature range 30 to 250°C. The products obtained were methane ethane, propane, and traces of C_4 hydrocarbons. About forty percent conversion was obtained. Temperature had little effect on either the relative proportion of products or on the extent of conversion. When the flowrate was reduced to one quarter of its original value, propylene was completely converted to methane, ethane and traces of C_3 and C_4 hydrocarbons. The activation energy of the overall reaction was 8.5 - 1.5K. cal. calculated for a steric factor of 0.1.

THE PRO-KNOCK ACTIVITY OF VARIOUS COMPOUNDS.

(A major portion of this was done with the collaboration of J. D. B. Ogilvie.)

Introduction

Internal combustion engines operate by the explosion of combustible mixtures. The energy liberated raises the temperature of the gases formed and pressure is exerted on the piston or moving part thus providing the motion which is transferred to the driving mechanism. In some circumstances, depending on the engine and the fuel used, the character of the combustion changes and a knocking sound results. This 'knocking' or 'pinking' is a high pitched metallic note like that produced by striking together pieces of metal and is due to an abnormally rapid explosion of a certain portion of the charge which is the last to burn, resulting in the formation of pressure waves in the gas. It occurs particularly when the engine is accelerating from a low speed, is laboring on a hill, or has heavy carbon deposits in its cylinders. Knocking operation causes a decreased output in power and,if prolonged or intense, overheating or mechanical damage can result. (1)

Violent knocking can be brought about by introducing certain compounds, called pro-knocks, into the air stream, or adding them to the gasoline used in an engine. It was thought that if a compound could be found which had sufficient pro-knock activity so that it would be effective in low concentrations (about two parts per million parts of air), it might be used as a barrage which would render inactive any automotive equipment which would pass through that barrage.

In this investigation, quantitative data were obtained on the pro-knock effectiveness of many compounds, and many radicals and elements that promote knocking were found.

1. Oxidation of Hydrocarbons

The complexity of oxidation was not fully recognized until Bone and his collaborators showed that a whole series of intermediate compounds were formed which subsequently gave rise to the end products. This led Bone to formulate the first comprehensive theory of hydrocarbon combustion (2).

All hydrocarbons, under suitable conditions of temperature and pressure, will unite slowly with oxygen without formation of flame and with no appreciable rise in temperature. The products of such an oxidation consist mainly of carbon monoxide, carbon dioxide, substances of a peroxydic character, alcohol, steam, aldehydes, acids and other compounds, but no free carbon or hydrogen. The rate of such a reaction does not conform with any simple order of reaction; it increases rapidly with increase hydrocarbon concentration and is little influenced by change in oxygen concentration. The temperature of initial combustion also varies with the hydrocarbon concentration.

There is a delay or induction period when any hydrocarbon-oxygen medium is introduced into a reaction vessel. During this period there is no appreciable pressure-change in the system and very little consumption of oxygen. This is followed by a period of relatively rapid reaction, during which the greater part of the hydrocarbon or oxygen, whichever is in defect, is consumed. The length of the induction period depends on many factors such as temperature, pressure, concentration, nature of the enclosing vessel, and the presence of traces of certain substances, e. g., nitrogen, peroxide, aldehydes and alcohols (3). The rate of the reaction also depends on the dimensions and the surface-

volume ratio of the enclosing vessel, and is accelerated by the addition of an inert gas.

These considerations have led to the suggestion that combustion in general proceeds by a chain mechanism. This postulates that when reaction occurs between suitably energized molecules, the heats of activation and reaction are not transferred by molecular collisions to the system as a whole, but by specific encounters with suitable reactant molecules which hand on the energy by quanta. The rate of reaction is related to the number and length of these reaction chains. The mechanism for the hydrocarbons can be shown by supposing that during the oxidation of original reactant R ,which is resistant to oxidation, an intermediate Y is formed which is less stable. On further oxidation of Y, oxygen atoms are supplied which accelerate the first step. Thus

$$Y + O_2 \rightarrow YO + O$$

$$O + R \rightarrow Y$$

$$Y + O_2 \rightarrow YO + O \quad \text{etc.}$$

The reaction chain may divide or branch, setting up new centres of activity

$$YO + O_2 \rightarrow YO{:}O + O$$

and the number of chains will increase. At some pressure limit, the rate of activation will be faster than the rate of deactivation (by collision with walls, molecular collisions, etc.) and sudden acceleration of the reaction will result. The actual course and mechanism of the hydrocarbon combustion has led to the advancement of many theories of oxidation.

1. Theories of Oxidation

There have been many theories advanced to account for the experimental results obtained, but the best known of these appears to be the stepwise formation of hydroxyl compounds, and the peroxide theory.

Early theories (4, 5) attempted to explain oxidation by assuming that carbon and water were the initial products or that the hydrogen burned preferentially to carbon. These theories were discarded when the complex intermediate products were found.

The Hydroxylation Theory

The hydroxylation theory in its present form is able to give an account of the course of combustion from slow reaction to detonation and defines the nature of the intermediate compounds and the order found. It was first advanced by Armstrong (6) to account for the formation of aldehydes in slow oxidation of methane as found by Bone and Wheeler It was developed in its present form by Bone (2).

The slow oxidation of a hydrocarbon involves a succession of hydroxylations and thermal decompositions mainly as follows:

For methane

$$CH_4 \rightarrow CH_3OH \rightarrow \underbrace{CH_2(OH)_2}_{H_2O + H_2:C:O} \rightarrow \underbrace{\begin{matrix}HO\\H\end{matrix}\!\!>\!C:O}_{CO + H_2O} \rightarrow \underbrace{\begin{matrix}HO\\HO\end{matrix}\!\!>\!C:O}_{CO_2 + H_2O}$$

In all cases, save for acetylene, the initial product of oxidation is always an alcohol. Then a dihydroxy alcohol is formed which decomposes into water and an aldehyde. The next step is the conversion of the aldehyde either to a lower aldehyde or into the corresponding fatty acid. Further hydroxylation occurs with subsequent breakdown of the dihydroxy compound so produced. Secondary reactions can occur

due to thermal decompositions, condensations or interaction of the intermediates giving a variety of products including lower hydrocarbons, peroxides, free carbon and hydrogen.

The brief induction period is explained as the time necessary to form a definite amount of aldehyde which remains constant throughout the subsequent reaction period.

This theory agrees very well with the analytical results obtained from slow oxidations, and agrees at least qualitatively with explosion reactions. However there is doubt as to the initial step since a termolecular collision is necessary, also the effect of catalysts is hard to explain since alcohols and aldehydes, while they do have some effect on the reaction, have relatively slight effect compared with that of the peroxides, which is the reverse of what is expected from the theory.

The Peroxide Theory

The peroxide theory in direct opposition to the hydroxyl theory postulates that any alcohols are formed as a by-product rather than an intermediate oxidation product. It was first formulated by Bach (8) and by Engler and Wild (9). According to this theory the initial product of combustion of a hydrocarbon is an alkyl peroxide or alkyl hydrogen peroxide. For methane the oxidation would follow:

$$CH_4 + O_2 \longrightarrow CH_4(O_2) \quad \text{or} \quad CH_3.O.O.H \qquad (1)$$

$$CH_4(O_2) \longrightarrow HCHO + H_2O \qquad (2)$$

Methyl alcohol could result from either the autoxidation of a methane molecule by its peroxide or by intramolecular change.

$$CH_4(O_2) + CH_4 \begin{cases} \longrightarrow 2CH_3OH \\ \longrightarrow CH_4(O_2)CH_4 \longrightarrow 2CH_3OH \end{cases}$$

The alkyl peroxide formed is in a high energy state and may do

one of several things. (i) It may revert to a normal state and radiate energy in so doing and form a stable peroxide, (ii) it may break up again, losing the excess energy by radiation, (iii) the compound may rearrange as shown in (2) giving highly active products, or (iv) collision may occur. If it encounters a fairly active fuel molecule or product therof, or oxygen molecule it will raise its energy so that it will react. The active products may collide and activate other fuel molecules thus setting up a reaction chain.

The strong points in favour of this theory are first its simplicity, since a bimolecular addition reaction between an oxygen molecule and a hydrocarbon molecule is necessary for the first step which is more probable than the termolecular collision necessary for the hydroxylation theory. Secondly, a peroxide product fits in better with the evidence with regard to positive and negative catalysts of such oxidations.

That a reconcilaition between the peroxide theory and the hydroxylation theory may not be impossible is suggested by a footnote in Bone's paper (10) where he states that a transient physical association between a hydrocarbon molecule and an oxygen molecule might exist until hit by a second hydrocarbon molecule with consequent immediate formation of two molecules of the mono-hydroxy-compound as the first recognizable chemical result.

Atomic Chain Theory

Norrish (11) has proposed an Atomic Chain Theory which differs from the hydroxylation theory only in its explanation of the initial step. He visualized the initial steps as

$$CH_4 + O \longrightarrow CH_2 + H_2O + 48 \text{ Kcal.}$$

$$CH_2 + O_2 \longrightarrow HCHO + O + 15 \text{ Kcal.}$$

The initial oxygen atoms are assumed to be formed by the production of formaldehyde through a surface reaction,

$$CH_4 + O_2 \xrightarrow{\text{surface}} HCHO + H_2O$$

and the subsequent oxidation of formaldehyde to formic acid liberating an oxygen atom.

$$HCHO + O_2 \rightarrow (H_2CO_3) \rightarrow H\ COOH + O$$

The reaction chain could be terminated by

$$O + CH_4 + X \rightarrow CH_3OH + X + 88\ \text{Kcal.}$$

or

$$O + \text{Surface} \rightarrow 1/2\ O_2$$

This theory differs from the peroxide theory in that it postulates the propagation of reactivity by atoms and radicals and not by an energy-chain mechanism. The addition of an inert diluent gas to a medium reacting by an energy-chain mechanism should cause a decrease in the reaction velocity whereas the reverse is true.

On the basis of this theory, it can be shown that the most reactive mixture should be one containing hydrocarbon and oxygen in the ratio 2:1 as has been found experimentally (3). The induction period is assumed to be the time necessary for an equilibrium quantity of formaldehyde to be built up at the surface.

Other Theories

Lewis (12) postualtes the first step as a dehydrogenation, with subsequent oxidation of both the hydrogen and the unsaturated hydrocarbon. This would necessarily mean that a saturated hydrocarbon and its unsaturated relative would behave similarly on oxidation. This theory was supported by Berl and Winnacker (13) and Steacie and Plewes (14). However Pidgeon and Egerton (15) and Mardles (16) have shown that the oxidation of a saturated hydrocarbon and its unsatur-

ated relative behave differently on oxidation.

Ubbelohde (17) indicates that the chain carrier is an aldehyde radical which would explain the similarity between hydrocarbon oxidation and aldehyde oxidation. The chain carrier radical postulated is

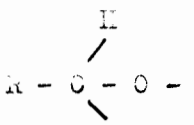

3. Oxidation of the Hydrocarbon Families.

Paraffins. These can be roughly divided into two groups, methane and ethane, and butane and higher. Propane is intermediate to these two. From the methane and ethane oxidations, aldehydes, acids, CO, CO_2 and H_2O have been isolated (2, 7, 18). At higher pressures the formation of alcohols is particularly noticeable (19). The products can be predicted from the hydroxylation theory. There is an induction period found with these. With propane, alcohols are obtained at higher pressures (20) and at atmospheric pressure, large amounts of peroxides are formed (21). None of these gases show very marked chemiluminescence. The concentration for maximum rate is two of hydrocarbon to one of oxygen.

The higher paraffins, from butane upwards show two modes of ignition at two different temperatures. With large molecules such as these, a deduction of the oxidation mechanism from an inspection of the products is different, and especially so if there is more than one mode of oxidation as would appear possible. Edgar (22) has shown that in a long molecule, the chief point of attack is the end methyl group. In a branched hydrocarbon molecule, the longest branch is attacked and oxidation proceeds till the point of branching is reached. The higher paraffins show an increased reaction rate for similar temperatures, also peroxides are much easier to isolate. The concentration for maximum rate decreases to about one for one for hexane. There is

considerable chemiluminescence.

Using a two percent mixture, at atmospheric pressure, the following stages in the combustion of n heptane have been distinguished (23, 24)

(1) 150 - 200°. Small possibly heterogeneous reaction.

(2) 250 - 350°. Primary reaction with rapidly increasing velocity, using 3 mols. of oxygen per mol. of fuel (lower ignition point with cold flames 270 - 300°)

(3) 350 - 470°. Subsequent reaction raises the oxygen consumption to 4.70 mols. per mol. of fuel. The velocity of both primary and subsequent reactions decreases rapidly with rise in temperature (temperature coefficient 0.85 / 10° rise from 380 to 470°)

(4) 470 - 510°. Velocity of primary reaction continues to decrease, but the subsequent reaction becomes faster and above 490° the final amount of oxygen used is greater. Inflammation occurs at about 490°.

This same paper also describes the much greater stability of 2, 2, 4 - trimethyl pentane to oxidation, no combustion being detected below 490°.

Olefins. The mechanism of oxidation of the olefins is better understood than that of the paraffins, owing to the greater certainty about the primary step in their oxidation. Peroxides are readily formed from the liquid olefins at room temperature but in many cases the peroxide is sufficiently stable for the reaction to stop at this stage. The reaction probably is

$$CH_3(CH_2)\,CH = CH_2 + O_2 \rightarrow CH_3(CH_2)_2CH - CH_2$$
$$\qquad\qquad\qquad\qquad\qquad\qquad\qquad\qquad\qquad\qquad\qquad\qquad\quad | \quad |$$
$$\qquad\qquad\qquad\qquad\qquad\qquad\qquad\qquad\qquad\qquad\qquad\qquad\quad O - O$$

At high temperatures a similar peroxide is probably the first step.

In contrast with the paraffin series, there is an absence of strong chemiluminescence (25) and also acetaldehyde has but a small influence on their combustion (14). The products can easily be explained by the hydroxylation theory after the peroxide has been formed. The non-knocking characteristics of olefin peroxides also indicate a different mechanism of oxidation.

Aromatic Hydrocarbons. Benzene does not oxidize until a fairly high temperature, 500° C, is reached, but once the benzene nucleus disrupts, very reactive and easily oxidized products are formed. When side chains are present, attack begins on the α-carbon atom of the side chain. There is an induction period, and very little chemiluminescence.

Naphthenes. The process is probably very similar to that of the primary hydrocarbons, the only additional complication is the rupture of a C - C link at some stage of the oxidation. Very little work has been done with the naphthenes.

3. Effect of Catalysts

The presence of minute quantities of certain materials has a marked effect on the rate of the oxidation. The rate may be changed such that the products from the reaction with and without the catalyst are different. The length of the induction period is very much shortened and the ignition temperature is lowered by positive catalysts. A number of positive catalysts have been discovered. The chief of these are nitrogen peroxide and other oxidizing catalysts. Aldehydes in many cases facilitate the combustion of hydrocarbons. Lead tetraethyl before it is oxidized also accelerates combustion. Iodine and many iodine compounds act as positive catalysts in some instances, and negative catalysts in other instances.

There are a large number of negative catalysts, among these are inorganic halides, alkyl iodides, carbon tetrachloride, inorganic sulphides, amines, nitrites and inorganic compounds of phosphorus, arsenic, antimony, bismuth, vanadium, boron, silicon, tin, lead, etc. The metallic antiknocks are also good negative catalysts. Lead tetraethyl, when decomposed, in most cases raises the initial ignition temperature of hydrocarbons almost 150° C.

II. Physical Aspects of Combustion.

In the previous sections it was seen that most of the investigations reported were carried out using a slow combustion method. Actually the combustion of hydrocarbons can occur in one of three ways depending on the conditions of temperature, pressure, composition of the mixture, and source of heat. It may occur as a slow combustion without the appearance of a flame and the reaction takes a measurable time to go to completion. At higher temperatures inflammation occurs; the oxidation auto-accelerates and the reaction goes to completion in a very short time accompanied by the emission of a considerable amount of light. Under suitable conditions, an extremely rapid reaction occurs almost instantaneously over a large portion of the charge. This detonation as it is called is extremely violent.

In order to initiate flame in a mixture of a hydrocarbon and air, it is necessary that its composition should lie within a range of mixtures bounded by the lower and upper 'limits of inflammability'. Within these limits, self-propagation of flame will take place after ignition has been effected. At any given composition, there are actually three explosion limits. There is a pressure below which no explosion will occur called the 'lower explosion limit'. If the pressure is above this, ignition will occur unless the pressure is above a certain pressure where again no explosion will occur. This is the 'upper explosion limit'. At a still higher pressure however, a third limit is found at pressures above which ignition will always occur. Up to the pressure of the lower limit, deactivation by the walls maintains

equilibrium between the formation and destruction of chain carriers. Above the first limit the formation of chain carriers just exceeds the rate at which the chains are broken so that a slow reaction is changed abruptly into a very rapid one. This is supported by the fact that the addition of an inert gas which would prevent diffusion to the walls, lowers the limit; whereas a reduction in diameter of the containing vessel which would increase chain-breaking, raises the limit.

The upper limit is due to gas phase deactivation. Thus an addition of an inert gas to the mixture narrows the limit. At a somewhat higher pressure the conditions no longer remain isothermal, the heat of reaction is no longer dissipated and fresh chains are initiated in the explosive medium owing to the increased temperature. Thus ignition can again be effected, and a rapid temperature rise results with auto-acceleration of the reaction.

The range of inflammability in a homologous series narrows progressively as the combustible increases in molecular weight; thus the range 5.4 - 14.8% for methane may be contrasted with approximately 1.2 - 4.2 % for hexane (26). When endothermic combustibles are considered, the range is very much wider owing to their exothermic decomposition in combustion, e. g. for acetylene the range is 3.3 - 52.3 % (26).

Ignition limits, inflammation limits and ignition temperature are all affected considerably by the method of ignition (spark or heated surface), by the shape and size of the vessel, and by the degree of turbulence. The latter raises the ignition temperature but widens the limits of composition in which inflammation may occur. Increase of pressure may also appreciably affect ranges of inflammability.

The rate and nature of flame movement in a given gas-air mixture can vary widely with the conditions of experiment. Any factor which influences the area of the flame will influence its speed in a proportionate degree. Also any movement in the mixture ahead of the flame, due either to the expansion of the burnt products or to an external agency will also affect it. Other factors that control it are the initial temperature and pressure of the mixture and the nature and concentration of the inflammable gas.

When the inflammation is in an asymmetrical combustion chamber, a complicated combustion may occur due to the effect of resonance set up in the mixture itself. Resonance gives rise to vibrations of the flame front which increases the area of the flame surface and augments surge effects. This tends to be exponential and increases until the influence of the walls checks the effect. Such vibrations may lead to a 'detonation wave', the sudden greatly enhanced and constant speed of flame movement in which the flame is accompanied by a pressure-wave travelling with the speed of sound; or the inflammability may extinguish itself during a particularly extensive backward vibration.

With the higher paraffin hydrocarbons, a chemiluminescence occurs at a temperature below the ignition temperature. This is called 'cool flames'; an analysis of the products of combustion at this stage shows that aldehydes are present. The flame temperatures for the paraffin hydrocarbons are in the vicinity of 1900° C. The unsaturated hydrocarbons have a slightly higher flame temperature, usually about 50° higher. The flame speeds are of the order of 60 - 260 cm. per second with air mixtures and between 1000 and 4000 cm. per second with oxygen mixtures.

Detonation also can occur only between certain well defined 'limits of detonation' which are influenced by the shape and size of the vessel, initial temperature, diluents etc. Detonation is not set up instantaneously after the action of the igniting agent. The detonation wave is formed by the juxtaposition of a flame and a compression wave and is set up at the moment when the flame front and the front of the compression wave coincide. The compression wave is set up ahead of the flame front immediately upon ignition of the charge. But since the velocity of the flame is increasing, it overtakes the compression wave and sets up the detonation wave. The detonation wave may be set up by reflections of the compression wave from the walls of the confining vessel and it may be necessary for several increases due to reflected waves before actual explosion sets in. The phenomenon has also been obtained when the interior walls of the confining vessel presents irregularities (27). As these irregularities favor an increase of pressure in the front of the compression wave, they cause a kind of auto-ignition of the mixture, leading to detonation at a point which the flame has not yet reached.

Once it has been set up, the detonation is propagated at a strictly uniform velocity in a stable mixture. The velocity is between 1000 and 4000 metres per second. The presence of very small quantities of inert gases or of impurities do not usually modify to any appreciable extent the velocity of propagation of an explosion wave. Water vapour is an exception to this (28). The presence of antiknocks does not modify the velocity of propagation.

Photographic evidence has shown that the detonation wave travels with a 'spin'. There is doubt as to whether the whole body of the gas rotates or, as is more generally believed, the head of detonation alone

follows a helical track.

It is improbable that a true detonation could be set up in an internal-combustion engine chiefly on account of the small length of the cylinder. Furthermore, the mixtures used, being diluted by the nitrogen in the air, are much less explosive than those used to study detonation waves. However it is possible for combustion to be propagated in an engine at a relatively high velocity although less than that of a true explosion wave, which results in knocking operation.

III. Knock

1. Combustion in Internal Combustion Engines.

When the inflammation of the gasoline-air mixture is effected by the passage of the igniting spark, the movement of the flame across the combustion chamber is very similar to its movement in an explosion chamber of constant volume in a laboratory experiment. After a slow start in the plug-body, the flame accelerates until about half the total path to the opposite wall has been traversed, then checks and subsequently travels at a nearly uniform or slightly decreasing speed until the end of inflammation. In non-knocking operation that is all that occurs.

If for some reason conditions change, e. g. the compression pressure is increased a little, or the speed of the engine is diminished on account of increase of load, knocking may set in. The flame burns the mixture at much the same speed as before, then begins to vibrate and suddenly accelerates after about three-quarters to seven-eighths of the total path has been traversed. Sometimes, but not invariably, ignition of unburnt mixture ahead of the flame precedes or is synchronous with this sudden acceleration. At this point a reillumination or 'after glow' flashes back from the flame front with the speed of sound through the burnt products and a pressure pulse or shock-wave accompanies this after glow. The impingement of this shock-wave on the walls of the combustion chamber sets up vibration in the metal giving the 'knock'. The pressure waves travel at a speed of 800 to 900 metres a second.

Knocking fuels give a very 'thin' flame front and a pronounced reillumination when the shock-wave is sent back, but with non-knocking fuels, such as benzene, there is a continuous zone of combustion behind the flame front, and, even though in certain circumstances acceleration

of the flame is observed towards the end of its travel, there appear to be insufficient residual energy in the burnt portions to develop a real shock-wave.

Two knocks can result if the flame front is complex. If the foremost portion of the flame front touches the end wall of the combustion chamber prior to knock, the last part of the charge to burn will be separated into two sections by a wall of flame and the combustion-chamber walls. Then knock can occur in these two regions at slightly different times. Knock may occur after peak pressure because, owing to the rounded shape of the flame, a portion of the charge may be unburnt although part of the flame may have reached the end wall. When severe knock occurs before any of the flame reaches the cylinder wall, there is no evidence of multiple knock.

Antiknocks such as lead tetraethyl have little effect in delaying the normal travel of the flame of a mixture unless the flame travel is very slow and vibratory (29) and unless the antiknock is already decomposed prior to the arrival of the flame (30). Thus the processes which occur in front of the flame during the heating of the gaseous mixture are hindered by the antiknock, but it has little effect on the setting up of a true detonation in a detonating mixture and very little effect on the adiabatic ignition temperature.

Thus, knock is a result of intense compression waves occasioned by the enormously enhanced rate of combustion which occurs in the last part of the charge when exposed to certain conditions of temperature and pressure. If the rate of pressure rise is great, the local concentration of reactants increases and the loss of energy for a given volume is diminished, with a consequent rise in reaction rate. The temperature to which the gases are exposed not only influences the reaction rate but substances are formed by slow oxidation prior to the actual arrival of

the flame which affect the subsequent rate of combustion. It is not certain to what extent such substances are produced as a result of the temperature of the flame itself or as a result of the hot surfaces to which the gases are exposed, but since increased length of flame travel, temperature of valves, and carbonized surfaces all favour knock it is concluded that it is not merely a matter of the effect of the temperature of the flame.

In knocking operation there is a loss of power and performance. In heavy duty engines, this may be the only result of continued knocking, but in high duty engines, such as for aircraft and torpedo boats, knocking is very serious and may wreck the engine in a few minutes by causing seizure (31).

2. Theories of Knock

From a consideration of the previous sections it might seem that knock was similar to, if not identical with detonation. However the evidence seems to indicate that it is not a true detonation, but that it is a type of combustion intermediate between inflammation and detonation. It is similar in that it is a violent and almost instantaneous reaction of a presensitized fuel-air mixture but it is neither as violent nor as rapid as a true detonation. The velocity is 1000 feet per second, that of a true detonation as high as 10000 feet per second; the pressure development is also much less than that of a true detonation. It is also unlikely from the conditions of mixture charged, temperature, pressure, and vessel shape and size that a true detonation could occur in an engine cylinder.

There is much controversy regarding the cause of the knock and a concise, clear statement of the different theories that have been proposed is very difficult. The situation is further complicated due

to the fact that a large number of experiments have been performed under conditions widely different from those existing in an engine cylinder. From these data much conflicting evidence is found which has led to the many theories of knock.

The mechanical knock theory was advanced by Dickinson (32), and in an early paper of Midgley and Boyd (33). It was assumed that the knock was due to the impact of the metal parts in the engine cylinder. They did not attempt to explain the origin of the force which supposedly caused the impact.

The free hydrogen theory postulates that hydrogen is liberated by the cracking of hydrocarbons in the gasoline prior to any extensive oxidation. The knocking is then caused by the rapid combination of the hydrogen with oxygen. Acetylene which likewise has a high rate of reaction with oxygen may also be formed by hydrocarbon cracking. This theory is supported by the fact that the rates of flame propagation of these two substances are about ten times that of gasoline-air mixtures. The fact that many antiknock compounds do combine with hydrogen also supports this theory. Steele (34) points out that addition of hydrogen to the engine cylinder causes violent knocking, and that stable hydrocarbon molecules such as benzene and methane are less prone to knocking.

Clark and Henne (35) studied the spectrum of non-knocking and knocking operation of an engine. They found that during knocking operation the spectrum of the first quarter of the combustion period was intense and extended into the ultra-violet region, and that of the succeeding portion greatly diminished in energy. The gaseous mass may absorb the radiation which would tend to decompose them into hydrogen or lighter constituents which then burn with a higher velocity producing

the knock as described in the free hydrogen theory. The activation of the hydrocarbon would then be dependent upon the density of the fuel-air mixture. Wendt and Crimm (36) held that the explosion flame is promoted by the emission of electrons from the reacting molecules which activated the unburnt gas by ionization, detonation resulting if the temperature and pressure were sufficiently high.

When combustible mixtures are ignited in tubes, the flame may begin to vibrate violently after travelling a certain distance. These rapid vibrations generate a high pitched note that resembles certain types of knock. This note was associated with knock by Morgan (37) who advanced the flame vibration theory of knock. Although this might account for certain of the notes in an engine knock, it does not account for the pronounced metallic knock. Egerton and Gates (38,39) account for the noise by compression waves set up by the enhanced vibratory combustion near the cylinder walls. Maxwell and Wheeler (40) noted that a vibratory combustion during knocking started a shock wave which caused detonation of the unburned fuel.

The theory of auto-ignition by pressure is due to Ricardo (41) who supposed that the portion of the charge which is first ignited compresses the unburnt portion causing heating. When the temperature rise exceeds the rate at which the heat can be dissipated, the remaining portion ignites spontaneously and almost simultaneously throughout, with resultant knocking. This implies a tendency to knock proportional to the spontaneous ignition temperature of the fuel. There is a close parallelism between ease of autoxidation and susceptibility to knocking for many fuels. This is not the case in all instances, however, as Tizard and Pye (42) state that carbon-disulphide has a lower ignition temperature than heptane but the latter is more susceptible to knock. However Withrow and Boyd (43) who obtained simultaneous flame and

pressure data by photographic means showed that when knock occurred there was spontaneous ignition in the part of the charge ahead of the flame part, accompanied by a very rapid rise in the cylinder pressure.

The high pressure wave or detonation wave theory as put forth by Midgley and Boyd (33), suggests that knocking results from the impact of a high-velocity, high-pressure wave against the cylinder walls and head. In normal combustion, the differential between the pressure immediately in front of the flame front and the lower pressure behind it is very small, but in detonating combustion the flame front is moving at a very high velocity and is preceded by a region of dense gas at extremely high pressure which strikes the top and sides of the combustion chamber. Callendar (44) further discussed this theory and observed that the increased susceptibility to knock found in a long cylinder agreed with this theory. He states that a compression wave which crosses the cylinder with a velocity greater than that of sound would cause practically instantaneous ignition by compression as it passed. He proposed a different theory to account for the ignition ahead of the flame front.

Callendar (44) proposed the nuclear drop theory and it was accepted in a modified form by other authors. He suggested that when the gasoline was atomized in the air, the drops as they evaporated, left a residue or nucleus consisting of the higher boiling constituents of the fuel. These nuclei would serve as foci of ignition since the higher members of a hydrocarbon series are more easily ignited. Chemical action should be easier at the liquid-vapour interface as a result of strain due to surface tension. Also the drops could absorb radiation more readily than vapour. Carbon particles would likewise induce ignition by combining with lower boiling components forming nuclei of much lower

ignition temperature than the pure vapour.

Callendar (44) later found that peroxides are formed freely with detonating fuels in the period of low-temperature combustion which precedes ignition. He suggested that the peroxides accumulated in the nuclear drops during rapid compression, and acted as primers for the simultaneous ignition of the drops. This theory implies that the kind of oxidation essential to knocking is a liquid phase, and not a gaseous phase, phenomenon.

Moureau, Dufraisse and Chaux (45) agreed with this liquid phase reaction. They showed that peroxides were formed at 160° by the higher boiling petroleum fractions and by the paraffin hydrocarbons.

Egerton and Gates (46) proposed a theory similar to that of Callendar. They accept the evidence that peroxides are essential to knocking, but declare that the detonation can take place in the gaseous phase. They do admit however that liquid droplets are likely to be present in the charge of liquid fuel. Egerton and Gates also differ from Callendar's theory by regarding the peroxides, not as primers for the ignition of the drops, but as catalysts of the main process. Egerton declares definitely for a chain mechanism of engine combustion with the peroxides initiating the chain. Egloff, Schaad and Lowry (47) also favour a theory involving reaction chains of this type.

Mondain-Monval and Quanquin (48) differ from other peroxide theories for they assumed that the peroxide is formed not from whole molecules and oxygen, but from already fragmented molecules which give alcoholic peroxides of the type R O O H. Ubbelohde and Egerton (50) and Egerton, Smith, and Ubbelohde (51) investigated the part played by peroxides. Peroxides of the type $C_2H_5O\,|\,OC_6H_5$ or $C_2H_5O\,|\,OH$ which can split readily to give radicals C_2H_5O-, give a pro-knock effect; while peroxides which cannot be

thus disrupted, such as $CH_3CH(O)-CH_2(O)$ had no marked pro-knock effect.

They pointed out the similarity of this theory with that of Hinshelwood, Williams, and Wolfenden (51), that chain-branching in the combustion of hydrogen is due to a similar type of fission, HO¦OH into hydroxyl radicals. They suggested that the peroxide radical also takes part in chain-branching.

Rice (52) noted the relation between knock ratings for heptane isomers and the number of molecules of lower hydrocarbons produced from them during their thermal decomposition. This he argued showed that knock was due to thermal decomposition of the hydrocarbon before oxidation. Most observers agree that knock is caused by some sort of presensitization of the last part of the charge, explainable on a chain reaction mechanism. Beatty and Edgar (53) point out that the end gas is subjected to slow oxidation by a chain mechanism which gives active products. These may bring about further oxidation and the formation of additional active products, continuing the reaction chain, or they may be deactivated by an unfavorable collision. So long as this deactivation process predominates the net effect is merely a partial oxidation of a portion of the original fuel and a slow rise in the temperature of the mixture and at the arrival of the flame front, normal combustion takes place. When the temperature and time factors are such that knock can occur, the kinetics of the reactions in the end gas are modified in the following way. As the temperature rises, the number of active molecules formed in unit time increases somewhat and the probability of their deactivation is much less. This starts chain branch-

ing and at the critical point at which the probability of chain branching approaches unity, there is a sudden and very considerable increase in the concentration of activated oxidation products in the end gas. The resulting mixture is far more inflammable than the original mixture and its combustion may be abruptly completed by a flame which spreads at a rate much greater than in normal inflammation. This does not correspond in velocity to a true detonation wave for here the molecular collision efficiency is much less than that occuring in a detonation wave; for detonation the probability of chain branching is unity.

3. Measurement of Knock

With the development of the modern high compression engine, the importance of an accurate knowledge of knocking tendency became apparent. The economies of marketing gasoline made it essential that the oil companies should know the rating of the fuel they were making. Up until 1928, no standard method of knock rating had been established, although many methods of comparing fuels had been suggested.

The earliest methods depended upon the observation of knock in engines by ear. Ricardo (54) in 1921 devised a method of comparing knocking tendency by expressing it in terms of the "Highest Useful Compression Ratio", this being the highest compression ratio at which the engine could be operated on the fuel in question without audible knock. Other methods consisted of determining the spark advance for various knock intensities; measuring the time required to rupture a diaphram of known thickness; determination of power at various rates of fuel flow at throttle setting for incipient knocking; comparison of the temperature in a plug located in a cylinder, etc. In some cases an audiometer was used to measure the knock intensity. Bomb tests and chemical analysis have also been tried to measure the knocking tendency.

A very popular system of expressing anti-knock values which is still found quite frequently in the literature today, is the 'aniline equivalent scale'. This represents, in terms of aniline, a knock suppressor, the knock effect of a substance when measured in a solution of 1 gram molecule per litre of solution in a reference gasoline, or as many grams per litre as there are units in the molecular weight of the substance.

In 1928, the Co-operative Fuel Research Committee standardized the knock testing technique. The method decided upon makes use of the bouncing pin indicator first used by Midgley in 1922 (55). In this indicator, a steel pin rests on a thin steel diaphragm which is in direct contact with the combustion chamber. When knock occurs the pin is given sufficient impulse to be driven upwards, thereby closing a pair of contacts and thus causing current to flow. The contacts are adjusted so that they do not close during non-knocking combustion. The electric circuit contains a hot-wire element. A thermocouple, placed near the hot wire element, is connected to a millivoltmeter, the reading of which varies with the temperature of the wire, and thus with the knock intensity. This millivoltmeter is known as a knockmeter. It does not give an absolute measure of knock intensity, but gives a comparative indication of the knock intensity between fuels. To compare fuels on the same basis, a set of standard reference fuels had to be established.

To establish a scale for measuring relative knocking tendency, two hydrocarbons, normal heptane and iso-octane (2, 2, 4-trimethylpentane) as suggested by Edgar (32) in 1927, were selected. Normal heptane has a very low anti-knock value and iso-octane has a high anti-knock value; both are definite, reproducible compounds having similar physical char-

acteristics. The knocking tendency of any given fuel to be rated can be expressed in terms of an equivalent mixture of iso-octane and heptane. The octane number of a fuel is the whole number nearest to the octane number of that mixture of iso-octane and normal heptane which the motor fuel matches in knock characteristics. The octane number is defined by, and is numerically equal to, the percentage by volume of iso-octane in a mixture of iso-octane and normal heptane. Thus, by definition, normal heptane has an octane number of zero and iso-octane of 100.

Since these two fuels have a relatively high cost, secondary reference fuels are used. These consist of stable, straight-run gasolines, one of comparatively high knocking tendency and another of low knocking tendency. Mixtures of these have been carefully calibrated in terms of octane number directly against heptane and iso-octane.

A carefully controlled procedure is essential in a knock-testing method because knock is affected by a large number of engine variables. Some of these are compression ratio (54), throttle opening (56), engine speed (57), spark timing (58), mixture ratio (58), mixture temperature (57), jacket temperature (57), and intake air temperature (57). Standardization of the test equipment was thus necessary.

The engine which was evolved for these tests is a single-cylinder, valve-in-head, variable-compression engine. The power output of the engine is absorbed by a form of induction motor-generator which runs at constant speed. It operates as a motor to start the engine and as a generator to absorb the load and to control the speed. No attempt is made to measure the power. The Ethyl Type 30-B Knock Testing Engine is operated at 900 rpm., the compression is varied by inserting shims in the engine block and raising the engine head. The compression is kept constant for a given octane range. This engine is now

considered obsolete and the Co-operative Fuel Research Engine has been adopted.

The C. F. R. engine is also a variable compression engine. The compression in this can be varied readily by raising the engine head. The spark and rocker arms are automatically adjusted. The specifications for operating this engine are given in the American Society of Testing Materials pamphlet D 357-41T.

The knock rating engine is standardized to give a knock rating that will agree with road tests. As road tests vary with the make of the car and in fact with different cars of the same make, the average is taken. Since the automotive industry is always modifying their engines, there is a drift away from the octane ratings as given on the C. F. R. engine but with several modifications of the original specifications, e. g. mixture temperatures, etc., the engine has kept fairly well in line with the road tests.

4. Knock Characteristics and Lead Susceptibilities of Fuels

The fact that isomeric hydrocarbons may have very widely different tendencies to knock led to the investigation of the relation between the molecular structure of hydrocarbons and their knocking characteristics, e. g. normal heptane begins knocking at a compression ratio of below 3 to 1, while its isomer,2, 2, 3 - trimethyl butane, does not begin to knock until the ratio is raised to 13 to 1 (59).

The following relationships are found for the paraffin hydrocarbons. For the normal or straight-chain paraffin hydrocarbons there appears to be a regular increase in tendency to knock with increase in the length of the carbon chain in the molecule. The knock increase per carbon atom

increase in length, is substantially constant. The successive addition of methyl groups to a carbon-atom chain results in a decreased tendency to knock. The relationship here is also regular. For a given molecular size, i. e. for isomers, there is less tendency to knock as the structure arrangement becomes more compact. The actual number of carbon atoms in the paraffin hydrocarbon has no relation to knocking tendency. The greater the number of carbon atoms in the molecule, the greater is the range between the best and the worst isomer.

In general the olefins show less knock tendency than the corresponding paraffins. The effect of lengthening the carbon chain unbroken by a double bond appears to be similar to that found in the case of the paraffins. In the straight-chain olefins, the tendency to knock decreases by fairly regular steps as the double bond is progressively nearer to the centre of the molecule. The knocking tendency of these compounds appears to be determined by the largest unbroken straight carbon chain, irrespective of the size of the molecule.

The cyclic hydrocarbons have superior anti-knock qualities to the corresponding straight chain paraffin hydrocarbons. The presence of an unbranched side chain results in a decrease in aniline equivalent. Lengthening the side chain, whether it is branched or unbranched increases its knocking tendency. The effect on knock of branching of a side chain is very great; a highly branched or centralized side chain may make the compound superior in antiknock value to the parent cyclic compound. The effect of position of side chains on these cyclic compounds appears to be very small. The cyclic hydrocarbons

containing a single double bond in the ring are very similar to the saturated cyclic hydrocarbons. Here again lengthening of the unbranched side chain results in a progressive decrease in anti-knock value. However, the effect of position isomerism is much greater than for the corresponding saturated compounds.

The aromatic hydrocarbons have antiknock qualities definitely superior to the paraffin hydrocarbons. The addition of a progressively lengthened straight saturated side chain to the benzene nucleus results in a progressive increase in anti-knock value up to n - propylbenzene and then further increase results in a progressive lowering of the antiknock quality. Addition of methyl groups to the benzene nucleus results in a progressive increase in anti-knock qualities. Position isomerism exerts a considerable effect and para/positioned side chains are superior to meta and to ortho. Branching of the side chains containing more than three carbon atoms results in an increase knocking tendency.

The 'lead susceptibility', that is the increase in octane number of fuels produced by the addition of a fixed proportion of lead in the form of tetraethyl lead, varies greatly with the types of gasolines. It is determined not only by the hydrocarbons present, but may be markedly affected by small amounts of impurities. In general, natural gasolines have a high lead susceptibility, cracked gasolines are next and straight-run gasolines the lowest.

For the pure hydrocarbons there is a rough relationship between critical compression ratio and lead susceptibility. For paraffins and naphthenes, the higher the critical compression ratio the greater is the lead susceptibility; for olefins and acetylenes, increase in compression ratio produces no marked change in lead susceptibility; and for unsaturated cyclics, increase in compression ratio produces a decline in lead

susceptibility. A few aromatic hydrocarbons which have been investigated were found to show relatively high lead susceptibilities.

IV. Antiknock Compounds

Three distinct methods have been considered for improving the knock-rating of fuels: a fuel of high knock rating is blended with one of lower rating; a very small amount of an "antiknock reagent" can be added to the fuel; or it has been considered that a catalyst could be applied to the surface of the combustion chamber. These methods are discussed below.

Blending of Fuels

There are a number of fuels which show little tendency to knocking. These can be added in relatively large proportions (10 - 60%) to a knocking fuel to give a fuel of reasonably good antiknock properties. Cracked gasoline, especially vapor phase cracked fuel, is much better than straight run gasoline. This is due to the unsaturated compounds present and also due to the lower sulphur content. Natural or casing-head gasoline also has good anti-knock qualities. These are widely used to improve gasoline stocks.

Aromatic compounds are also good antiknock fuels. Benzene has been added to gasoline to improve its rating for many years. The more complex or irregular the structure of the molecule, the better is its non-detonant qualities. The terpenes also have excellent antiknock properties (60). Alcohol is also a very good non-knocking fuel and is used to blend fuels. Iso-octane although not used in commercial blends of gasoline has a very high knock rating.

It is difficult to decide whether the effect obtained in a blend of non-knocking fuel with a knocking fuel is merely the sum of the partial effects of the two, or whether the non-knocking fuel also acts as an inhibitor of the knock caused by the other fuel. There are a few indications that non-knocking fuels also exert a slight antiknock effect (61)

Antiknock Compounds

Midgely and Boyd (62, 63, 64) discovered the existence of several compounds, which when added to a motor fuel in small quantities caused a considerable increase in the knock rating of the fuel. This led to the further discovery of a large number of compounds which suppressed the knocking tendency far out of proportion to the amount added. The most effective of these compounds are organo-metallic compounds. Some nitrogen containing compounds are also quite effective. The following is a list of the more important antiknocks classified according to their chemical structure.

1. Nitrogen Compounds

These are true antiknock compounds. The better of these show measurable effect in a concentration as low as o.1%, an amount which can hardly be considered sufficient to modify the bulk concentration of the fuel. The antiknock effect is not due to the presence of the nitrogen alone, since some nitrogen containing compounds (nitro-, nitrites and nitrates) promote knocking. The effectiveness apparently depends upon a special type of linkage between the nitrogen and the organic radicals. In this class amines show the greatest effect. Table I shows the relative effectiveness of several amines. The values listed are the reciprocal of the number of moles giving the same antiknock effect as one mol. of aniline.

TABLE I (65)

Comparison of Antiknock Activity of Several Amines

(Numbers are reciprocals of the moles giving the same effect as one mol of aniline.)

Ammonia	0.9	Toluidene	1.22
Ethyl amine.....	0.20	m-Xylidene	1.4
Diethyl amine	0.50		
Triethyl amine	0.14	Monomethyl aniline 1.4	
Triphenyl amine.	0.09	Monoethyl aniline 1.02	
Aniline	1.0	Dimethyl aniline 0.21	
Diphenyl amine	1.5	Diethyl aniline	0.24

The presence of an aromatic linkage to the nitrogen greatly increases the antiknock effect. Side chains on the aromatic ring also increases the effectiveness. Secondary amines are in general better than primary or tertiary. Amides (20), imines (67), carbamides (20) and cyanogen compounds (67,68) have been shown to have antiknock properties, but to a much lesser extend than the amines.

2. Other Group Five Elements

(a) Phosphorous and arsenic (20). Some of these compounds are known to be oxidation inhibitors, but there is very little mention of antiknock properties.

(b) Antimony (20, 69) Trivalent antimony acts as an antiknock compound, while pentavalent antimony is a pro-knock. Antimony triphenyl and trichloride are effective antiknocks.

(c) Bismuth (20, 61, 67, 70). Some bismuth compounds are rather good antiknocks, e. g. bismuth trimethyl, triethyl and triphenyl.

3. Halogens

Although halogens, particularly the lighter ones, are generally considered to possess pro-knock tendencies, several halogen compounds are antiknocks. Carbon tetrachbride (71) ammonium halides (71), alkyl

halides, particularly iodides (20, 64, 65) chloro, bromo and iodo naphthalene (71), iodine (20,72) and phenyl halides have all been reported as being antiknock compounds. Iodine compounds are stated to be the best, bromine next, and chlorine the least effective (20).

4. Sulphur, Selenium, Tellurium.

Several sulphur compounds such as inorganic sulphides (7), organic sulphur compounds and sulphur itself are antiknocks. Selenium compounds have a much greater antiknock tendency than sulphur and tellurium more than selenium. Selenium diethyl (21, 61, 70) is quite a good antiknock and selenium diethyl (20, 61) is fair. Tellurium diethyl (61) is a strong knock inhibitor and tellurium diphenyl (61) slightly less so.

5. Other Non-metals.

(a) Boron (20) has some antiknock effect.

(b) Silicon (20, 71). Silicon tetraethyl is a fair antiknock.

6. Metals.

A great many metals, both their salts and organo-metallic compounds, have antiknock properties. Here the action is identified more closely with the element itself rather than with the type of linkages (61). There has been much discussion as to whether uncombined metals have or have not antiknock effect, without any definite conclusion having been reached. The most effective antiknock compounds known belong to this type.

The lighter metal compounds have been found not to have very great effect. Among the potassium compounds the gallate, oxalate and citrate (20); ethylate (73), and iodide (72) are effective. Potassium vapours acting in the oxide form are more effective than tetraethyl lead. Barium carbide (74) has also been reported as having antiknock properties.

However, it is mainly the heavy metallic elements that possess

the greatest antiknock activity. Lead compounds are the best commercial antiknock compounds known. It appears that tetravalent lead compounds almost always have antiknock power, while bivalent lead compounds are ineffective (20). Lead tetraethyl is the best antiknock known and is added to most commercial gasoline in quantities varying from 0.5 to 6.0 m. l. per gallon. Lead tetramethyl (70), lead tetrapropyl (20) and many other lead compounds (21, 61, 70) have all been studied and found to be effective in varying degrees.

Iron, cobalt and nickel are also very effective. The carbonyls are next to tetraethyl lead in activity (20, 61, 70, 75, 76). Iron carbonyl has been widely used in some European countries in improving commercial gasoline. Iron acetyl acetone (70) is also effective.

Chromium phenyl (86) and molybdenum carbonyl (75) also have a slight effect.

Tin tetramethyl, tetraethyl and tetraphenyl (20) are fairly good, and some of the stannic halides have also been reported as antiknocks (21, 61, 70, 72).

Compounds of zinc (71), cadmium (61), mercury (77, 78), cerium (20, 66), thallium (79), vanadium (20) and titanium (61) have also been found to be antiknock agents. Thallium vapour is a very good antiknock, being more effective than lead tetraethyl.

The following tables show the relative effectiveness of a number of anti-knock compounds:

TABLE 2 (6, 44, 45)

Relative Effectiveness of
Different Compounds of the Same Element

(Number is reciprocal of the number of mols giving the same effect as one mole of aniline)

Element	Ethyl Compound	Phenyl Compound
Iodine	1.09	0.88
Selenium	6.9	5.2
Tellurium	26.8	22.0

TABLE 3 (80)

Relative Antiknock Effectiveness

(Reciprocal of the number of mols giving the same effect as one mol of aniline)

Lead tetraethyl	118	Bismuth trimethyl	23.8
Lead tetraphenyl	70	Bismuth triethyl	23.8
Lead diphenyl dimethyl	115	Bismuth triphenyl	21.4
Lead diphenyl diethyl	109	Stannic chloride	4.1
Lead diethyl chloride	79	Stannic iodide	15.1
Lead thioacetate	10	Monophenyl arsine	1.6
Cadmium dimethyl	1.24	Triphenyl arsine	1.6
Titanium tetrachloride	3.2		

In all cases where the element is the determining factor rather than the linkage, the change from ethyl to phenyl causes at most a 20% decrease in activity (61). The effectiveness varies with position in the periodic table, increasing down the groups.

7. Aromatic Compounds.

In general aromatic compounds possess antiknock activity; this activity decreases with hydrocarbon side chains but increases with hydroxyl or amine groups (81). Phenyl chloride (71), iodide (20, 72), sulphide (20) nitrite (82), monophenyl and triphenyl arsines (11), diphenyl oxide (20), dihydroxy benzene (21, 70), phenol (66), cresol (20) and quinone (20, 66) have been reported to possess antiknock properties.

8. Ketones and Esters.

In general these do not show very great pro- or anti-knock activity. Some ketones (81) particularly higher ones are effective, the methyl and ethyl esters, and salts of boric, silicic and acetic acids (71), some of the naphthenic acid esters (83), furocyanic acid esters (84), the esters of palmitic, oleic, myriste, and lauric acids (20), and potassium gallate, oxalate and citrate (20) are antiknocks.

9. Inorganic Salts

Copper nitrate (85) hydroxy compounds (81) and water (20) also have antiknock properties.

Non-detonation Catalysts Fixed on the Inside of the Motor.

It has been proposed that the inside of the explosion chamber of the cylinders could be painted with substances which give reversible chemical reactions of the type that are endothermic at high temperatures and exothermic at low temperatures. Carbonates of lead, copper, calcium, magnesium, sodium or potassium, mixed with an inert material such as silica, have been patented (85). The oxides of vanadium, cobalt, and rare earth metals, especially cerium have also been recommended (86). The efficiency of such a method is low, and fouling and other mechanical difficulties are also to its disadvantage.

Compounds are also added to gasoline in small amounts, not to increase the antiknock rating, but to preserve the antidetonant qualities of cracked gasoline. Aniline, hydroquinone, naphthalene, and anthracene (87) have all been found to inhibit the charge on storing. In general any antioxidation catalyst is good.

V. Pro-knock Compounds

Compared with the large number of data available on antiknock compounds very few existed on pro-knock compounds until very recently. This is not surprising, since the search was for particularly effective antiknock materials for improving gasoline. Pro-knock compounds are materials which when added to gasoline in small amounts, increase the knocking of an internal combustion engine. Most of these were discovered during the search for anti-knock compounds, or from a study of the intermediate products in the combustion of hydrocarbons.

Here again there are knocking fuels as well as the true pro-knock compounds. Ethers and aldehydes are in general knocking fuels and the addition of a fairly large amount of these substances will cause a decrease in the octane rating of a fuel (20).

Organic peroxides are reported as being among the best knock inducers (66). Ozone (33) has an effect comparable with the antiknock effect of lead tetraethyl. Hydrogen peroxide (77) is also fairly effective. Dimethyl (88), diethyl (66, 88) and ethyl hydrogen peroxides (66) are among the best; ethylidene peroxide (88) slightly less so. Acetyl (88), benzoyl (20, 89), cetyl benzoyl (88), and diacete peroxides (88) are very effective also. Methyl, and ethyl ketone peroxides (90) and olefin peroxides are not effective (20, 66, 88, 91).

The organic nitrites are also quite powerful pro-knock agents; ethyl (91), propyl (70, 91) butyl (20, 92), amyl (20, 89) and isoamyl nitrites have been investigated. The corresponding nitrates (93), nitro compounds and oxides of nitrogen, NO, NO_2 (20, 61, 66, 89, 91) are much less effective although some have a pronounced effect.

The lighter halogens exhibit pro-knock tendencies. Both bromine and chlorine (20, 66, 94) have been reported as effective, as are several of their organic compounds. The activity reported appears to be chlorine greater than bromine, greater than iodine. Indeed, iodine and several of its compounds are reported as being anti-knock agents.

Among the more intensified studies of this pro-knock effect is that included in a report by Stacey and Masson (95). The following compounds are listed as "inducers" of knock.

nitroso-isopropyl-p-toluidine
thiocarbanilide
allyl-iso-cyanate
allyl-iso-thiocyanite
amyl salicylate
methyl sulphate
ethyl nitrite
isopropyl nitrite
amyl nitrite
amyl ether
mercuric diphenyl
tin tetraphenyl
silicon tetraphenyl
tin tetraphenyl and worm seed oil
petrolatum
benzaldehyde
heptaldehyde
methylnonyl ketone
zinc diethyl
amyl mercuric iodide
lead triphenyl iodide
phenyl mercuric iodid
cetyl alcohol
stearic acid
cobalt oleate
cadmium bromide
ammonia (gas dry)

They concluded that nitrogen when present as an organic nitrate or nitrite, was a pro-knock, and when present in the amine form, either an anti-knock or neutral. Esters formed by the action of nitric acid on alcohols were found to be inducers. Iodine in some compounds showed up as anti-knocks, and in other cases as pro-knocks.

In a more recent report by Lapeyrouse and Lebo (96) the octane blending improvement (O. B. I.) of 300 compounds are given.

Here $O.\ B.\ I. = \frac{C - A}{X}$

C = octane number of blend of X in the base stock

A = octane number of base stock

X = proportion of blending agent (fractional part)

Those with a high negative O. B. I. are

o- p- ditolyl p- phenylene diamine	-300
allyl isocyanate	-200
aliphatic hydroxy amines	-1000
zinc salt of the diketone $C_5H_7O_2$	-940
iron (ferric) salt of the diketone $C_5H_7O_2$	-940

A comparison might be made here with one of the better pro-knocks investigated in this research. Chloropicrin gave an O. B. I. value of -16,700.

In a memorandum by Sugden (97) giving an account of work done in England phosphorous trichloride, phosphorous oxychloride and carbon tetrachloride are listed as having stopped an engine either by causing the pistons to stick, or by fouling the spark plugs. Carbon bisulphide and chlorine are given as compounds which caused "considerable knocking".

Recent work has been done at the Thomas and Hochwalt laboratories (98) on sabotaging friendly gasoline, i. e. gasoline stores which must be abandoned. As a result of tests made on twelve Delcolite engines they found that adding small amounts of resins would be effective in rendering gasoline unuseable. They indicate that the best resin for this purpose is paradura 10 - P, a commercial oil-soluble phenolic resin made by condensing a paratertiary alkyl phenol with formaldehyde. A solution of 10 grams per gallon will quite effectively gum the piston of an engine after about 1 gallon per cylinder of the doped fuel has passed through an engine. Other compounds suggested, in order of effectiveness, are paradura 367, super bechacite 1001, rosin ester or santoresin, china-wood oil, and PCl_3 or $PNCl_2$. Metal naphthanates are also mentioned as effective in sticking an engine.

The work that is reported in the following sections was done up to September 1, 1941. Similar work was undertaken in the United States. This work is reported in papers by T. Midgley Jr. and A. L. Henne (99). The following are the better pro-knocks that they have investigated.

sulphur trioxide	phosphorous sulphochloride
nitrogen chloride	phosphorous tribromide
n butyl dichlorophosphine	phosphorous trichloride
sulphur chloride	phosphorous oxychloride
1 - chloro - 1 - nitropropane	chloropicrin
1, 1 - dichloro-1-nitroethane	thioxylchloride

sulphuryl chloride

The best one reported is sulphur trioxide which on a gasoline containing 5.36 ml. of tetraethyl lead per imperial gallon, required 11 parts per million of air by volume to produce a ten octane decrease.

They have also determined the action of these compounds on an unleaded fuel in an endeavor to determine the mechanism of the pro-knock action. They observe that while it requires much greater concentration of adulterant in an unleaded fuel than that required in a leaded fuel to cause the same octane decrease, the pro-knock activity is not simply counteracting of the lead tetraethyl. The effect seems to vary with the pro-knock agent and with the base stock of the fuel. Some pro-knocks, like phosphorous oxychloride, reduce the octane number of the leaded gasoline by counteracting the effect of the tetraethyl lead, and when this effect has been completely counteracted, no further pro-knock effect is obtained by adding more of such materials; nor do these compounds show any pro-knock effect in unleaded fuel. Other compounds like isoamyl nitrite have the same effectiveness in unleaded as in leaded fuels. Still others, like sulphur trioxide which counteracts the lead tetraethyl, also

affects the unleaded fuel.

Qualitative and semi-quantitative work was carried out in these laboratories (100) using a Chevrolet engine and testing the effectiveness of a compound injected into the air intake, by the audibility of the resulting knock. Some 197 compounds were tested which indicated the compounds to be investigated on the knock testing engine. The more effective compounds that were found were chloropicrin, bromopicrin, isoamyl nitrite, normal butyl nitrite, tertiary butyl nitrite, thionyl chloride, nitromethane, 2 - nitro propane, acetoacetic ester and isopropyl ether.

VI. Theories of Pro- and Antiknock Action

A theory of antiknock action must not only account for the inhibiting action of certain compounds, but also the action of knock inducers. It must explain not only why organo-metallic compounds like tetraethyl lead are effective but also why some organic compounds, notably the amines, are antiknock agents. The theory must explain why one molecule of tetraethyl lead in 200,000 of gasoline should be as effective as a 25 percent benzene addition in suppressing knock. The effect appears to be chemical rather than a physical phenomena and their action occurs in the brief time interval prior to the inflammation of the charge. A theory of antiknock action must account for the fact that the change from normal to knocking combustion is abrupt rather than continuous.

Theories of Antiknock Action.

The film theory of antiknock action postulates that the antiknock acts as a poison to destroy the catalytic activity of the walls. Jolibois and Normand (101) suggested that lead tetraethyl was decomposed and the atoms of lead were deposited first on sharp edges and points or at the "active spots" in the cylinder, increasing their radius of curvature and thus making them less capable of initiating combustion. This theory fails to account for the anti-detonant properties of compounds such as amines, and also fails to explain why knocking recommences as soon as an ordinary fuel is used although lead and its oxides should continue to cling to the walls. However, under some conditions, there has been found a continued inhibiting effect in vessels used for oxidation experiments in the laboratory. Sokal (86) also regarded combustion as fundamentally heterogeneous and reduced knocking by coating the walls of the chamber with

a material containing either carbonates or oxides of lead, cerium and other elements.

The theory that the antiknock absorbs radiations or intercepts electrons was put forth by Midgley (102) and by Wendt and Grimm (36). The antiknock promoted the combination of ions previous to combustion, thus reducing the rate at which the combustion accelerated. The heavier elements in the lower right-hand corner of Mendeléeff's table pick up negative charges easily, hence they should form good antiknock compounds. As evidence they stated that the lighter elements in each periodic group were pro-knocks and the heavier ones often antiknocks. Experimental evidence was advanced for this theory by Wendt and Grimm who found the recombination of ions above a pool of benzene with tetraethyl lead was more rapid than without tetraethyl lead. These results have been challenged by several authors. This theory implies that knock inducers should act by increasing ionization, an effect which has not been observed.

The action of antiknock compounds in minute amounts is explained quite well on the basis of Callendar's droplet theory. Since the drops form only a small proportion of the total fuel, and if the compound were concentrated in these drops, the effect would be out of all proportion with its concentration in the total fuel mixture. Many antiknock compounds have low volatility and would remain in the liquid phase if such were present. He postulates that the metallic antiknock should be decomposed to free metal which would then decompose the peroxides as fast as they were formed. Moureau, Dufraisse and Chaux (45) visualize the antiknock compound as forming an unstable oxide, followed by mutual destruction of the peroxides.

Egerton and Gates (46) also suggest that it is the metal of the anti-knock compound which prevents the accumulation of the peroxides. Thus only metals capable of forming peroxides such as potassium, sodium, manganese or lead can act as antiknocks by forming a metal peroxide from the fuel peroxide. This metal peroxide subsequently decomposes, regenerating the metal. Organic antiknocks act similarly but are not as effective since they would not be regenerated as easily.

The action of the antiknock agent is explained on the auto-ignition theory by increasing the spontaneous ignition temperature of the fuel. Several metal compounds were found to retard pre-ignition combustion as noted by Egerton and Gates (46) and others. Schaad and Boord (103) found that there was no effect of antiknock agents on the ignition temperatures of certain organic vapours when a direct-current break spark was used for ignition; but the antiknock increased the current required when ignition was caused by a heated wire. They explain this by suggesting that some pre-ignition oxidation took place before the current required for ignition was reached. Thus knock-suppressors were capable of decreasing this pre-ignition oxidation, while knock-inducers were shown to promote it. There is much controversy about the elevation of the spontaneous ignition temperature by antiknock agents. Lewis (104) found that certain pro-knock compounds raised the ignition temperature of some fuels, and on other fuels lowered the ignition temperature. He concluded that there was no relation between change of spontaneous ignition temperature and pro- or antiknock activity. This opinion is expressed by other authors (105, 106)

In contrast to the supposed inhibiting effect of the antiknock compound expressed in the above theories are some theories which regard the antiknock as an accelerator.

Dickinson (32) showed that multiple spark plugs tend to reduce knock. Clark, Bergmann and Thee (105) include a theory of knock suppression that suggests that the tetraethyl lead decomposed to lead particles which become incandescent and act as multiple miniature spark plugs causing uniform combustion. On this theory, it is not the speed of the oxidation which causes knocking, but its unevenness. Charch, Mack and Boord (80) modify this theory by assuming that since the particles of metal are liberated in a hot oxidizing atmosphere, they must be capable of immediate oxidation. The heat developed by this oxidation raises the temperature around the particle which promotes combustion and thus there is partial oxidation homogeneously throughout the entire volume. With aromatic amines the hydrocarbon radicals attached to the nitrogen oxidize more readily than the fuel and so spread the region of oxidation. Lewis (104) suggested substituting the idea of flameless combustion for active combustion ahead of the flame front.

Ubbelohde and Egerton (49) and Egerton, Smith and Ubbelohde (50) in connection with their peroxide theory of knock give the qualities of a good antiknock. They state that it must be (a) oxidized, (b) dispersed so as to be almost a vapour and (c) capable of being oxidized to a higher oxide. When tetraethyl lead, iron carbonyl, etc. are used, metallic oxides are formed as an essential part of their mechanism. They consider the antiknock to act either (i) by being peroxidized so as to remove oxygen from the active chain carriers or (ii) by mutual destruction of peroxides or (iii) by removing energy from the chain carriers. They do not exclude the possibility that antiknocks may have a surface action.

From all these theories and from experimental evidence available one is led to conclude that the antiknock action is to inhibit the pre-

flame combustion in the engine. There is no time lag or induction period in the action of an inhibitor, as is sometimes the case for a positive catalyst, provided the inhibitor is available in its reactive form. Whether the reaction involved is considered as peroxidations, hydroxylations, thermal or oxidative decompositions etc., a general term such as chain reactions covers all these. The specific method by which the pro- or antiknock affects the propagation of these reaction chains remains unknown although evidence points to an oxidation mechanism. The pro-knock materials are usually of a chemical type which would be expected to initiate oxidation processes and it appears probable that their function is mainly that of starting reaction chains at a rate much greater than that which results from normal reaction. If the deactivation of the chains carriers is not also increased, the critical point is reached, where the chains are formed faster than they are broken, in a shorter time giving the charge a greater opportunity to knock. It may be necessary to enlarge this to include the extension and breaking of chains,as well as initiation of these chains,as the pro-knock activity.

Since there is such a marked difference in the relative effectiveness of metallic antiknock agents and the organic compounds, it seems indicated that there is a fundamental distinction between their modes of action. The theory put forth by Egerton, as mentioned above, that the action is due to the oxide formation from the antiknock compound seems to explain as well as any their action. The difference in degree of action seems to be due to the ease with which metal can form active oxide or atom,while the organic antiknock compounds cannot undergo such reversible reactions as readily. The action of the active oxide or atom is one of inhibiting the formation of the reaction chains, thus

reducing pre-flame combustion and preventing any rapid combustion of the last part of the charge until the flame front has reached it. Before an actual mechanism of antiknock action can be developed further experimentation is necessary.

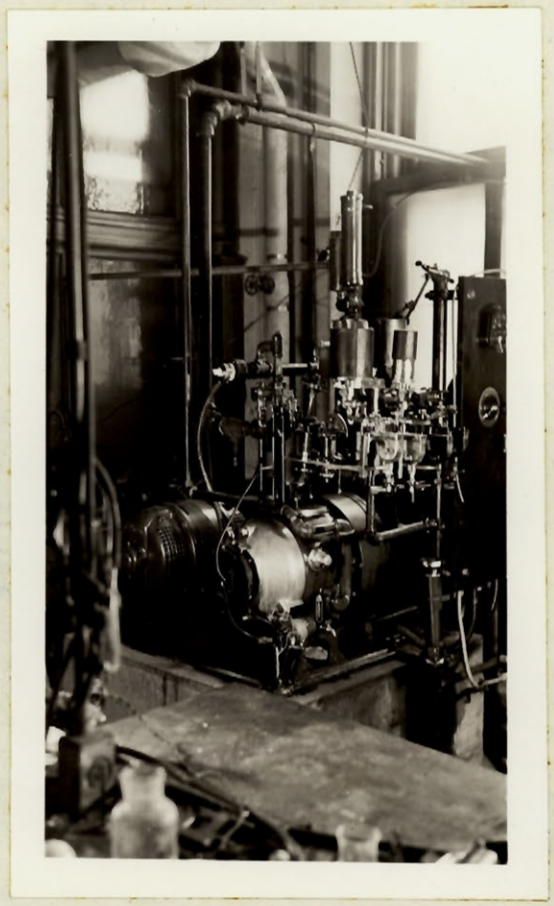

Fig. 1. Ethyl Knock Testing Engine, Type 30-B

EXPERIMENTAL

The investigation consisted essentially of determining the octane drop caused by various concentrations of a compound added to the air intake of, or dissolved in, the gasoline used in a knock testing engine. The octane number of the gasoline was first determined and then the rating of the fuel with the pro-knock added. The decreases in the octane rating of the fuel were found for several concentrations of the pro-knock agent and the graph of octane decrease vs. concentration was established.

For this, an Ethyl Knock Testing Engine, Type 30-B, as pictured in figure 1, was used. Although this engine is now obsolete for accurate fuel testing, it was found to be quite satisfactory for these investigations where absolute octane ratings were not required. The results obtained in checking the octane numbers of gasoline agreed closely with those determined by the company which supplied the gasoline. Also results of tests conducted on this type 30-B engine and similar tests conducted on a more modern Co-operative Fuel Research - American Society for Testing Materials Knock Test Unit in another laboratory were in good agreement.

The gasoline used for these experiments was an 80.5 octane leaded aviation fuel of 72.6 octane cracked base stock, as supplied to the R. C. A. F. by Shell Oil Company. This gasoline was used because it had the most convenient octane rating that could be used on the 30-B engine without modifying the engine. A leaded gasoline was used since these would be met in field applications. The reference fuels were the fuels listed as A-6, F-3, and C-12, as supplied by Standard Oil Development Company.

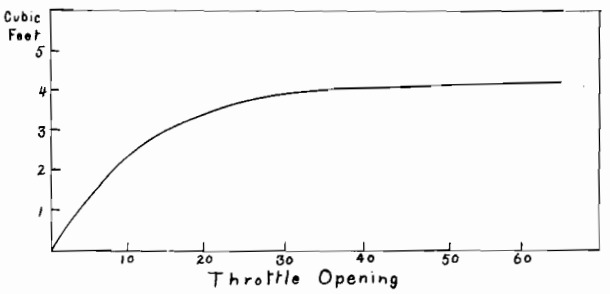

Fig. 2, Air Consumption

Fig. 2. Air Consumption

Since it was desired to express the concentrations of pro-knock compounds used as parts by volume per million of air consumed by the engine, the air consumption of the engine was determined. For this a 200 cubic feet per minute gas meter was attached in series with a 45 gallon drum and to the air inlet of the engine. The drum acted to smooth out pressure variations. One inch diameter rubber and glass tubing was used throughout the set-up. The resistance of the calibration apparatus, as measured by a simple U type water gauge, was less than four inches of water. Measurement of the rates of air consumption at various throttle openings were made. The graph of air consumption in cubic feet per minute against throttle opening in degrees is given in figure 2.

The conditions of operation of the engine were as follows: at full throttle for an octane range of 70 to 80, a compression pressure of 133 $\pm$ 2 pounds per square inch was used; for an octane range of 60 to 70, 126 $\pm$ 2 pounds per square inch was used. The throttle was set at 18° as this particular setting gave a conveniently wide linear range of knockmeter readings for a ten octane range. The engine speed was maintained constant at 900 revolutions per minute and a spark advance of 15° was used. The spark gap of the spark plugs was set at 0.025 inches. The bouncing pin contacts were maintained approximately 0.01 inches apart, but were adjusted from time to time to maintain a wide knock-meter range at the $18^{\bullet}$ throttle setting.

For every compound, at least five octane determinations were necessary to establish a curve of octane decrease vs. concentration. The standard method of determining the octane number of a gasoline requires about two hours per determinators and is accurate to $\pm$ 0.1

of an octane number. An accuracy of only $\pm$ 0.5 of an octane number was considered satisfactory in this work, so a more rapid method, although less accurate, was devised. The average time for each determination was reduced to about ten minutes.

The method consisted essentially of calibrating the knockmeter scale. However a simple calibration of octane number against knockmeter reading was not satisfactory since, under constant engine conditions, the knockmeter reading was not always constant for a single octane rating. However, for two fuels of different octane ratings, the difference in the knockmeter deflections for the fuels was constant to within one scale division. For example, for a fuel of octane number 70, the knockmeter reading for successive determinations might be 80, 82, 78, and for a fuel of 80 octane, the corresponding readings might be 50, 53, 48; the difference in knockmeter reading is 30 $\pm$ 1 for this ten octane range. A range such as this was readily obtained by suitable adjustment of the bouncing pin contacts, and the knockmeter rheostat. A calibration of change in knockmeter scale with change in octane number resulted in a straight line (figure 2 (a))

The detailed procedure of one determination was:

1. The 80 octane fuel used in these tests was standardized by the usual method, using standard reference fuels.

2. The knockmeter reading for this fuel was then determined.

3. A knockmeter calibration graph was established using standard reference fuels over the desired range.

4. The knockmeter readings for several tests using an adulterant were taken. Before and after each of these, the knockmeter reading for the 80 octane fuel was checked. The octane change for each of these was then readily determined from the graph.

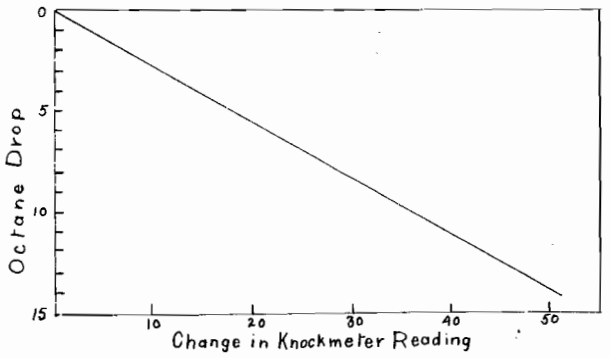

Fig 2a Typical Calibration Curve

Fig. 2(a) Typical Calibration Curve.

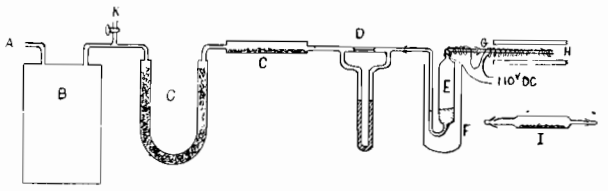

Fig 3, Apparatus for Adding Liquids to Air Intake.

A: Compressed air line.
B: Large drum.
C: $CaCl_2$ and P_2O_5 drying tubes
D: Butyl phthallate flowmeter.
E: Pycnometer containing liquid.
F: Heating or cooling bath.
G: Inlet tube, heated if required.
H: Air inlet to engine
I: Pycnometer for solids.
K: Excess air outlet.

Fig. 3. Apparatus for Adding Liquids to Air Intake.

5. From time to time the calibration graph was checked by using a standard reference fuel. The position of the curve might have changed very slightly over a period of time. The newly determined position would then be used as the calibration graph for further determinations.

All readings were taken at maximum knock air-fuel ratio.

Since gaseous, liquid and solid compounds were used, various techniques were required to admit their vapours into the air inlet of the engine.

The liquid compounds were generally handled by bubbling a small air or nitrogen stream through the compound. This air stream then joined the air taken into the engine. In some cases the liquid had to be heated or cooled, and in all cases the small air or nitrogen stream had to be perfectly dry.

About five c. c. of the liquid was placed in a pycnometer E (figure 3) which was then closed with ground glass caps and weighed. The pycnometer was then placed in the set up as shown. Air was taken from a compressed air line and passed into a 45 gallon drum to smooth out minor pressure changes in the line. Part of the air from this drum, the amount controlled by adjusting outlet K, was then passed through a long calcium chloride tube and over phosphorous pentoxide C to dry it well. The air flow was measured on a dibutyl phthallate flowmeter D. The air or nitrogen was bubbled through the liquid in the pycnometer E and then into the air inlet of the engine, carrying the vapour of the liquid with it. In cases where the oxygen of the air decomposed the compounds, nitrogen was used as supplied in cylinders by the Dominion Oxygen Company. The outlet valve on the cylinder was attached directly to the flowmeter D. If the compound was too volatile, an ice or ice-salt bath was placed around the

the pycnometer. If it were a high boiling point compound, the pycnometer was heated electrically. In this latter case, the inlet tube G was also electrically heated throughout its length to prevent condensation of the vapour there. The concentration of the vapour in the air entering the engine was controlled by varying the air or nitrogen flow as measured on the flowmeter.

The air or nitrogen was blown through for ten minutes and the knockmeter reading at maximum knock air-fuel ratio was found during this time. A stop watch was used to time this interval. The pycnometer was then removed, caps put on, and reweighed. From the loss in weight of the pycnometer and the air consumption the concentration in number of parts of compound as vapour per million of air was determined.

At least five such determinations were made for each compound and the data thus obtained were plotted, octane drop vs. concentration, on a semilog graph paper. The concentration necessary to give a ten octane drop was determined from this curve.

A similar technique was used for handling solids with an appreciable vapour pressure. For these a horizontal type of pycnometer was used (figure 3). The dried air or nitrogen was passed above the compound and into the engine. If heating was required to increase the vapour pressure over the compound, the tube was placed in a heating coil.

Compounds which were gases at room temperature were handled in a different manner. They were added by displacement with an inert liquid from a suitable burrette attached to the inlet tube (figure 4). In most cases mercury was used as the displacing medium, but in cases where the mercury reacted with the gas, e. g. for chlorine, concentrated sulphuric acid was used; with still other gases, a high boiling satur-

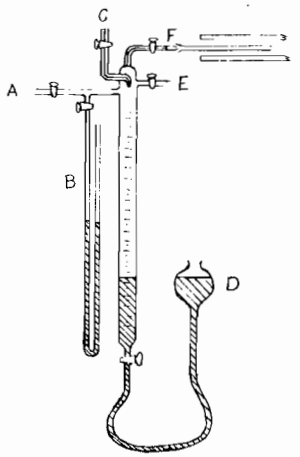

Fig 4. Gas Displacement Apparatus.
A: Gas Inlet. D: Leveling Bulb.
B: Mercury Manometer E: To Vacuum Pump.
C: To Mercury Reservoir F: To Engine Air Intake.

Fig. 4. Gas Displacement Apparatus.

ated paraffin hydrocarbon was used.

The vessel containing the gas was attached to A (figure 4), and the apparatus evacuated through E. Then the gas was admitted into the burrette until the pressure was about atmospheric, and stopcock A was closed. Final adjustment of the pressure to atmospheric was done by moving the levelling bulb D. Stopcock F was then opened and varying flows of the displacing liquid were admitted into burrette, the rate being controlled by the stopcock C. The rate was measured by noting with a stop-watch the time for 5 or more c. c. to be displaced.

For gases that were better than about thirty parts per million for a drop of ten octane, it was necessary to dilute them previously with dry air, following which the mixture was displaced from the burrette.

In solution work 5 c. c. of the liquid was diluted to 500 c. c. with gasoline. A quantity of this stock solution was diluted to 200 c. c. This fuel was then tested in the engine and the knockmeter reading recorded. Increased quantities of the stock solution were diluted to 200 c. c. and knockmeter readings taken until a ten or more octane drop was noted.

When solids were used in solution work, a weighed quantity was dissolved in 500 c. c. of gasoline and this was used as a stock solution from which other dilutions were made.

RESULTS

The concentration necessary for ten octane drop was the reference selected to compare the relative effectiveness of the compounds tested. Those compounds that were tested in solution were calculated as parts per million of air by using the relationship that 1000 c. c. of gasoline, which was consumed in two hours, was equivalent to 3960

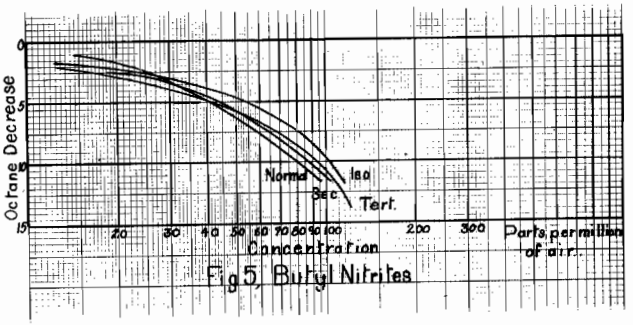

Fig. 5. Butyl Nitrites.

cubic feet of air which was consumed in the same time. The results are arranged as nearly as possible into groups of related compounds. The graphs of octane drop vs. concentration in parts of compound as vapour per million of air are also given in the accompanying figures.

1. Butyl Nitrites

Table 4

	P.p.m. for 10 octane drop
n Butyl nitrite	82.5
Isobutyl nitrite	107.0
Sec. butyl nitrite	88.0
Tert. butyl nitrite	95.5

The complete graphs for these compounds are shown in figure 5. Normal butyl nitrite has the lowest required concentration. Branching of the chain seems to increase the amount required.

2. Amyl Nitrites

Table 5

	P.p.m.
n Amyl nitrite	62.0
Isoamyl nitrite	63.0
Tert. amyl nitrite	92.0
Nitrite of sec. butyl carbinol	92.0
Nitrite of diethyl carbinol	93.0

Figure 6 shows these curves. Again the normal is the best. Branching at the end of the chain as in isoamyl nitrite does not appear to have much effect. Branching near the nitrite group has the greatest effect. There would appear to be an optimum branching effect above which increased branching has little or no effect.

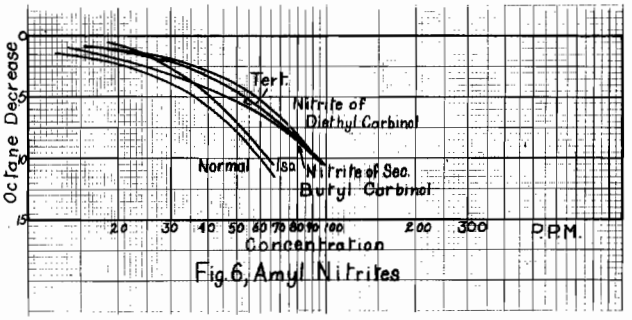

Fig. 6, Amyl Nitrites

Fig. 6. Amyl Nitrites

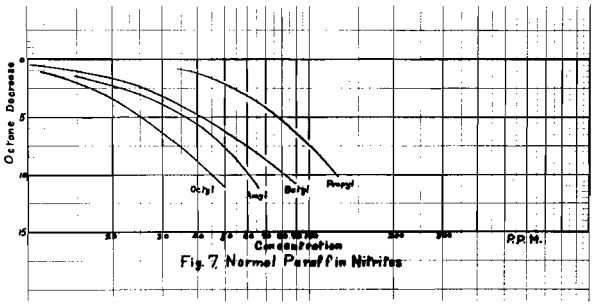

Fig. 7. Normal Paraffin Nitrites.

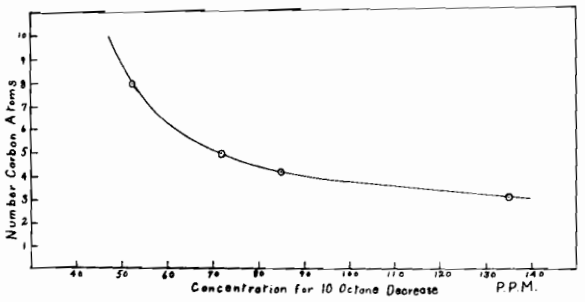

Fig. 8. Normal Paraffin Nitrites

Fig. 8. Normal Paraffin Nitrites

3. Normal Paraffin Nitrites.

Table 6

	P. p. m.
n Propyl nitrite	125.0
n Butyl nitrite	82.5
n Amyl nitrite	62.0
n Octyl nitrite	45.0

From table 6 and figure 7, it is apparent that the pro-knock quality improves with increased length of carbon chain, at least to the eight membered carbon chain. Figure 8 is the plot of number of carbon atoms in the chain vs. the concentration for ten octane drop. This curve seems to become assymtotic to the 20 p. p. m. line and does so around the 16 membered chain.

4. Bromine and Nitro Substituted Methanes.

Table 7

	P. p. m.
Tetra nitro methane	88.0
Bromo nitro methane	21.5
Monobromo trinitro methane	15.7
Dibromo dinitro methan	11.4
Tribromo nitro methane (bromo-picrin)	8.2

The curves for these are shown in figure 9. Tetranitro methane is much better than nitro methane (a value for this obtained by extropolating the curve of figure 4, would be above 300 p. p. m.) Also the mon-trinitro methane is better than monobromo mononitro bromo/methane, giving some indication as to the effectiveness of the nitro radical. But the bromine radical has considerable more pro-knock effect than the nitro group; in fact the pro-knock effect of the nitro groups seems to be almost negligible with that of bromine. As will be shown later, this is only true after the first nitro group has been added to the nucleus. Figure 10 shows the concentration in parts per million

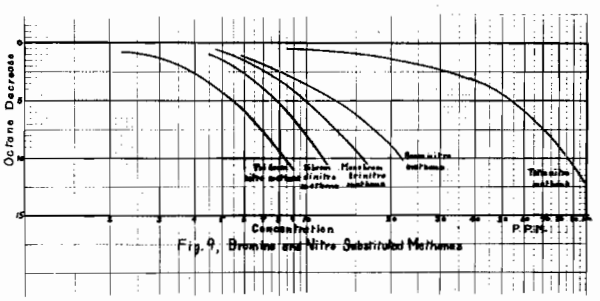

Fig. 9. Bromine and Nitro Substituted Methanes.

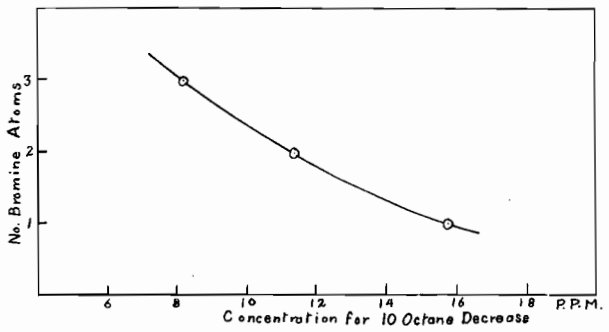

Fig. 10 BromoNitro Substituted Methanes

Fig. 10. Bromo-nitro Substituted Methanes.

for the ten octane drop vs. number of bromine radicals. This curve would have a greater slope if the nitro groups were not present on the molecule.

5. Chloro-nitro Substituted Paraffins.

Table 8.

	P. p. m.
2 Chloro-2 nitro propane	91.4
1 Chloro - 1 nitro ethane	28.9
Trichloro-nitro-methane (chloropicrin)	15.6
1, 1 Dichloro - 1 nitro ethane	12.4

These are shown in figure 11. It appears that the radicals are most effective when on the end carbon atoms, for in table 6, increased length of carbon atom chain caused increased pro-knock activity, whereas here the 1 chloro-1 nitro ethane is far better than 2 chloro-2 nitro propane. It is rather surprising that 1, 1 dichloro-1 nitro ethane is better than trichloro nitro methane. Evidently the increased length of chain has a greater pro-knock effect than the third chlorine radical.

Bromine compounds appear to be better than the corresponding chlorine compounds, e. g. bromopicrin is nearly twice as powerful as a pro-knock as chloropicrin.

6. Halogens and Hydrogen Halides.

Table 9.

	P. p. m.
Iodine	56 (approx.)
Chlorine	40.0
Bromine	16.2
Hydrogen Fluoride	90
Hydrogen Bromide	62
Hydrogen Chloride	30
Iodine trichloride	10.8
Iodine monochloride	18.5
Iodine monobromide	15.5

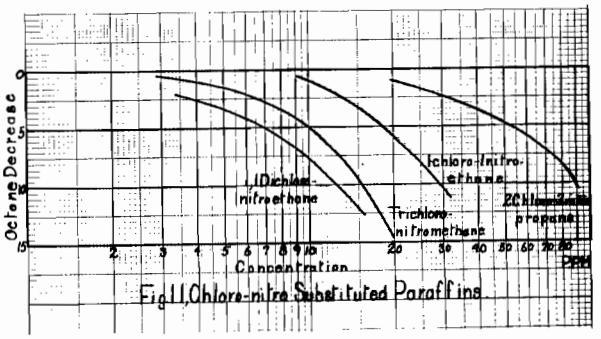

Fig. 11. Chloro-nitro Substituted Paraffins

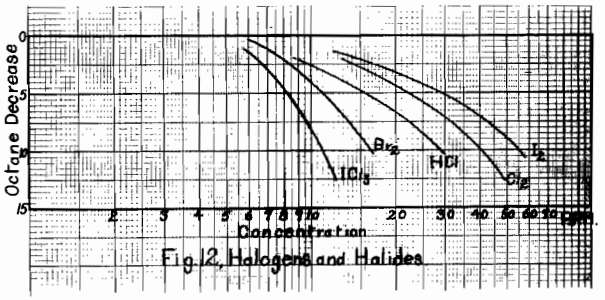

Fig. 12. Halogens and Halides.

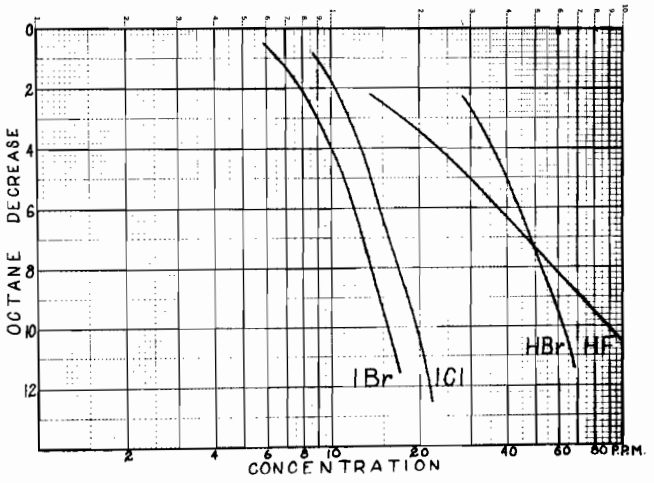

Fig. 13. Halogen and Halides.

In table 9 and figures 12 and 13, bromine appears to be the best of the halogens except in the case of hydrogen bromide which was not as effective as hydrogen chloride. No explanation for the discrepancy can be given. The value listed for iodine is only approximate since there was some condensation of the iodine in the intake tube. The iodine halide compounds are better than the halogens alone which would make it seem that the approximate value for iodine is much too high. From a consideration of these compounds, iodine would appear to be nearly as good if not better than bromine.

7. Halogen Substituted Methanes.

Table 10.

	P. p. m.
Methyl chloride	195
Methylene chloride	68.0
Chloroform	44.0
Carbon tetrachloride	33.0
Difluoro-dichloro methane (freon)	125

Table 10 and figure 14 shows the effect of increased substitution of the hydrogens of methane with chlorine. This is further shown in figure 15 where the relationship of number of chlorine atoms on the methane base is plotted against the concentration required for ten octane drop. It is interesting to notice that the substitution of a nitro radical for the fourth chlorine radical (as in chloropicrin) reduces the p. p. m. very markedly, from 33 down to 15.6

Fluorine here has less pro-knock effect than chlorine. The two fluorine radicals on difluoro dichloro methane increase its stability which may explain the fact that it is not as effective as dichloro methane alone.

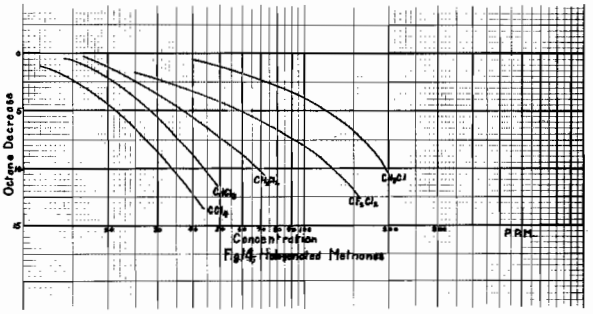

Fig. 14. Halogerated Methanes.

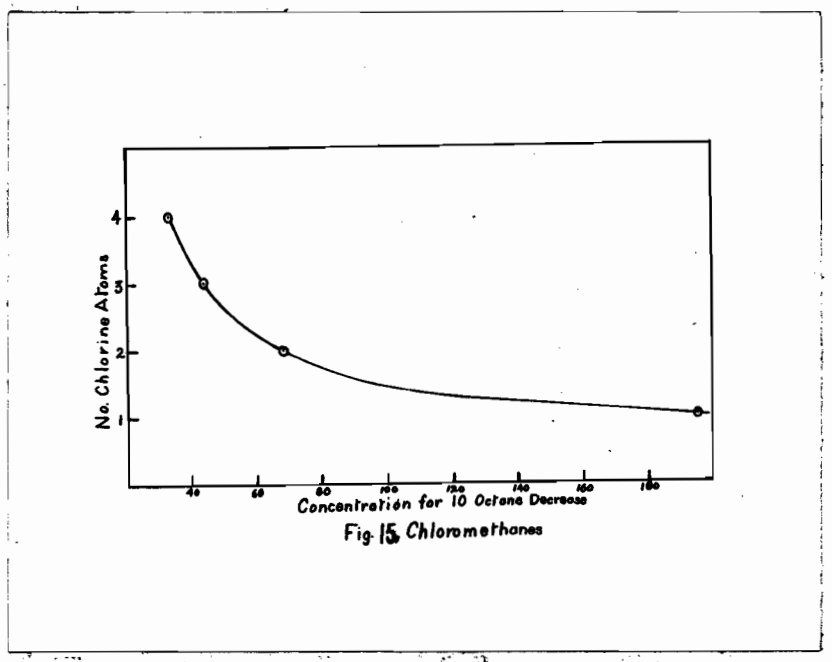

Fig. 15. Chloromethanes.

8. Chlorethanes

Table 11

	P. p. m.
Ethyl chloride	156
Ethylene dichloride	78.0
1,1,2-Trichloroethane	55.0
1,1,2,2 Tetrachloroetnane	40.0
Pentachloroethane	27.0
Hexachloroethane	18.4

Figure 16 again shows the effect of substitution of the hydrogen of a paraffin with a chlorine radical. In figure 17, the curve of a number of chlorine atoms on an ethane nucleus against concentration in parts per million for ten octane decrease is plotted.

9. Oxychloride and Inorganic Halides (Figures 18 and 19)

Table 12

	P. p. m.
Thionyl chloride	15.1
Selenium oxychloride	8.3
Phosphorous oxychloride	7.7
Chromium oxychloride	7.7
Vanadium oxychloride, vandium chloride (50-50 mixture)	7.1
Aluminum trichloride	14.5

The oxychloride groupsare very good pro-knocks. The oxygen atom appears to have a pro-knock effect as can be seen by comparing phosphorous oxychloride with phosphorous trichloride (in Table 13). However it is possible that the increased pro-knock effect is due to the pentavalent phosphorous rather than the oxygen radical.

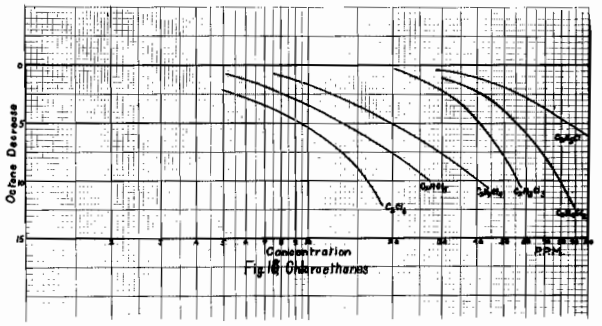

Fig. 16. Chloroethanes.

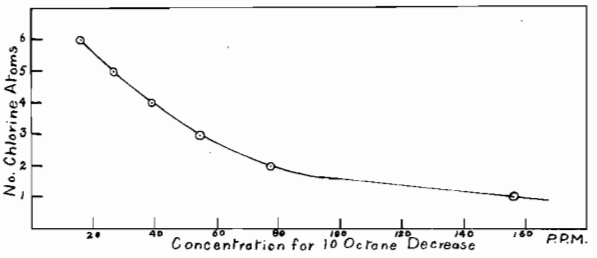

Fig. 17. Chloroethanes

Fig. 17. Chloroethanes.

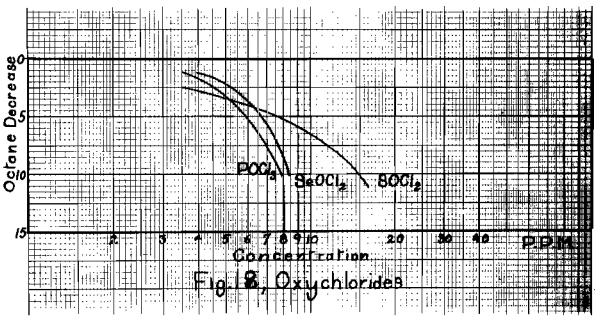

Fig. 18. Oxychlorides.

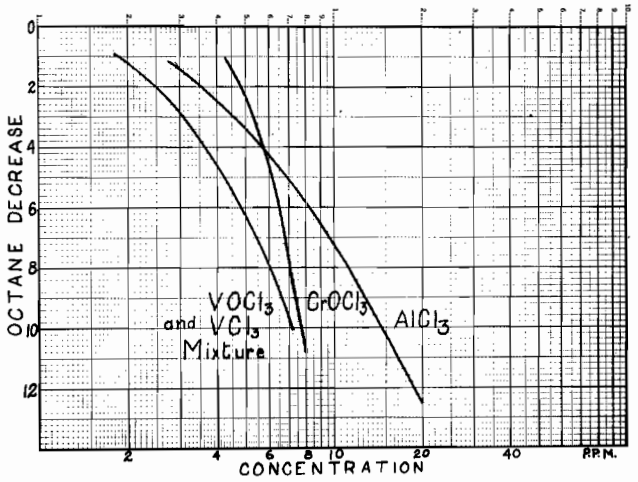

Fig. 19. Oxychlorides.

10. Arsenic, Antimony and Phosphorous Halides

Table 13.

	P. p. m.
Dichloro-methyl arsine	3.8
Cacodyl Chloride (in air stream)	4.2
(in solution)	5
Lewisite (in solution)	4.6
Arsenic tribromide	4.6
Arsenic trichloride	5.8
Arsenic trifluoride	11.0
Antimony pentachloride	6.1
Phosphorous pentachloride	6.5
Phosphorous trichloride	8.6
Phosphorous trifluoride	31.5
Phosphorous pentafluoride	40

The octane drop concentration curves for these are shown in figure 20 and 21.

Arsenic compounds are the best pro-knock compounds investigated during this study. Dichloro-methyl arsine is the best pro-knock found to date. Antimony compounds and then phosphorous compounds are the next best.

The substitution of a methyl radical for one chlorine on a chloride increases the pro-knock effect as was noted in section 5. The fluorine radical is again shown to be inferior to the chlorine radical in pro-knock activity. Increased halogen substitution is shown again to increase the effectiveness, c. f. phosphorous trichloride and phosphorous pentachloride.

Both lewisite and cacodyl chloride when dissolved in the gasoline reacted to some extent forming a slight milky precipitate. This precipitate is probably an arsenic oxide, for when cacodyl chloride was added to the unleaded base stock, a heavy white precipitate resulted. This would thus decrease the effectiveness of the compound added as

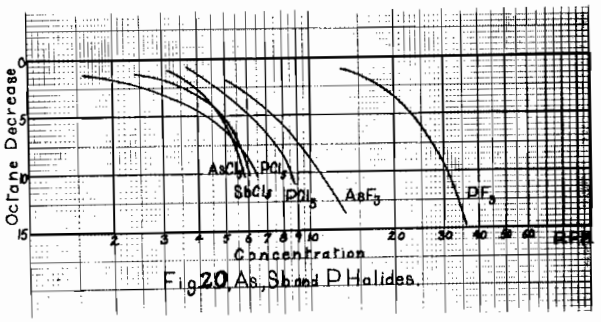

Fig. 20. As, Sb, and P Halides.

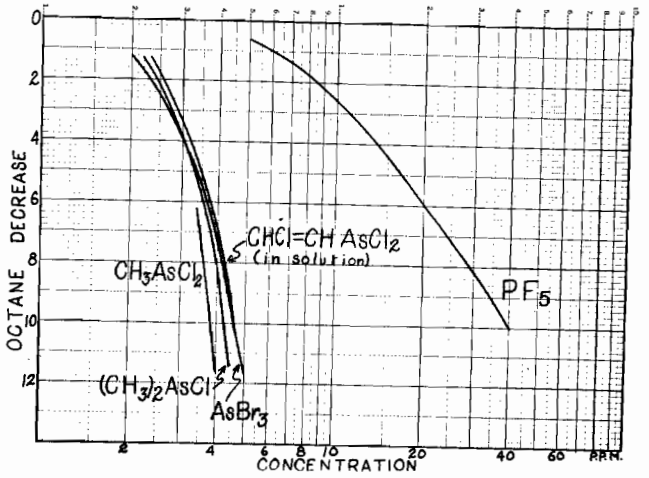

Fig. 21. As, Sb, and P Halides

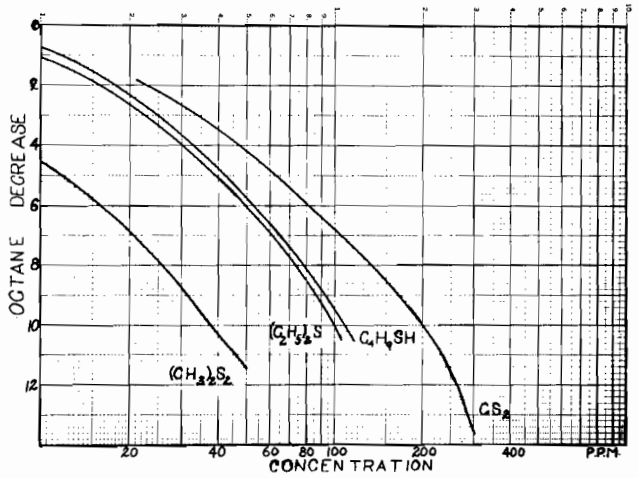

Fig. 22. Sulphides and Mercaptans.

is seen in the values for cacodyl chloride where the compound was better by one part per million in the air stream than in solution. If a similar amount of effectiveness was removed from the lewisite in dissolving it in gasoline, the value when using it in the air stream would be about 3.8 which would make it at least as effective as methyl dichloro arsine.

11. Sulphides and Mercaptans

Table 14

	P. p. m.
Carbon bisulphide	205
n Butyl mercaptan	108
Ethyl sulphide	100
Methyl disulphide	37

Figure 22 shows the concentration octane decrease curves for these. Increase sulphur content in an organic compound lowers the concentration required for the same pro-knock effectiveness. A sulphide linkage appears to be more effective than a mercaptan linkage for ethyl sulphide is better than n butyl mercaptan in spite of the decreased length of the chain.

12. Other Organic Sulphur Compounds

Table 15

	P. p. m.
Methyl isothiocyanate	285
Methyl thiocyanate	115
n Propyl sulphone	132
Benzene sulphonyl chloride	54

The curves for these are shown in figure 23. The thiocyanate radical- SCN is much more effective than the isothiocyanate radical - -NCS.

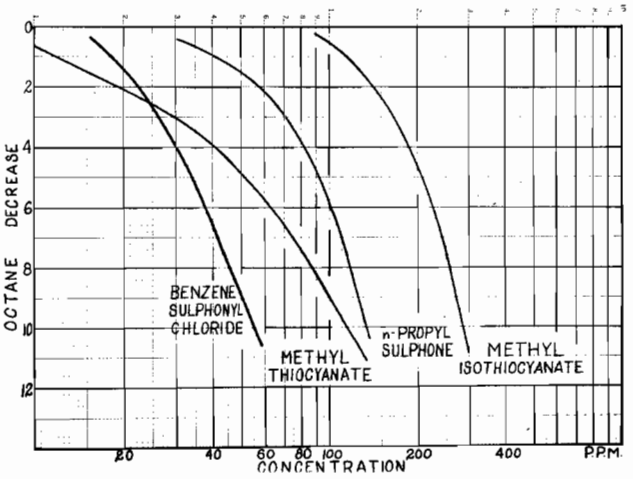

Fig. 23. Organic Sulphur Compounds.

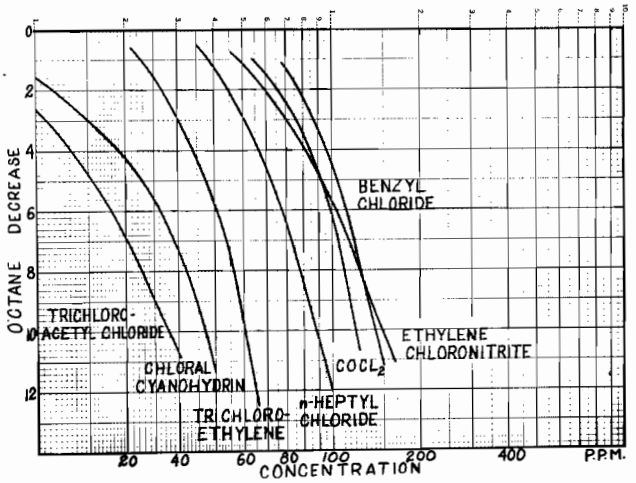

Fig. 24. Miscellaneous Organic Halides.

13.Miscellaneous Organic Halides (Figure 24)

Table 16

	P. p. m.
Ethylene chloronitrite	150
Diethyl chloroamine (approx.)	164
Benzyl chloride	141
Ethyl hypochloride (approx.)	135
Phosgene	120
n Heptal chloride	88
Trichloroethylene	51
Chloral cyanohydrin	37
Trichloroacetyl chloride	28

In the monochlorosubstituted paraffins, the effect of chain length is not as great as it is for the mononitrites. The shorter chained monochlorides are more effective than the corresponding nitrites, but the longer chained chlorides are far less effective than the nitrite. This is shown in the following abbreviated table.

Table 17.

Concentration of compounds necessary for 10 octane decrease

	Nitrite	Chloride
Methyl	300	195
Ethyl	200	156
n Heptal	49	88

The value obtained for ethyl hypochloride is only approximate because even though nitrogen was used through the pycnometer, it decomposed very rapidly. With diethyl choroamine there was apparently a very mobile equilibrium with some isomer which made it difficult to establish the concentration octane drop curve.

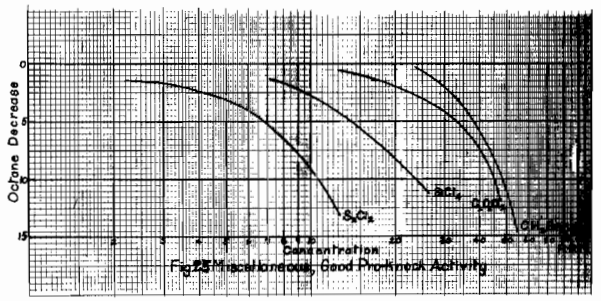

Fig. 25. Miscellaneous, Good Pro-knock Activity.

14. Miscellaneous (Good Pro-knock Activity) (Figure 25)

Table 18

	P. p. m.
Methylene bromide	48.3
Oxalyl chloride	45.1
Silicon tetrachloride	23.0
Sulphur chloride	10.6

The bromine radical is here shown to be better than the chlorine radical since methylene chloride required 68.0 p. p. m.

Silicon tetrachloride is better than carbon tetrachloride which required 33.0 p. p. m. Here again this may be due to the decreased stability and ease of hydrolysis of silicon tetrachloride, or it may be that silicon is a better pro-knock nucleus than carbon.

15. Miscellaneous (Poor Pro-knock Activity) (Figures 26 & 27)

Table 19

	P. p. m.
2 Nitro-butinol-1 acetate	310
Sulphur hexafluoride	195
Acetyl nitrate	140
n Butyl thionitrite	130
Boron trifluoride	115
Cyanogen bromide	113
Ethyl sulphite	100
Trichloroethyl nitrite	76.0
Ethyl orthosilicate	23.0

The thionitrite linkage is not as effective as the ordinary nitrite linkage, n butyl nitrite only required 82.5 p. p. m. Ethyl sulphite is much better than either the nitrite or the chloride, a long chained sulphite might be quite effective.

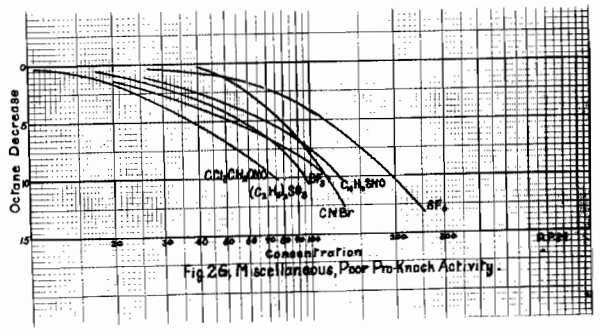

Fig 26, Miscellaneous, Poor Pro-Knock Activity.

Fig. 26. Miscellaneous, Poor Pro-knock Activity.

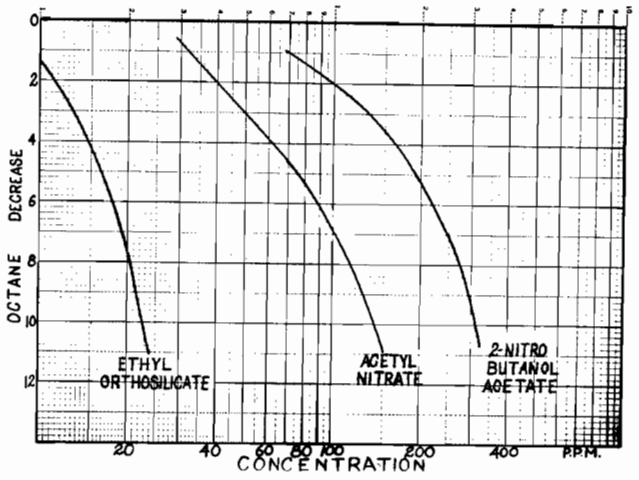

Fig. 27. Miscellaneous Compounds.

16. Compounds with no Pro-knock Effect.

Table 20

(No octane decrease at the concentration indicated.)

	P. p. m.
Diacetyl ortho nitric acid	12
Stibene (approx.)	50
Isopropyl ether	440
n Butyraldehyde	453
Cyanogen	600
n Butyl borate	
Ascaridal	
Nitrous oxide	

(A saturated solution in gasoline of the following compounds was used.)

Triphenyl-chloromethane
Ammonium azide
Nitro acetal dioxine
Picryl chloride
Triphenyl phosphine sulfide

17. Solution Data.

The following is the result of work done by dissolving the compounds in the gasoline and testing the octane number of the resulting mixture. This was done to see if there was any difference in the results obtained by adding the compounds in the air stream and those obtained by using solutions and to find if possible a compound suitable for use in sabotaging gasoline stores.

Table 21

Results of Solution Work

Adulterant	P.p.t of fuel by volume	Remarks	P.p.m. calculated	P.p.m. when added to air stream
Chloropicrin	0.6	causes faint cloudiness	12.0	15.6
Bromopicrin	0.7	faint cloudiness	13.0	8.2
Dibrom dinitro methane	0.7	no visible change	15.0*	11.4
1, 1 dichloro-1, nitro ethane	0.7	no visible change	12.0*	12.4
Trinitro bromo methane	0.9	no visible change	17.0*	15.7
Silicon tetrachloride	0.9	slight colorless ppt.	16.0	23.0
Phosphorous oxychloride	1.2	brownish ppt.	26.5	7.7
Selenium oxychloride	1.5	brownish-yellow ppt.	43.5	8.3
1-chlor-1-nitro ethane	1.6	no visible effect	36.0*	28.8
Pentachlorethane	1.6	no visible effect	27.0	
Carbon tetrachloride	1.9	no visible effect	40.0	33.0
Tetrachloroethylene	2.1	no visible effect	41.5	
Tetrachloroethane	2.1	no visible effect	40.5	
2-chloro-2-nitro propane	2.3	no visible effect	41.0*	91.4
1,2 Dichloroethylene	2.4	no visible effect	63.0	
Chloroform	2.5	no visible effect	62.5	40.0
Tert-butyl chloride	2.5	no visible effect	45.5	
Dichloromethane	2.9	no visible effect	68.5	
1,1,2-trichloroethane	3.1	no visible effect	67.0	55.0
Tetranitro methane	3.5	greenish colour	38.5	88.0
n-Butyl nitrite	3.8	greenish colour	67.0	82.6
Nitroform	4.8	greenish colour; part did not dissolve	101	
Isoamyl nitrite	5.0	greenish colour	74.5	63.0
n octyl nitrite	5.8	no visible effect	62.5	45.0
Monochloroethane	5.8	no visible effect	156	
Ethyl sulphite	9.2	no visible effect	143	100

* Calculated using an approximate density.

In this solution work a gasoline leaded to 80.5 octane from a 72.6 octane base stock was used. This leaded gasoline reacted in many cases with the compound added before the 'doped' gasoline had entered the engine. This was particularly noticeable with the chlorides which caused a precipitation of the lead. As the lead does not precipitate out immediately in most cases but may require as long as twelve hours, the octane decrease would depend on the time between preparing the stock solution and using it. The results are of use in determining the effect of sabotaging gasolines, when sufficient time has been allowed, but if any reaction occurs between the gasoline and the adulterant outside the engine, they are not of value in determining the effect of use in an air barrage. It would appear that the effect of adding the compound in the air stream and in the gasoline is about the same if no reaction occurs.

Some metal naphthenates of unknown molecular weight were investigated in solution. The results are shown in table 22. They were found to gum up the piston rings and valves very badly and to cause a heavy formation of carbon in the cylinder, necessitating frequent overhauling of the engine.

Table 22

Metal Naphthenates Investigated in Solution

Metal Naphthenate	Octane decrease caused by adding 0.3 gram per 100 c.c	Octane decrease adding 0.03 gram per 100 c.c.	Octane decrease adding 0.003 gram per 100 c.c.
Cobalt	1.5	1.5	1.0
Zinc	0.8	0.0	0.0
Copper	2.3	0.8	0.4
Manganese	1.8	1.2	0.8
Chromium	4.2	1.1	0.8
Iron	3.0	0.0	0.0
Mercury	16.0	2.5	0.0
Lead	0.8	0.3	0.0
Magnesium	1.2	0.0	0.0
Potassium	insoluble in gasoline		
Vanadium	10.0	1.8	1.0
Nickel	3.3	2.0	0.3

Tests on Unleaded Fuels

As stated previously, all the above tests were carried out on 80.5 octane gasoline, leaded to this value from a base stock of 72.6 octane. It was thought desirable to find out if the pro-knock effect obtained was partly or wholly due to reaction with the tetraethyl lead of the gasoline. To do this, chloropicrin was tested on the unleaded base stock and on an unleaded 80.5 octane fuel made from reference fuels. The results obtained are shown in table 23. Again the values given are the concentration necessary for 10 octane decrease.

Table 23

Pro-knock Effect of Chloropicrin in Different Fuels.

	P. p. m.
80.5 octane leaded fuel	15.6
72.6 octane unleaded base stock (in solution)	72.8
72.6 octane unleaded base stock (in air stream)	72.5
80.5 octane reference fuel	86.0

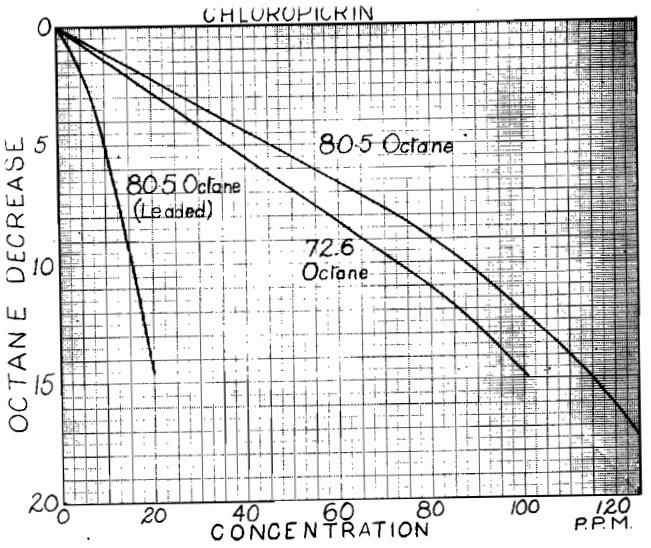

Fig. 28. Chloropicrin in Unleaded Fuels.

The graph of concentration against octane decrease is shown in figure 28. It is seen from this that a large part of the effect is counteraction of the tetraethyl lead but there is still a considerable effect on the unleaded gasoline. The graph of concentration against octane decrease on the unleaded fuel is linear for quite a portion of the curve. The effect on two types of unleaded fuels is shown.

Cacodyl chloride when dissolved in the unleaded 72.6 octane gasoline reacted forming a heavy white percipitate. The solution above the precipitate had a slightly less octane rating, 3000 p. p. m. reduced the rating by 3 octane units.

Although it was seen that there was a greatly decreased effect on an unleaded fuel, it was felt that this would not hinder the investigation since the fuel used in the German aircraft contains around 5.73 ml. of tetraethyl lead per imperial gallon (99). If, as shown, most of the effect is due to the presence of tetraethyl lead, the concentration necessary for a ten octane decrease on the fuel used in German aircraft should be somewhat less than that found for the 80.5 octane gasoline used here. The gasoline in these tests had only about 1.5 ml. of tetraethyl lead per imperial gallon.

Discussion of Results

The most effective pro-knock radicals yet investigated are the halides. The order of increasing activity is fluoride, iodide and chloride about the same, and then the bromide radical. The effectiveness of the halide radicals may be due to their ability to act as chain carriers (107). The combustion process, which is a chain mechanism, would be accelerated by the presence of chain carriers. There is one instance of the sulphite radical being much more effective than the chloride radical,

but further work is necessary to ascertain the use that can be made of this radical.

The best elements for the nucleus of an ideal pro-knock are the middle elements of groups V (b) and VI (b). The group V elements are better than those of group VI. The order of effectiveness in group V is arsenic better than antimony better than phosphorous. The marked activity of these elements may be due in part to their great ease of hydrolysis which would liberate halogen halides from the compound.

The presence of a nitro group on a paraffin halide appears to have an accelerating effect on the halides present, c. f. chloropicrin 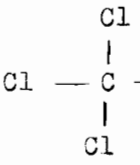 and carbon tetrachloride 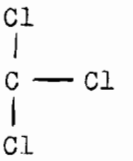 , the former requires only 15.6 p. p. m. for 10 octane decrease whereas the latter requires 33 p. p. m. This increased pro-knock activity cannot be due to the activity of the nitro group, for tetranitro methane requires 88 p. p. m.

A methyl radical also has an accelerating effect as is shown in several compounds, c. f. 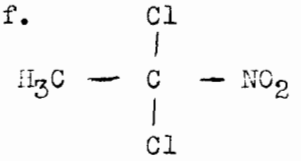 and 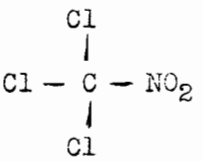

and 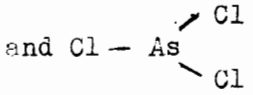 and 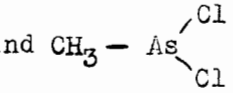 The concentration is decreased from 15.6 to 12.4 p. p. m. in the first case, and from 5.8 to 3.8 p. p. m. in the second case.

Branching in a long organic molecule decreases its pro-knock effectiveness as shown in the butyl and amyl nitrites. Increasing the

length of the chain also increases its pro-knock activity. These conclusions are in agreement with the anti-knock qualities of organic compounds; increase in chain branching and decrease in chain length of a fuel increases its octane rating (108).

The metal naphthenates show the effect of the metal atom since the naphthenate radical probably has anti-knock properties (109). Mercury and vanadium naphthenates were the most effective. A very effective pro-knock might result if pro-knock radicals were placed about these elements.

These metal napthenates gummed up the engine very rapidly. This fact is important when considering a compound suitable for sabotaging gasoline stocks. This sticking was also found by the Thomas and Hochwalt laboratories (98).

From these results one can postulate the structure of an "ideal" pro-knock. The kernel should be arsenic, or possibly mercury or vanadium. It should be a bromide, with a methyl radical on one of the valency bonds. This compound might be further increased in activity by using a halogen substituted carbon radical instead of the methylene radical. Since the one nitro radical was able to increase the pro-knock activity of the halogen substituted compounds,it would be desirable to place such a radical on this halogen substituted carbon radical. The structure of the final compound might be for example

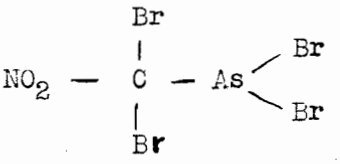

Such a compound would be a solid and further investigation is necessary to see how this could be modified to make it a more suitable compound to use although it is possible that this could be used by dispersing it

in the air as a vapour which would solidify as a fine dust. Synthesis of, and tests with compounds of this type are projected for the near future.

Sufficient data from which to postulate a mechanism of pro-knock activity are not available. The pro-knock action seems to depend mainly on the elements constituting the molecule and to some extent upon their arrangement in the molecule. Most of the 'pro-knock' elements are in groups IV, V, VI, and VII and in series 2, 3, 4 and 5. Very few elements outside this section had any pro-knock activity; mercury is about the only exception. The pro-knock activity of a group appears to increase as its position approachs series 4.

Attempts to relate the relative pro-knock effectiveness of the various compounds to other properties of the molecules, such as heats of formation, and combustion were impossible since sufficient data of this nature were not available. However there does appear to be a relation between pro-knock activity and the catalytic effect of these compounds on the rate of oxidation of butane. A relation between the concentration required for a ten octane decrease and that required to give optimum reduction in half time value is indicated (110).

Whether the use of pro-knock compounds as a weapon in chemical warfare is practical, cannot be stated. Estimates of the octane drop required to render an aeroplane engine inactive vary, and no quantitative data are available. It is essential that this should be determined before any real estimate of the value of pro-knocks in military tactics can be made. If field trials demonstrate that the action of a pro-knock can, in fact, hinder operation of military motorized equipment, at least of certain types, it would seem perfectly justifiable to seek still further for compounds of increased pro-knock activity.

Bibliography

(1) Dickinson, H. C. Oil and Gas J. 29, 24 (1931)

(2) Bone, W. A. and Townend, D. T. A. Flame and Combustion in Gases, Longmans, Green and Company, 1927.

(3) Bone, W. A. Bakerian Lecture, Prov. Roy. Soc. 137, 243 (1932)

(4) Kersten, W. J. prakt. Chem. 84, 311 (1861)

(5) Misterli, T. J. Gasbeleucht 48, 802 (1905)

(6) Armstrong, H. E. J. Chem. Soc. 83, 1088 (1903)

(7) Bone, W. A. and Wheeler, R. V. J. Chem. Soc. 1074 (1903)

(8) Bach, P. B. Compte. rend 124, 951 (1897)

(9) Engler, C. and Wild, L. A. Ber. 30, 1669 (1897)

(10) Bone, W. A. J. Chem. Soc. 1933, 1614.

(11) Norrish, R. W. Proc. Roy. Soc. A 150, 36 (1935)

(12) Lewis, J. S. J. Chem. Soc. 1927, 1555

(13) Berl, E. and Winnacker, K. Z. phyik. Chem A148, 26 (1930)

(14) Steacie, E. W. R. and Plewes, A. C. Proc. Roy. Soc. A146, 583 (1934)

(15) Pidgeon, L. M. and Egerton, A. C. J. Chem. Soc. 1932, 661, 676

(16) Hardles, E. W. J. Trans. Faraday Soc. 27, 681 (1931)

(17) Ubbelohde, A. R. Science of Petroleum, Vol. 4, page 2937, Oxford University Press, 1938.

(18) Bone, W. A. and Hill, S. G. Proc. Roy. Soc. A129, 434 (1930)

(19) Newitt, D. M. and Hoffner, A. E. Proc. Roy. Soc. A 134, 591 (1931)

(20) Marek, L. F. and Hahn, D. A. The Catalytic Oxidation of Organic Compounds in the Vapor Phase, Chemical Catalog Company, 1932

(21) Pease, R. N. J. Am. Chem. Soc. 51, 1839 (1929)
52, 5106 (1930)
55, 2753 (1933)
56, 2034 (1934)

(22) Edgar, G. Ind. Eng. Chem. 19, 145 (1927)

(23) Pope, I. C., Dykstra, F. J. and Edgar, G. J. Am. Chem. Soc. 51, 1875, 2203, 2213 (1929)

(24) Beatty, H. A. and Edgar, G. J. Am. Chem. Soc. 56, 102 (1934)

(25) Prettre, M. Ann. Comb. Liq. 6, 7, 269, 533 (1931)

7, 699 (1932)

Bull. Soc. Chim. Franc. 51, 1132 (1932)

(26) Wheeler, R. V. J. Chem. Soc. 113, 45 (1918)

(27) Laffitte, P. Ann. Phys. 4, 623 (1925)

(28) Laffitte, P. and Breton J. Compt. rend, 183, 284 (1926)

(29) Egerton, A. C. Proc. Roy. Soc. 114, 137, 152 (1927)
116, 516 (1927)

(30) Lorentzen, J. Z. Angur. Chem. 44, 131 (1931)

(31) Beale, C. O. B. Science of Petroleum, Vol. IV p. 3072

(32) Dickinson, H. C. J. Soc. Auto. Eng., 8, 558 (1921)

(33) Midgley, T. Jr. and Boyd, T. A. Ind. Eng. Chem. 14, 894 (1922)

(34) Steele, S. Nature, 131, 725 (1933)

(35) Clark, G. L. and Henne, A. L. J. Soc. Auto. Eng. 20, 264 (1927)

(36) Wendt, G. L. and Grimm, F. V. Ind. Eng. Chem. 16, 890 (1924)

(37) Morgan, E. J. Soc. Auto. Eng. 16, 8 (1925)

(38) Egerton, A. C., and Gates, S. F. Proc. Roy. Soc. A114, 402 (1927)

(39) Egerton, A. C. Nature, 121, 876 (1928)

(40) Maxwell, N. and Wheeler, R. V. Ind. Eng. Chem. 20, 1041 (1928)

(41) Ricardo, H. R. Aut. Engineer 11, 92 (1921)

J. Soc. Aut. Eng. 10, 308 (1922)

(42) Tizard, H. T. and Pye, D. R. Phil. Mag. 1922, 79
1926, 1094

(43) Withrow, L. and Boyd, T. A. Ind. Eng. Chem. 23, 539 (1931)

(44) Callendar, H. L., King, R. O. and Sims, C. J. Engineering 121 475, 509, 576, 605 (1926)

(45) Moureau, C., Dufraisse, C., and Chaux, R. Compt. rend 184, 413 (1927)

Chim et Ind. 17, 99 (1927)

(46) Egerton, A. C., and Gates, S. F. J. Inst. Petr. Tech. 13, 281 (1927)

Nature 119, 427 (1927)

(47) Egloff, G., Schaad, R. E. and Lowry, C. D. Jr. Ind. Eng. Chem. 21

785 (1929)

(48) Mondain-Monval, P. and Quanquin, B. Ann. Chim. 15, 309 (1931)

(49) Ubbelohde, A. R. and Egerton, A. Nature 135, 67 (1935)

(50) Egerton, A. C., Smith, F. L. and Ubbelohde, A. R. Phil. Trans. Roy. Soc. 234, 433 (1935)

(51) Hinshelwood, C. N., Williams, C. and Wolfenden, P. Proc. Roy. Soc. A147, 48 (1934)

(52) Rice, F. O. Ind. Eng. Chem. 26, 259 (1934)

(53) Beatty, H. A. and Edgar, G. Science of Petroleum Vol. IV, p. 2927

(54) Ricardo, H. R. Auto. Eng. 11, 51, 92 and 130 (1921)

(55) Midgley, T. Jr., Thomas, W., and Boyd, T. A. J. Soc. Auto. Eng. 10, 7 (1922)

(56) Mac Coull, N. J. Soc. Auto. Eng. 22, 457 (1928)

(57) Stansfield, R. and Thole, F. B. Ind. Eng. Chem. Anal. Ed. 1, 98 (1929)

(58) Roesch, D. J. Soc. Auto. Eng. 19, 17 (1926)

(59) Lovell, W. G., Campbell, J. M., and Boyd, T. A. Ind. Eng. Chem. 26, 1105 (1934)

(60) Graetz, A. Ann. office nat. comb. liquides, 3, 69 (1928)

(61) Callingaert, G. Science of Petroleum, Vol. IV, p. 3024

(62) Midgley, T. Jr. and Boyd, T. A. J. Soc. Auto. Eng. 15, 659 (1920)

(63) Midgley, T. Jr. and Boyd, T. A. Ind. Eng. Chem. 14, 589, 849, 894 (1922)

(64) Midgley, T. Jr. and Boyd, T. A. Ind. Eng. Chem. 15, 421 (1923)

(65) Boyd, T. A. Ind. Eng. Chem. 16, 894 (1924)

(66) Egerton, A. C. Science of Petroleum, Vol. IV, p. 2914

(67) Cross, R. U. S. Patent 1,883,595 Oct. 18

(68) Rozenstien, L. and Hund, W. J. U. S. Patent 1,920,766, Aug. 1.

(69) John R. U. S. Patent 1,753,294 April 8.

(70) Kalichevsky, V. A. and Stagner, B. A. Chemical Refining of Petroleum, Chap. 8, Chemical Catalog Co. 1933

(71) I. G. Farbenind, A. G., British Patent 334,181 April 27, 1929.

(72) Kettering, C. F. and Midgley, T. Jr. U. S. Patent 1,635,216 July 12.

(73) Layng, T. E., and Youker, M. A. Ind. Eng. Chem. 20, 1048 (1928)

(74) Bone, C. A. French Patent 733,497, Mar. 15, 1932.

(75) Danner, P. S. Can. Patent 332,361 May 9, 1933.

(76) Longenus, M. Asphalt Teerind. Z. 26, 519 (1926)

(77) Ducamp, A. J. Brit. Patent 335828, Dec. 4 (1928)

(78) Hosmer, F. E. Brit. Patent 309,191 April 5 (1928)

(79) Egerton, A. C. U. S. Patent 1,771,169 July 22.

(80) Charch, W. H., Mack, E. Jr. and Boord, C. E. Ind. Eng. Chem. 18, 334 (1926)

(81) Endo, E. J. Fuel Soc. Japan 11, 564 (1932)

(82) Bassett, H. P. U. S. Patent 1,641,520 Sept. 6

(83) Rosenbaum, R. R. U. S. Patent 1,841,254 Jan. 12

(84) Rosenstien, L. Brit. Patent 349,475 Nov. 18, 1929

(85) Sokal, E. Brit. Patent 285,145 Nov. 11 (1925)

(86) Sokal, E. J. Soc. Chem. Ind. 43, 283 (1924)

(87) Egloff, G., Faragher, W. F. and Morrell, J. C. Refiner Nat. Gas. Mfr. 9, No. 1, 80 (1930)

(88) Schmidt, A. W., Generich, H., Schalz, G. and Mohry, F. Braunkohle, 35, 535 (1936)

(89) Mardles, E. W. J. J. Chem. Soc. 1928, 822

(90) Callandar, H. L. Engineering 123, 147 (1927)

(91) Beatty, H. A. and Edgar, G. Science of Petroleum, Vol. IV, p. 2927

(92) Clark, G. L. and Thee, W. C. Ind. Eng. Chem. 18, 528 (1926)

(93) Clark, G. L. Br. J. Radiology 23, 112 (1927)

(94) Moureau, C., Dufraisse, C. and Chaux, R. Ann. office nat. comb. liquides, 2, 233 (1927)

(95) Stacey, H. R. and Wasson, J. I. Antiknock Characteristics of Various Chemical Compounds. Standard Oil Development Research Laboratories.

(96) Lapeyrouse, M. and Lebo, R. B. Antiknock Characteristics of Individual Chemical Compounds. Mar. 25, 1937.

(97) Sugden, S. Memorandum on Attack of Internal Combustion Engines by Means of Chemical Agents. Ptn. 1271 (P21455) 1940

(98) Thomas and Hochwalt Laboratories "Chemical Treatment of Oils..(Gasoline Satotage)", 1941.

(99) Midgley, T. Jr. and Henne, A. L. Div. B, Serial Nos. 13, 24, 67 (1941)

(100) Ogilvie, J. D. B. Masters Thesis, McGill University, 1940.

(101) Jolibois, P. and Normand, G. Compt. rend 179, 27 (1924)

(102) Midgley, T. Jr. J. Soc. Auto. Eng. 7, 489 (1920)

(103) Schaad, R. E. and Boord, C. E. Ind. Eng. Chem. 21, 756 (1929)

(104) Lewis, J. S. J. Chem. Soc. 1930, 2241

(105) Clark, G. L., Brugmann, E. W. and Thee, W. C. Ind. Eng. Chem. 17, 1226 (1925)

(106) Ormandy, W. R. and Craven, E. C. J. Inst. Pet. Tech. 10, 335 (1924)

(107) Hinshelwood, C. N. Kinetics of Chemical Change, Oxford University Press, 1940.

(108) Lovell, W. G. and Campbell, J. M. Science of Petroleum, Vol. IV, p. 3004

(109) Egloff, G., Faragher, W. F. and Morrell, J. C. Oil and Gas J. 28 (29), 116 (1929)

(110) Gillies, A. Private communication.

THE DYNAMIC SORPTION OF BUTANE AND AMMONIA ON CHARCOAL

(in collaboration with J. D. B. Ogilvie)

THE DYNAMIC SORPTION OF BUTANE AND AMMONIA ON CHARCOAL

(in collaboration with J. D. B. Ogilvie)

TABLE OF CONTENTS

Introduction

Sorption has been studied in many ways, most of which dealt with a static system. With the development of the service respirator, it became necessary to study sorption in dynamic systems, in an effort to relate performance of the respirator in the field to laboratory tests. A new method of studying dynamic sorption was developed in this laboratory (1) and the sorption of butane and ammonia were studied using this method.

Sorption

Gases are sorbed on solids by interaction of the unsatisfied fields of force of the surface atoms of the solid, with the fields of force of the molecules striking the solid surface. This phenomenon has led to a great many investigations which showed sorption to be a function of pressure. Since sorption is, in one sense, simply an instance of the distribution of a substance between two phases, it might be anticipated that Nernst's Distribution Law would apply. Thus it was postulated that the sorption would follow a modified form of Henry's Law. This law holds for many cases at low concentrations, but deviations are numerous.

The best known attempt to modify the sorption isotherm beyond the Henry's Law region is the so-called Freundlich isotherm,

$$x = kp^{1/n} \qquad \text{(i)}$$

Here x is the amount sorbed, p is the pressure of the sorbate, and 1/n and k are constants for a given system at a given temperature. Two great defects are inherent in this relation. It only holds over narrow ranges of pressures, and it is purely empirical, having no theoretical basis. A more exact formulation was postulated by Langmuir (2). He obtained a formula from considering that the sorbed layer is only one molecule thick when complete, and that sorption was due to the actual condensation of the molecules arriving at the surface from the gas, followed by a re-evaporation after a longer or shorter time. From equating the rate of condensation to the rate of evaporation, the equation

$$\frac{x}{m} = \frac{abp}{1 + ap} \qquad \text{(ii)}$$

was obtained, when a and b are constants. Other formulae of a similar

type have also been postulated (3,4).

The amount of gas sorbed is a function of temperature. Except in a few instances, where complicating factors intrude, the amount sorbed at a given pressure is always found to decrease with rise in temperature, which necessarily follows from the fact that the heat of sorption is always positive. The effect of temperature on sorption was first investigated by Miss Homfray (5) and Titoff (6) who found a linear relation between the logarithm of the amount sorbed and the temperature. The magnitude of the temperature coefficient is quite large. With some sorbants and sorbates the mechanism of sorption changes with temperature.

The amount of sorption of different sorbates has been found to be in the order of their boiling points. Heat is always evolved on sorption, the heat of sorption is greater in the earlier stages, falling off as sorption proceeds further. Lamb and Coolidge (7) express the heat for changing amounts of sorption by an expression of the form,

$$q = ax^b \qquad (iii)$$

where a and b are constants, q is the total or integral heat, and x the total volume of vapour sorbed. In all cases the heats of sorption are always greater than the latent heats of vaporization to which many authors have tried to relate them. Attempts also have been made to relate heats of sorption to heats of reactions.

Static sorption studies indicate that sorption occurs very rapidly at first, then decreases rather sharply to approach the equilibrium value, which may take weeks to complete (8) In mixtures of gases a preferential sorption of one or the other is found; the presence of one gas lowers the amount sorbed of the second gas (9).

Mechanisms of Sorption

Sorption on solids is generally classified according to the type of force involved in binding the sorbed atoms or molecules to the surface atoms of the solid. There are two distinct types of sorption, the "molecular" or "van der Waals" type, in which the forces are the van der Waals forces which produce condensation in liquids; and 'chemisorption' defined as co-valent combination of the sorbate with the surface atoms.

In molecular sorption, the heat of sorption is low, the binding to the surface is not very strong, and the sorption is fully reversible, since the gas may be easily pumped off. This sorption may be an actual condensation of liquid into the very small channels and capillaries in the porous solid. In such spaces, the concavity of the meniscus in the fine capillaries produces a lowering of the vapour pressure below that over a plane surface, thus facilitating condensation. This type of sorption is most marked with gases below, or close to, their critical temperatures. The close relation between the ease of liquefaction and the extent of this type of sorption is of course due to the similarity of the forces involved. The molecules of the sorbed gases are not dissociated on the surface. It is also probable that the molecules are more or less mobile in the sorbed layer, and can move along the surface.

Chemisorption involves the actual setting up of co-valent bonds between the sorbate and the sorbant. The heat of sorption for this type is almost three times as great as that for the molecular type. The sorption may be somewhat reversible, but usually a high temperature is necessary to remove all the sorbate. The binding may be so strong that the underlying atoms are torn away upon removal of the sorbed gases. Thus

the adhesion of oxygen to tungsten is very strong, for at high temperatures, the tungsten is removed with the oxygen as the oxide. The chemisorbed layer of atomic oxygen will not react with hydrogen until temperatures are reached where the oxygen begins to evaporate slowly from the surface. The reactivity of the chemisorbed gases may be greatly enhanced giving a catalytic action to the sorbant.

This mechanism predisposes one to expect that the layer of sorbed molecules will not exceed on molecule or atom in thickness since the combining capacity of the surface atoms will probably be satisfied by the presence of a single layer of atoms of gas on the surface.

There are other types of chemisorption which occur due to a chemical reaction on the surface of the sorbant. Some gases are decomposed by hydrolysis by the water sorbed on the surface of the sorbant, e. g. phosgene on charcoal. Decomposition of the sorbate may be catalysed by impregnants in the sorbent. The products of the decomposition might then be sorbed.

Solution in sorbed water may occur. This is not true sorption; but charcoal which has been saturated with water will remove gases from surroundings by solution of the gas in the water. This is also true when amounts less than the saturation value of water are present on the charcoal.

Experimental results have indicated that in many cases, both molecular sorption and chemisorption are operating simultaneously. This is clearly indicated in cases of sorption in which an extremely high temperature coefficient is present. It is also shown in sorptions which increase with temperature.

Taylor (10) suggested that just as an activation energy is necessary to bring about co-valent combination of atoms, so the process of chemisorption requires an activation energy. Thus at very low pressures, sorption takes place by van der Waal sorption due to the small activation it requires. At higher temperatures sorption will take a different form, as chemisorption, since the molecules of the sorbate have now attained the considerable energy of activation required to combine by co-valent forces with the surface. Polanyi (11) also points out that free valencies at a surface would not attract molecules, until these have jumped over a potential barrier.

The preceding discussion has dealt mainly with static sorption systems where the amount of sorption is found by measuring the volume of gas which disappears from the gas when it is brought into contact with the sorbing solid surface. In some cases the weight of the gas sorbed in a sealed system is measured by a microbalance (18). A dynamic sorption can also be studied, with the sorbate in an inert carrier such as air.

Dynamic Sorption

Dynamic sorption studies became important when the respirator was first developed as a defensive weapon. In these studies, a mixture of the sorbate in an inert carrier, such as air, is passed over a charcoal bed. The rate at which the gas is taken up depends upon the rate at which it is supplied. The governing rate factor may be either the actual process of sorption, or the diffusion of the sorbate from the air stream to the surface of the charcoal. Thus the presence of the carrier gas may interfere with the true sorption velocity.

Dynamic studies enable efficiency as well as capacity data to be studied. The sorption should increase linearly with time if the rate

of supply is constant, and should reach a point when the charcoal ceases to be 100% efficient and there is an appearance of gas in the effluent air stream. The time of this occurrence is called the service time or breakdown time. The rate of sorption will decrease at this point until at a further time, there is zero sorption. At this time the amount of sorbate on the charcoal is in equilibrium with the gas stream being passed over it.

Since most investigations have been conducted with the aim of increasing the knowledge of service respirators, they deal mainly with service time. Thus most of the theories of dynamic sorption have tried to predict service time and to explain its variation with other factors.

Theories of Dynamic Sorption

There are two main treatments of the data obtained from, and the mechanism involved in, the dynamic sorption on charcoal. Mecklenberg (12, 13) made the assumptions that the sorption was a condensation of the toxic gas in the capillaries of the charcoal and that the velocity was that of a heterogeneous reaction, and thus the Nernst equation could be used. With these assumptions he derived equations for all the quantities concerned in dynamic sorption. Danby, Davoud, Everett, Hinshelwood, and Lodge in England, later developed their mechanism from purely theoretical considerations and gave mathematical expression to all the measurable quantities.

Theory of Danby et al

This theory was treated first in a simple form which gave fair agreement with experiment, then in a detailed form involving the solution of a partial differential equation.

The simple theory makes assumptions that are not by any means fulfilled in practice. It assumes that the interaction rate will follow the equation for a reaction of the first order which assumption is likely to be closely fulfilled. It assumes further that each successive element of charcoal functions with complete efficiency for a certain time and then passes completely out of action, an assumption which cannot be more than approximately fulfilled.

The concentration, then, is stated to decrease exponentially with length of bed travelled, and to increase exponentially with time, viz.

$$c = c_0 e^{\frac{-kl}{L}} e^{\frac{kbt}{L}} \qquad \text{(iv)}$$

where K is a measure of the rate of sorption reaction, L is the linear flowrate, b is the rate of exhaustion, c is the initial concentration of the sorbate in the gas stream and c_0 the concentration of the gas after passing through a length l of the charcoal bed, and T is time from the start of the gas flow.

From this they obtained an equation for the service time T

$$T = \frac{N_0}{c_0 L} \quad (\lambda - \lambda c) \qquad \text{(v)}$$

where N_0 is the initial number of active centres per cc. of charcoal, λ is the total length of the charcoal bed, and λc the 'critical length'. The critical length is defined as a length of charcoal bed below which there would be immediate breakdown. Above this length there would be a linear relation between the service time and the bed length.

When the flow rate is varied, the column length being kept constant, a corresponding relation appears

$$T' = \frac{\lambda N_0}{c_0} \left[\frac{1}{L} - \frac{1}{Lc} \right] \qquad \text{(vi)}$$

where L_c is critical flowrate above which breakdown is instantaneous.

In the more detailed theory, the assumption that saturation is rapid and complete is removed, and it is considered that the saturation of the charcoal column is gradual. The fundamental equation for the removal of a gas in a sorbing column is given as

$$-\frac{\partial c}{\partial l} = \frac{1}{L}\left[\frac{\partial x}{\partial \tau} + \frac{\partial c}{\partial \tau}\right] \qquad \text{(vii)}$$

and is independent of any assumptions as to the mechanism of the removal. $\partial c/\partial l$ is the rate of concentration change of gas in the air stream with length, $\partial c/\partial t$ the rate of sorption of the gas by the charcoal with time. It was then assumed that the rate of removal of the gas is proportional both to the concentration of gas in the air stream, c, and to the concentration of active centres N per cc. of charcoal. This gave

$$\frac{\partial x}{\partial \tau} = kcN \qquad \text{(viii)}$$

It was also assumed that, on an average, each active centre deals with n molecules of gas before becoming inactive. Thus if the actual number of active centres per cc. is N_o', then they are treated as $n N_o' = N_o$ active centres of unit activity. One centre of unit activity was assumed destroyed each time a molecule of gas was sorbed. The assumption is made too that the heat of reaction or of sorption is conducted away immediately.

Substituting equation (viii) in equation (vii) and solving yields equations for critical length and service time:

$$\lambda_c = \frac{L}{N_o k} \ln \; c_o / c' \qquad \text{(ix)}$$

where c' is the concentration of the emerging gas at breakdown time,

and

$$T' = \frac{1}{kc_o}\left[\ln\left(e^{kN_o\lambda/L} - 1\right) - \ln\left(c_o/c - 1\right)\right] \qquad (x)$$

From this latter equation is obtained the relations

$$T' = \frac{N_o}{c_o L}\left(\lambda - \lambda_c\right) \qquad (xi)$$

$$T' = \frac{N_o \lambda}{c_o}\left[\frac{1}{L} - \frac{1}{L_c}\right] \qquad (xii)$$

and

$$T' = \frac{1}{kc_o}\left[\frac{kN_o\lambda}{L} - \ln\frac{c_o}{c'}\right. \qquad (xiii)$$

These predict that the service time will vary:

(a) with the specific properties of the charcoal, as with k and N ,

(b) linearly with the column length λ,

(c) linearly with the reciprocal of the flow rate L, but at flow rates greater than L_c, the breakdown time is zero,

(d) with the reciprocal of the initial concentration c_o when c_o is sufficiently small.

The critical length λ_c should vary with the logarithm of the initial concentration, c_o.

The experimental data presented show that for carbon tetrachloride, nitrous fumes, arsine, and hydrogen sulphide, the service time relations agree with those predicted.

A consideration of the simple theory indicates that the concentration of the sorbing gas should fall off exponentially with the length of the charcoal bed, since

$$c = c_o e^{\frac{-kl}{L}} e^{\frac{kbT}{L}} \qquad (iv)$$

At various times, t_1, t_2, etc. the gradients would be as those shown in figure 1 where concentration is plotted against column length. A similar figure would be obtained for the amount of sorption along the bed. c' here is the concentration at breakdown time, λ_c, the critical length. The concentration gradients from the detailed theory would be formed according to the relation

$$C = \frac{C_o}{e^{-kc_oT}\left(e^{kN_o l/L} - 1\right) + 1} \qquad (XIV)$$

The gradients are shown in figure 2 for various times. The gradient changes shapefrom an exponential curve as shown at T_1 to an inflected curve at T_4. Hereafter the curves are similar and move along the bed at a constant rate. The service time is shown in both these figures as the point where the concentration at length λ reaches c', i. e. the first detectable trace of gas.

2. The Mecklenberg Theory.

Mecklenberg visualized the charcoal bed, after gas had been passing for some time, as divided into three parts:

(a) a length next to the front surface saturated with gas,

(b) a "working" length in which the sorption process was taking place,

(c) a length not yet reached by the gas.

He considered the "working" length and assumed that the gas was being sorbed by condensation in the capillaries of the charcoal. He further assumed that he was dealing with a "mathematical" charcoal, i. e. one that had all the capillaries equal to one another and of constant cross-section; and that the gas diffused out of the air stream to the outer surface of the charcoal with a velocity similar to that given by Nernst for a heterogeneous

FIGURE 1.

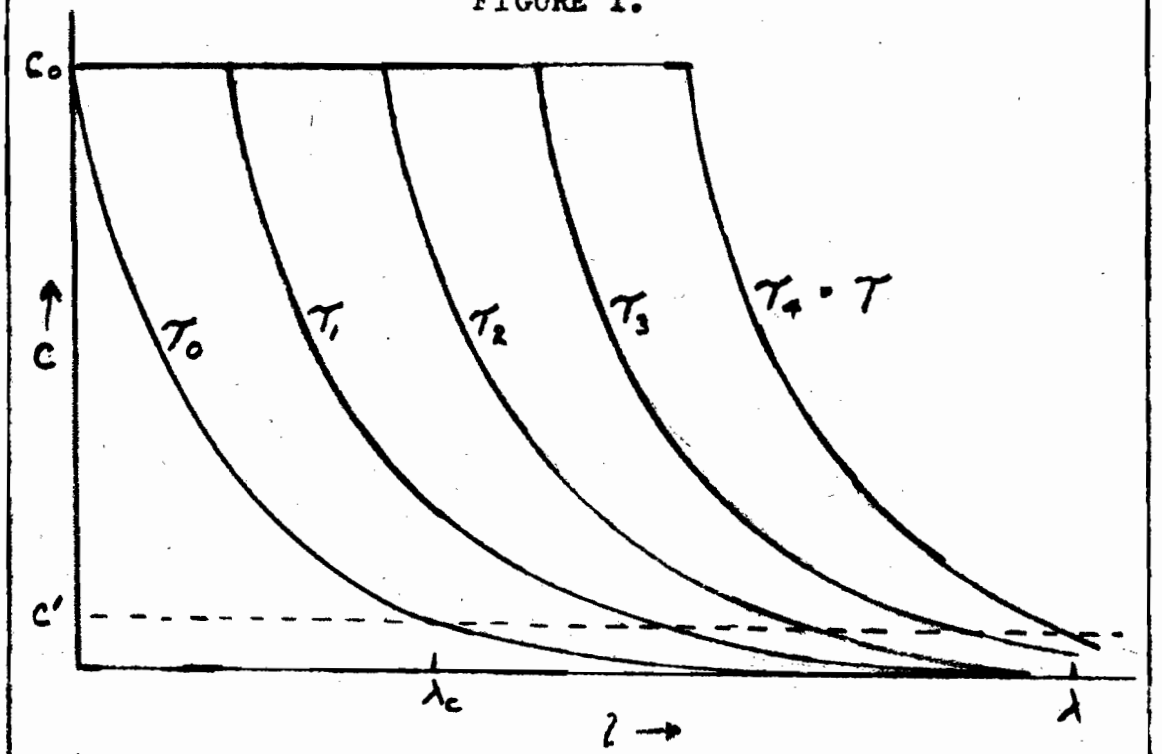

FIGURE 2.

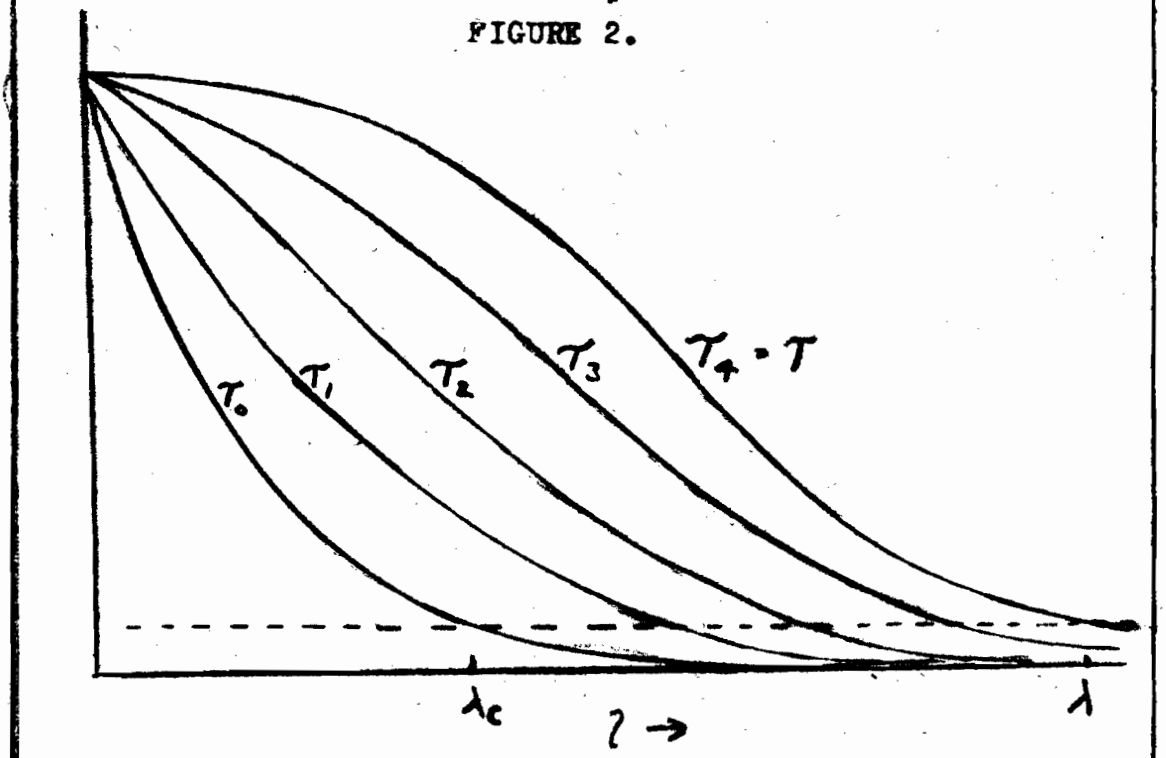

CONCENTRATION OF TOXIC GAS AT DIFFERENT DISTANCES ALONG THE COLUMN.
(a) Simple Theory
(b) More Detailed Theory

reaction:

$$- \frac{dC}{dt} = \frac{DF(C - C^1)}{\delta} \qquad \text{(xv)}$$

where C is the partial pressure of the toxic gas in the air outside the charcoal capillaries, C^1 is the vapour pressure of the gas inside the capillaries, D is the diffusion coefficient of the gas in air, F is the outer surface of the charcoal grains per cc. exposed for the diffusion, δ is the thickness of the gas layer sorbed on the charcoal grains and t is the time.

He derived the following equations for the service time T^1 and the dead length h.

$$T^1 = \frac{kQ}{v\, c_o} (L - h) \qquad \text{(xvi)}$$

and

$$h = \frac{\delta}{DF} \cdot \left(\frac{KQ}{v}\right)^{n-1} \left(\ln \frac{c_o - c'}{c_x - c'} - \frac{c_o}{c_o c'} \right) \qquad \text{(xvii)}$$

where k is the maximum amount of gas sorbed by the charcoal, is the linear velocity of the air stream over the charcoal, L and Q the length and cross-section of the charcoal bed, respectively, KQ is that portion of the cross-section of the cell not actually filled with charcoal, c_x the minimum detectable concentration of the gas, and n is a constant.

From equation (xvii) Mecklenberg was able to predict that the dead length, h was:

(a) inversely proportional to the square root of the cross-section Q,

(b) directly proportional to the square root of the velocity since n is usually about 0.5,

(c) directly proportional to the diameter of a single charcoal grain, and

(d) directly proportional to the logarithm of the initial concentration, c_o.

Mecklenberg confirmed the last two predictions by experiment. The first two predictions were confirmed by Engel (15).

Shilow, Lepin and Wosnessensky (16) studied the sorption of chlorine from air streams on different types of charcoal. Their apparatus enabled them to determine the service time of, and the amount of chlorine sorbed in, different sections of a cell. They attempted to dfine dead length by two constants,

$$h = \frac{\tau'}{\theta} \qquad \text{(xviii)}$$

where τ' is the initial loss of time of protective action and is the coefficient of protective action. This coefficient is given as

$$\theta = \frac{T}{L} = \frac{\text{service time}}{\text{bed depth}} \qquad \text{(xix)}$$

They found that for chlorine concentrations varying from 0.66% to 1.36%, the equation

$$c_o \times T = \text{Constant} \qquad \text{(xx)}$$

was valid.

Mecklenberg (13) applied their data to his equation for service time as a function of:

(a) the diameter and length of charcoal bed,

(b) the velocity and initial concentration of the gas stream,

(c) the capacity and specific surface of the charcoal, and,

(d) the vapour pressure of the sorbate in the capillaries of the charcoal.

The equation was confirmed by these data.

Dubinin, Parshin and Pupuirov (17) in an investigation of short charcoal beds found that there was some protective action even with bed lengths shorter than the dead length. They concluded that dead length was purely a mathematical fiction and that it had no physical significance.

Mecklenberg pointed out that at the beginning of a run, there would be no liquid in the capillaries of the charcoal and in consequence, the term c'of his equation would be zero, which would modify his equation to

$$h = \frac{\delta}{DF}\left(\frac{KQ}{v}\right)^{n-1}\left(\ln\frac{c_o}{c_x} - 1\right) \qquad \text{(xxi)}$$

As the gas is sorbed, c' would increase gradually to its maximum value C_o. Thus the curve of the service time - bed length plot would be linear over most of its length, but at some point it would curve in towards the origin and cut the axis at a point closer to the origin than the dead length obtained by extrapolationof the straight portion of the curve. Mecklenberg determined such a curve for chloropicrin.

Shilow et al (16) from a consideration of their results, constructed a series of gradients, at different times, along the charcoal bed. Their diagram is shown in figure 3. They indicate that the shapes of the curves representing the early stages of sorption such as OQ, OR differs from those at later stages of sorption as OA, OB, etc. The curve OD represents the final shape of the concentration gradient. They noted that the curves at all stages of the initial sorption started from the point O, which represented the initial concentration of the gas stream. They point out that the areas OPQ, OQR, etc. increased until the area OCD was reached and then this remained constant. They also state that after this building up period, the velocity of the gradient through the bed becomes constant.

From equation (xvii) Mecklenberg derived an expression for the decrease in the concentration of the gas in the air stream in the charcoal bed.

$$c = c_o e^{-\frac{DF}{\delta}\left(\frac{v}{KQ}\right)^{n-1} s} + c' \qquad \text{(xxii)}$$

where s is the distance along the bed. This exponential curve is shown in figure 4 by CDB. The curve according to this equation should always be similar to the initial curve, that is exponential at all points and the charcoal bed up to C′ should be saturated.

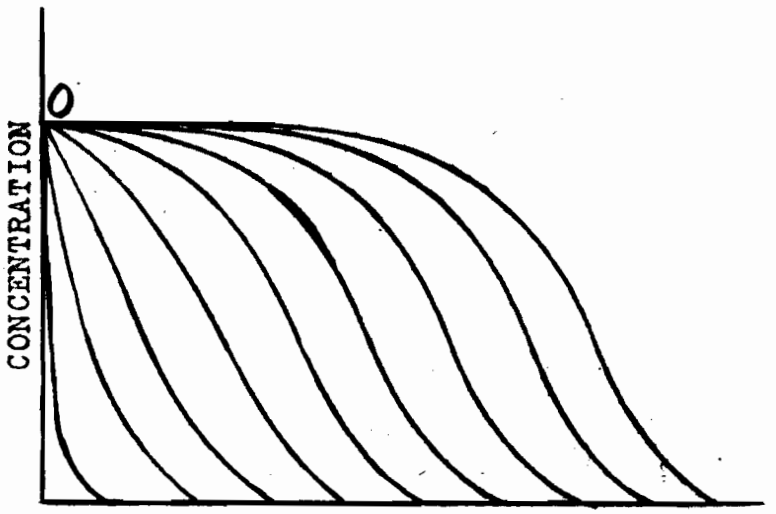

GAS PHASE GRADIENTS (SHILOW)

FIGURE 3.

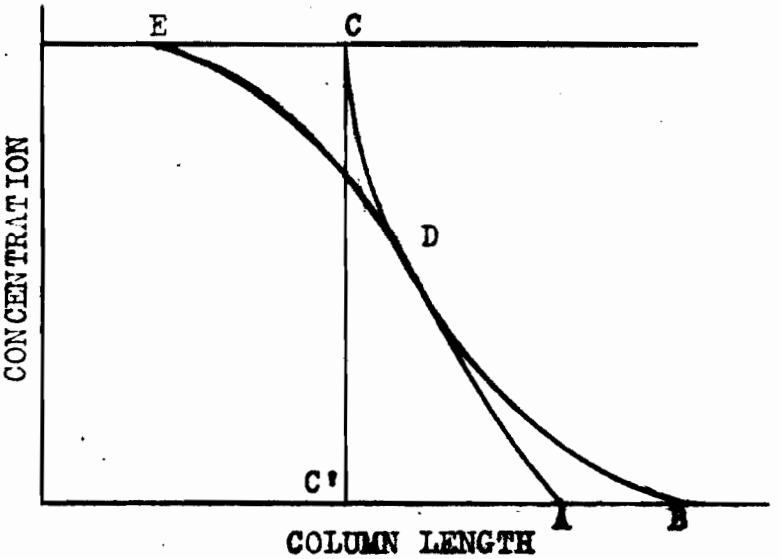

"MATHEMATICAL" (CDF) AND ACTUAL (EDA) CONCENTRATION GRADIENTS (MECKLENBERG)

FIGURE 4.

The actual gradient is of the shape EDA which Mecklenberg explains in the following way. He points out that in the derivation of equation (xxii) a "mathematical" charcoal was assumed which possessed capillaries of uniform and constant cross-section, and that Nernst's diffusion law was assumed to hold for the diffusion of the gas from the air stream to the charcoal surface. An actual charcoal has capillaries that vary in size and in shape. The smaller capillaries cause a shortening in the bottom part of the gradient from DB to DA. The upper part of the curve is explained by him as due to the presence of larger capillaries which are assumed not to fill as rapidly as the remainder and are not filled as equation (xxii) requires. Thus the curve is displaced into the form EDA. In addition he states that the outside capillaries would fill up rapidly, according to equation (xxii) but that the sorbate in the outside capillaries would slowly migrate into the inner capillaries. This migration is slower than the outer sorption so that after the initial rapid condensation there follows a slow condensation which also acts to displace the curve from CD to ED. Only in the mid part of the concentration gradient does the equation hold.

Mecklenberg considered the process of sorption of a gas to consist of two parts.

(a) The first period is building up of the sorption gradient or working layer to its constant shape. He defined the working layer as the length of charcoal bed long enough to reduce the concentration of the effluent gas to its"threshold" value, that is the limiting concentration, below which the presence of the gas in the air can no longer be detected by the detection reaction used in the experiment.

(b) The second part is the movement of this gradient, once it is built up, through the charcoal bed with a constant linear velocity.

The general process of sorption which he pictures is as follows. A charcoal bed of length l is considered, into which a gas-air mixture is entering. Consider the air stream and the bed as split up into differential layers perpendicular to their longitudinal axis. In the case of the air stream, the layers are indicated by 1, 2, 3 etc, the charcoal layers are designated as a, b, c etc. The air stream layer 1 is considered first. In passing through charcoal layer a, the air stream 1 will give up a part of its gas; a further part of the gas is given up to layer b, c, d, etc. Finally, as a result of these removals, the concentration of the gas falls off to the threshold value at charcoal layer s_1. Exactly the same process is repeated with the layers 2, 3, 4..... of the air stream, only using the charcoal layers s_2, s_3, s_4.....This does not occur at a similar relative distance along the axis as s_1 because the stream has had to pass over partially saturated charcoal. As the process continues, each particular layer of charcoal will take up less and less gas from each successive differential amount of air that passes over it. Finally, at some time t_x, when a differential amount of air, x, enters the bed, layer a becomes saturated and the sorption gradient has reached its full length and extends through the bed to some layer s_x. The bed length to layer s_x is thus the working layer. The next differential amount of air will saturate layer b and the gradient will extend one layer past s_x. The gradient then moves through the bed with a constant velocity.

For the first differential amount of air the front trace of gas has moved through the charcoal bed from the front surface to a point s, during the differential time interval. When the second differential amount of air enters, the front trace of gas moves a distance s_2-s_1 in an equal time

interval. When the gas reaches s_1, its concentration has been considerably lowered in passing over the partially saturated charcoal of the section to s_1 so that the distance $s_2 - s_1$ must be shorter than the length s_1. Similarly the distance travelled by the third amount of air $s_3 - s_2$ is less than $s_2 - s_1$. Thus the front trace of gas moves through the charcoal with a constantly decreasing velocity, reaching a constant minimum velocity when layer a becomes saturated. Shilow et al confirmed this behaviour with chlorine at a concentration of 2.13%.

Comparison and Experimental Proof of these Theories.

Evidence in favour of these theories is found in the investigations of many workers. The variation of sorption data such as service time, dead length and sorption capacity with the various independent factors has been investigated and a comparison of the results with the predicted relations is given.

1. The service time. The theories of Mecklenberg and of Danby et al predict the following variations:

(a) Variation with bed length. Both theories predict a linear relation. Mecklenberg further predicted that the linear relation failed at shorter bed lengths, curving towards the origin. This behaviour of the service time bed length curve has been noted by many authors. Shilow et al and Dubinin et al show this for chlorine; Danby et al for hydrogen sulphide, carbon tetrachloride, nitrous fumes and arsine; Mecklenberg for chloropicrin; Ismailov and Sigalovskaya (18) for the vapours of benzene, n-heptane, phenol, naphthalene and carbon disulphide; and Ruff (19) for solutions of acetic acid and phenol in water.

Dubinin (17,20) expressed service time in a different form,

$$T = \phi L - \tau \qquad \text{(xxiii)}$$

where ϕ is the coefficient of protective action, L the bed depth, and τ the protective time loss due to the very rapid penetration of the gas at the start of the run. The relation of this and the equation

$$h = \frac{\tau}{\delta} \qquad \text{(xviii)}$$

as deduced by Shilow et al, which includes τ the initial loss of time of protective action, and δ the coefficient of protective action, is seen more clearly by consideration of figure 5. The coefficient of protective action is the slope of the linear portion of the service time - bed length curve, and the protective time loss is the intercept of the extrapolation linear relation on the negative service time axis.

(b) Variation with flow rate. Both theories predict a linear relation between the service time and the reciprocal of the flow rate. Danby et al show good agreement with this relation with the gases tested. The critical flow rate which they postulate however has not been verified experimentally.

(c) Variation with the cross-section of the bed. Mecklenberg equation (xvi) indicates a direct linear relation which his experiments verify.

(d) Variations with the physical constants of the charcoal. Danby et al and Mecklenberg both predict a linear variation of the service time with the diameter of the charcoal grains. This has been confirmed by the experiemntal findings of both.

(e) Variation with initial concentration. Danby et al predicted that the service time will vary as the reciprocal of the initial concentration for very low initial concentrations. They found this relation to hold quite well for carboh tetrachloride, hydrogen sulphide, nitrous fumes and arsine up to concnetrations of 1%. Shilow et al also predict this and show a linear relation for chlorine in concentrations from 0.66 to 1.36%.

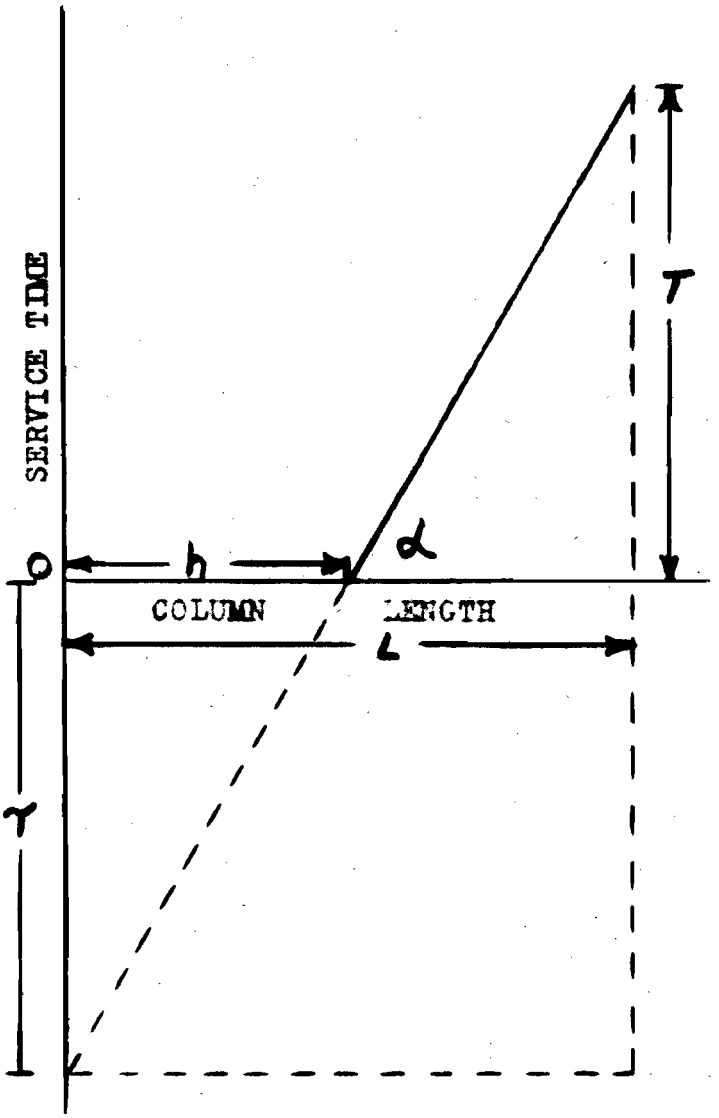
SERVICE TIME
T
h
α
COLUMN
LENGTH
L
γ
COEFFICIENT OF PROTECTIVE ACTION

FIGURE 5.

2. The dead length. This has been previously mentioned as a means of measuring the residual activity of the charcoal at the service time. Mecklenberg has shown that the true dead length is shorter than that originally taken. The original dead length,h, is really a mathematical fiction which enables one to predict the service time over the linear portion of the service time bed length curve.

Allmand (21) has developed an equation for the dead length,

$$h = \frac{Q - \ln Y_B}{K_o} \left(\frac{V}{A} \right)^{1/2} d \qquad \text{(xxiv)}$$

where Q is a coefficient perculiar to charcoal and vapour, Y_B the fraction of the entering concentration of the vapour transmitted at service time, V the volume of air flow per unit time, A the cross-section of the charcoal bed, d the average diameter of a charcoal granule, and K_o a constant which is equal to $(1/T)^{1/2}$. The relations that this equation predicts are identical with those predicted by Mecklenberg from equation (xvii).

(a) Variation with cell and charcoal characteristics. The dead length has been predicted to vary with the reciprocal of the cross-sectional area of the charcoal bed and directly with the diameter of the charcoal granules. Mecklenberg (13) and Engel (15) have confirmed these relations using chloropicrin.

(b) Variation with flow rate. Mecklenberg from equation (xvii) predicted that

$$h = \text{const.} v^{(1-n)}$$

where n is a constant which is usually about 0.5. Thus the dead length should vary with the square root of the linear velocity. From equation (ix) of the theory of Danby et al, the critical length should vary directly

as the flow rate. Engel has confirmed its dependence on the square root of the flow rate.

(c) Variation with initial concentration. Both theories from equations (ix) and (xvii) predict a linear relation between the dead length and the logarithm of the initial concentration. This was confirmed by experiments on chloropicrin and on chlorine by Shilow et al.

3. Sorption Capacity. In static systems the sorption capacity of a given charcoal depends on the molecular weight and boiling points of the sorbing gas. Engel noted that this is true for dynamic systems.

In dynamic systems, most of the work has dealt with the service time of the charcoal and few investigators have determined the total sorbing capacity of the charcoal. The volume activity of a charcoal has been used, however, as an indication of its protective power. It is measured by sorbing carbon tetrachloride under the given experimental conditions until it is detected in the effluent stream.

$$\text{Volume activity} = \frac{\text{Increase in weight of the charcoal}}{\text{volume of charcoal}} \times 100$$

In the theory of Danby et al the dynamic sorption of gases, the sorptive capacity of the charcoal is expressed in terms of a capacity constant, N_o, the number of active centres each of which is capable of removing one molecule of sorbate, and a rate constant K which determines the rate of removal of the sorbate from the gas stream. These are assumed in the theory to be independent of factors such as initial concentration, flow rate etc.

In Mecklenberg's service time equation

$$T' = \frac{kQ}{vC_o}(L - h) \qquad \text{(xvi)}$$

k is the maximum amount of sorbate which the charcoal is capable of taking

up under the experimental conditions. He investigated its dependence on the initial concentration of sorbate, chlorine, and found that it followed the Freundlich isotherm,

$$k = ac_o^{\,b} \qquad \text{(xxv)}$$

where a and b are constants; for chlorine a = 8.38 and b = 0.164.

Ruff found that the Freundlich isotherm was followed for liquids in aqueous solution.

Syrkin and Kondraschow (22) in an investigation of the dynamic sorption of organic vapours found that the amount sorbed by the whole bed was related to time by the equation:

$$\log \frac{A}{A - c} = 0.434KT \qquad \text{(xxvi)}$$

where A is the maximum sorption, c the amount sorbed in time, T, and K a constant. K was found to vary with temperature according to the formula

$$\tau = \frac{K_{T_2}}{K_{T_1}}^{\frac{10}{T_2 - T_1}} \qquad \text{(xxvii)}$$

The following experiments were done to obtain numerical data for the sorption of butane and ammonia on charcoal under various conditions, and to test further the relations derived by the various authors cited above.

EXPERIMENTAL

Apparatus

The apparatus used in these investigations consisted essentially of a charcoal cell mounted on one arm of an analytical balance, to permit the sorption to be followed by weight as a function of time. Provision was made for measuring the mixture of air and sorbate admitted to, and for sampling and analysis of the effluent gas stream from the cell. This type of apparatus was first described by Pearce (1) and was used here with minor modifications.

A detailed description of the apparatus may be simplified by considering separately the following systems: air purifying, sorbate, charcoal conditioner, the sorption cell, the effluent gas stream, and the analysis.

Figure 6 shows the apparatus diagrammatically.

Air was introduced from a compressed air line to a 45 litre ballast volume V_1 (figure 6). This ballast volume eliminated the small pressure variations which occurred in the line. Since carbon dioxide is appreciably sorbed by charcoal, it was removed from the air stream by passing it through three soda-lime tubes, B, connected in series. Water vapour was also removed, using four calcium chloride drying tubes, A, three anhydrous phosphorous pentoxide tubes (which were in effect the soda-line tubes, the latter material being used to prevent plugging of the tubes), and three sulphuric acid bubblers, C, in series. This system could be used to obtain air of any desired humidity by adjusting the concentration of the acid in the bubblers. The present study was confined to the use of dry air, hence concentrated sulphuric acid was used. The rate of air flow was measured with a rotary wet test meter, D, filled with butylphthallate, inserted in the line

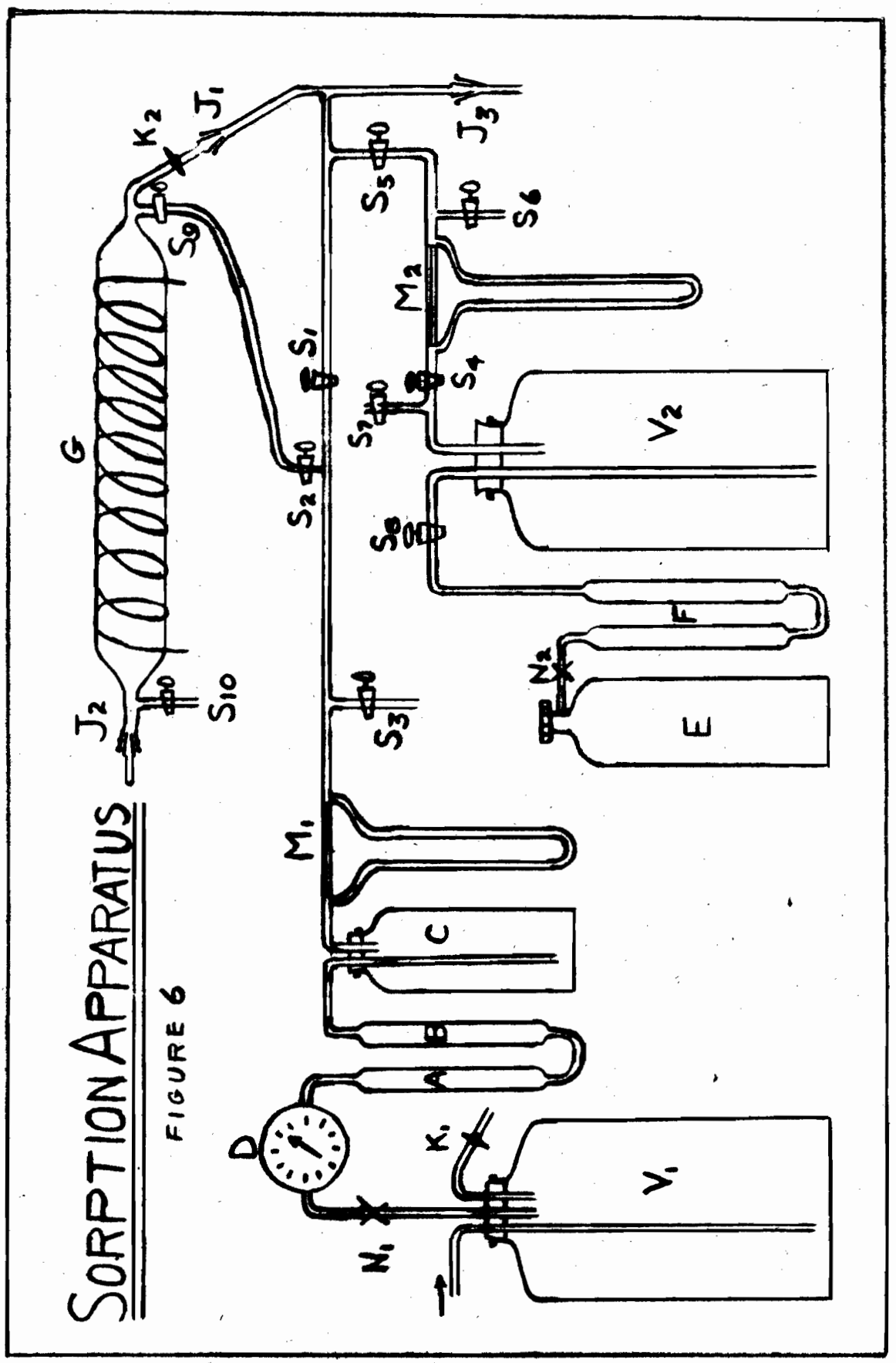
SORPTION APPARATUS
FIGURE 6
G
J2
S10
J1
K2
S9
S8
S1
S2
S3
S4
S5
S6
J3
M1
M2
A
B
C
D
K1
N1
V1
V2
E
F
N2

between the ballast volume and the soda-lime tubes. Setting of the flow rate was facilitated by a calibrated capillary flowmeter, M_1, of the usual type. Butyl phthallate was used as the manometer fluid. Regulation of flow was accomplished by a blow off valve, K_1, which consisted of a screw clamp on a short length of rubber tubing, for rough adjustment, and a metal needle valve, N_1, for finer control. The air could be admitted to the cell, to the conditioner, or to a fume hood as desired, by suitable adjustment of stopcocks, S_1 and S_2 and S_3.

The sorbate was admitted directly from the storage cylinder E. It was dried by passing it through four calcium chloride drying tubes, F, in series. After passing through the 50 litre ballast volume, V_2, the sorbate entered the air stream through the stopcock S_4. Rough regulation of the flow rate was obtained by a scratch on the stopcock, while finer control was accomplished by adjusting the needle value, N_2, on the cylinder. The flow rate was measured by the calibrated capillary flowmeter, M_2, containing butyl phthallate as the manometer fluid. Stopcocks, S_5 and S_6, allowed the sorbate stream to be admitted to the air stream or diverted to a fume hood. The whole sorbate system could be evavuated through stopcock S_7.

The charcoal was conditioned in a stream of dry, carbon-dioxide-free air in the conditioner G, which was constructed from a pyrex tube about a foot long and two inches in diameter. It was heated electrically, and insulated with asbestos. A slide wire rheostat, regulating the current, permitted the temperature to be controlled. The conditioner was mounted above the cell and at a slope of about thirty degrees with the horizontal. The ground joint J_1 allowed the conditioner to be removed for refilling, which was done through the ground joint J_2 at the upper end. The air stream for conditioning entered through the stopcock S_9, and was allowed to escape through the stop-

cock S_{10} on the upper end. The conditioner was connected to the ground joint J_1 by a short length of rubber tubing fitted with a screw clamp K_2.

The charcoal was allowed to fall into the cell from the conditioner, by opening the screw clamp K_2 and gently tapping the conditioner. Since the charcoal always fell from a constant height, the packing of the granules in the cell was constant, as shown by the fact that reproducibility of results was readily obtained. No moisture or carbon dioxide could contaminate the conditioned charcoal, since it only came into contact with dry, carbon-dioxide-free air, after being conditioned.

The charcoal cell (figure 7a) consisted of a piece of glass tubing 4 cm. inside diameter and 21 cm. long. A brass cap was fitted over the top and sealed to the glass with de Khotinsky cement. A section of thin brass tubing 1.5 cm. in diameter and 7 cm. long was soldered through the centre of the cap and extended down into the cell. A brass ring about a quarter of an inch wide, with small projections on each side was sealed around the outside of the cell at the bottom. A detachable brass cap, similar to the one at the top was machined to fit snugly around the brass ring, and could be drawn against the bottom of the ring to form an air-tight seal by oblique slots operating over the projections on the ring. A length of brass tubing extended downward from the centre of the brass cap.

The charcoal was supported on a circular disc of metal gauze of the type generally used in respirators. To allow the air to flow freely out of the cell, this gauze disc rested on a ring of glass tubing about half an inch in height. The cell was marked off in centimeters so that the depth of charcoal in the cell could be varied from one to five centimeters. Two thermocouples, T_1 and T_2 were inserted into the cell through the bottom, the positions of the junctions being altered as desired. The thermocouple wires were copper

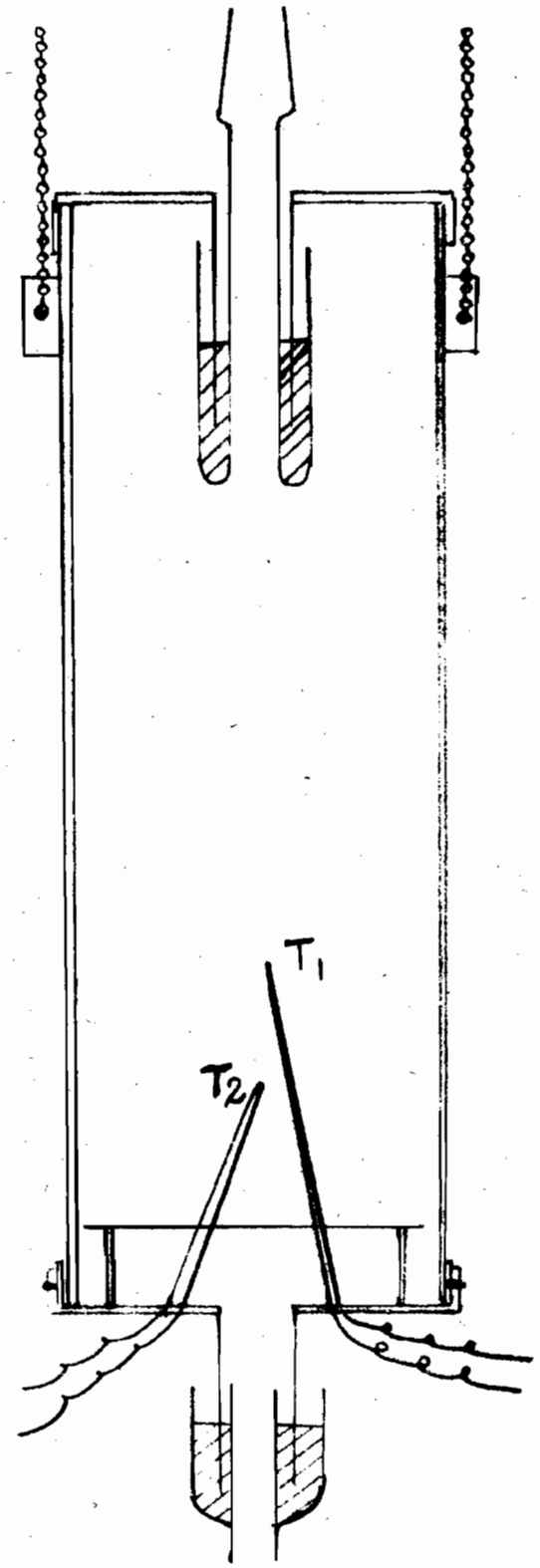

FIG. 7 A

FIGURE 7
CHARCOAL CELLS

and constantan B and S gauge number 28. They were coiled loosely outside the cell, so as not to interfere with the weighing, and connected to fixed binding posts. Temperatures were measured on a Cambridge unipivot millivoltmeter with a thermal scale.

The cell was suspended by two light chains from one arm of an analytical balance adapted for this purpose. To allow the cell to move freely and to prevent escape of any gases from the cell, the brass tubes dipped into cups containing butyl phthallate. These cups were attached to the inlet line at the top by a ground joint J_3 and to the outlet line at the bottom. The weight of the empty cell assembly was about 200 grams.

When greater accuracy in the weight of the amount of gas sorbed was desired, and where equilibrium weights were sufficient, a modified cell was used, (figure 7b). This was made from pyrex tubing, 4 cm. in diameter and 8 cm. long, fitted with ground joints at either end. The charcoal rested on a piece of gauze as in the previous cell. This cell could replace the former, being connected to the air line by the ground joint J_3. Weight could not be followed as a function of time with this, but it could be removed when sufficient time had been allowed for equilibrium, sealed with ground joint caps, and weighed accurately on an analytical balance.

The gas stream leaving the bottom of the cell (hereafter called the effluent stream) passed through one arm of a T tube to the fume hood. A short length of glass tubing to contain test papers was inserted in the exit line. To sample the effluent stream, evacuated pipettes were connected to the other arm of the T tube by a capillary tube. The bore of the capillary tube was such that the bulbs filled at a rate less than the rate of gas flow from the cell.

The analysis of the effluent stream was carried out in the apparatus

shown diagrammatically in figure 8. The sample pipette H was supported at an angle of about thirty degrees and the gases were displaced from the bulb with mercury from reservoir L.

For butane analysis, the gases from the bulb, after mixing with dry, carbon-dioxide-free air were passed through a quartz tube, Q, about three feet long and 1/4 inch in diameter. This quartz tube was heated for about one foot of its length in an electric furnace, P, to a temperature of 1000° C. A rheostat and an ammeter were used to maintain the temperature. The carbon dioxide formed during the combustion was absorbed in standard sodium hydroxide solution in the absorption tube R. For efficient absorption a sintered disc bubbler, U, of the type shown in the figure was used, and a few drops of butyl alcohol added to reduce the surface tension of the solution so that a fine foam was obtained. The oxygen stream which was purified by passing through a soda-lime tube, W, was regulated to give about three inches of foam. Standard hydrochloric acid was used to titrate the excess sodium hydroxide using phenalphthalein as the indicator. For dilute gases 1/10 normal standard solutions were used while for more concentrated gases, 1/2 normal solutions were used.

For ammonia, the apparatus used was slightly different. The ammonia mixture displaced from the bulb was absorbed directly in standard sulphuric acid after mixing with carbon-dioxide-free air stream to obtain the necessary degree of foaming in the absorbing liquid. Standard sodium hydroxide was used to titrate the excess acid, using a solution of methyl red and brom-cresol green as indicator.

Procedure

Details of the experimental technique will be much clearer if the procedure of a typical experiment is described and the results recorded.

The charcoal was dried in the conditioner for twelve hours at 150° C in a stream of dry carbon-dioxide-free air, and allowed to come to equilibrium

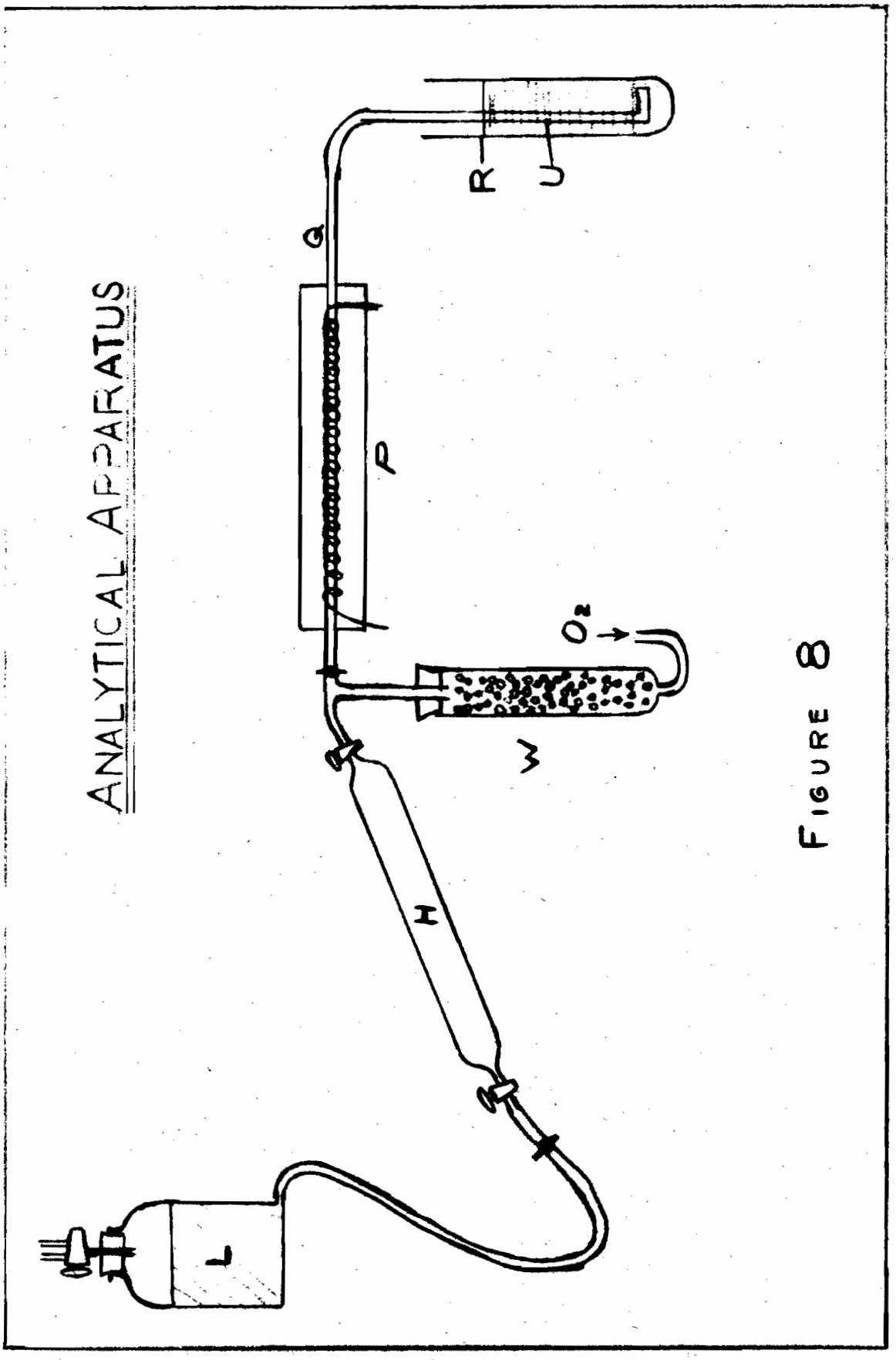

FIGURE 8

with the air of the desired moisture content at room temperature for a further twleve hours.

Since sorption is very dependent on the temperature of the charcoal, it was important that room temperature be kept reasonably constant for all runs. Before and during all experiments, room temperature was set and held at $22.5^{\circ} - 0.5^{\circ}$ C. Variations in atmospheric pressure appeared to have little effect on the amount of sorption.

The cell was thoroughly flushed out using the dry carbon-dioxide-free air. The air stream was then diverted through the stopcock S_3 while the weight of the empty cell was determined. Care was taken to have the cell swinging freely in the liquid seals. Charcoal was then admitted to the cell to the desired depth and its weight determined, without air passing through the cell. Dry air was passed through the cell, and regulated to the desired flow rate, using the blow off valve K_1 and the needle valve N_1. With the air stream being diverted through S_3, the sorbate stream was then regulated to the desired value using the scratched stopcock S_4 and the needle valve N_2. At the beginning of the experiment the flow was set by adjustment of the scratched stopcock and regulated thereafter by the needle valve, which was found to give finer control. The zero weight of the charcoal cell was next found with the air stream passing through the bed. The zero thermocouple readings were also taken. When conditions were steady, the sorbate was directed into the air stream, a stop-watch started, and the initial reading on the wet-test meter taken. Thereafter, weight and temperature readings were taken at two minute intervals. Samples of the effluent stream were taken at appropriate intervals, the first being taken shortly after the beginning of the experiment, the second immediately after the bottom thermocouple reading had reached its maximum value, and the others at regular

intervals until the end of the experiment. The time between samples was determined by the sorbate and air flow rates and the depth of the charcoal bed.

The atmospheric pressure, room temperature, and the temperature and pressure of the air stream in the wet test meter was read when convenient.

When the charcoal was no longer absorbing, as indicated by constant weight readings for a period of at least fifteen minutes, and by the thermocouple readings having returned to their original values, a final sample of the effluent stream was taken. The final air meter reading and time were determined. Both the air and sorbate streams were diverted to the fume hood, and the final static weight of the cell, charcoal and sorbate determined. The net weight of the gas sorbed as indicated by the difference between the initial and final static weights and the zero and final weights with the air stream passing through the cell should check.

For analysis the bulbs were connected in the analytical apparatus (figure 8) and the gases displaced as described previously. About five minutes was allowed for the displacement to ensure complete combustion and absorption. The percent sorbate in the effluent gas was determined by titration of the excess absorption solution.

The accuracy attained in the analysis of the sample bulbs was about $\pm$ 5% due to variations in the sorbate and air flow rate. The analytical method was quite accurate, duplicate prepared samples agreeing to within 1%. One part in 10,000 of sorbate in air could be detected. Weight readings were accurate to about $\pm$ 0.005 of a gram.

Moisture and carbon dioxide determinations on the air stream showed that it contained undetectable amounts of carbon dioxide (less than

1:10000) and less than 0.004% moisture.

A sample data sheet is shown here.

6/2/42

Run 84

Air: 2.6 (3 l./min) Butane: 30.0 (24 c.c/ min)

Room Temp. 23°C Atm. Pressure 759 mm. Hg.

Height of charcoal bed	4 cms.
Weight of charcoal plus cell	31.38 gms.
Weight of cell	3.59
Weight of charcoal	27.79
Final weight	35.34
Butane sorbed	3.96

Air meter

Temperature 23°C Pressure 3.70 Hg.

Initial meter rdg 48.556
Final " " 60.427
11.871 cu ft. Time 114 mins.

$$\text{Air rate} = \frac{11.871}{114} \times 28.3 \times \frac{273}{296} \times \frac{853}{760} = 3.045 \text{ l./min.}$$

* Time	Weight	T_1	T_2	W
0	32.02	24.0	24.0	
2	32.11	27.0	24.0	0.09
6	32.33	31.0	28.0	0.30
10	32.53	32.0	29.5	0.51
18	32.99	33.5	31.5	0.97
34	33.93	30.5	34.0	1.91
50	34.87	26.5	31.0	2.85
70	35.71	23.5	26.0	3.69
90	35.96	23.0	23.5	3.94
110	35.98	23.0	23.0	3.96

* Analysis

Bulb	Time of Sampling	c.c. H_2SO_4	c.c. N_aOH	c.c. neutralized by CO_2	K	$\%C_2H_{10}$ in air stream
4	25	10.20	9.93	.03	.1045	.003%
1	110	3.13	2.92	7.08	.0935	.660%

$$K = \frac{\text{normality}}{1000} \times 22.4 \times \frac{100}{V} \times \frac{T}{273} \times \frac{760}{P}$$

V = vol. of sample bulb T = room temp.

P = atm. press. % = K(c.c. N_aOH)

*These tables have been greatly condensed.

$$\frac{x}{m} \quad \frac{3.96}{27.96} \quad \frac{22400}{58} \quad 54.9$$

$$\text{Partial Pressure} = \frac{24.0}{3096} \times 760 = 5.70 \text{ mm. Hg.}$$

$$\text{Corrected height} = \frac{27.79}{6.57} = 4.23 \text{ cms.}$$

Note Bulbs, at slow flow rates necessary for ammonia, required approximately six minutes to fill. In calculations, the sample was considered as having been taken in 3 minutes after the bulb was opened. For butane, much larger flows were possible and a larger capillary allowed the bulbs to fill completely in two minutes. The sample was then considered to be taken one minute after sampling was started.

In desorption experiments the charcoal was saturated under the desired conditions of air and sorbate rate, pure sorbate being used in most cases until equilibrium was attained. The conditions of sorbate and air flows were changed to those desired for desorption and the weight-time readings and temperature readings taken at suitable intervals. Sample

bulbs were taken at appropriate times. This was continued until a new equilibrium weight was established.

The charcoal used in all these experiments is Canadian S. B. T. 95 - 96 and is silver impregnated. The ammonia used was anhydrous ammonia as supplied by Canadian Industries Limited. The butane was 99.5% pure and was used without further purification except for the removal of any water vapour present. It was obtained from the Ohio Chemical and Manufacturing Company.

RESULTS.

A. Ammonia

The weight increase of the charcoal bed with time, the temperature rise with time and the analysis of the escaping gases were carried out using ammonia concentrations from 5 parts per 1000 up, and flowrates of 0.16 - 3.2 cm. per second, and at column lengths of 3, 4 and 5 centimeters of charcoal as previously described. The service time, dead length, amount of sorption and escaping concentration were calculated.

1. Amount of Sorption

The increase in weight of the charcoal bed as the ammonia-air mixture was passed over it is shown as a function of time for various concentrations, flowrates and column lengths, in figures 9 and 10. It is seen that the weight increases linearly with time until the service time is reached. The slope of this linear section depends on the ammonia flowrate (as figure 10 shows) and is independent of the air flowrate (figure 9). After the service time is reached, the weight falls off gradually with time until a constant weight is reached, at which time the charcoal is in equilibrium with the ammonia-air stream being passed over it.

The equilibrium sorption weights are given in tables 1 and 2 for various concentrations, flowrates and column lengths. The column length was determined using an average centimeter bed, which weighed 6.57 gram. This was the average weight of a centimeter bed length determined from the weights of all the beds used throughout the work. The column lengths given in the tables 1 and 2 are approximate. The correct bed lengths, calculated from the weight of charcoal have been used however in plotting graphs of the column length. Figures 11 and 12 show that the equilibrium weight sorbed

Table 1

Weight Sorbed (Grams) at Various Air Rates

(NH_3 flow = 60 cc. /min.)

Air Rate cc./min.	Column Length (cms.)		
	5	4	3
0	3.65	-	2.16
100	1.67	1.34	1.00
200	1.08	0.89	0.67
300	0.92	0.76	0.59
550	0.34	-	-
2000	-	-	0.10

Table 2

Weight Sorbed (Grams) at Various Ammonia Rates

(Air flow = 200 cc./min.)

NH_3 Rate cc./min.	Column Length (cms.)		
	5	4	3
15	0.55	0.43	0.32
42	0.92	0.79	0.59
60	1.08	0.89	0.67
100	1.45	1.18	0.87

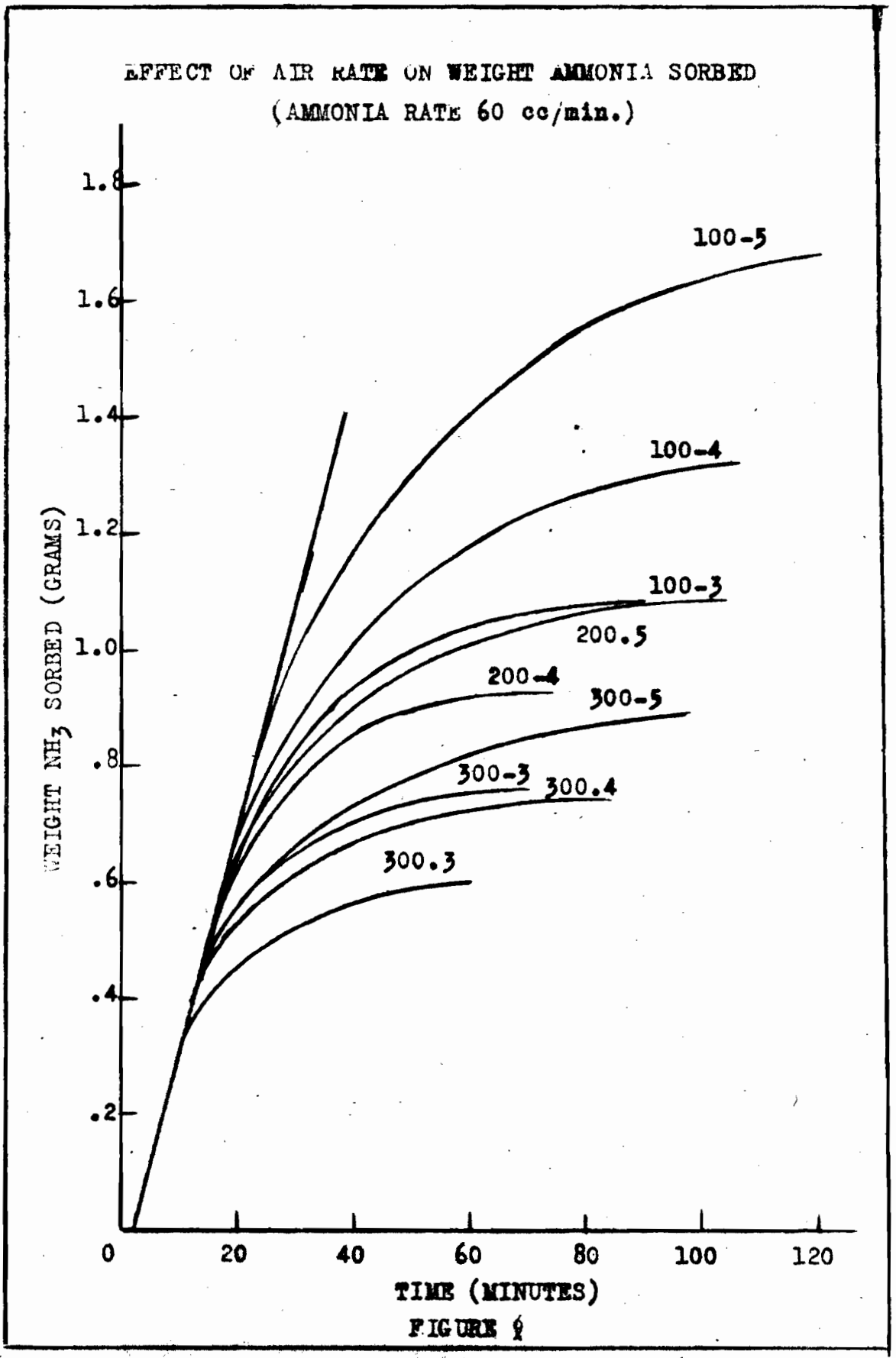
EFFECT OF AIR RATE ON WEIGHT AMMONIA SORBED
(AMMONIA RATE 60 cc/min.)
WEIGHT NH_3 SORBED (GRAMS)
1.8
1.6
1.4
1.2
1.0
.8
.6
.4
.2
0
20
40
60
80
100
120
TIME (MINUTES)
100-5
100-4
100-3
200.5
200-4
300-5
300-3
300.4
300.3

FIGURE 9

EFFECT OF AMMONIA RATE ON WEIGHT SORBED
AIR RATE 200 cc./min.

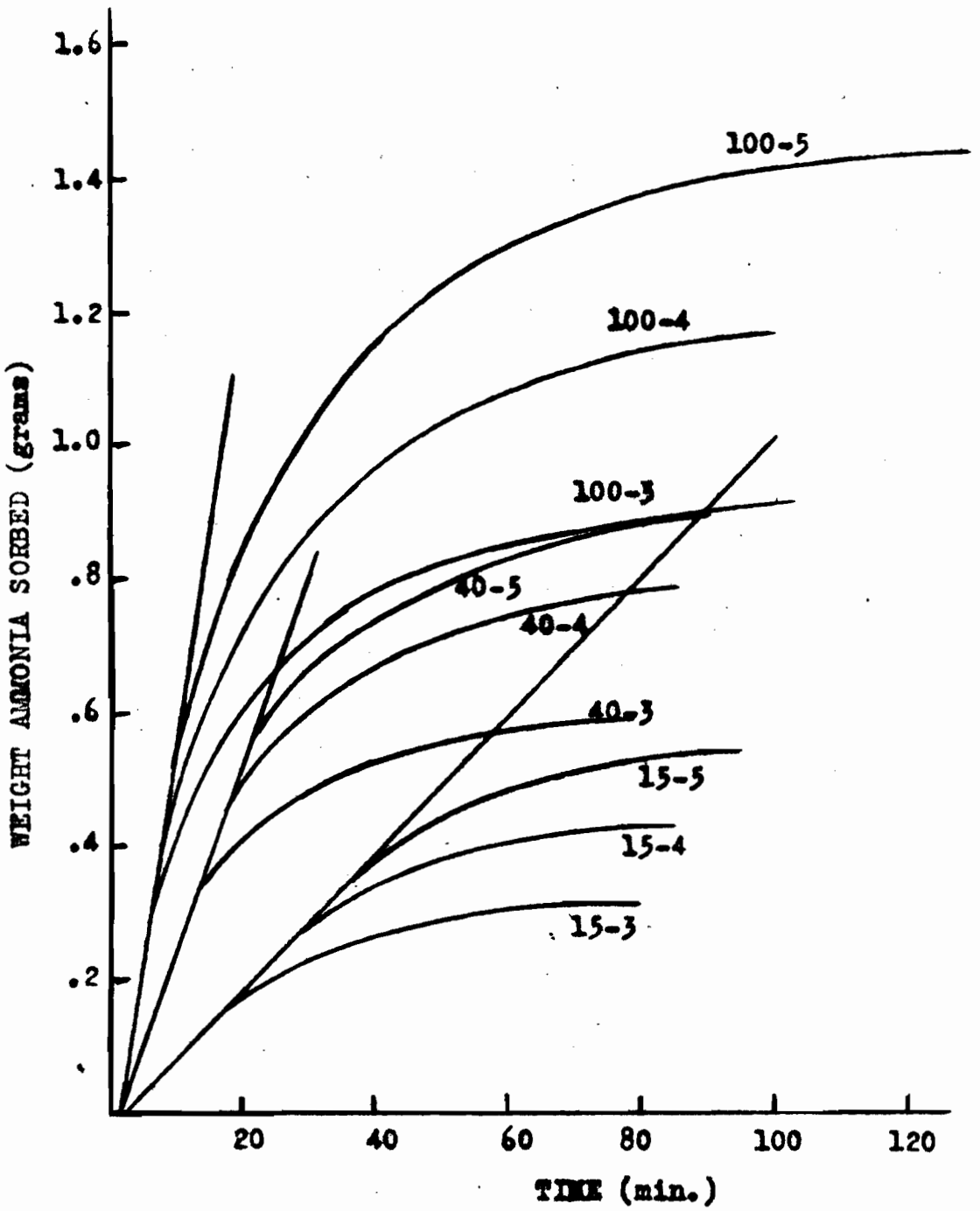

FIGURE 10.

Table 3

Volume Sorbed per Gram at Various Air Rates

(NH_3 rate = 60 cc./min.)

Air Rate cc./min.	Column Length (cms.)		
	5	4	3
0	145	-	146
100	69.0	68.8	69.2
200	44.0	44.0	45.5
300	38.2	38.0	38.2
550	25.4	-	-
2000	-	-	12.5

Table 4

Volume Sorbed per Gram at Various NH_3 Rates

(Air rate = 200 cc./min.)

NH_3 rate cc./min.	Column Length (cms.)		
	5	4	3
13.2	19.8	-	-
15	21.2	21.2	21.7
42	38.9	39.4	38.6
54	40.6	41.1	-
60	44.0	44.0	45.5
100	59.4	59.4	58.2

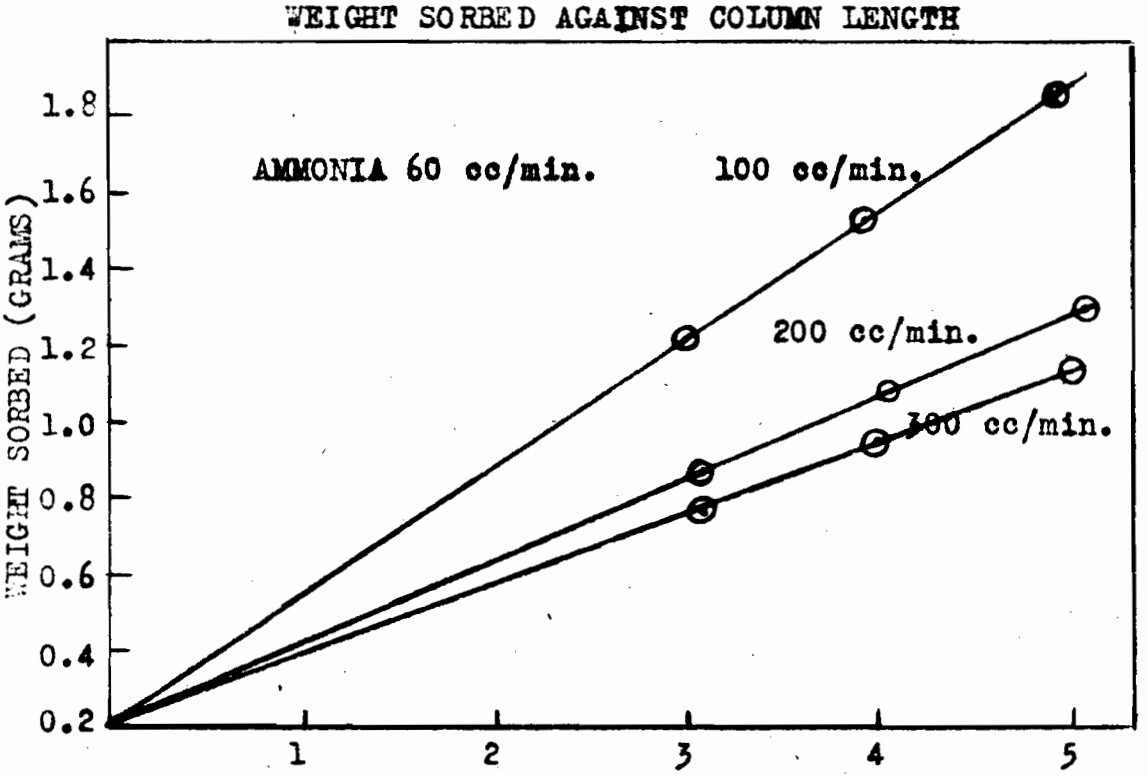

(VARIABLE AIR FLOW)
FIGURE 11.

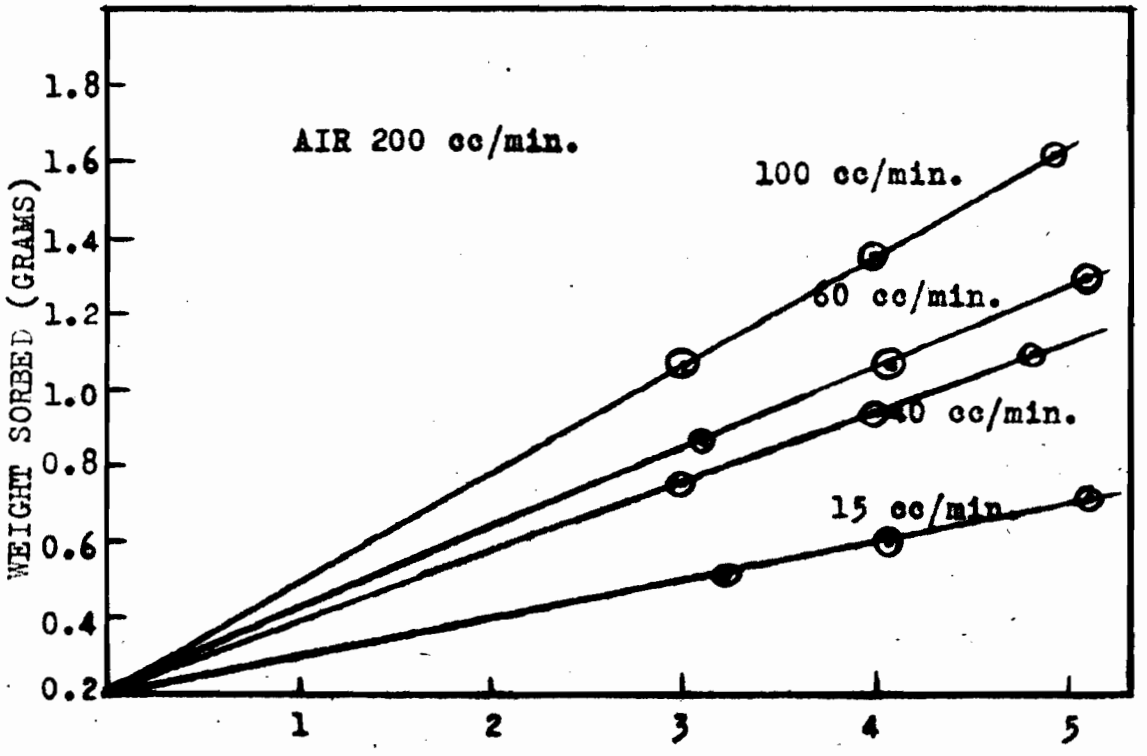

(VARIABLE AMMONIA FLOW)
FIGURE 12

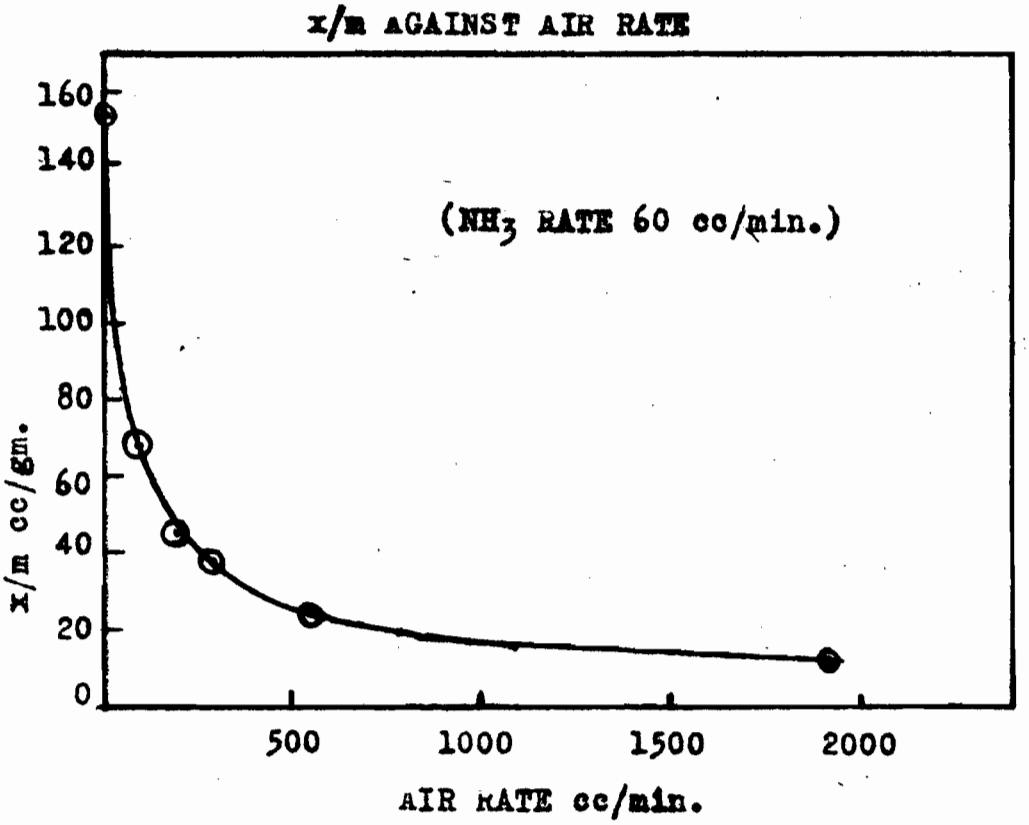

FIGURE 13.

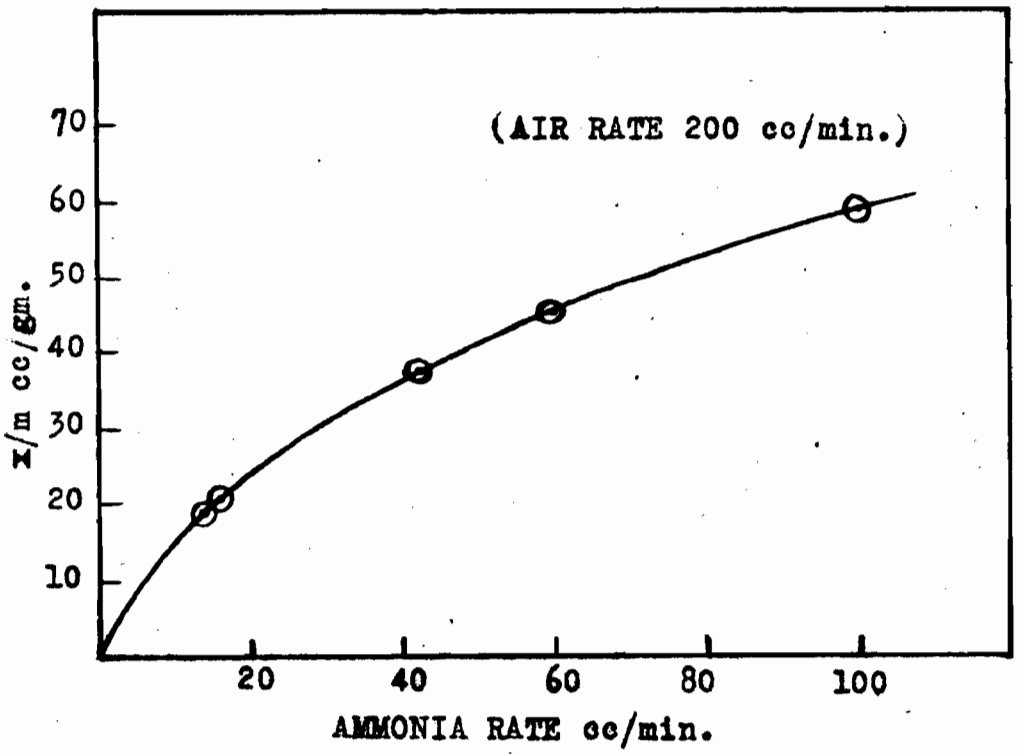

FIGURE 14.
x/m AGAINST AMMONIA RATE

is a linear function of column length at constant concentration.

The variation of the equilibrium sorption, expressed as the volume sorbed per gram of charcoal (x/m) with the rates of flow of the ammonia and air streams, is shown in tables 3 and 4 and in figures 13 and 14. It is seen that at constant ammonia flow, the effect of increasing the air flowrate from zero is quite marked at first but the effect diminishes at higher air rates. When plotted as the logarithm of the volume sorbed per gram of charcoal against the logarithm of the air rate, a straight line is obtained (figure 15). The effect of increased ammonia flow is to increase the amount of sorption. A linear relation is obtained between the logarithm of x/m and the logarithm of the ammonia flowrate (figure 16).

The data for the variation of the equilibrium sorption with partial pressure are given in table 5. Over the range of 50 mm to 760 mm of Hg. partial pressure, the relation is linear with no indication of attaining a constant value of x/m at higher partial pressures. Below 50 mm. partial pressure the curve bends downwards toward the origin as the partial pressure is further decreased (see enlarged graph figure 17.) The logarithm of the equilibrium sorption plotted against the logarithm of the partial pressure gives a straight line (figure 18) for partial pressures between 50 and 760 mm. and a second straight line of decreased slope for partial pressures below this.

Above 50 mm. the Langmuir or Freundlich isotherms may be applied, the equations being:

$$x/m = \frac{0.278P}{1 + 0.000555P}$$

and

$$x/m = 1.06P^{\frac{1}{1.31}}$$

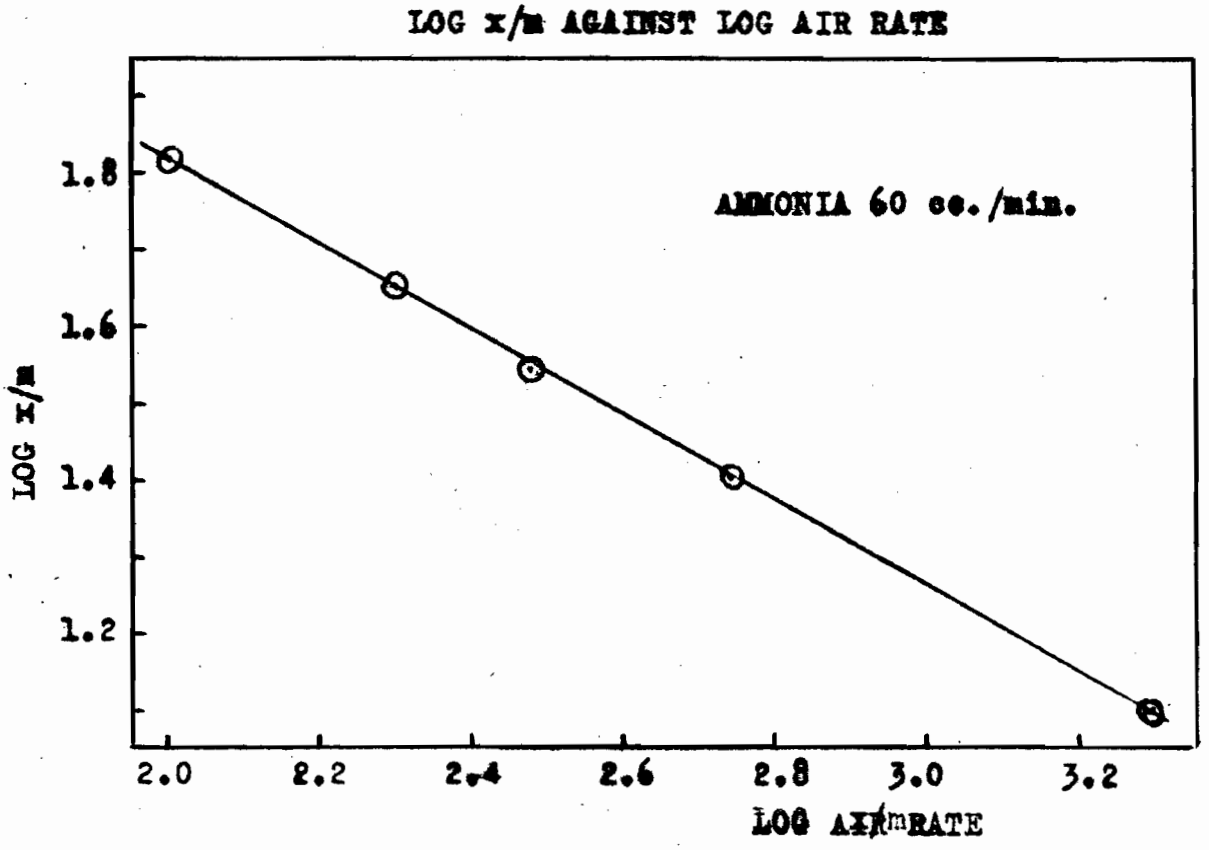

FIGURE 15.

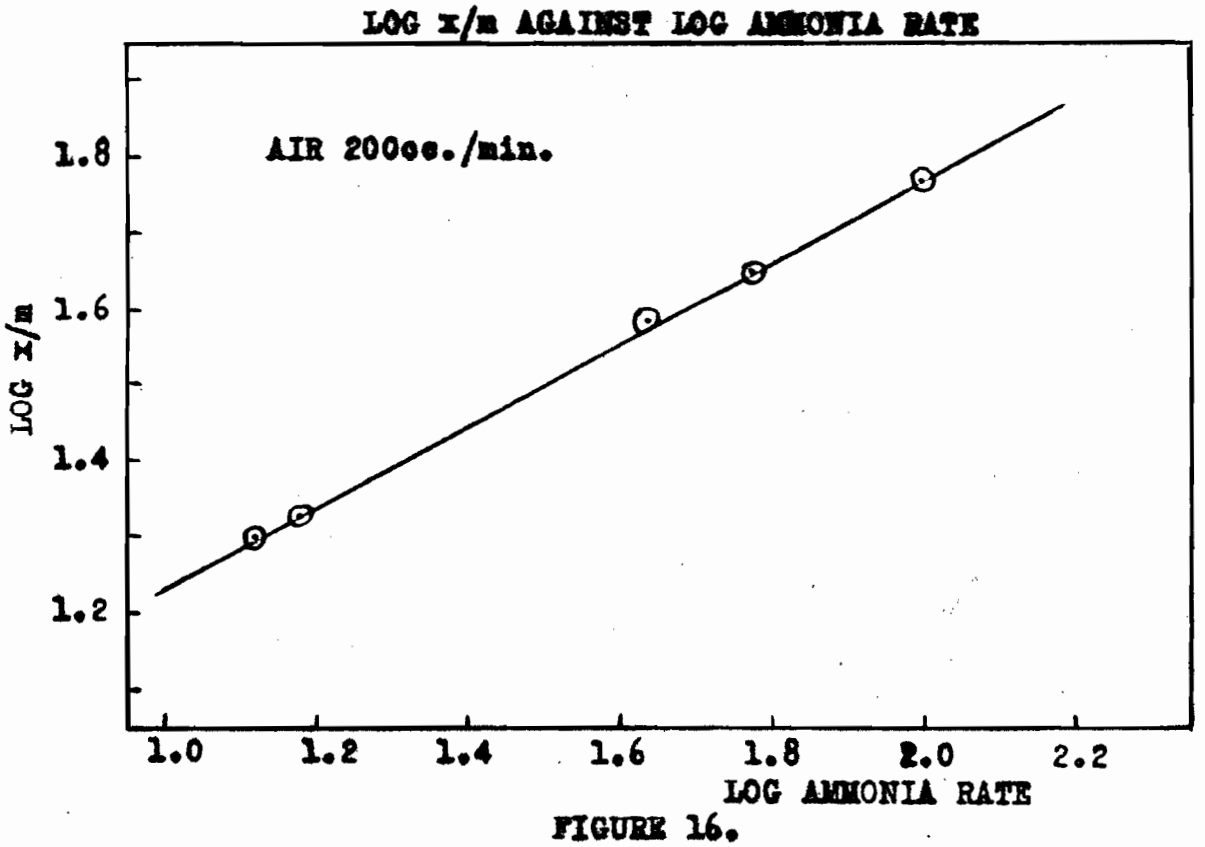

FIGURE 16.

where x/m is in cc. per gram of charcoal, and P in mm. of mercury. Other authors have found these isotherms to hold for dynamic systems of: chlorine (16), aqueous solutions (19), and chloropicrin (13).

The linear velocity of the ammonia-air stream, at constant ammonia concentration was found to have no effect on the equilibrium amount of ammonia sorbed. Table 6 shows the data for four runs of this nature at total flowrates from 0.16 to 1.79 cm. per second.

The slopes of the linear portion of the weight-time curves should give a measure of the rate of sorption during this time. Since all the ammonia is being sorbed, the slope should be equal to the rate ofsupply of the ammonia. It was found, however, that the rate of sorption in c. c. per minute was lower than the ammonia flowrate, see table 7. A graph of this slope against the ammonia flowrate is shown in figure 19. This will be further discussed in the analytical section and in the desorption studies.

Table 5

x/m (cc./gm.) with Various Partial Pressures of Ammonia.

Air Rate cc./min.	NH_3 Rate cc./min.	P.p. NH_3 mm. Hg.	x/m
0	60	760	145
54	200	465	103
150	97	300	67.2
100	60	285	69.0
200	100	254	59.4
200	60	175	44.8
100	20	132	38.2
200	42	132	38.9
300	60	127	38.2
500	100	132	38.2
550	60	75	27.5
200	15	53	21.2
2000	60	22.1	12.5
3270	60	13.7	11.2
3270	17	3.9	4.1
3270	14.7	3.4	5.7
3270	13.2	3.1	5.6
3270	3.4	0.79	2.3
3270	1.6	0.37	1.1

x/m AGAINST PARTIAL PRESSURE OF AMMONIA

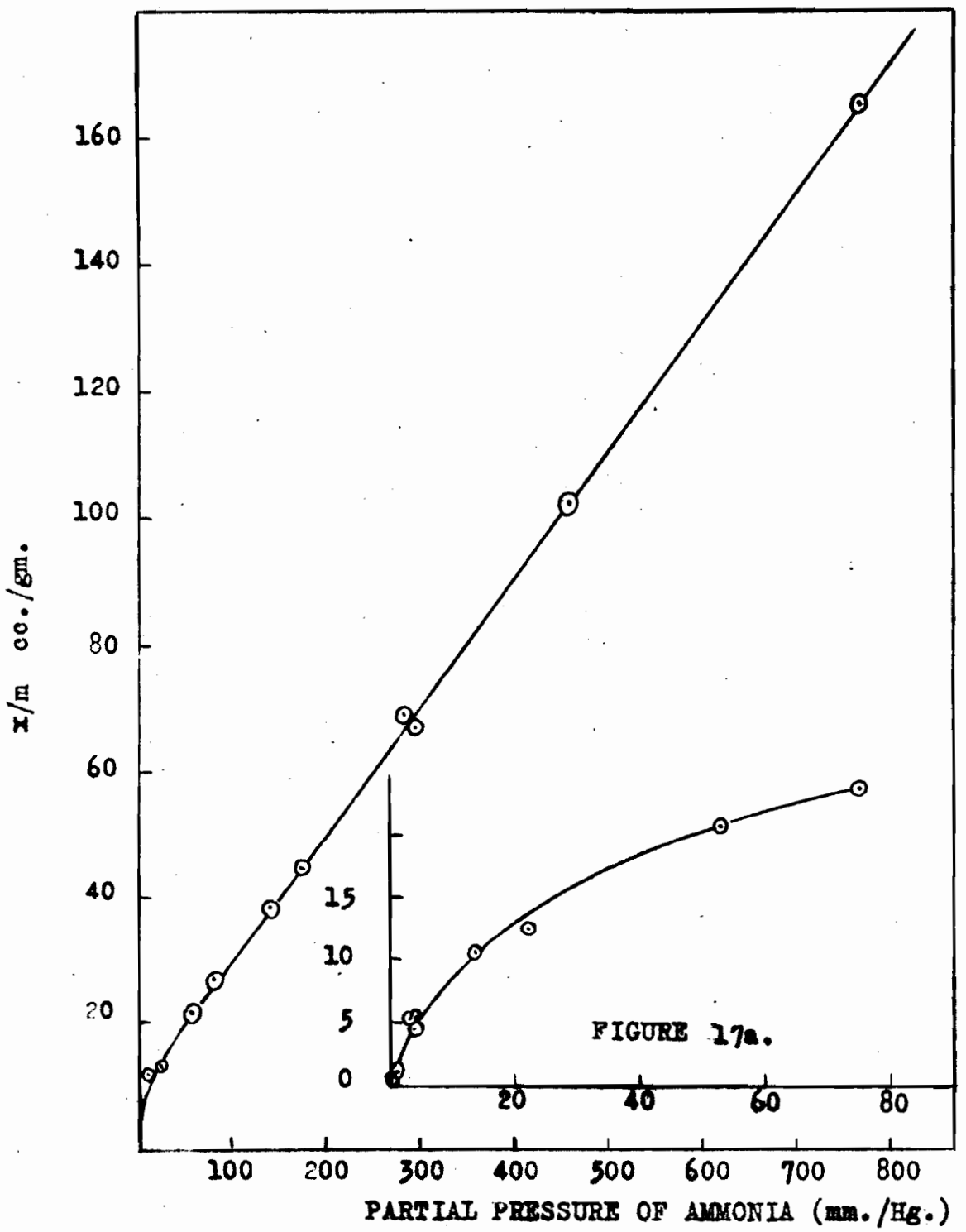

FIGURE 17a.

FIGURE 17

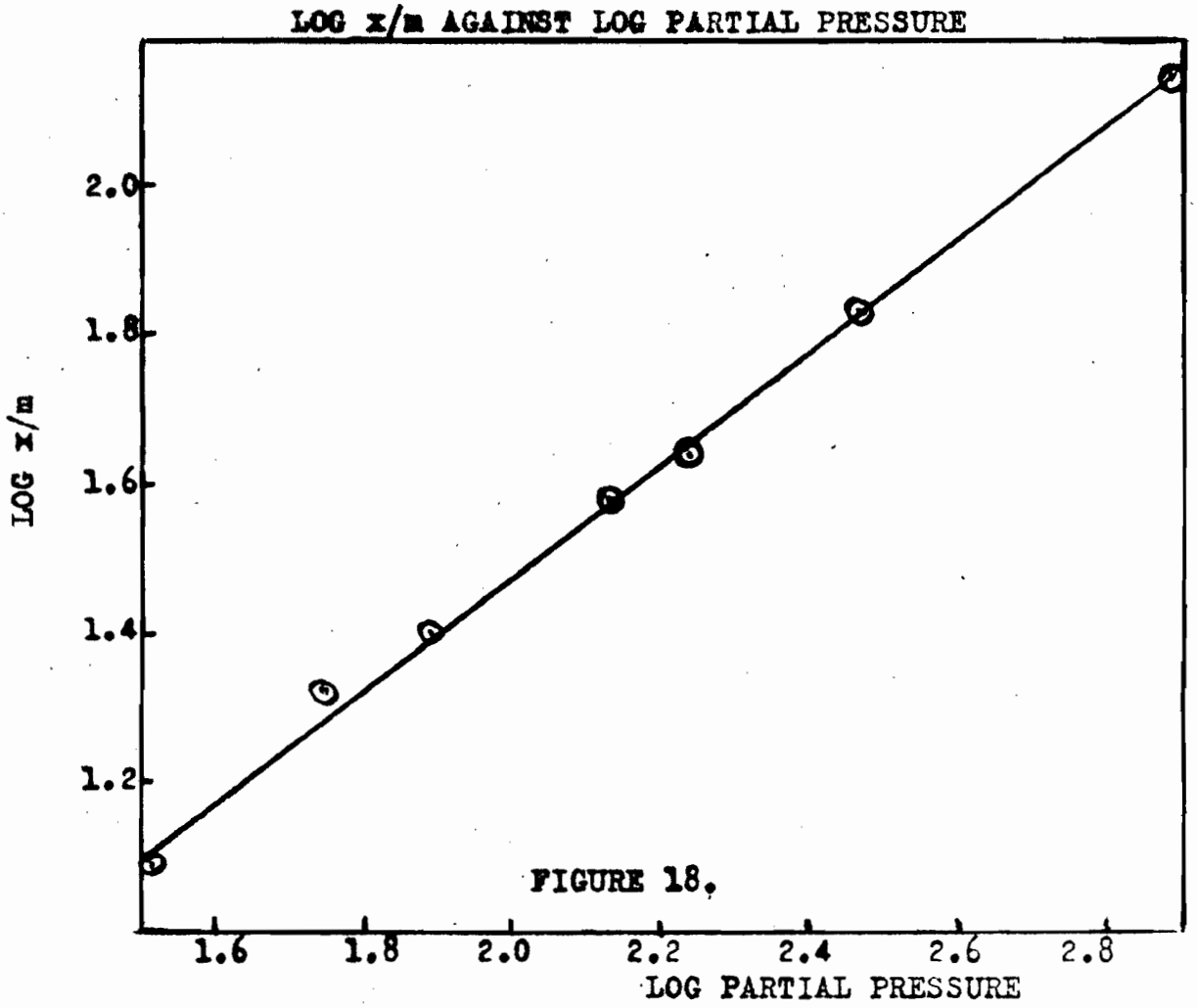

FIGURE 18.

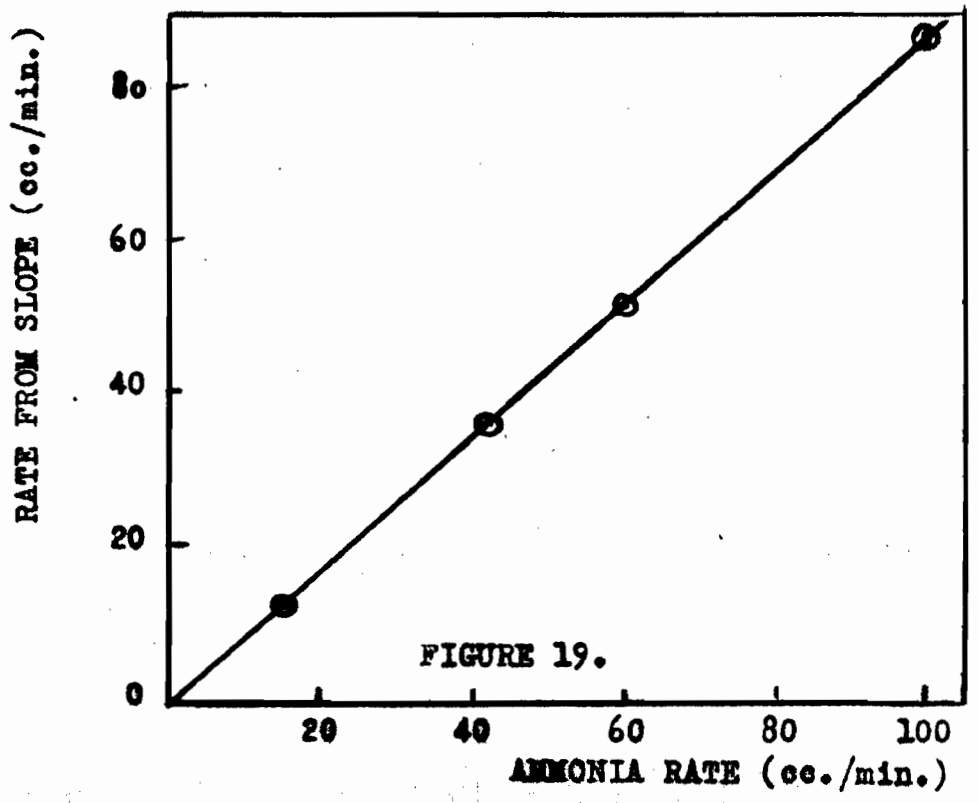

FIGURE 19.

Table 6

Effect of Total Velocity on Equilibrium Sorption at Constant Composition

Conc. %	Rate of flow cc./min.	W (gms.)	x/m cc./gm.	Velocity cms./sec.
16.7	120	0.92	11.2	0.16
16.7	242	0.92	11.4	0.32
16.7	360	0.92	11.2	0.48
16.7	600	0.95	11.1	0.79

Table 7

Calculated Slopes at Various Ammonia Rates.

Ammonia Rate cc./min.	Rate calculated from slope cc./min.
13	10.6
15.7	13.8
42.0	36.5
60	51.5
100	87.5

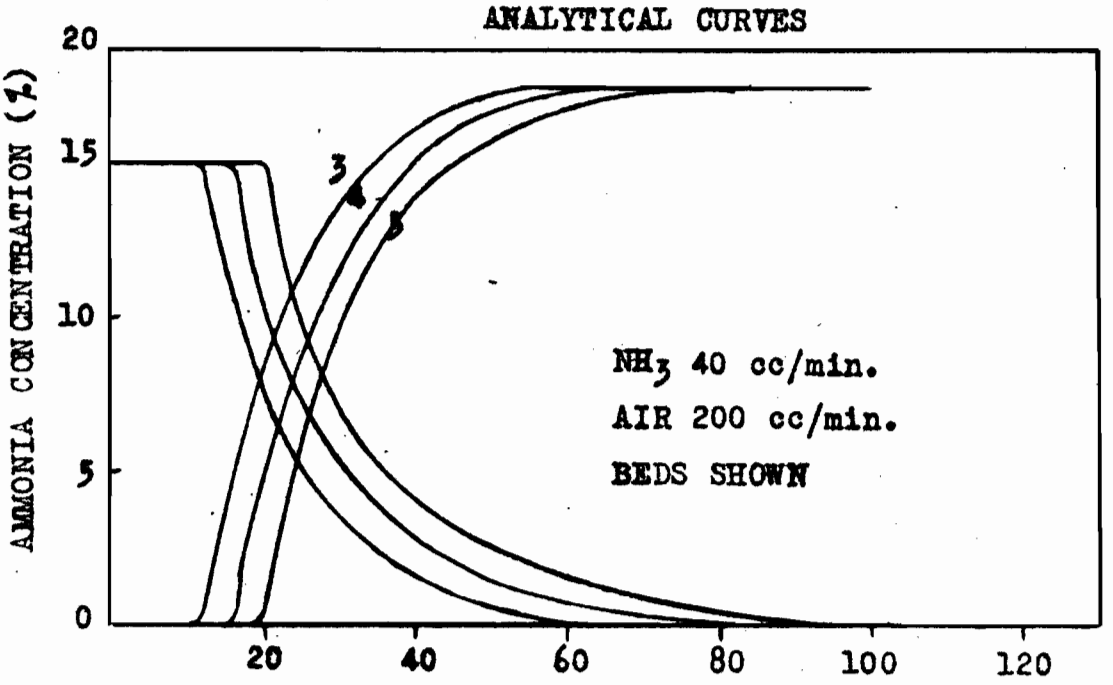

EFFECT OF BED LENGTH

FIGURE 20

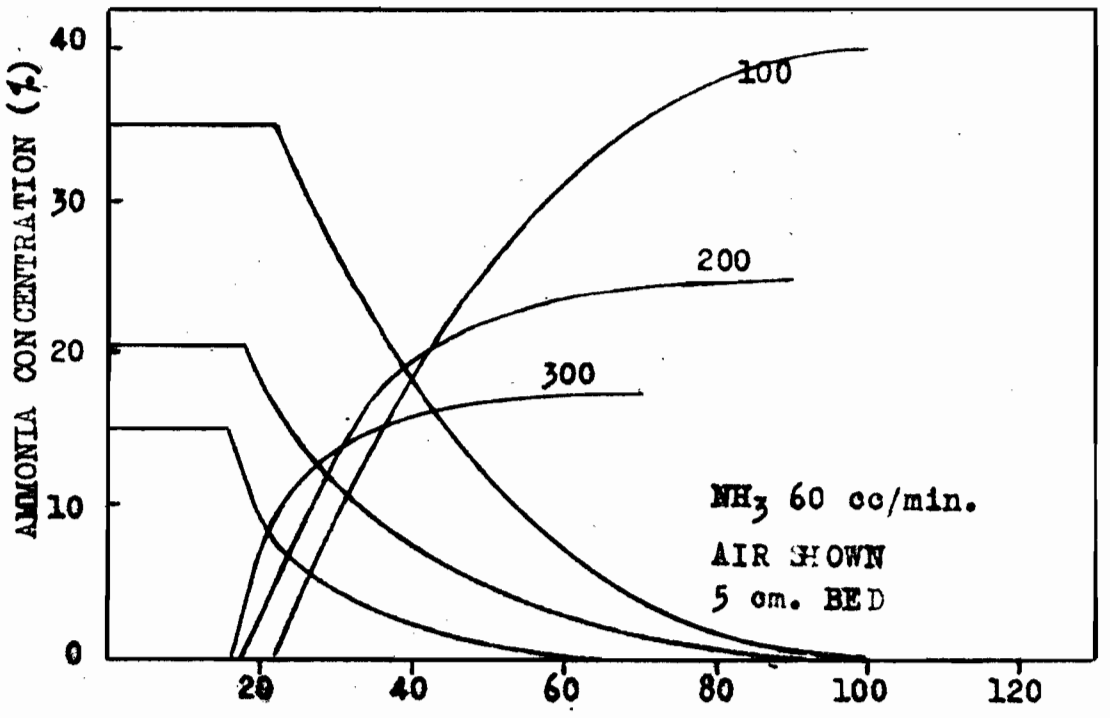

EFFECT OF AIR RATE

FIGURE 21.

2. Analytical Data

The concentration of ammonia in the escaping gases is shown as a function of time in figures 20 to 23 for various conditions. Figures 20, 21, 22 and 23 show the variation with column length, air flowrate, ammonia flowrate, and total linear velocity respectively. It is seen that no ammonia appears in the effluent gases until the service time is reached, indicating complete sorption of the ammonia supplied in the entering stream. After the service time, the concentration of ammonia in the escaping gases increases rapidly at first, but approaches a constant value when the charcoal bed is saturated. In these graphs the ammonia concentration is expressed as a percent concentration of the gas stream leaving the charcoal bed based on the metal flowrate of the gas stream entering the cell.

On the same graphs is plotted the differential amount sorbed as a function of time. This was obtained by graphical differentiation of the weight-time curves plotted in figures 9 and 10. When expressed in the same units as the concentration of the ammonia in the escaping gases, it is a complementary curve to that of the analysis of the effluent stream. It represents the percent of the total entering stream which is being removed by the charcoal bed at any time. It is, therefore, constant until the service time, and thereafter decreases, approaching zero when the charcoal bed is saturated.

In table 8 the data for the escaping concentration as a function of time are presented. If the escaping concentration of ammonia in the effluent stream is expressed as a function of time by plotting the logarithm of the reciprocal of the concentration, (1/c) against time as in figure 24, a curve is obtained in contrast to the predictions of

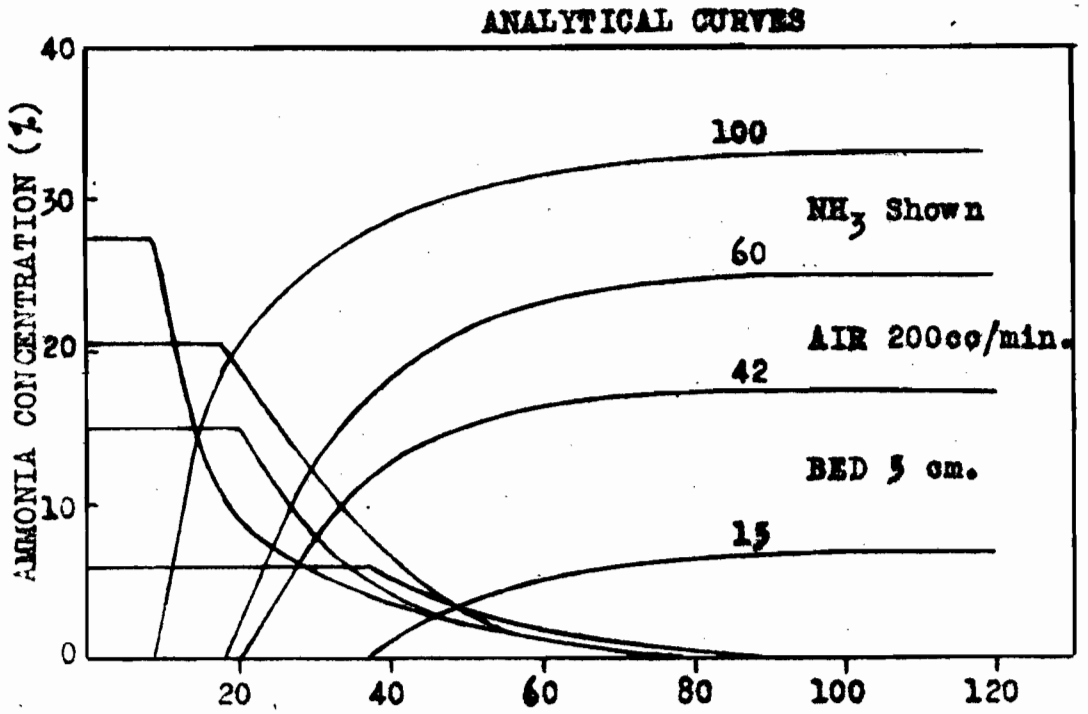

EFFECT OF AMMONIA RATE
FIGURE 22.

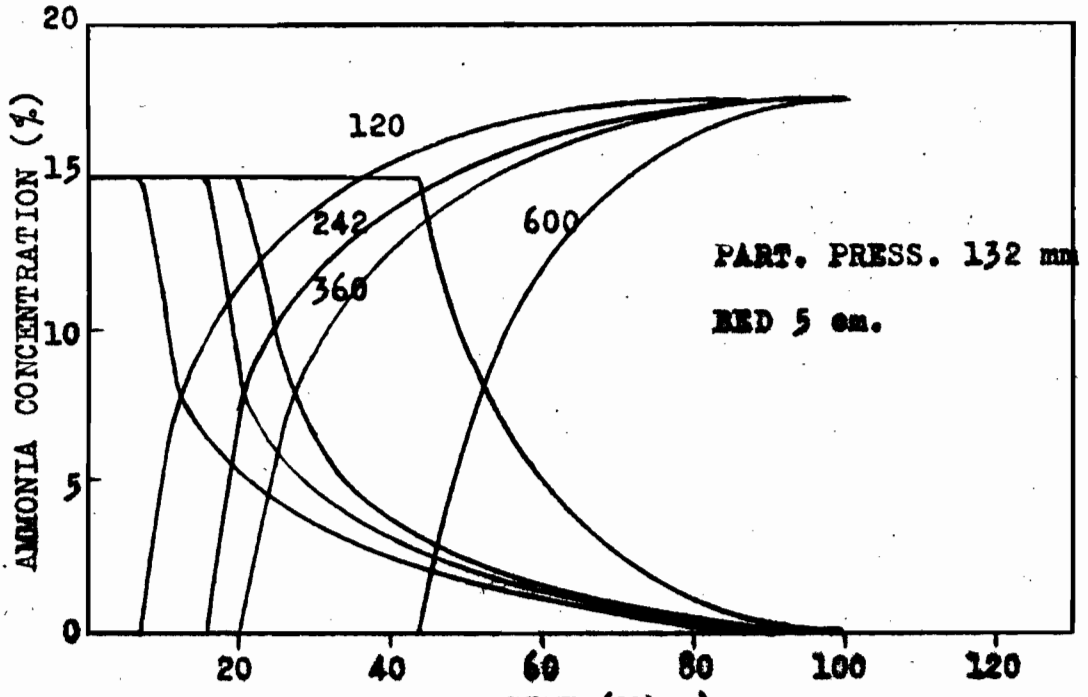

EFFECT OF FLOWRATE
FIGURE 23.

Table 8

Escaping Concentration as a Function of Time.

Time after Service Time mins.	Concentration c%	1/T	Log 1/c
4	4.3	.250	$\bar{1}$.366
10	10.2	.100	$\bar{2}$.992
14	12.0	.0712	$\bar{2}$.921
19	13.5	.0526	$\bar{2}$.870
25	15.0	.0400	$\bar{2}$.824
30	15.6	.0333	$\bar{2}$.807
40	16.3	.0250	$\bar{2}$.788
50	16.8	.0200	$\bar{2}$.775
60	17.0	.0167	$\bar{2}$.770
80	17.4	.0125	$\bar{2}$.760

ESCAPING CONCENTRATION

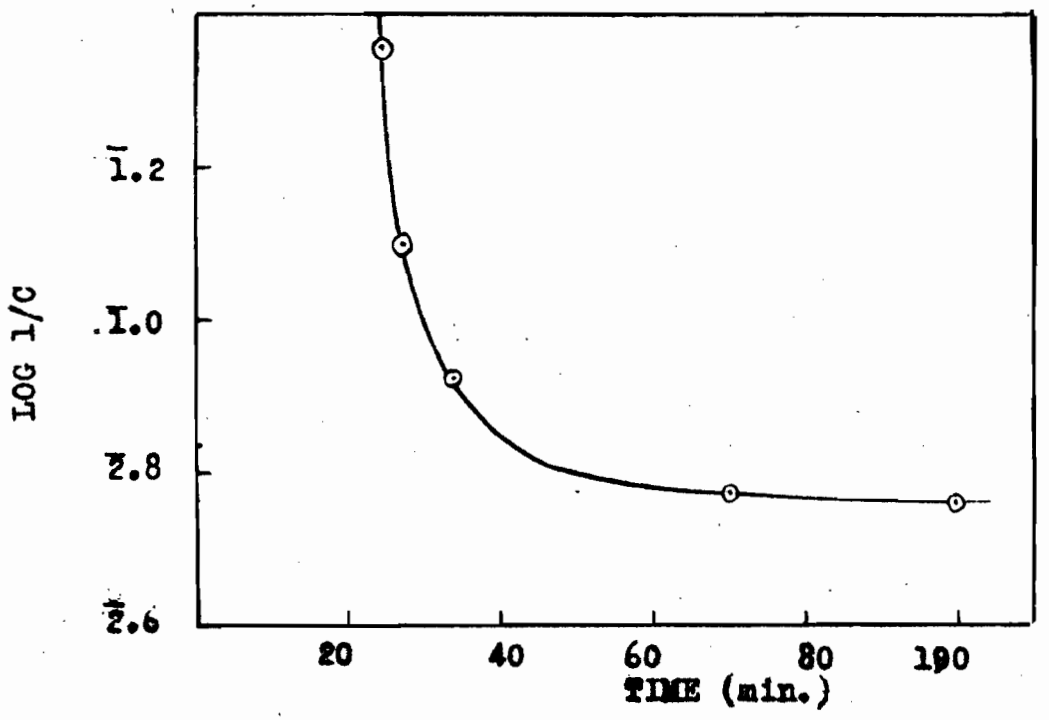

FIGURE 24.

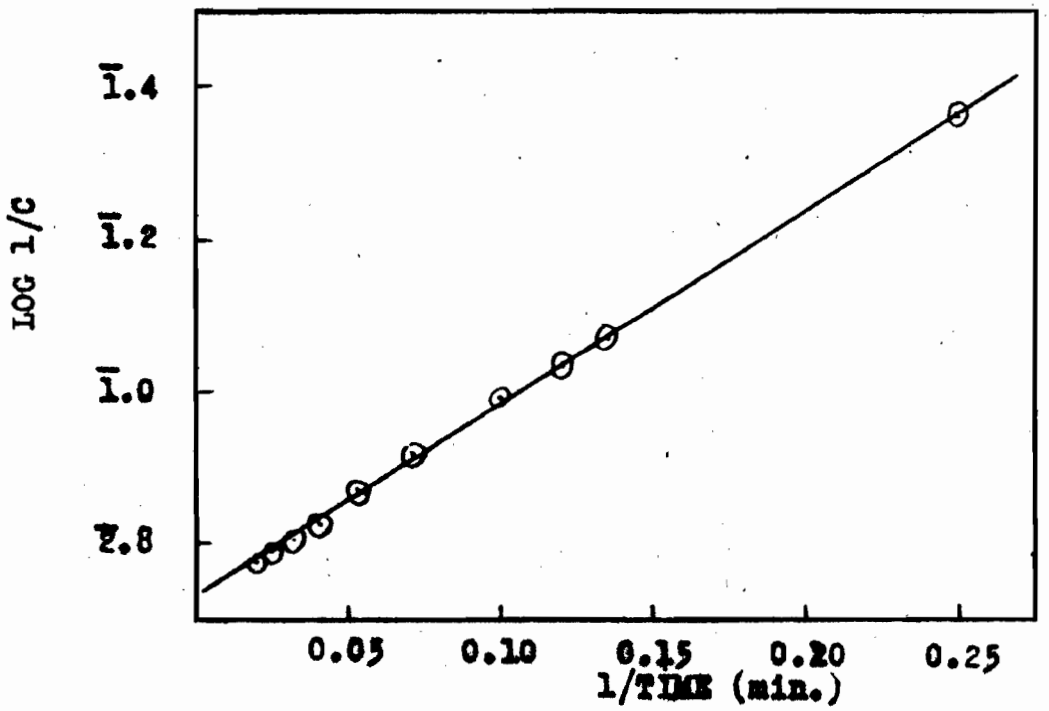

FIGURE 25.

Danby et al, who derive the equation for escaping concentration as

$$\ln\left(\frac{c_o}{c} - 1\right) = -kc_oT + \ln\left(e^{KN_o\lambda/L} - 1\right)$$

where c is the escaping concentration and T the time. They state however that this relation only holds when c_o/c is large, i. e. in the early stages of breakdown. From figure 24, it is seen that an approximation to a straight line is obtained for the first few minutes.

A linear relation is obtained, however, between the logarithm of the reciprocal of the escaping concentration and the reciprocal of the time (figure 25) if the time is measured from the service time. These data for escaping concentration are presented only for one run, All other runs gave similar results.

It may be noted that the sorption as indicated by the constant differential amount sorbed does not correspond to the ammonia flowrate as measured by the analysis of the escaping gases when the charcoal is saturated. This was found to be due to air displaced from the charcoal by the ammonia, and will be discussed later under the desorption studies which confirmed this behaviour.

The escaping concentrations calculated from the differential sorption curves would not, then represent the true concentration of ammonia in the effluent stream. The apparent weight of ammonia on the charcoal is less than that actually sorbed, by the weight of the air displaced.

3. Service Time Data

The service time was determined in these investigations as the time when the charcoal ceased to be 100% efficient in removing the ammonia from the air stream. This was the time at which the weight-time curves deviated from the linear relation. Service times calculated on this basis agreed within half a minute of those determined using a phenolphthalein or litmus test paper in the effluent gas line. The deviation between the observed weight and the actual weight sorbed due to the displaced air, would have no effect on the service time since, if the true weight of ammonia sorbed were plotted against time, the amount of ammonia taken up by the charcoal when the graph deviates from the linear relation would be greater, but the time at which this occurs would be unchanged.

The service times at various column lengths and rates of air and ammonia flow are given in tables 9 and 10 and are shown graphically as a function of these variables in figures 26 to 31. A straight line is obtained when the service time is plotted against column length, (figure 26 and 27), which if extrapolated cuts the column length axis at a positive length. This intercept is the "critical" or "dead" length. It was not possible to test the behaviour at very short bed lengths as the weight change would not be very large since ammonia is so poorly sorbed. Thus it cannot be stated whether or not the graph curves in towards the origin at short column lengths, as was found by Dubinin et al (17) and Mecklenberg (13). These extrapolated straight lines converge to a point below the origin. No theoretical significance has been attached to this fact.

The linear relation which was found to hold agrees with the theories of Danby et al and Mecklenberg which give the equations

Table 9

Service Time at Various Air Rates

(NH_3 flow 60 cc./min.)

Air Rate cc./min.	Column Lengths (cms)		
	5	4	3
100	22.5	17.5	12.5
200	16	12	8.5
300	14	11	8

Table 10

Service Time at Various Ammonia Rates

(Air flow - 200 cc./min.)

WH_3 Rate cc./min.	Column Length (cms.)		
	5	4	3
15	30	23	17
42	20.5	16	11.5
60	16	12	8.5
100	8	6	4

SERVICE TIME AGAINST COLUMN LENGTH

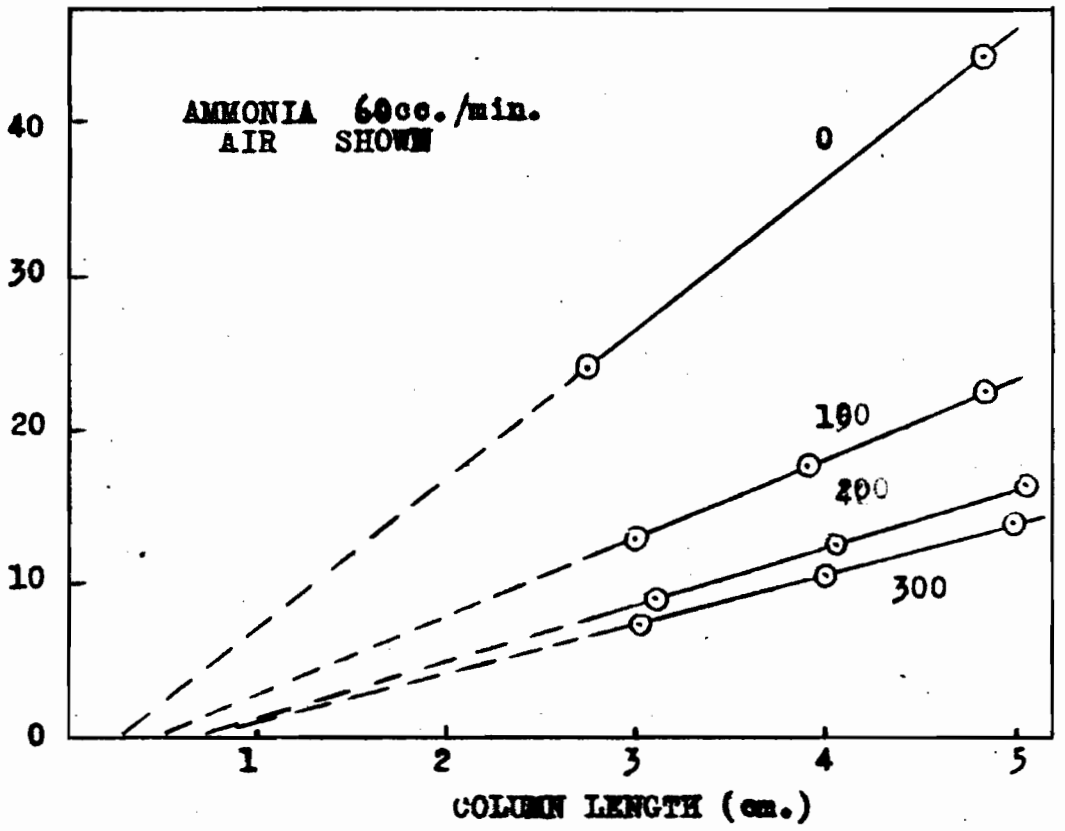

FIGURE 26.

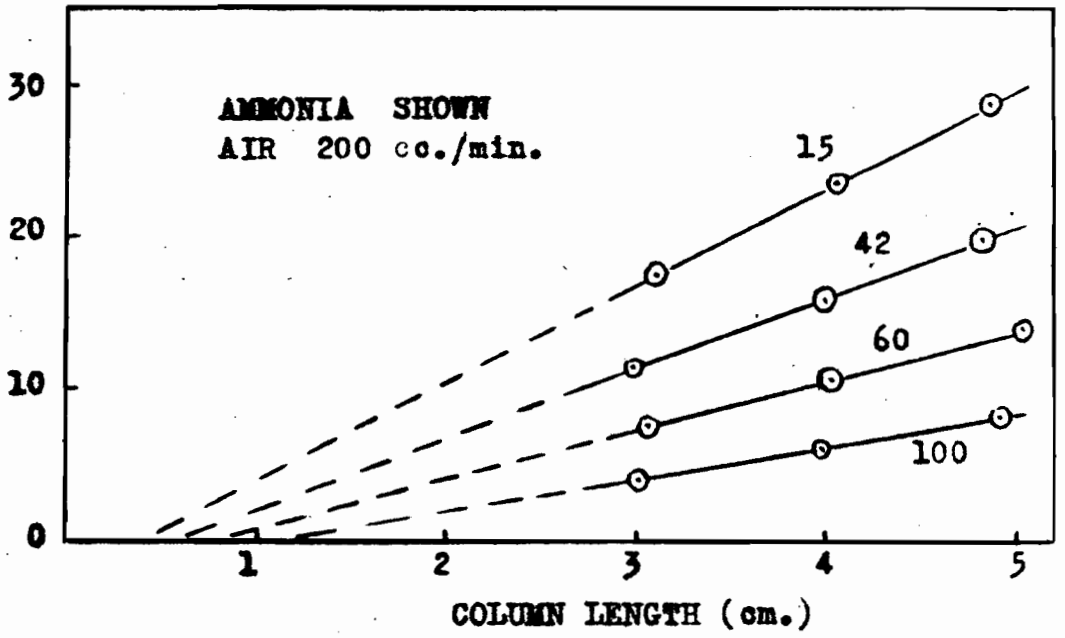

FIGURE 27.

$$T = \frac{N_o}{c_o L} (\lambda - \lambda c)$$

and

$$T = \frac{k}{v c_o} (L - L_c)$$

respectively. The slope of these curves is the coefficient of protective used by Shilow (16) and Dubinin (20) in their equations for the dead length and service time (equations xviii & xxiii)

Since the service time thus varies with column length, it is important in discussing its variation with flowrate, concentration, etc., that comparable runs be done at exactly equal column lengths. This was impractical so that "corrected" service times were used. These were determined by interpolation of the service time-column length graphs to the nearest integral column length. This corrected service time has been plotted in figures 28 to 31 and recorded in tables 9 and 10.

Figure 28 shows the effect on the service time of varying the rate of air flow at constant ammonia flowrate. The service time using 60 cc. per minute of pure ammonia is quite high but decreases rapidly at first as the air stream is increased, but the effect is not very great at air flowrates above 300 cc. per minute. When the logarithm of the service time is plotted against the logarithm of the air rate (figure 29) a straight line results.

The service time decreases also as the ammonia flowrate is increased at constant air rate as in figure 30, but the logarithm of the service time decreases linearly with the ammonia flowrate (figure 31). From the slopes of the logarithmic curves it is seen that the service time is much more dependent on the ammonia flowrate than on the air flowrate since the service time decreases exponentially with the ammonia rate but only with the 0.4 power of the air flowrate.

EFFECT OF AIR RATE ON SERVICE TIME

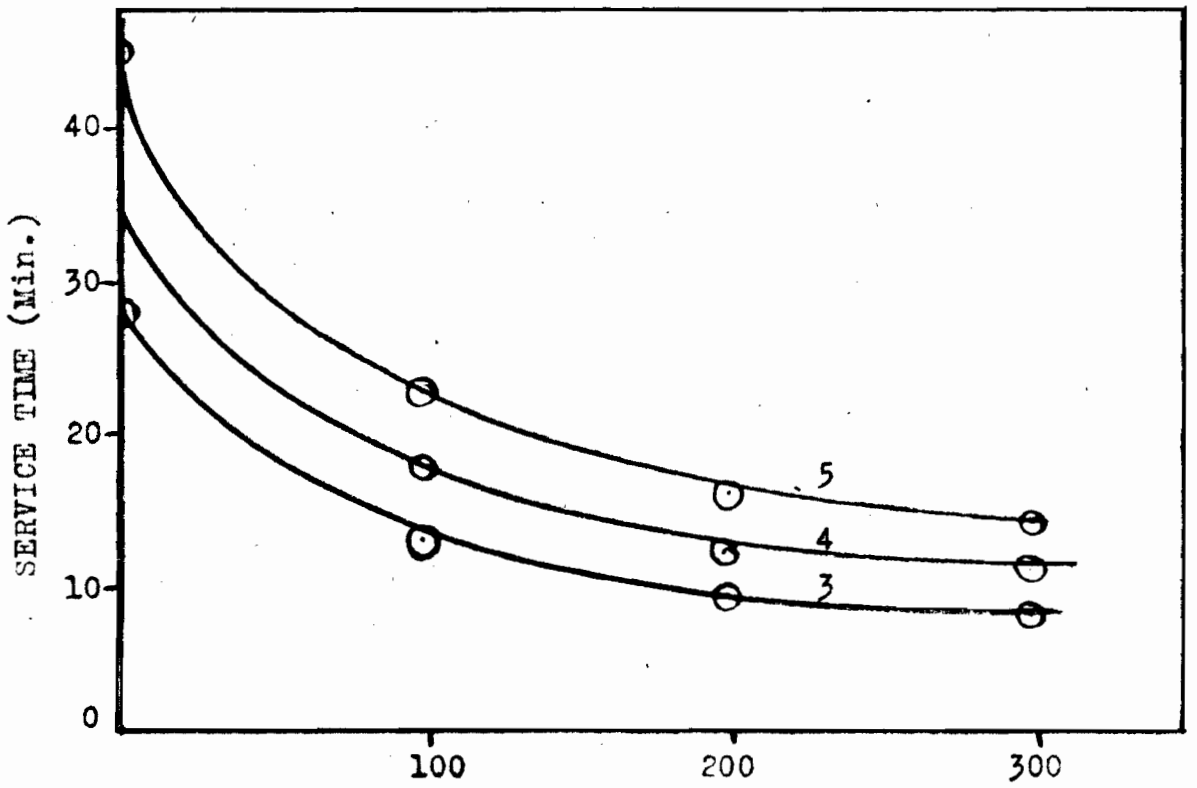

FIGURE 28.

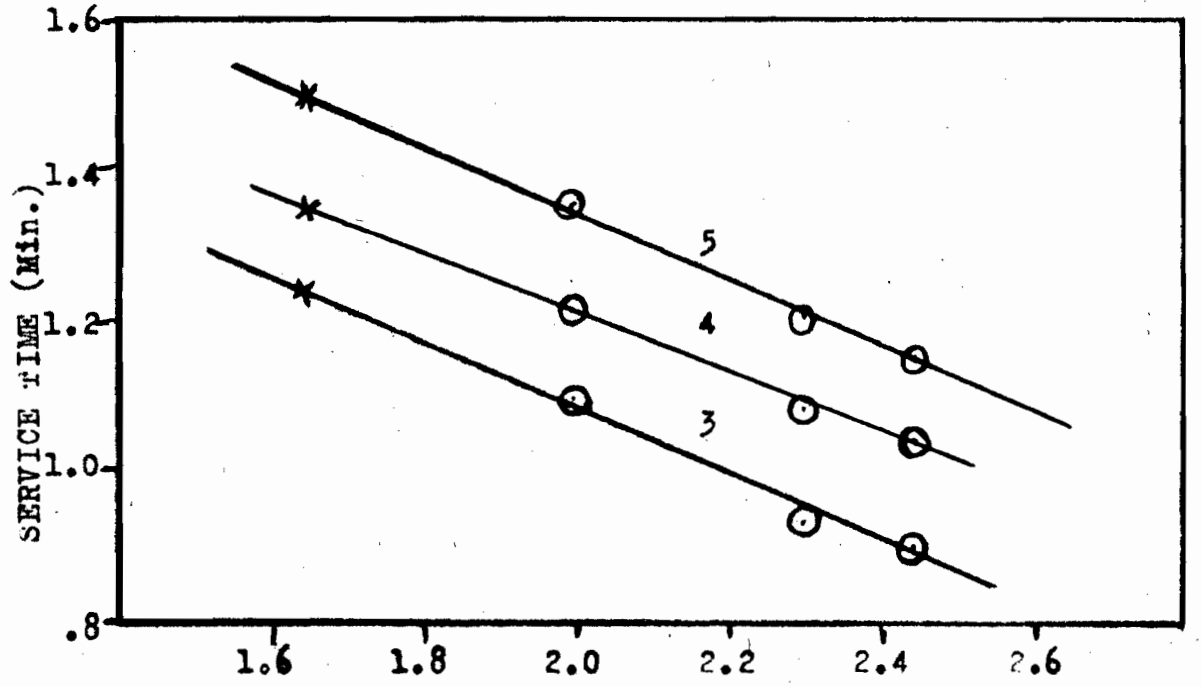

FIGURE 29

EFFECT OF AMMONIA RATE ON SERVICE TIME

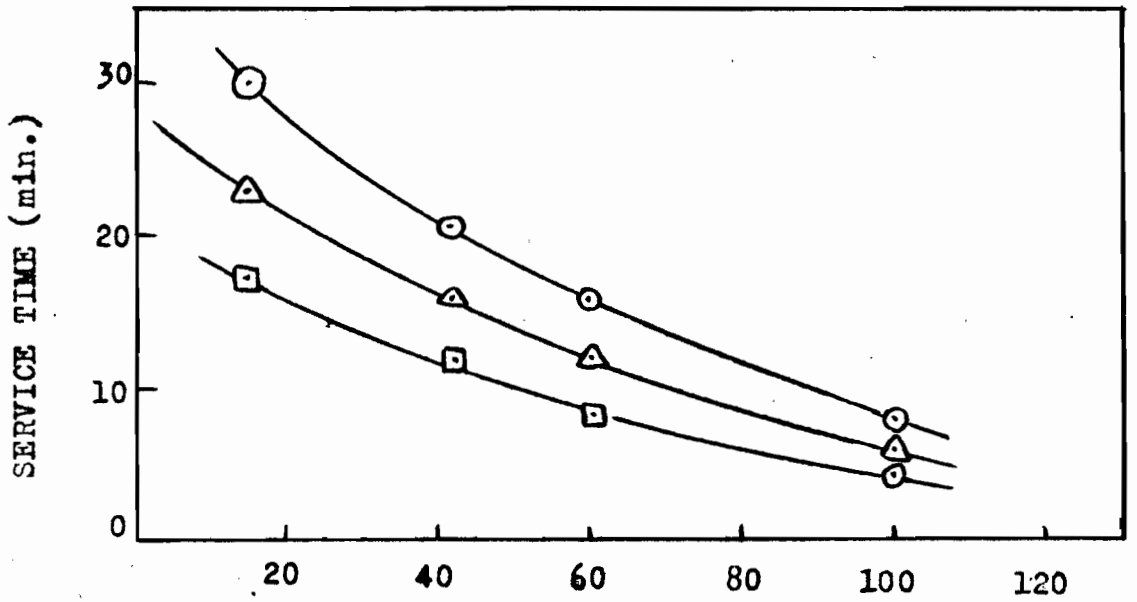

FIGURE 30

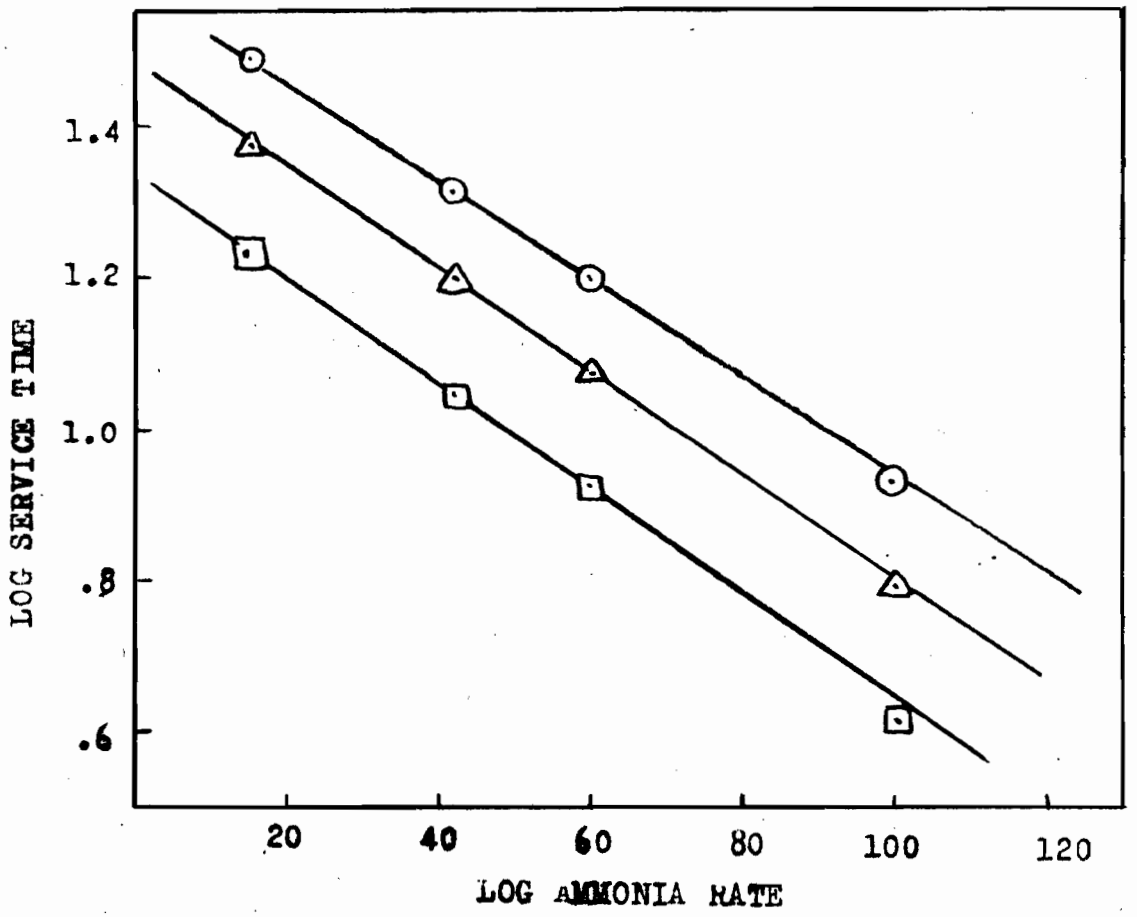

FIGURE 31

Table 11

Effect of Flowrate on Service Time at Constant Composition

Air Rate cc./min.	NH_3 cc./min.	Total cc./min.	Velocity (L) cms./sec.	Service Time min.	1/L
100	20	120	0.16	42	6.2
200	42	242	0.32	20.5	3.1
300	60	360	0.48	14	2.1
500	100	600	0.79	6	1.3

Table 12

Effect of Concentration on Service Time

(Flow rate = 250 cc./min.)

Air Rate cc./min.	NH_3 Rate cc./min.	Conc. (c_o) %	Service Time min.	$1/c_o$
150	97	39.2	9	0.0254
200	54	21.2	17	0.0470
200	60	23.0	16	0.0435
200	42	17.4	20.5	0.0576
235	19.5	7.65	22	0.131

At constant concentration of ammonia in the entering gas, the service time depends upon the reciprocal of the flowrate as shown in table 11 and figure 32. Extrapolation of the straight line so obtained intercepts the flowrate axis, corresponding to a "critical" flowrate, above which there would presumably be immediate breakdown of the charcoal bed, at this particular concentration. Experimental proof of the existence of this critical flowrate is, however, lacking.

At constant flowrate the dependence of the service time on the initial concentration of the ammonia in the entering stream was studied. The data obtained is given in table 12. A linear relation was found to hold (figure 33) between the service time and the reciprocal of the initial concentration over the range of ammonia concentrations of 17% to 40%, but which fell off rapidly at lower concentrations. Danby et al predicted a linear relation should be obtained at low, but not at high concentrations from the equation

$$T = \frac{1}{kc_o}\left(\frac{k N_o \lambda}{L} - \ln \frac{c_o}{c'}\right)$$

where $\ln c_o/c$ was assumed negligible at low concentrations and N_o on a_o appears to be much greater than the theory assumes. Shilow et al (16) have found a linear relation for chlorine over the concentration range of 0.66 to 1.36%

An illuminating way of showing this relation is to plot service time times initial concentration against the initial concentration (figure 34). It is readily seen that the relation

$$c_o T = \text{constant}$$

holds only at concentrations at some minimum value. Arnell (23) has also noted the increase of the product $c_o T$ from zero until it reaches a constant value.

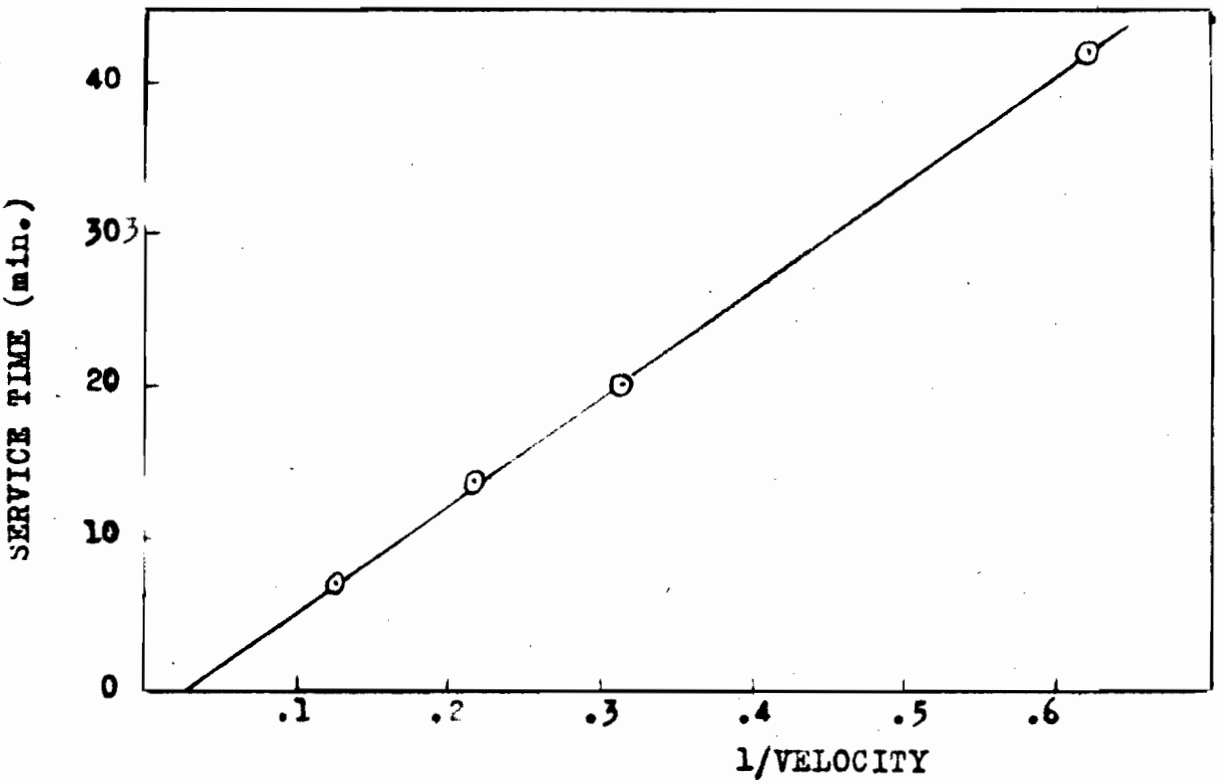

EFFECT OF FLOWRATE ON SERVICE TIME

FIGURE 32.

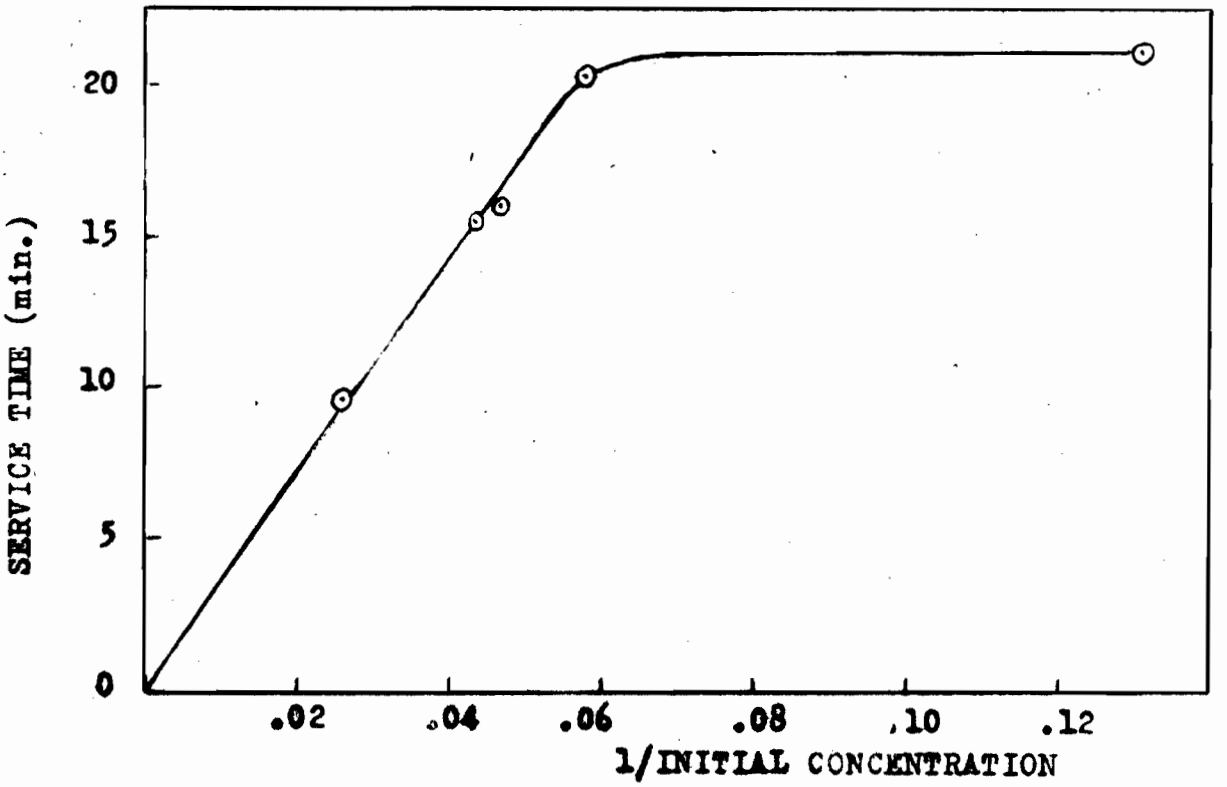

EFFECT OF INITIAL CONCENTRATION ON SERVICE TIME

FIGURE 33.

EFFECT OF INITIAL CONCENTRATION
ON SERVICE TIME

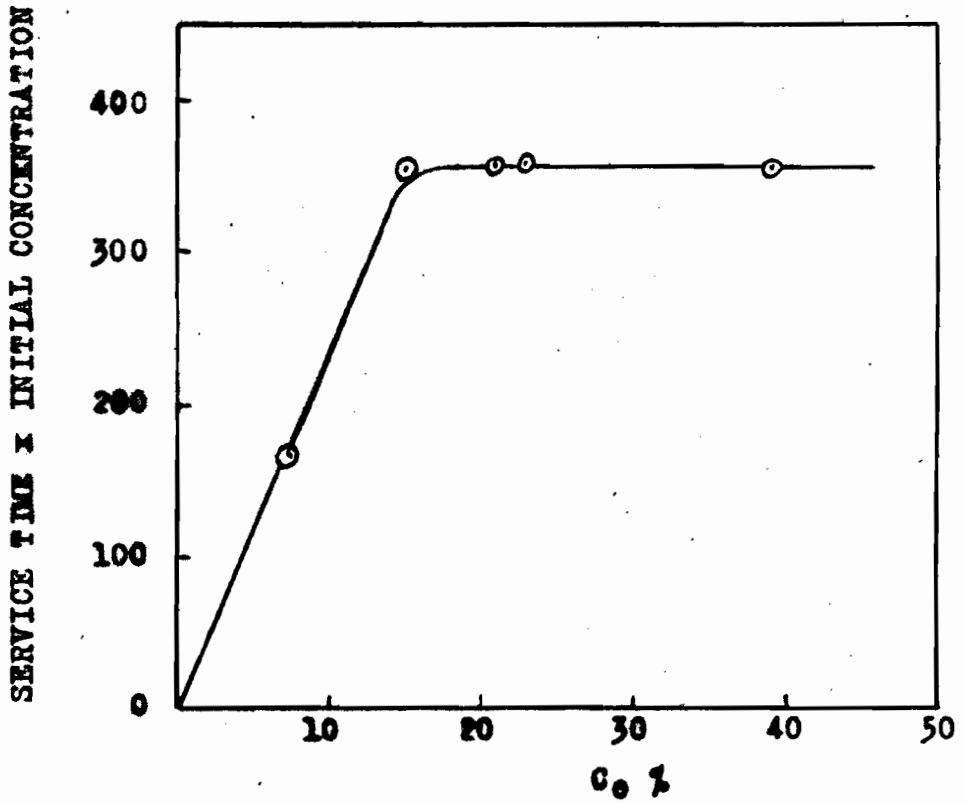

FIGURE 34.

4. Critical Lengths.

These are determined by the intercept of the extrapolated service time-column length curves. Roughly this critical or dead length increases with increase in the air flowrate at constant ammonia rate, and with increased ammonia rate at constant air rate similar to the decrease of the service time with these variables. The long extrapolation necessary in the curves shown in figures 26 and 27, makes the calculation of numerical values for the critical length rather inaccurate.

5. Temperature Data

The temperature rise in the bottom (T_2) and third from the bottom (T_1) centimeter charcoal layers is shown as a function of time for a number of typical cases in figure 35. The temperature rises rapidly in both layers at first to a maximum value and falls more slowly as the charcoal bed is cooled by the gas stream. The maximum temperature rise in the upper layer was found to be greater than that in the bottom layer, presumably due to heat losses by greater contact of the bottom layer with the surroundings.

Table 13 and figure 36 show that the maximum temperature rise is a linear function of the ammonia flowrate at a constant air flowrate. An increase in the air flowrate at constant ammonia rate has a slight cooling effect as shown in figure 37.

The relation between the maximum temperature rise and the linear flowrate is shown in table 14 and figure 38. The increase with increasing flow is due to the increased amount of ammonia sorbed per unit time. The cooling effect of the increased air flow is also shown by the graph.

Since sorption is affected greatly by change in temperature, the effect on the relations given previously is marked. The service time would be decreased where there is an appreciable temperature rise due to the sorption since the length of the working layer would be increased due to the decreased sorption capacity of the charcoal. This would increase the residual activity, and hence also the dead length.

The weight-time curves would slope off more gradually due to the decreased sorption when the bed is heating, and the continuance of sorption as the bed cools down to room temperature. This would increase the saturation time. Since the service time would be decreased and the saturation time increased, the escaping concentration would be lower at any given time.

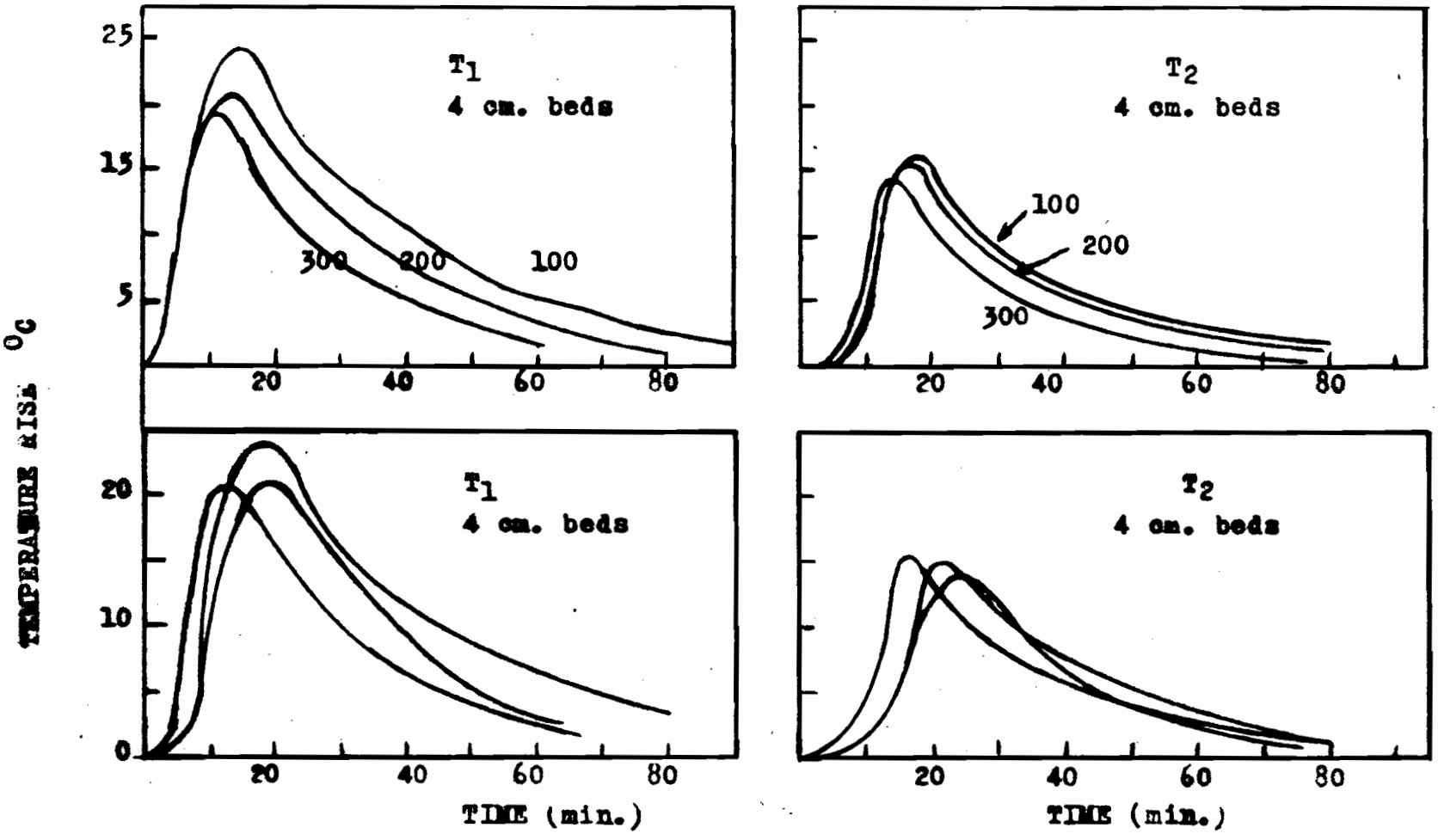

TYPICAL TEMPERATURE CURVES
AMMONIA 60 cc./min
AIR SHOWN

FIGURE35.

Table 13

Maximum Temperature Rise (°C)

NH_3 Rate cc./min.	Air Rate (cc./min.) 0	100	200	300
15			4.5	
42			16	
60	25.5	24.5	21	19.5
100			32	

Table 14

Effect of Flowrate on Maximum Temperature Rise

Velocity cc./min	120	242	360	600
ΔT_1	10.5	19	21	27
ΔT_2	9	12.5	16	19

MAXIMUM TEMPERATURE RISE DATA

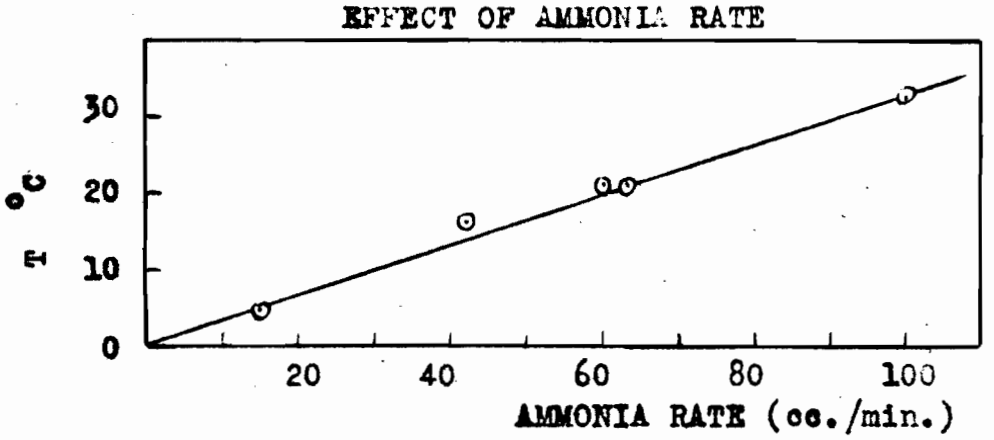

FIGURE 36.

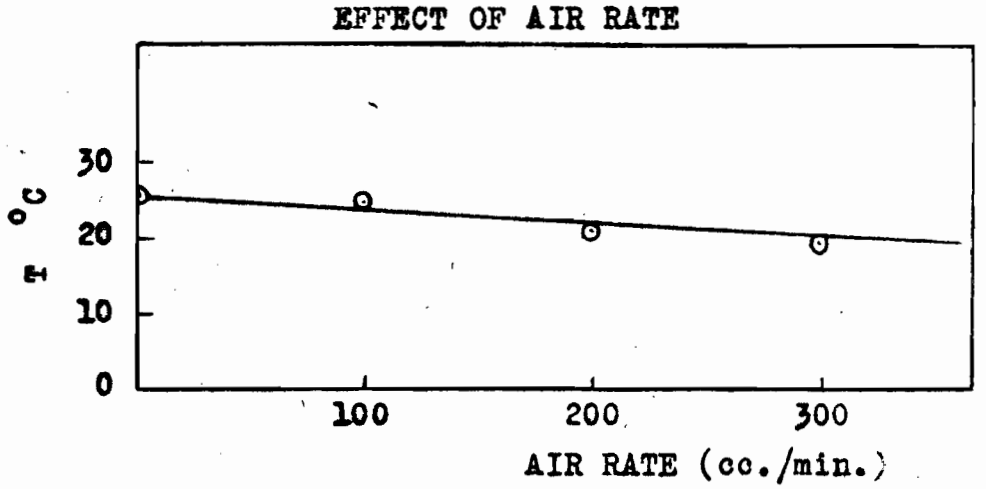

FIGURE 37.

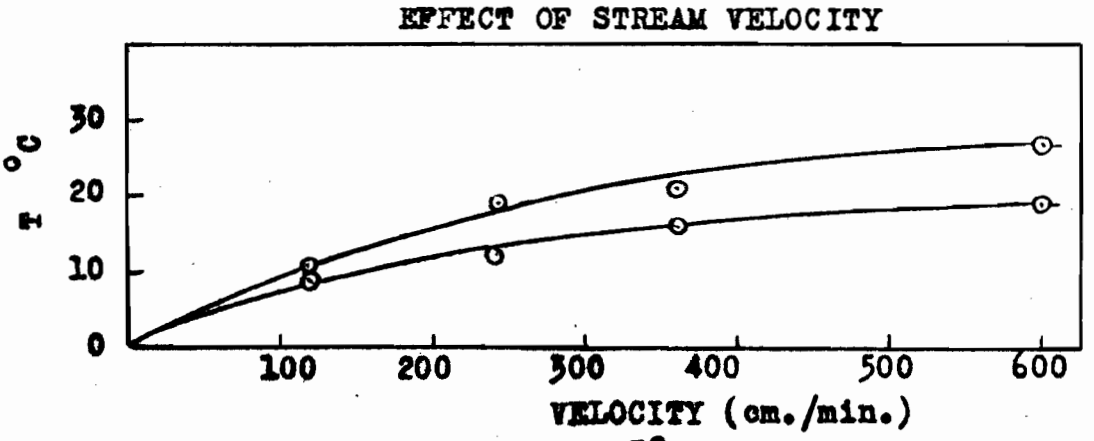

FIGURE 38.

Butane sorption was studied over the concentration range of 3 to 100 parts per thousand, with two runs of pure butane. The butane flowrate was varied from 9 to 71 cc. per minute and the air rate was varied from zero to 3000 cc. per minute. The flowrate was varied from 153 to 3100 cc. per minute. Since the amount sorbed was quite large, the sorption could be studied using short beds; the depths were varied from one to five centimeters.

1. Amount Sorbed

In table 15, the weight sorbed, and x/m data are presented. The height given in column one is the height calculated from the weight of the charcoal bed. The data in the last column give the number of cc. of butane sorbed per minute as determined by the slope of the linear portion of the weight-time curves, (some of which are shown in figures 39 and 40). This portion of the curve, since it depends solely on the rate of supply of the butane, should have a slope equal to the butane rate as indicated in column three. Here, as in the ammonia sorption, this difference is due to the air displaced from the charcoal.

In figure 39, the weight-time curves as determined directly from the weight readings, are presented. As in the case of ammonia sorption, the charcoal is 100% efficient until the service time when the curve ceases to be linear and butane is present in the effluent gas stream. The curve then bends to a horizontal straight line which is the saturation weight under those conditions. It will be noted that the curvature of these curves is more rapid than those found for ammonia. This is partly due to the more rapid removal of the heat of sorption by the greater air flow used in the butane sorption.

Table 15

Weight Sorbed and x/m Data.

Height (cms.)	Air Rate (cc./min.)	Butane Rate (cc./min.)	Partial Press. (min. Hg.)	Weight (grams)	x/m (cc./gm.)	Slope (cc./min.)
4.08	3130	53	12.7	4.32	62.0	51.6
1.94	3020	53	13.2	2.07	63.0	51.5
5.01	1590	53	24.5	5.80	68.0	51.5
4.09	1530	53	24.5	4.73	68.0	51.5
2.96	1520	53	24.5	3.43	68.0	51.5
2.13	1530	53	24.5	2.47	68.0	51.5
1.19	1520	53	24.5	1.38	68.0	51.5
3.96	500	53	72.8	5.26	78.1	51.4
3.95	0	71	760	5.98	89.2	69.1
4.12	0	53	760	6.26	89.2	51.5
4.00	3020	71	17.4	4.42	65.0	69.0
3.70	3020	30	7.5	3.60	57.2	29.0
2.18	3020	30	7.5	2.12	57.2	29.0
4.23	3045	24	5.7	3.96	54.9	22.6
4.16	3040	9	2.3	3.13	44.3	8.7
2.12	3000	9	2.3	1.66	45.1	8.8
1.27	3020	9	2.3	0.96	44.3	8.7
4.01	1500	30	15.0	4.34	63.7	29.0
2.09	1500	30	15.0	2.27	63.7	29.0
3.99	1403	30	15.9	4.26	62.6	29.0
3.88	151	2.7	13.7	4.20	63.7	2.5

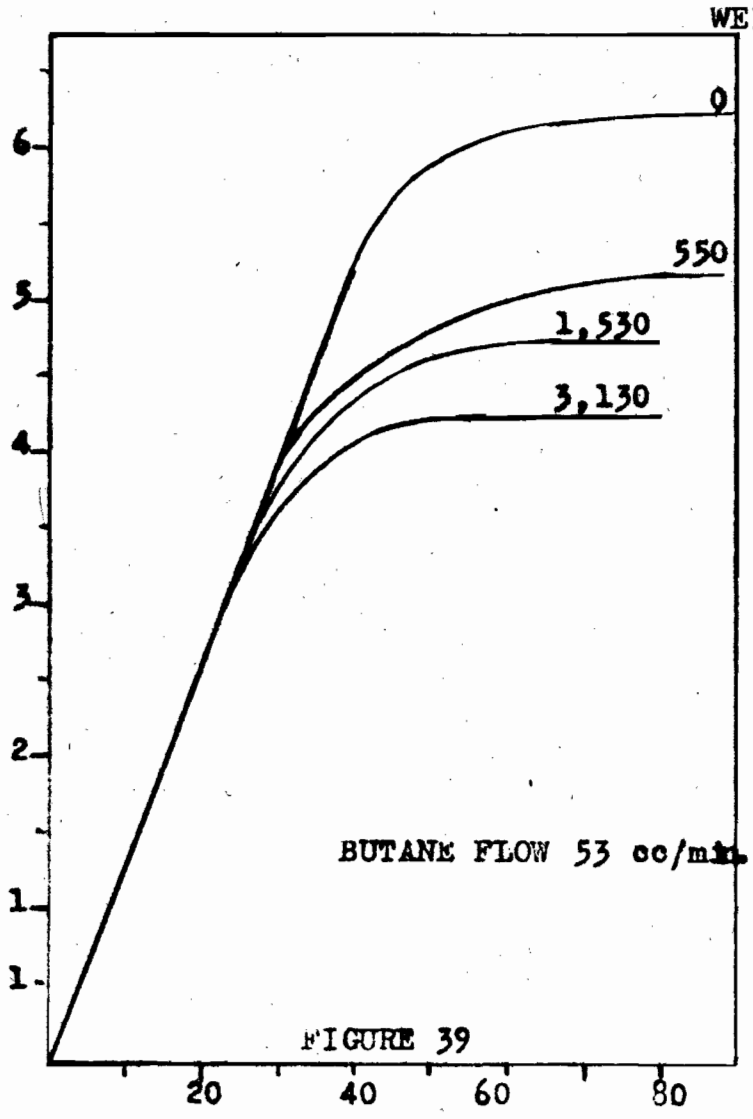

FIGURE 39

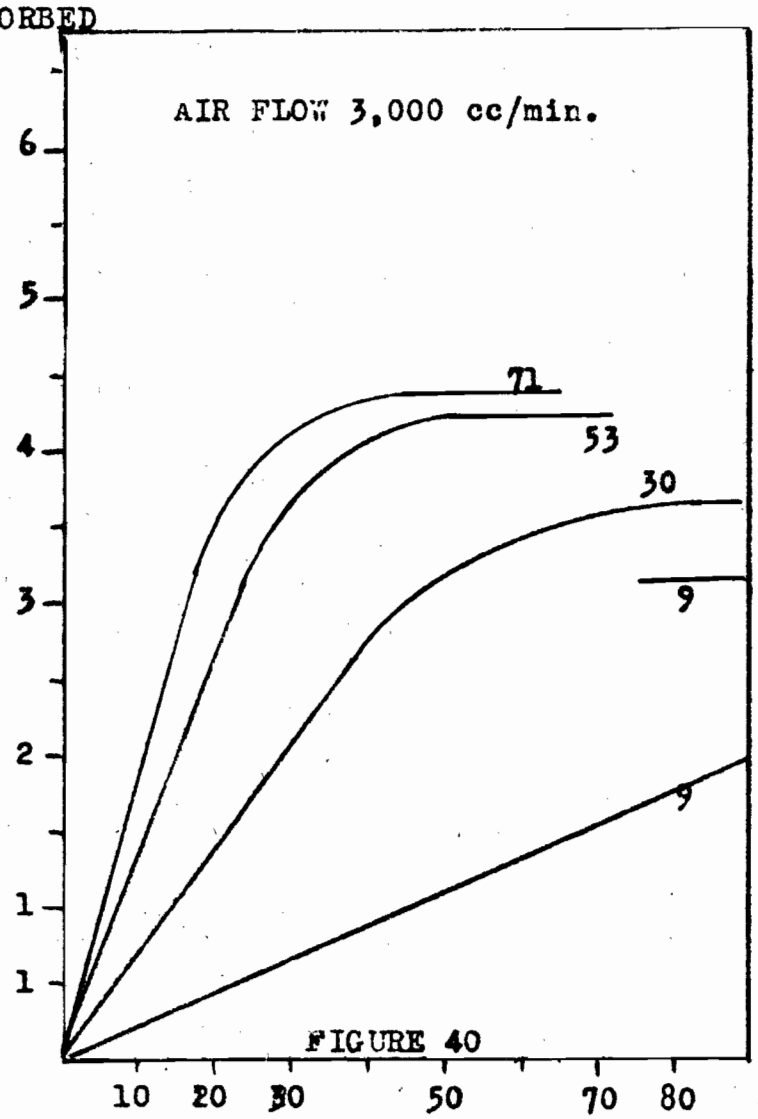

FIGURE 40

It is seen from the curves that the air rate has no effect on the initial slope, but that the final value increases as the air flow-rate is decreased.

In figure 40 a similar set of curves are shown with a constant air rate and variable butane rate. Here the slope of the straight line portion of the curve is not the same but depends on the butane rate. The saturation value increases as the butane flow is increased.

Figure 41 shows the variation in x/m (cc.'s per gram) due to the increased air rate. A smooth curve is obtained which decreases from the maximum value at zero air flow. The logarithm of x/m plotted against the logarithm of the air rate gives straight lines which converge. These are shown in figure 42.

The effect of butane concentration on x/m is shown in figure 43. Since the total flow rate is approximately constant, varying from about 3030 to 3090 cc. per minute, the partial pressure could be plotted instead of the flowrate. The logarithmic relation is shown in figure 44. Here the relation is linear for high butane concentrations but falls off for the low butane concentrations. This shows that log x/m varies directly as the logarithm of the initial concentration.

Figure 45 shows the complete curve of x/m against partial pressure of butane up to 760 mm. of Hg. This curve does not follow one Langmuir or Freundlich isotherm over its whole course, different pressure ranges require different isotherms. A portion of the curve for partial pressure below 70 mm. of Hg. is shown plotted on a larger scale in figure 46. The experimental points are not more than one division from the curve drawn which indicates that, in this respect at least, the experimental error is about $\pm$ 1% .

The curve shown rises steeply at first and then flattens off quite rapidly to a constant value of x/m. This behaviour is in contrast with that

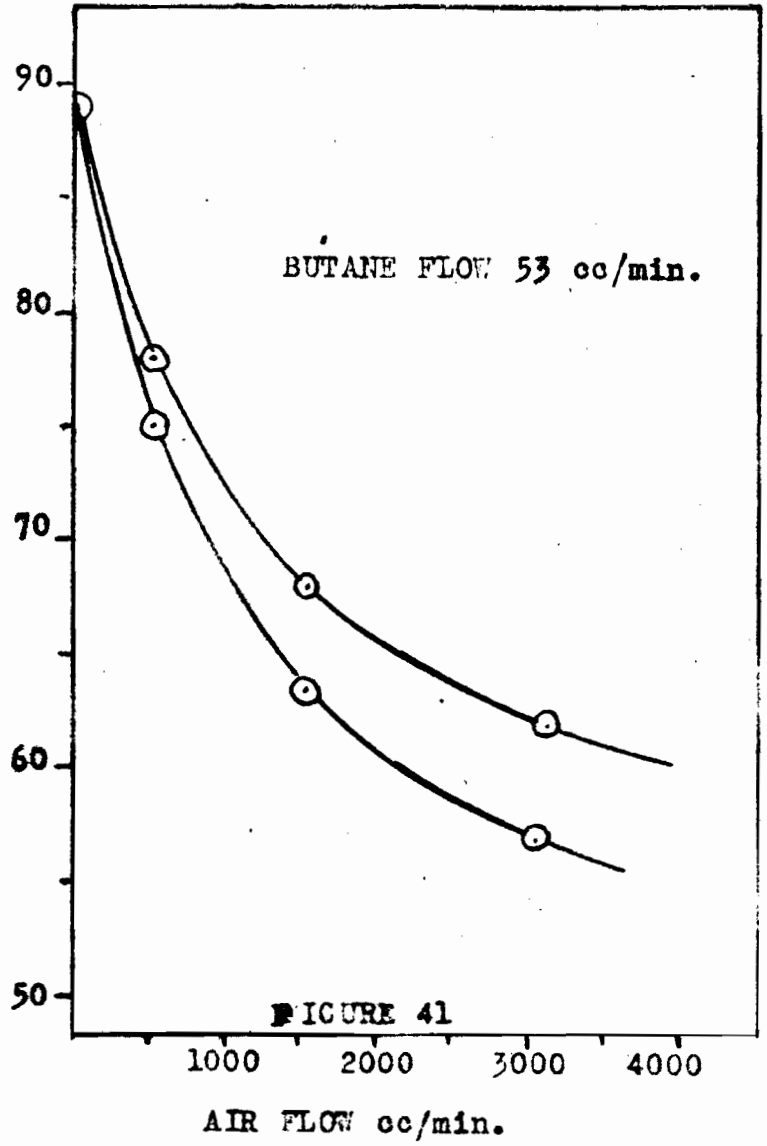

FIGURE 41

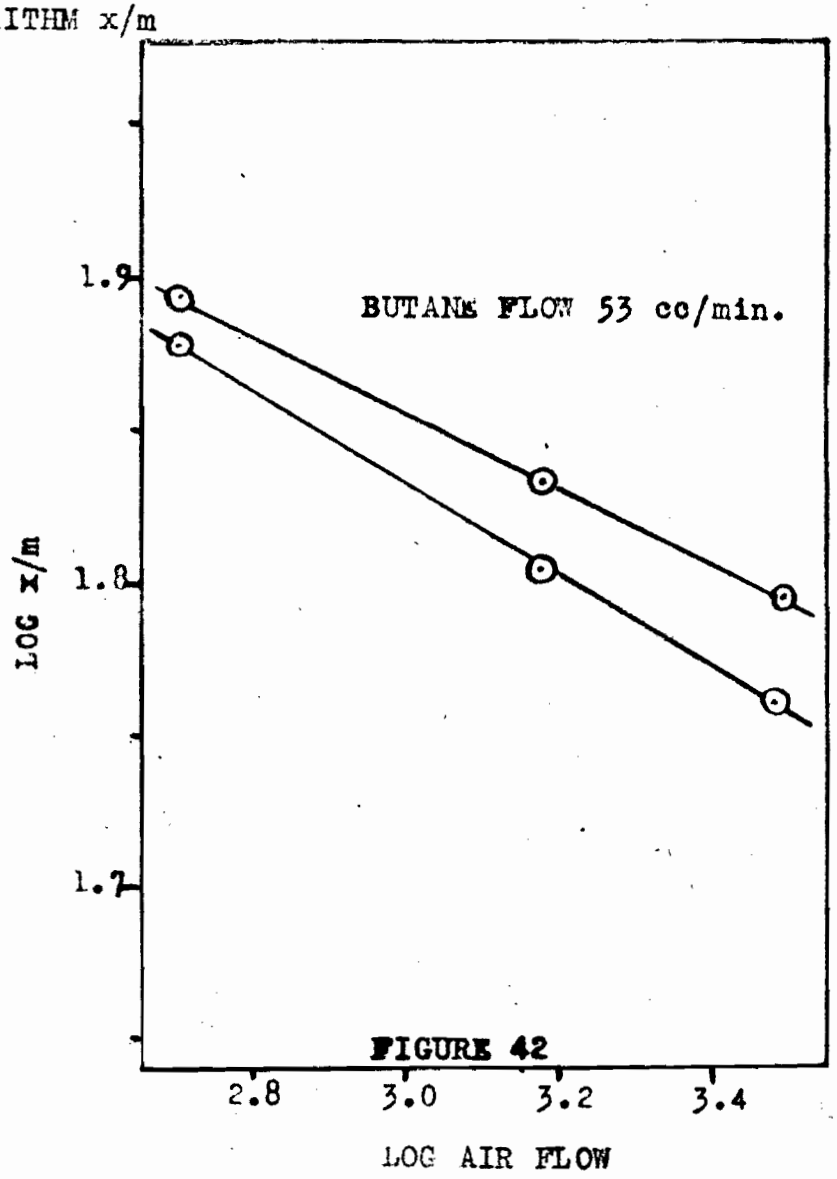

FIGURE 42

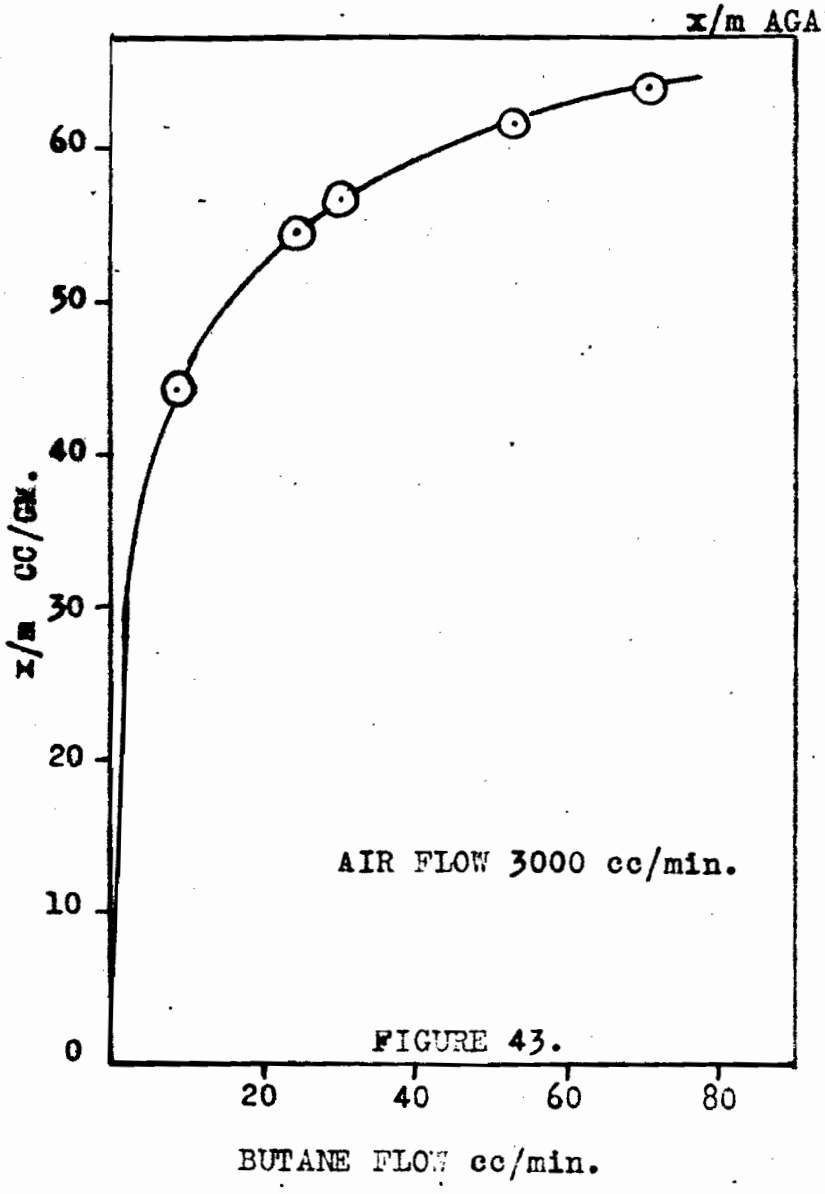

FIGURE 43.

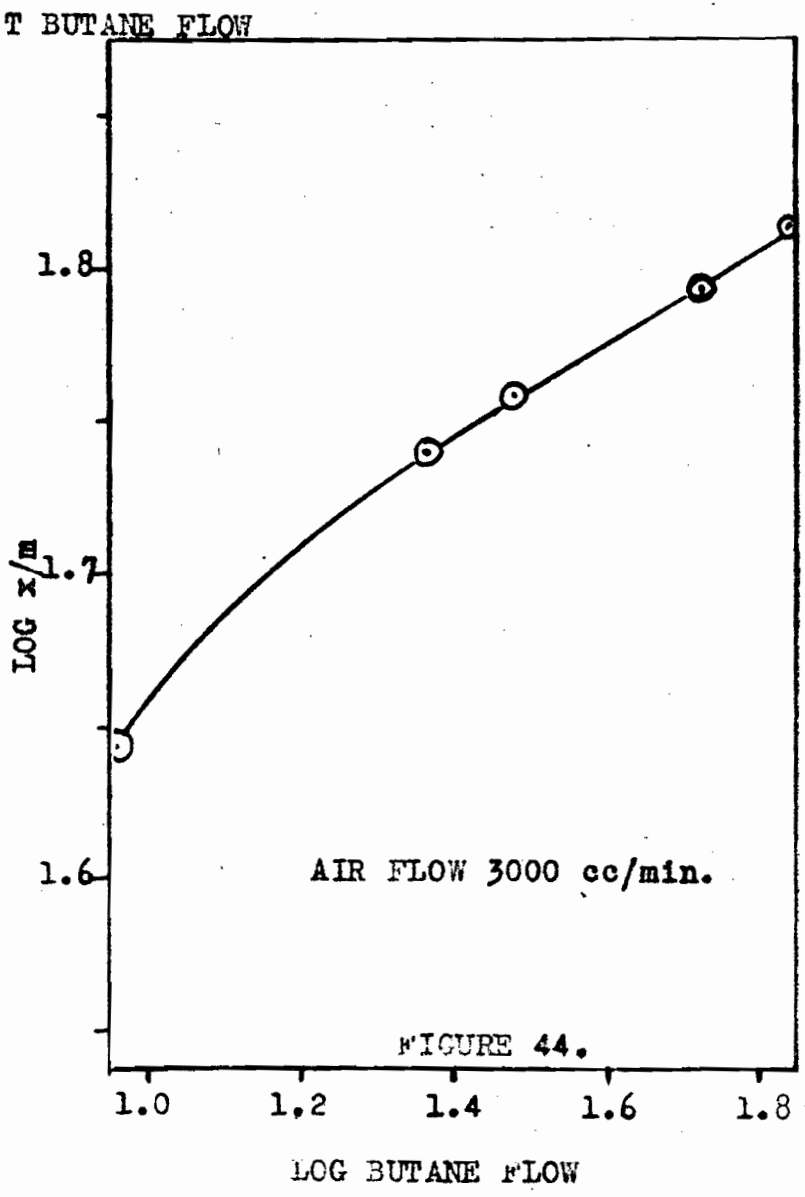

FIGURE 44.

SORPTION ISOTHERM OF BUTANE

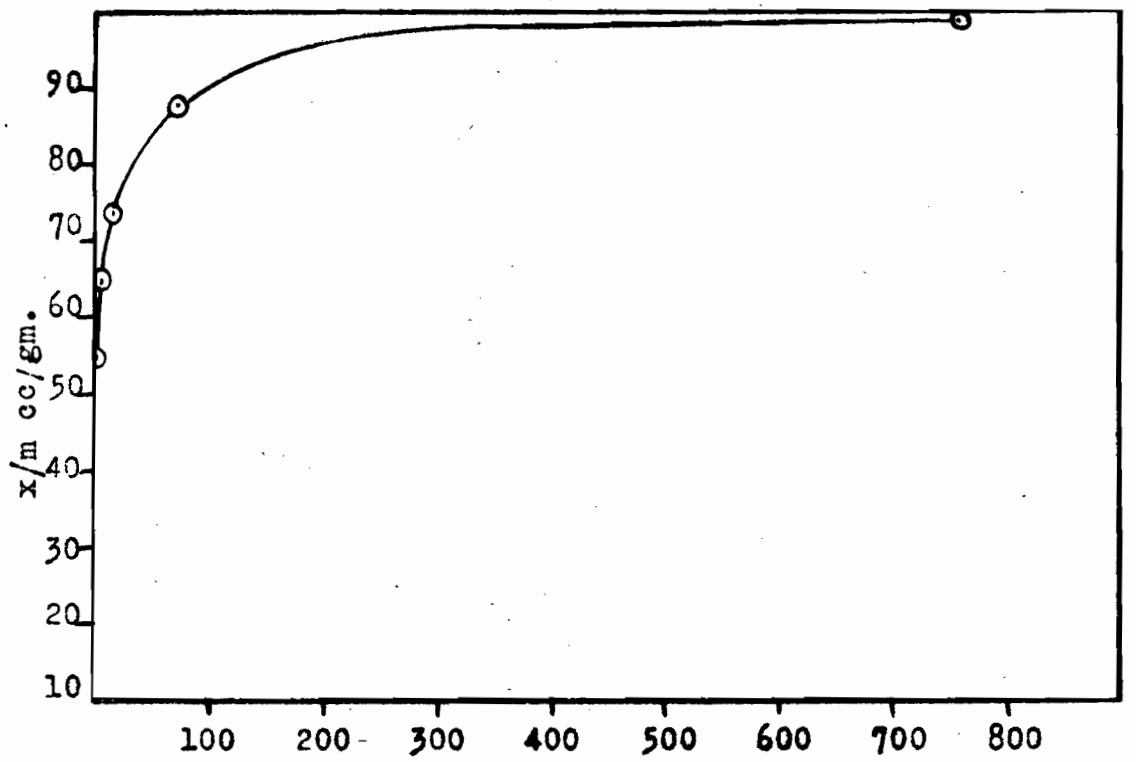

FIGURE 45.

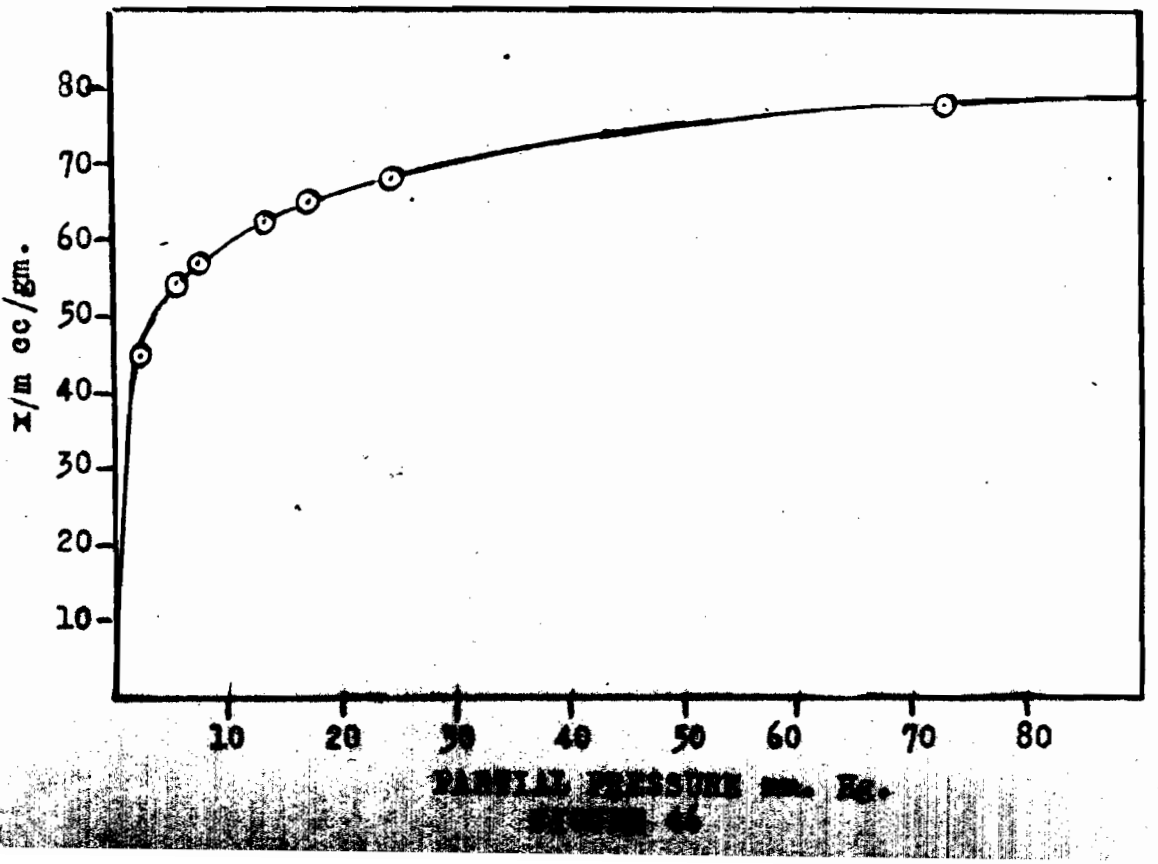

of ammonia, where the partial pressure curve was linear, rising towards the right, and did not reach a maximum value in the pressure range studied. This would indicate a different type of sorption mechanism in the two cases.

This difference is also shown in figure 47 where the logarithm of x/m is plotted against the logarithm of the partial pressure. This does not give the straight line relation found for ammonia sorption.

As in the case with ammonia, flowrate had no effect on the value of x/m in the ranges investigated, from 153 to 3180 cc. per minute.

In figure 48 the curve of cc. per minute calculated from the slope of the initial portion of the weight against time curves against actual butane rate (as found by analysis) was plotted. A straight line relation was obtained. The difference between the calculated and actual value is approximately the same as that found for ammonia, e. g. at 60 cc. per minute flowrate of sorbate, the difference for ammonia is 7.5 cc. per minute while that for butane is 2 cc. per minute. On a weight basis these correspond to 7.5 x 17 = 127 for ammonia (using the molecular weight) and 2 x 58 = 116 for butane. The difference in these two figures is well within the experimental error in determining the flowrates.

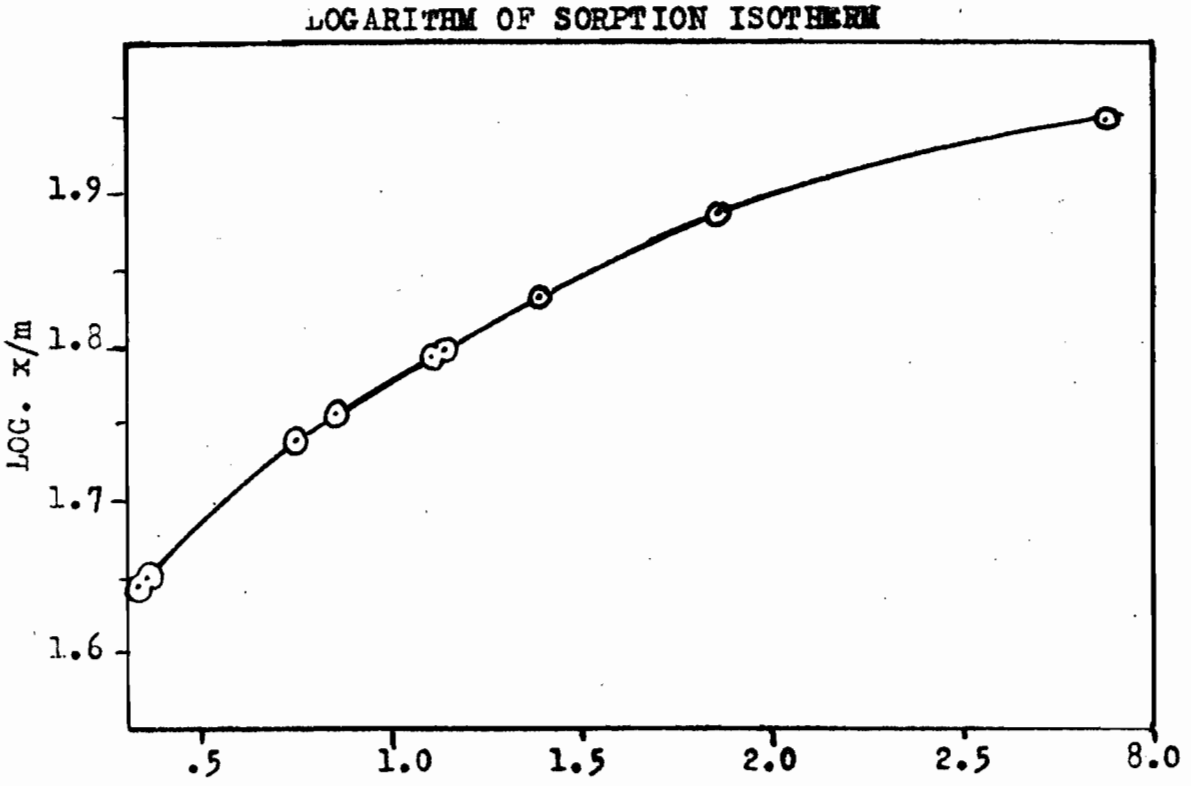

FIGURE 47.

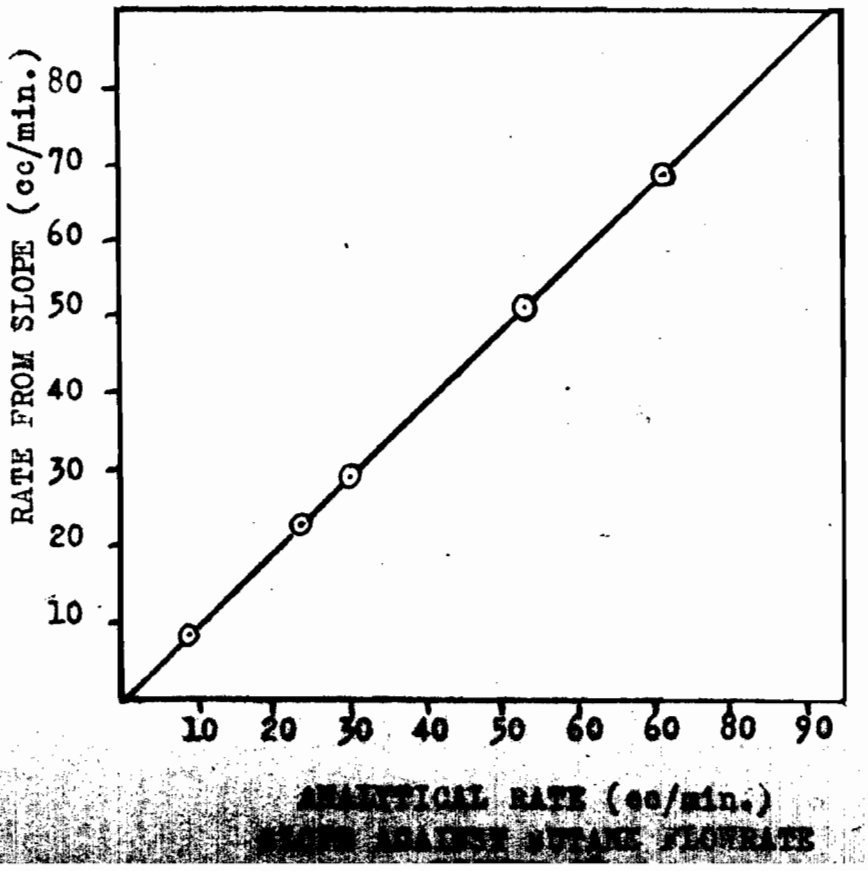

BUTANE FLOWRATE

2. Analytical Data

The data for the following sets of curves, figures 49 to 52 inclusive are not presented since they are too extensive. The curves, however, indicate the data adequately.

These curves are plots of grams of sorbate per minute against time. The curve starting from zero is the analytical curve of the effluent gases. The curve starting from the top is that obtained by differentiating graphically the weight-time as was indicated in the ammonia results. The analytical curve reaches a higher value than the differential curve due to the air displaced from the charcoal.

In figure 49, the curves obtained from the 5 bed depths of the 53 cc. per minutes butane rate, 1520 cc. per minute air rate runs, are shown. The curves are horizontal until the service times are reached, then break off rapidly and curve exponentially to a final horizontal line. The shape of the curves are similar after the first centimeter bed. In the one centimeter bed, the break is not so sharp but soon assumes a shape similar to the others.

The analytical curves, as will be shown later, can be used to determine the concentration gradients of the sorbate air stream throughout a five centimeter bed since the exit gas is, in fact, the gas that is in the working layer of the charcoal bed.

Figure 50 shows the analytical, differential sorption curves for 3000 cc. per minute air flow, four centimeter bed depths, and varying butane concentrations. It is seen that the initial slope of these curves is decreased as the butane concentration is decreased.

Figure 51 shows the effect of air rate on the curves. These are for a constant butane flow of 53 cc. per minute and 4 centimeter beds. The

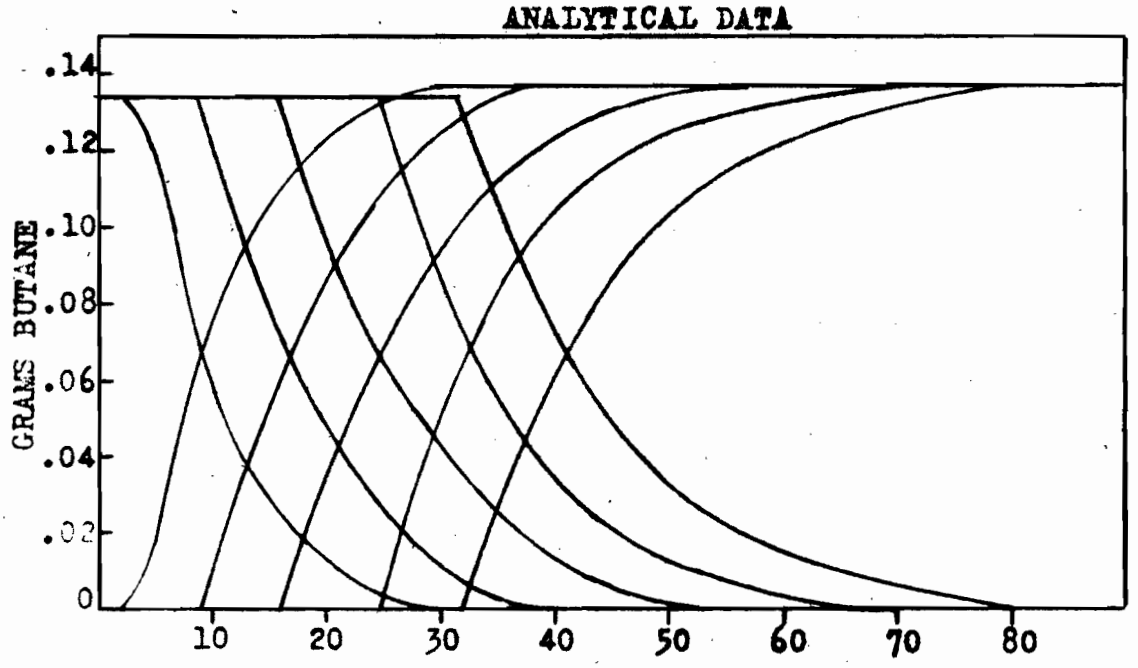

CONSTANT FLOW AND CONCENTRATION

FIGURE 49.

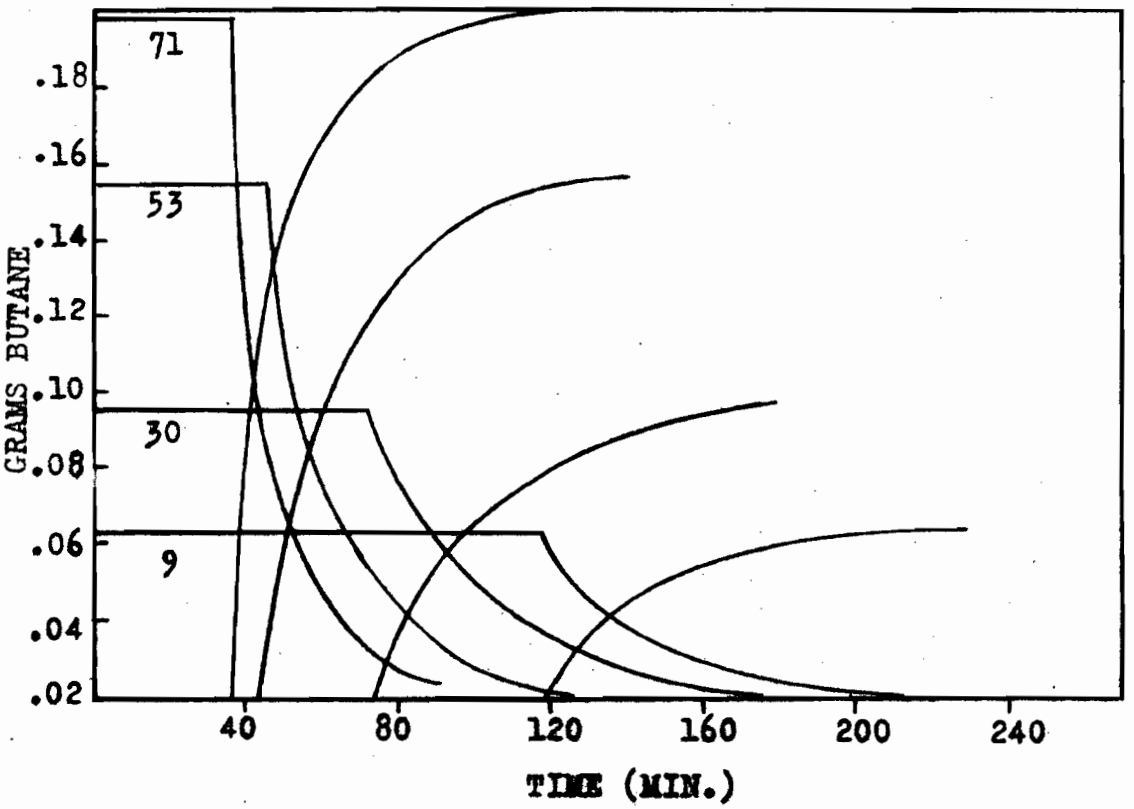

VARIABLE BUTANE CONSTANT AIR FLOW

FIGURE 50.

ANALYTICAL DATA

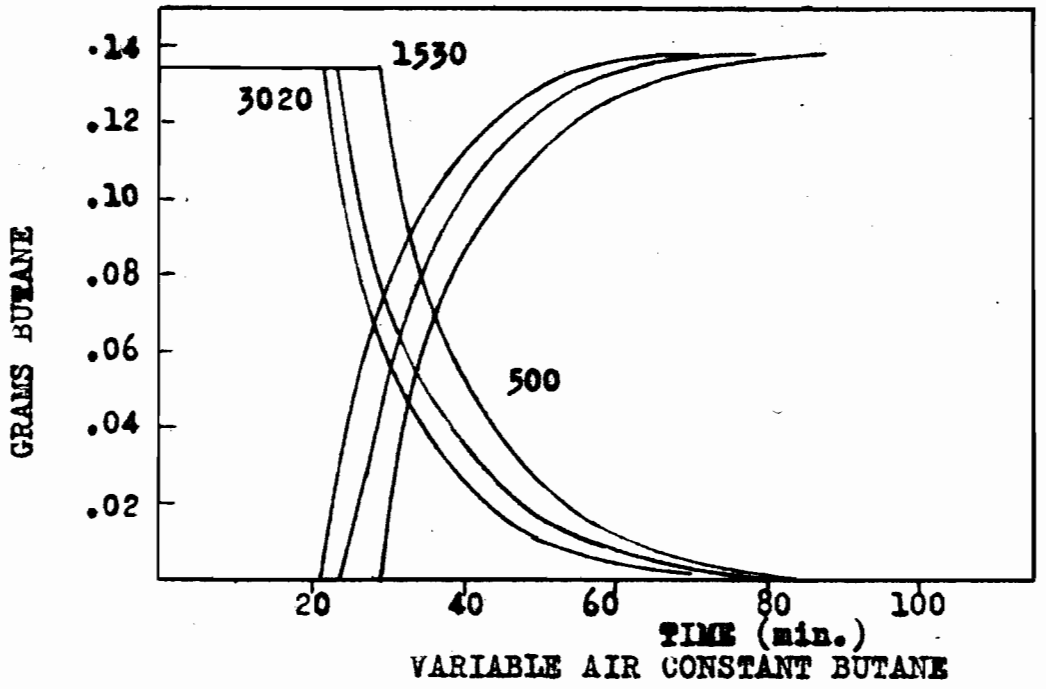

VARIABLE AIR CONSTANT BUTANE

FIGURE 51.

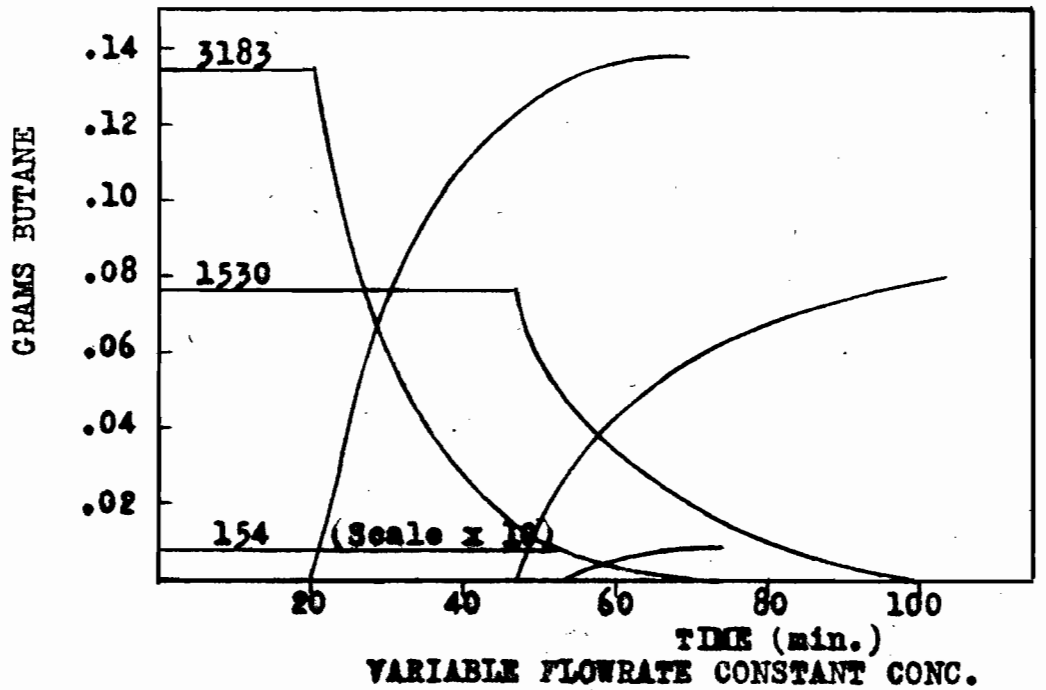

VARIABLE FLOWRATE CONSTANT CONC.

FIGURE 52.

shapes of the curves are not affected by the air rate except that the breaking point is shifted to higher times with decreased air flow.

The analytical and differential sorption curves for variable flow-rate and constant concentration are shown in figure 52. The partial pressure of the butane in the entering gases is 13.8 mm. of Hg. and the flowrate is varied from 154 to 3183 cc. per minute. The rate of change of these curves is decreased with decreased stream velocity. Thus the curves from the service time to completion for the 3183 cc. per minute rate extend over 50 minutes, while for the 154 cc. per minute they extend over 200 minutes. The weight per minute of butane is changed for the three runs since the partial pressure is constant.

The data for the relation of escaping concentration as a function of time are shown in table 16. These are the data obtained from one run, all other runs gave similar data. The time axis is started at the service time, setting it equal to zero. The concentration of the escaping gases is expressed as grams of butane per minute.

In figure 53, the logarithm of the reciprocal of the concentration of the escaping gases is plotted against time. A curve is obtained that is not linear, in contrast with the prediction of Danby et al. However they state that the straight line relation only holds when $c_o/$ is large; i. e. in the early stages of breakdown. It is seen that this is approximately true for the first few minutes. If the logarithm of the escaping concentration is plotted against the reciprocal of the time, a straight line relation is obtained as shown in figure 54.

Table 16

Escaping Concentration as a Function of Time.

(Butane rate = 53 cc./min.; Air rate = 1500 cc./min. Bed depth: 5 cms.)

Time (mins.) (Setting Service Time equal to Zero)	Concentration of escaping gases	log. c	log 1/c	1/T
0	0			
3.5	0.031	$\bar{2}.491$	1.509	0.286
8.5	0.062	$\bar{2}.792$	1.208	0.118
13.5	0.085	$\bar{2}.929$	1.071	0.0740
18.5	0.102	$\bar{1}.009$	0.991	.0540
23.5	0.116	$\bar{1}.065$	0.935	.0425
28.5	0.122	$\bar{1}.086$	0.914	.0349
33.5	0.129	$\bar{1}.110$	0.890	.0298
38.5	0.133	$\bar{1}.124$	0.876	.0260
43.5	0.136	$\bar{1}.134$	0.866	.0230
48.5	0.137	$\bar{1}.137$	0.863	.0205

ESCAPING CONCENTRATION

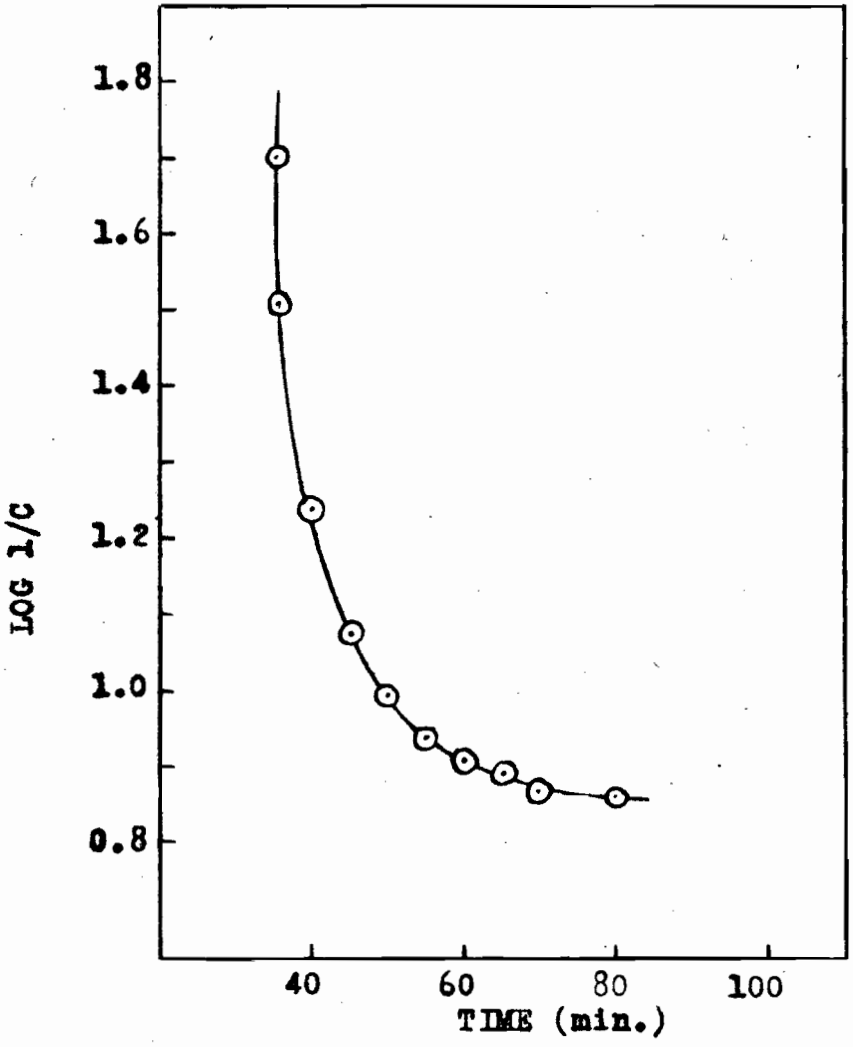

FIGURE53

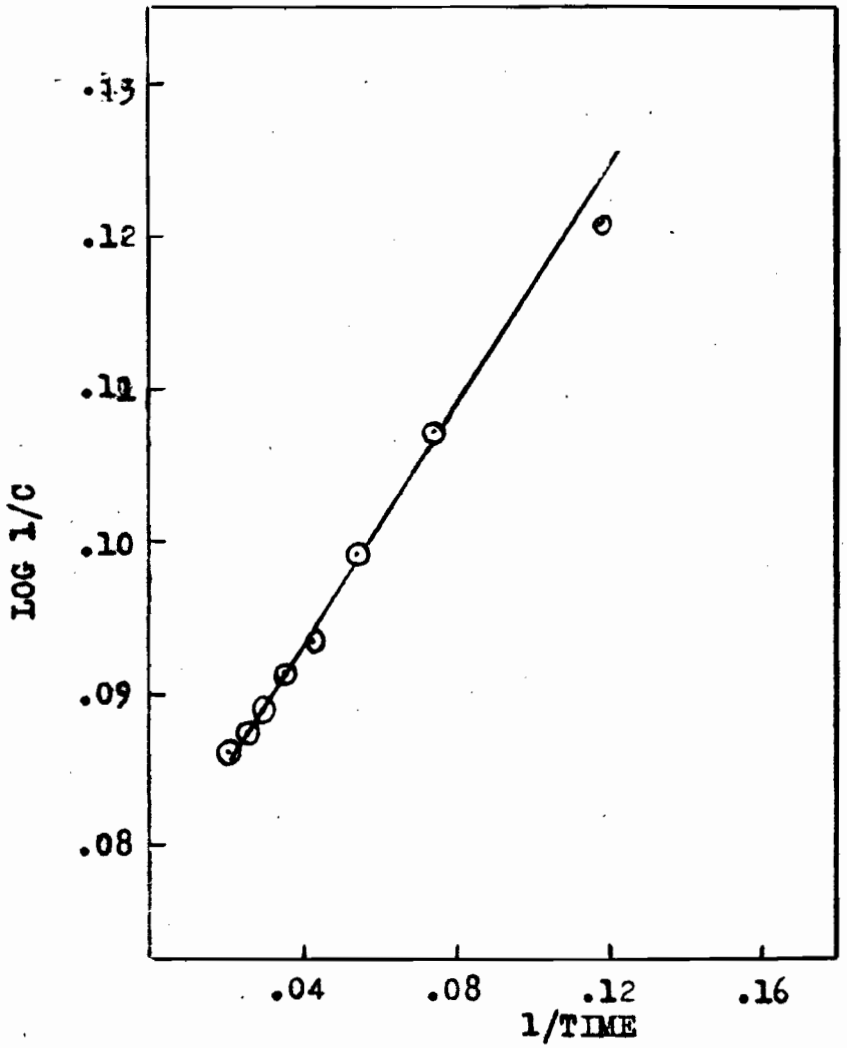

FIGURE 54.

3. Service Time Data.

The service time was taken as the break in the linear portion of the weight-time curves as in the case of ammonia. The data for the service time relations are given in Table 17. Here the first four columns are the same as those in table 15. In column 5 the observed service time is given while in column 6 the corrected service time is given.

Figure 55 shows the service time-column length relation for constant butane flowrate and variable air flowrate. Figure 56 shows similar curves for constant air flow and variable butane flowrates. The straight lines intersect at a common point off the graph, except for a high air rate and a low butane rate. The various critical lengths for these variables can be determined from these graphs. Here again the bed lengths used were too long to show the curvature of the graph towards the origin as described in ammonia.

In figure 57, the service times for a four centimeter bed and constant butane flow are plotted against air rate. The service time decreases from its maximum value at zero air rate but the rate of decrease becomes small at high air flowrates. The logarithm of the service time is plotted against the logarithm of the air rate in figure 58, and a linear relation is obtained.

The effect of varying the butane rate at constant air rate and constant bed length is shown in figure 59. The partial pressures corresponding to the butane flowrate are also shown. These determinations were made essentially at constant flowrate since the effect of changing the butane rate on the total flow is negligible. The relation of the logarithm of the service time and the logarithm of the butane rate is shown in figure 60. A linear relation was found. This is in contrast with the relation between ammonia rate and service time found in the previous section. In that case the logarithm

Table 17

Service Time Data

Height	Air Rate	Butane Rate	Partial Press.	Service Time	Corr. S. T.
4.08	3130	53	12.7	22.0	21.5
1.94	3020	53	13.2	7.0	7.5
5.01	1590	53	24.5	31.5	31.0
4.09	1530	53	24.5	24.5	24
2.96	1520	53	24.5	16.5	16.0
2.13	1530	53	24.5	9.0	8.0
1.19	1520	53	24.5	2.0	0.2
3.96	500	53	72.8	29.0	29.5
3.95	0	71	760	25.0	25.5
4.12	0	53	760	40.0	38.5
4.00	3020	71	17.4	17.5	17.5
3.70	3020	30	7.5	37.0	39.0
2.18	3020	30	7.5	19.0	16.0
4.23	3045	24	5.7	53.0	49.5
4.16	3040	9	2.3	129	123
2.12	3000	9	2.3	62.0	61.0
1.27	3020	9	2.3	34.0	30.5
4.01	1500	30	15.0	47.0	47.0
2.09	1500	30	15.0	21.5	20.5
3.99	1403	30	15.9	48.0	48.0
3.88	151	2.7	13.7	540	558

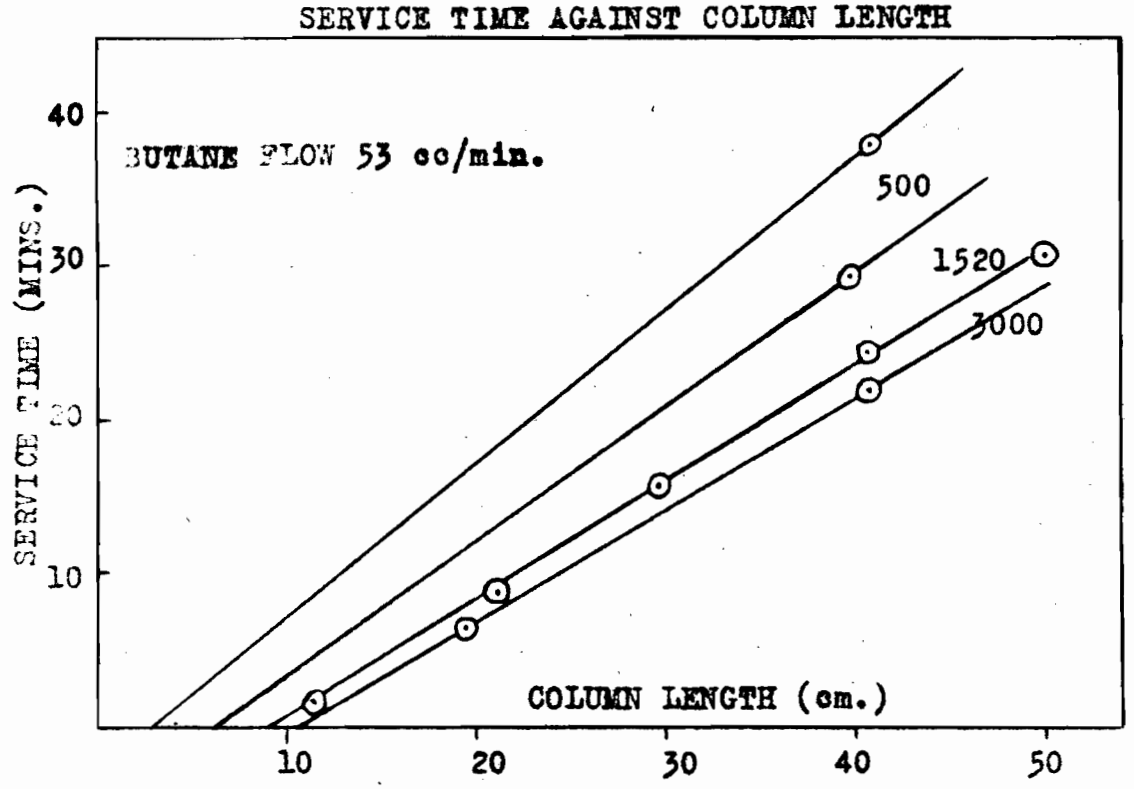

VARIABLE AIR CONSTANT BUTANE FLOW
FIGURE 55

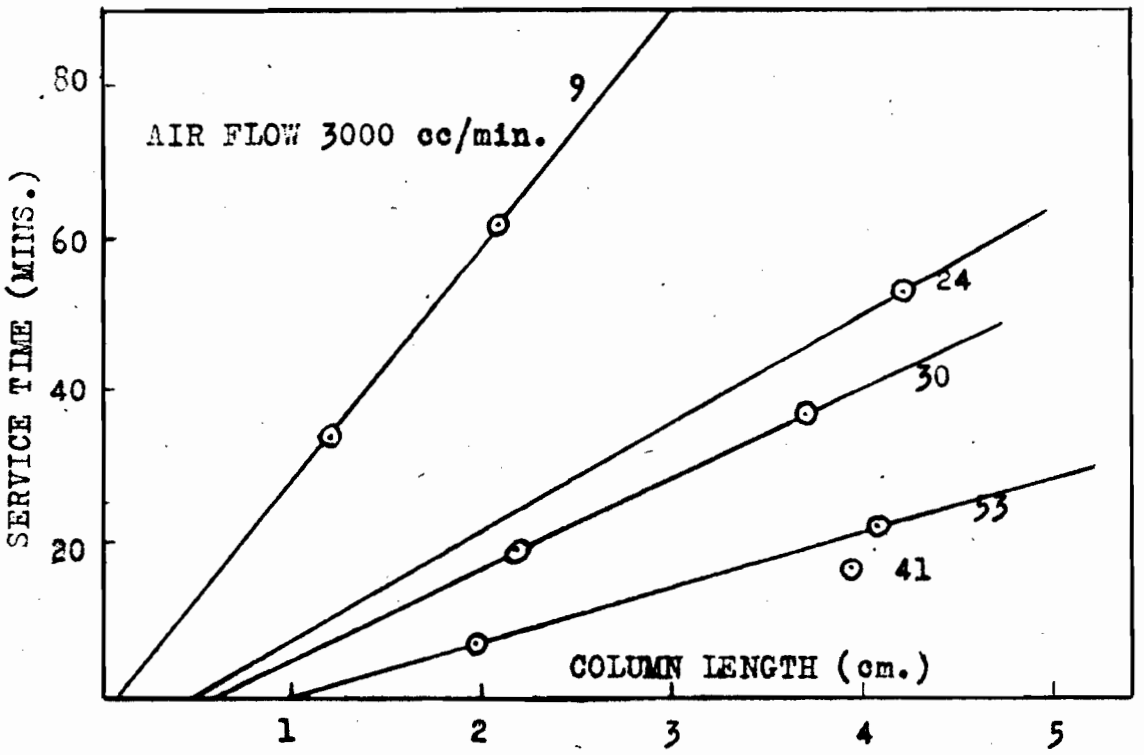

VARIABLE BUTANE CONSTANT AIR FLOW
FIGURE 56

SERVICE TIME AGAINST AIR RATE

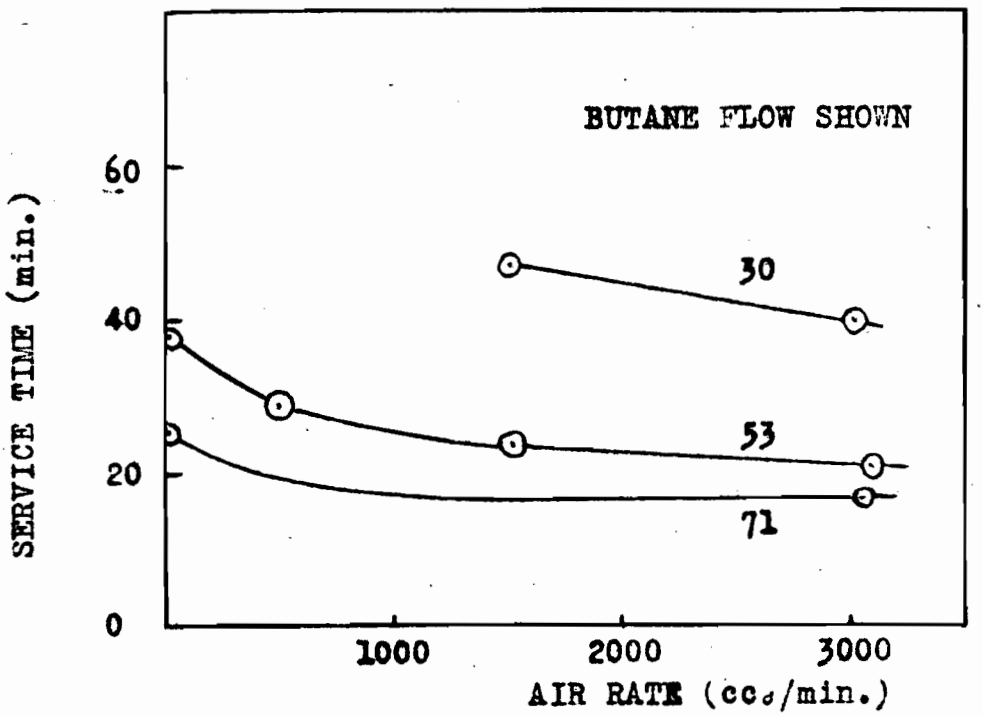

FIGURE 57.

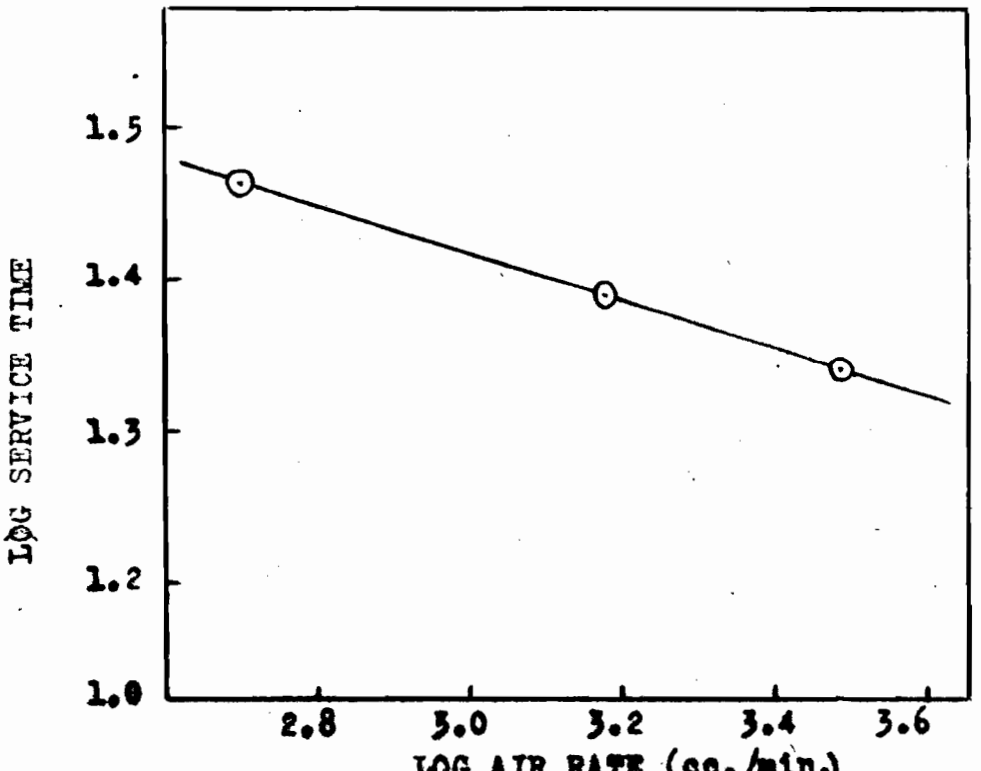

FIGURE 58.

SERVICE TIME AGAINST BUTANE RATE

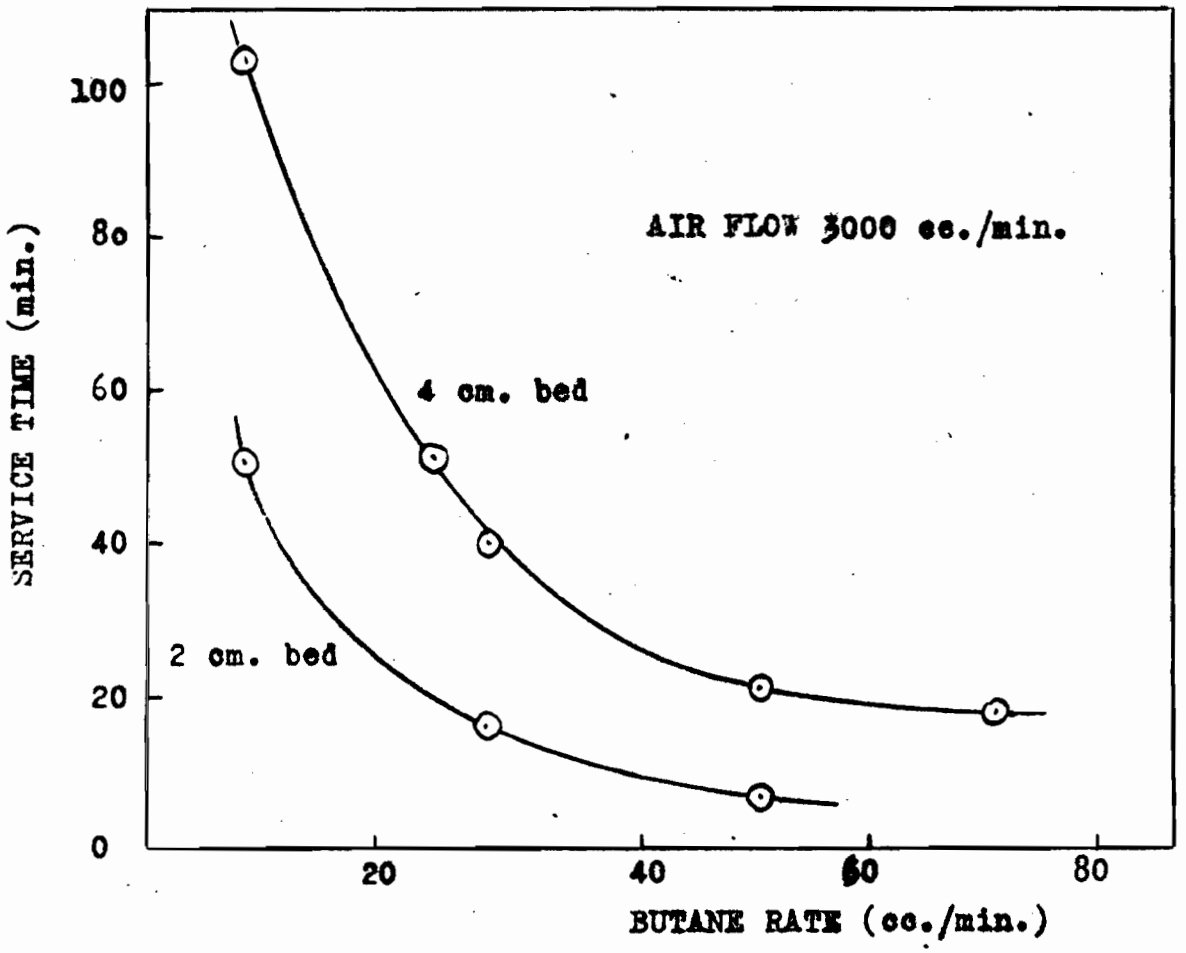

FIGURE 59.

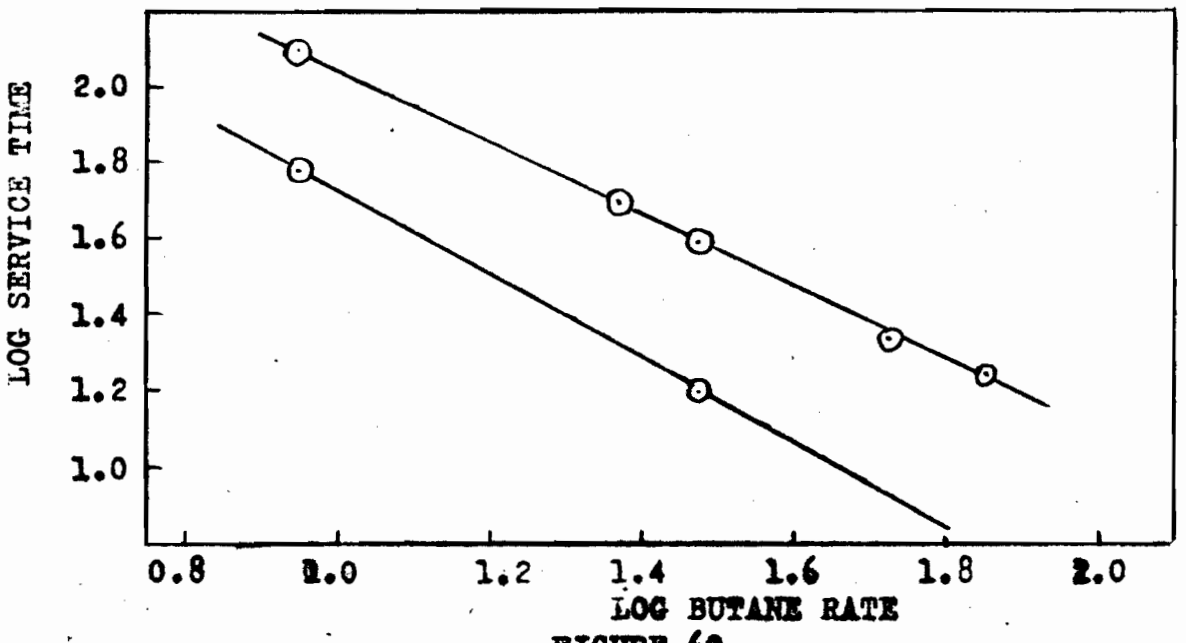

FIGURE 60.

of the service time plotted against the ammonia rate gave a straight line.

The theory of Danby et al and of Mecklenberg predicts that the service time varies inversely as the initial concentration for low concentrations. The date for the plot of service time against the reciprocal of the initial concentration are given in table 18. The plot of service time against $1/c_o$ is shown in figure 61 and a straight line is obtained which is in agreement with the Danby et al and Mechlenberg predictions. It is seen that the relation is followed within the error of the experiment. The abrupt curve that was found in the plot of ammonia concentration against $1/c_o$ is not seen in the concentration range studied here. The value obtained by multiplying the concentration and the service time, is approximately constant in agreement with the results of Shilow et al (16).

The data showing the effect of flowrate are shown in table 19. The concentration here is approximately constant and a four centimeter bed was used. The curve of service time against flowrate is shown in figure 62. The service time decreases rapidly with increase in flowrate at first, the effect is not so marked at flowrates greater than 1500 cc. per minutes.

The velocity of the gas stream through the cell is calculated from the rate (cc. per minute) and the cross-section of the cell. No attempt was made to determine the reduction in cross-section due to the presence of the charcoal. The service time was plotted against the reciprocal of the velocity in figure 63. A straight line relation is obtained which is in agreement with the equation of Danby et al,

$$T = \frac{M_e \lambda}{c_o}\left(\frac{1}{L} - \frac{1}{L_c}\right)$$

The critical flowrate, L_c, for the butane concentration used here as found by extrapolation of the straight line to the axis, is 10,000 cms. per second. This value, however, was not tested experimentally. This relation is also in agreement with Mecklenberg's theory.

Table 18

Service Time as a Function of Initial Concentration

Air Rate cc./min.	Butane Rate cc./min.	Initial Concen. (c_o) %	$1/c_o$	Corrected Service Time (min.)
3040	9	0.296	3.38	123
3045	24	0.788	1.27	49.5
3020	30	0.995	1.007	39.0
3020	53	1.695	0.590	21.5
3020	71	2.300	0.435	17.5

Table 19

Effect of Flowrate on Service Time

Air Rate cc./min.	Butane Rate cc./min.	Total Flow cc./min.	Velocity (L) cms./sec.	Corrected Service Time	1/L
151	2.7	154	12.22	558	.0818
1500	30	1530	121.4	47	.00823
3130	53	3183	252.4	21.5	.00396

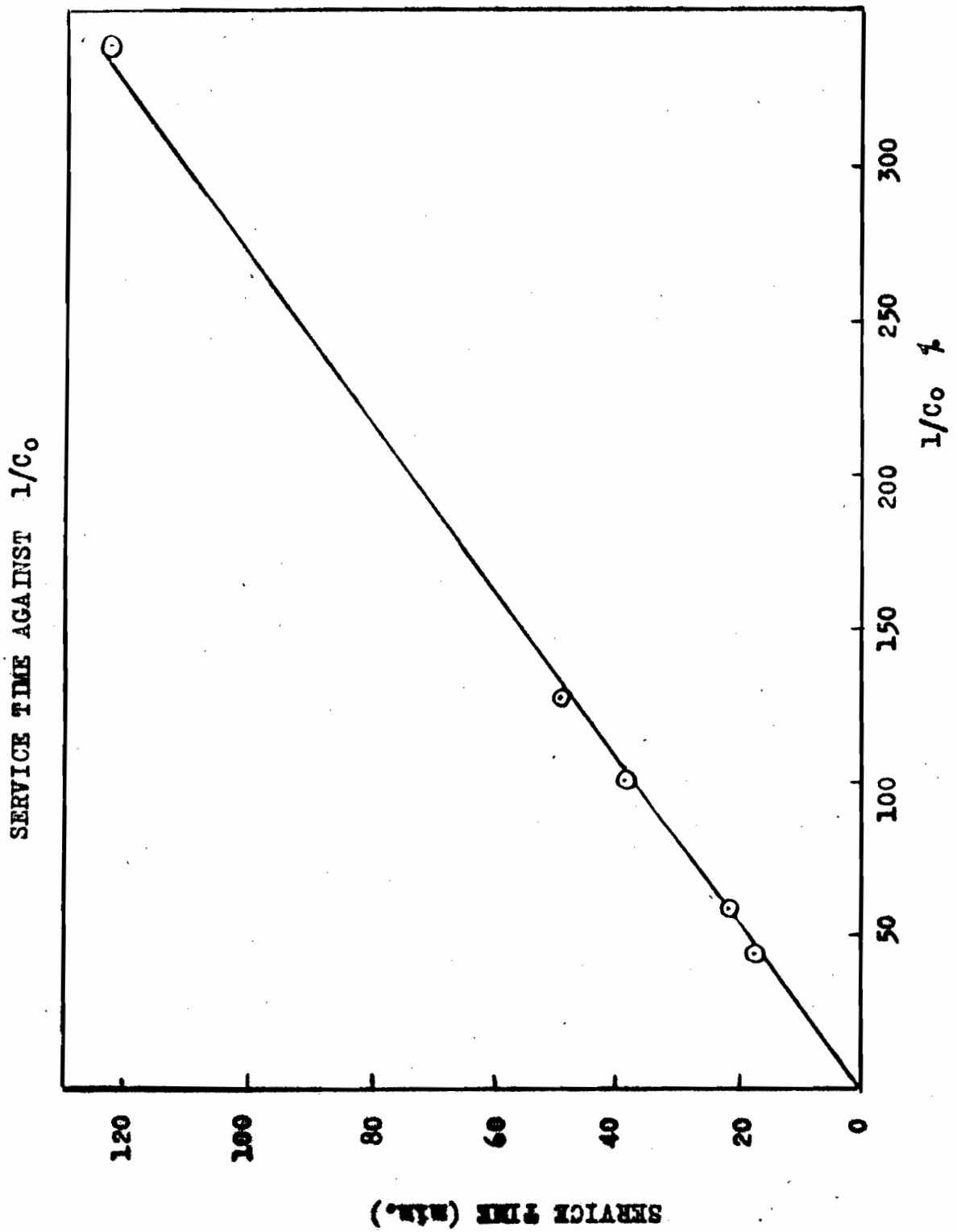
SERVICE TIME AGAINST 1/C₀
SERVICE TIME (min.)
1/C₀
0
20
40
60
80
100
120
50
100
150
200
250
300

FIGURE 61.

EFFECT OF FLOWRATE ON SERVICE TIME

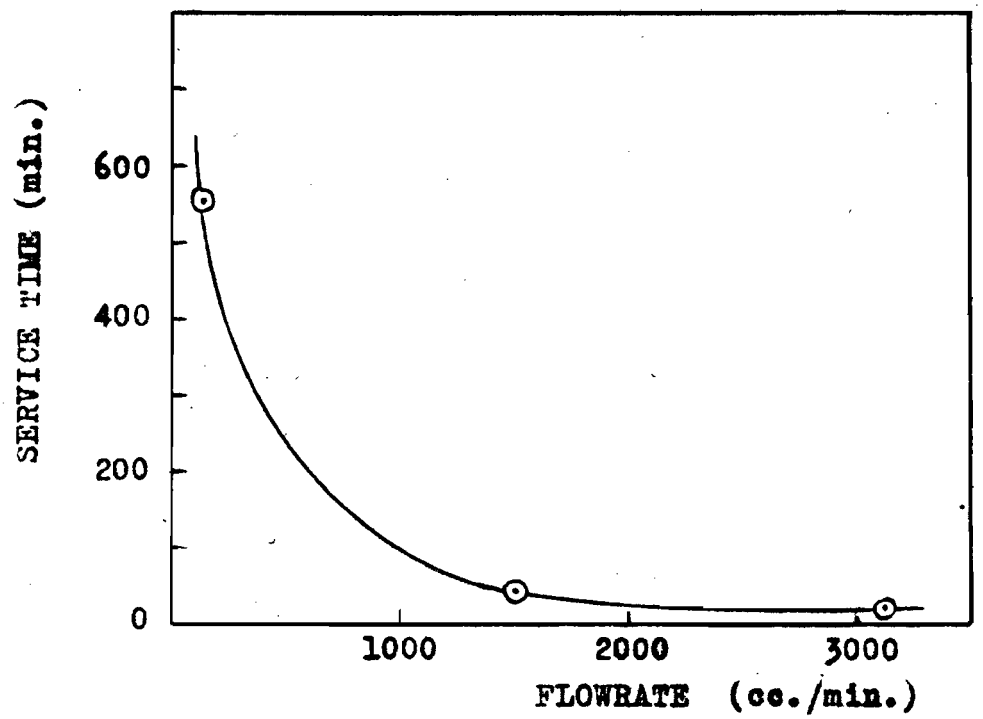

FIGURE 62.

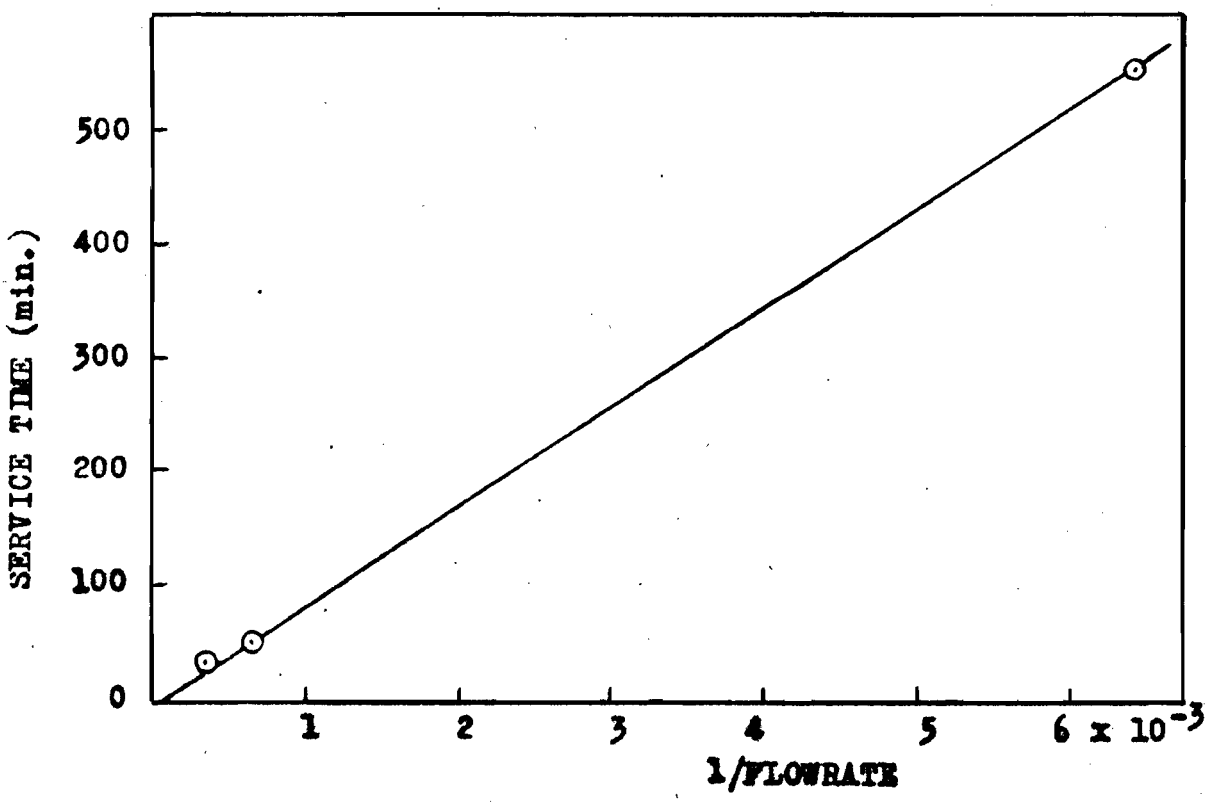

FIGURE 63.

4 Critical Lengths.

The data for the effect of variation in air rate are given in table 20. The plot of critical length against air rate is shown in figure 64. The critical length is increased by increasing the air rate, but the relative effect decreases as the rate becomes larger. In figure 65, the critical length is plotted against the logarithm of the air rate, and a straight line is obtained.

The theory of Danby et al predicts that the relation between critical length and concentration of the gas in the air stream follows the equation

$$\lambda_c = \frac{L}{kN_o} \ln (c_o/c' - 1)$$

where λ_c is the critical length, k is a constant, N_o is the number of active centers per cc. of charcoal which they assume constant, and c' the escaping concentration of the gas at service time, which will be a constant for any test to determine the service time. If L, the total flowrate, is kept constant, then the critical length should vary as the logarithm of the initial concentration (c_o). Thus the critical length plotted against the logarithm of the initial concentration should give a straight line.

The equation that Mecklenberg derives for the dead length

$$h = \frac{\delta r}{DF}\left(\frac{KQ}{v}\right)^{n-1}\left[\ln\frac{c_o - c'}{c_x - c'} - \frac{c_o}{c_o - c'}\right]$$

also predicts that it should vary with the logarithm of the initial concentration, if, as is assumed for his "mathematical" charcoal, the vapour pressure in the capillaries, c', is constant.

The data for the effect of concentration on critical length are given in table 21. In figure 66, the critical length was plotted against the partial pressure of butane. The critical length is seen to increase

Table 20

Effect of Air Rate on Critical Length.

(Butane flowrate 53 cc./min.)

Air Rate cc./min.	Critical Length (cms.)
0	0.57
500	0.75
1530	0.95
3130	1.03

Table 21

Effect of Concentration on Critical Length at Constant Flowrate

(Total flow 3050 cc./min.)

Partial Pressure of Butane mm. of hg.	Critical Length (cms.)
2.3	0.10
5.7	0.40
7.5	0.55
12.7	1.03
17.4	1.26

CRITICAL LENGTH AGAINST AIR RATE

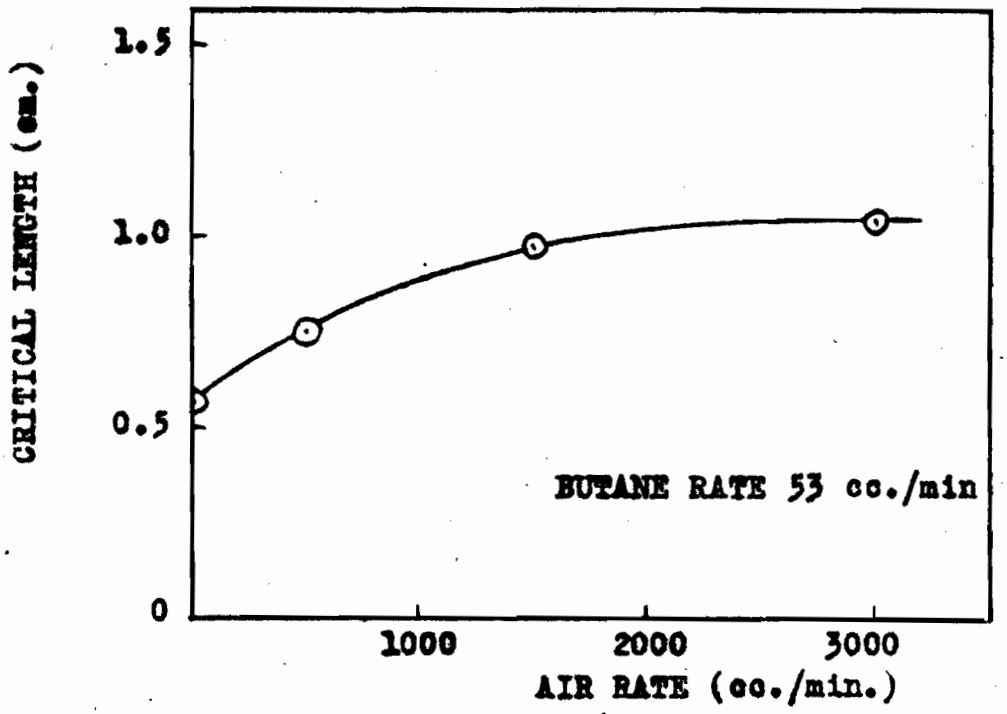

FIGURE 64.

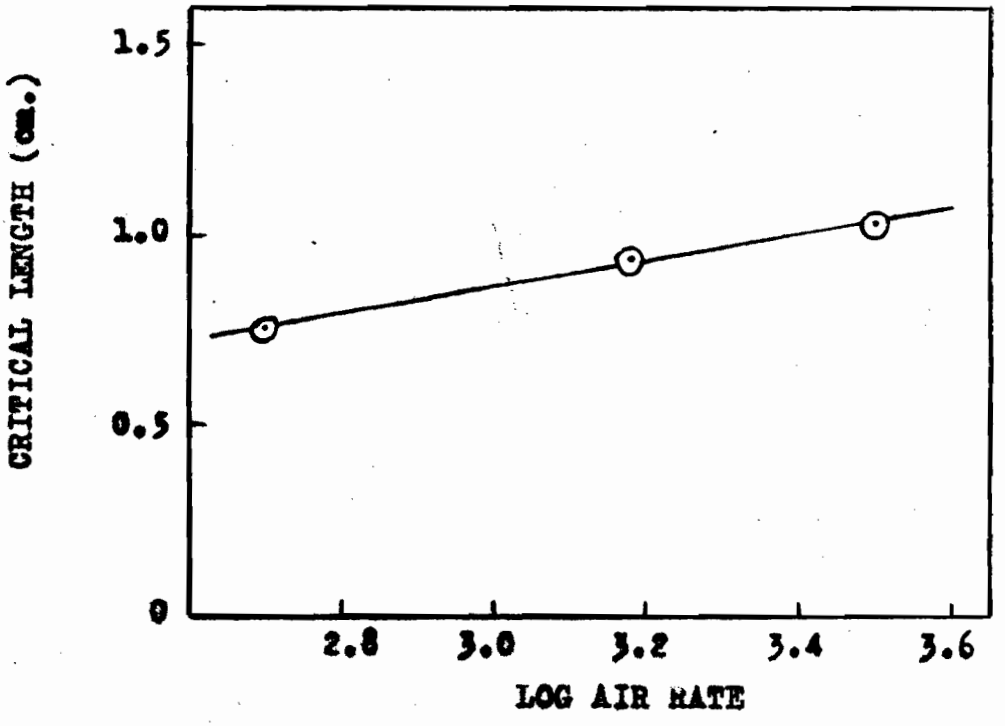

FIGURE 65.

EFFECT OF CONCENTRATION ON CRITICAL LENGTH

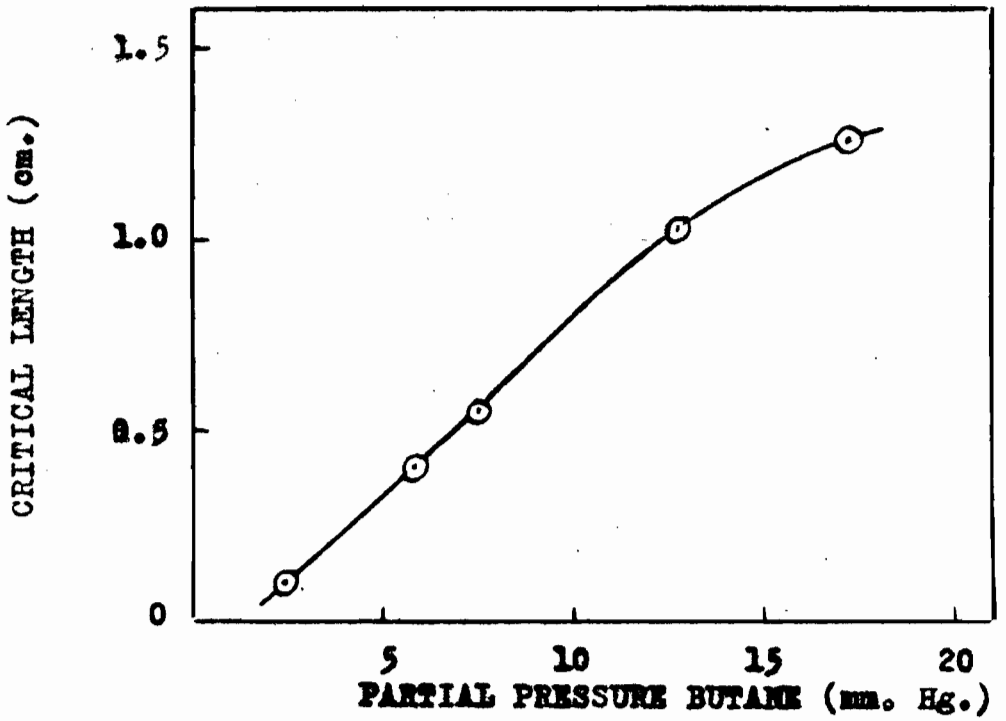

FIGURE 66.

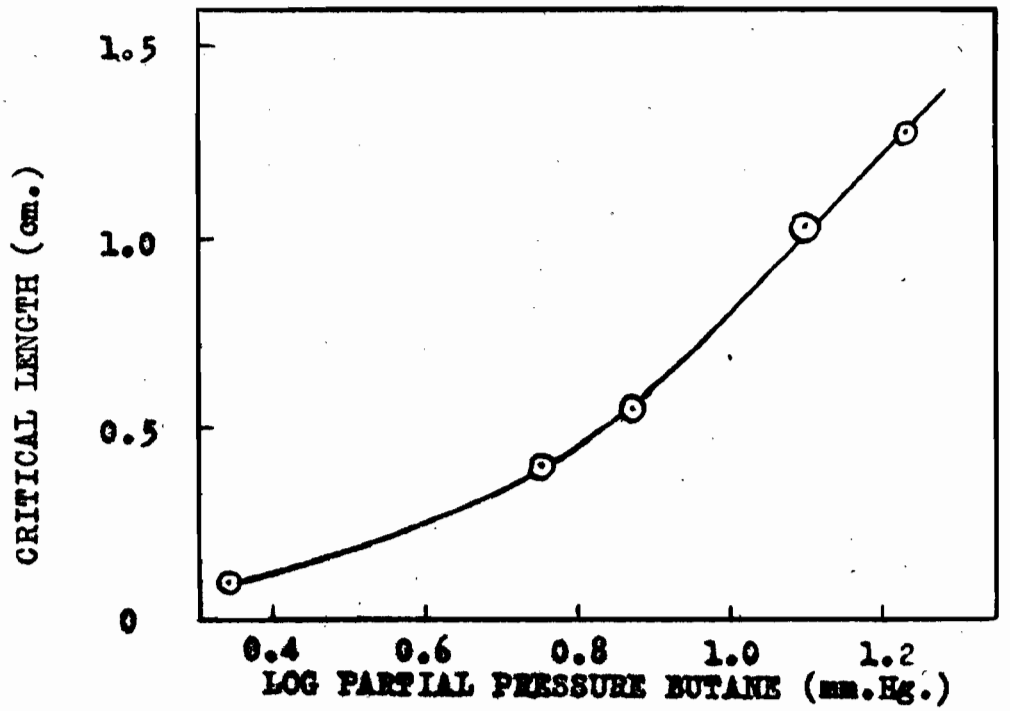

FIGURE 67.

with the partial pressure of butane, but the curve seems to tend towards a maximum at higher partial pressures. the critical length is plotted against the logarithm of the partial pressure as in figure 67, and a linear relation is found at higher partial pressures (above 7 mm. of Hg.), but the graph does not continue to be linear at partial pressures below this, but curves towards the origin.

5. Distribution of Butane in the Charcoal Cell.

(a) Distribution of Sorbed Butane.

From a consideration of the characteristics of sorption of 1, 2, 3, 4, and 5 centimeter beds, it is possible to determine both the distribution of the sorbate throughout a 5 centimeter bed, and the concentration gradient in the air stream passing through the bed, at various times. The concentration gradients for a five centimeter bed, at various times and with a butane flowrate of 53 cc. per minute and an air flowrate of 1520 cc. per minute, are determined in this section. Similar curves could be constructed for other flowrates reported in this investigation.

The data for the time of saturation of the 1, 2, 3, 4, and 5 centimeter beds are found in table 22. The curve of saturation time against bed depth is shown in figure 68. From this curve, the bed depth that is saturated in times 2, 4, 10 etc., are determined and plotted on the horizontal line of figure 70 corresponding to 1.16 grams of butane sorbed per centimeter of charcoal, which is the saturation concentration for the gas flows used.

The column lengths which have service times of 2, 4, 10 etc. as determined from figure 55, are plotted along the base line of figure 70.

The weight-time data for the 1, 2, 3, 4, and 5 centimeter beds are also found in table 22. The curves showing the plot of these data are given in figure 69. From these data, the number of grams of butane per centimeter sorbed in each centimeter layer at times 2, 4, 10 etc. were determined as shown in table 23, and this value assigned to the mid-point of that centimeter layer. These values were then plotted on figure 70 at their respective mid-points. The curves joining points of equal time were then drawn, giving the concentration gradients of the sorbed butane throughout the charcoal bed at the various times.

Table 22

Weight - Time Data

(Butane rate = 53 cc./min; air rate = 1520 cc./min.)

Time	Column Length (cms.)				
mins.	1.19	2.13	2.96	4.09	5.01
2	0.215	0.22	0.22	0.22	0.22
4	0.45	0.46	0.46	0.46	0.46
10	1.06	1.24	1.24	1.24	1.24
15	1.29	1.83	1.94	1.92	1.92
20	1.35	2.18	2.59	2.60	2.60
30	1.38	2.42	3.17	3.79	3.95
40		2.47	3.35	4.34	4.94
50			3.39	4.62	5.44
60			3.42	4.72	5.64
70				4.73	5.75
80					5.80

Table 23

Weight Increments (gms./cm.)

Time	Column Length (cms.)				
mins.	0.6	1.66	2.54	3.52	4.55
2	0.180	.016			
4	0.380	.053			
10	0.890	.180	.012		
15	1.080	.575	.108		
20	1.135	.880	.495	.009	
30	1.160	1.105	.904	.550	.174
40		1.160	1.060	.875	.650
50			1.110	1.090	.890
60			1.160	1.150	1.00
70				1.160	1.110
80					1.160

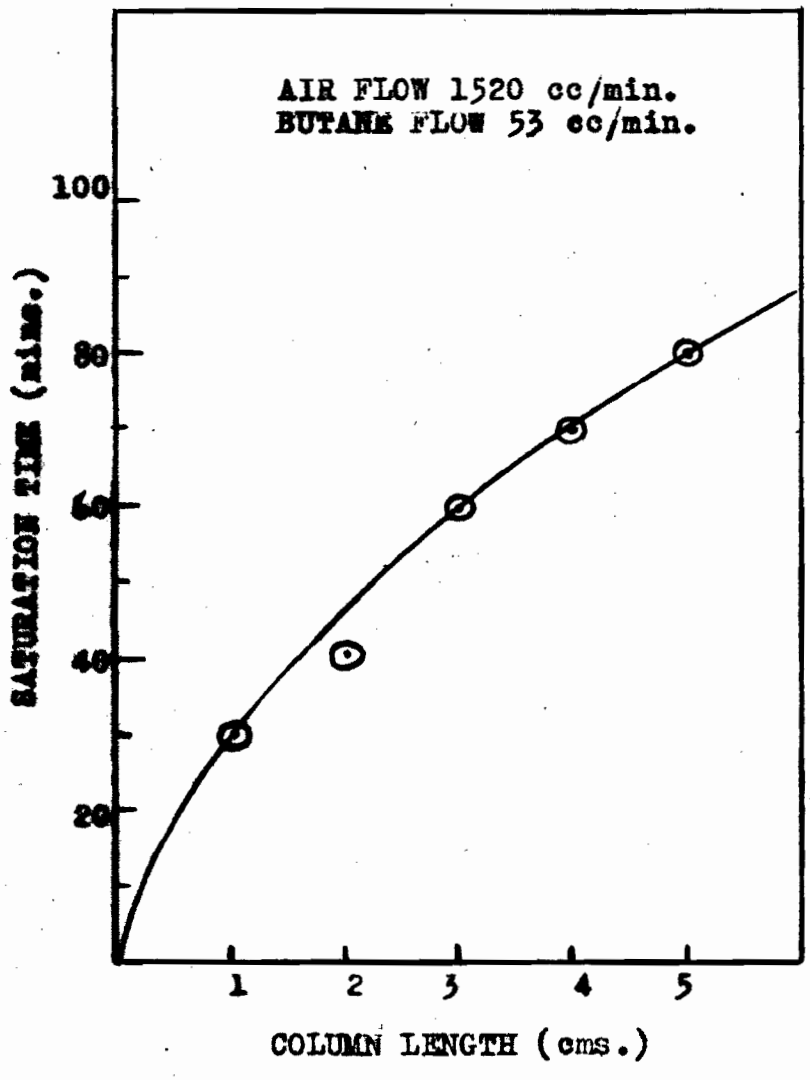

FIGURE 68

SATURATION TIME AGAINST COLUMN LENGTH

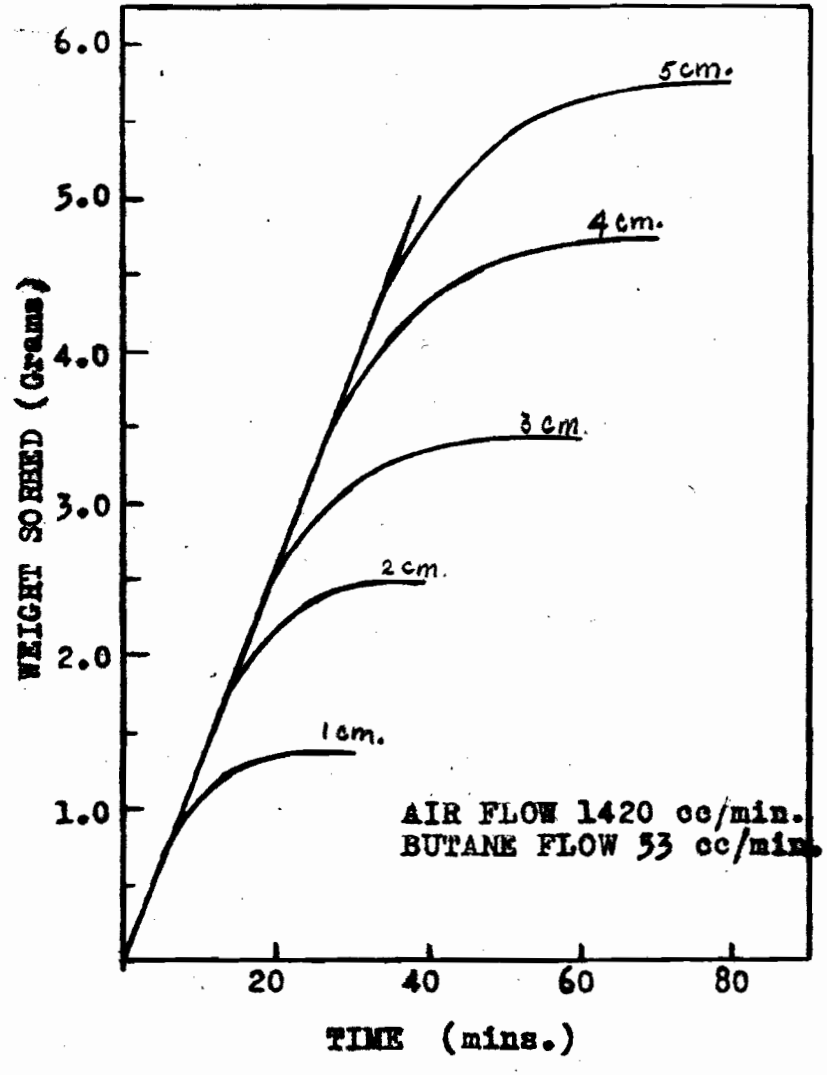

FIGURE 69

WEIGHT SORBED

CONCENTRATION GRADIENTS OF SORBED BUTANE

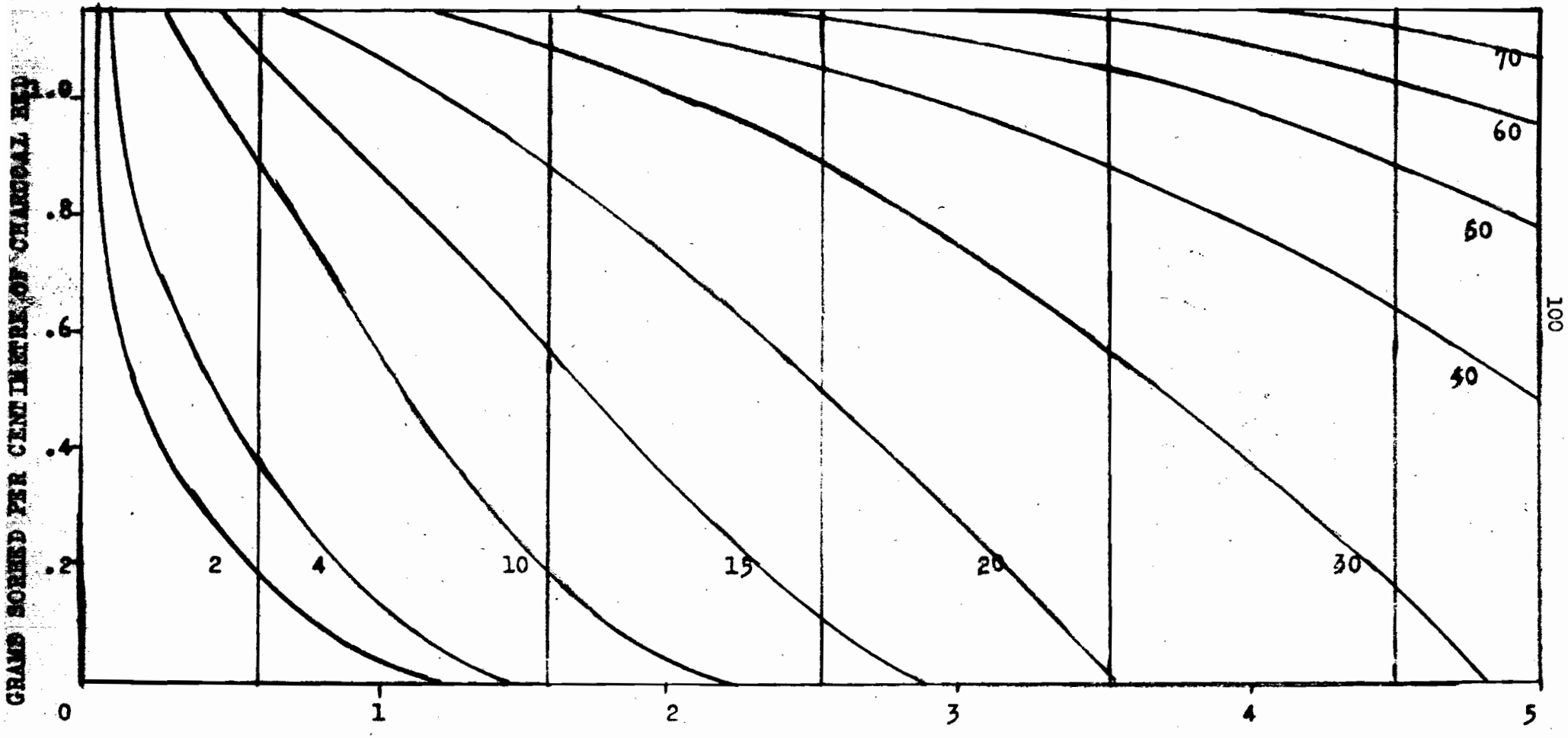

FIGURE 70.

From figure 70 it can be seen that the gradient is changing at times below 30 minutes until the final gradient is established. It will be shown later that actually the 30 minute gradient is not the final shape, but that there is a slight change in shape until the 60 minute gradient is established. The first gradients appear to follow the exponential curves of the "mathematical" charcoal of Mecklenberg, or the curves postulated in the approximate theory of Danby et al, but they leave this form as Mecklenberg predicted. This behaviour is in agreement with that predicted by the detailed theory of Danby et al.

Mecklenberg explains the falling off of the top part of the concentration gradient as due to the larger capillaries in the charcoal, and due to the slow migration of the outer sorbed material into the inner capillaries. But it appears that a third factor operating to increase the time required for saturation, is the temperature change due to the heat of sorption. As will be seen in the section 6, the temperature rise for butane (and also for ammonia) is quite high. Before the final saturation value can be obtained, this heat must be removed by the air stream, and this delays the time of saturation. This of course would not be so marked with very low initial concentrations.

These concentration gradients could also be obtained by graphical differentiation of the integral sorption curves shown in figure 71. These integral sorption curves are drawn from the data presented in table 22, and are a plot of the weight sorbed in grams against the bed depth in centimeters for constant times.

In figure 72 the differential weight of gas sorbed as given in figure 70 is plotted against time at different depths in the bed. The relation between the weight sorbed and the time appeared to follow an exponential curve of the type

$$x = W_s (1 - e^{-bt})$$

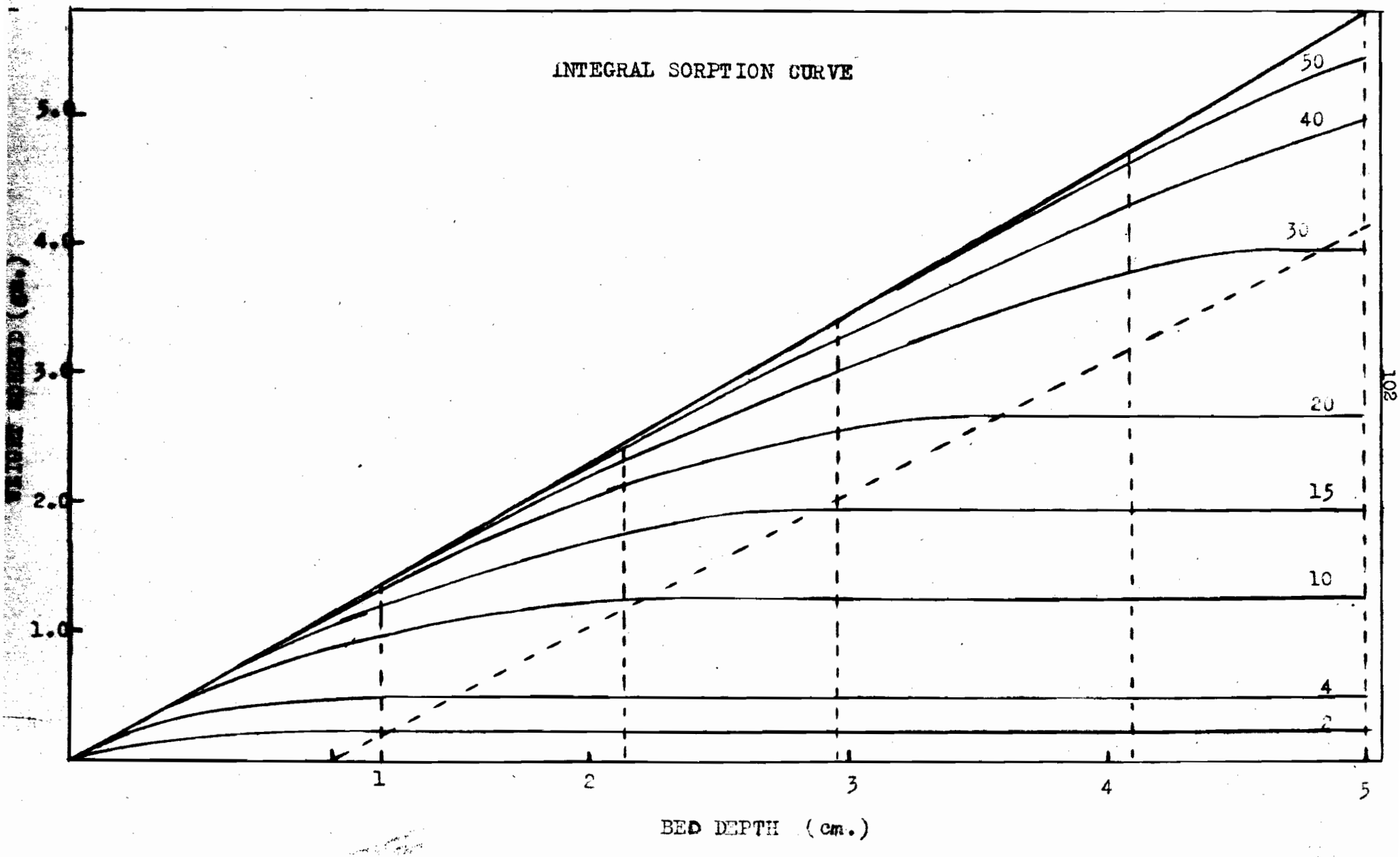
INTEGRAL SORPTION CURVE
5.0
4.0
3.0
2.0
1.0
50
40
30
20
15
10
4
2
1
2
3
4
5
BED DEPTH (cm.)

FIGURE 71

DIFFERENTIAL WEIGHT OF GAS SORBED AGAINST TIME

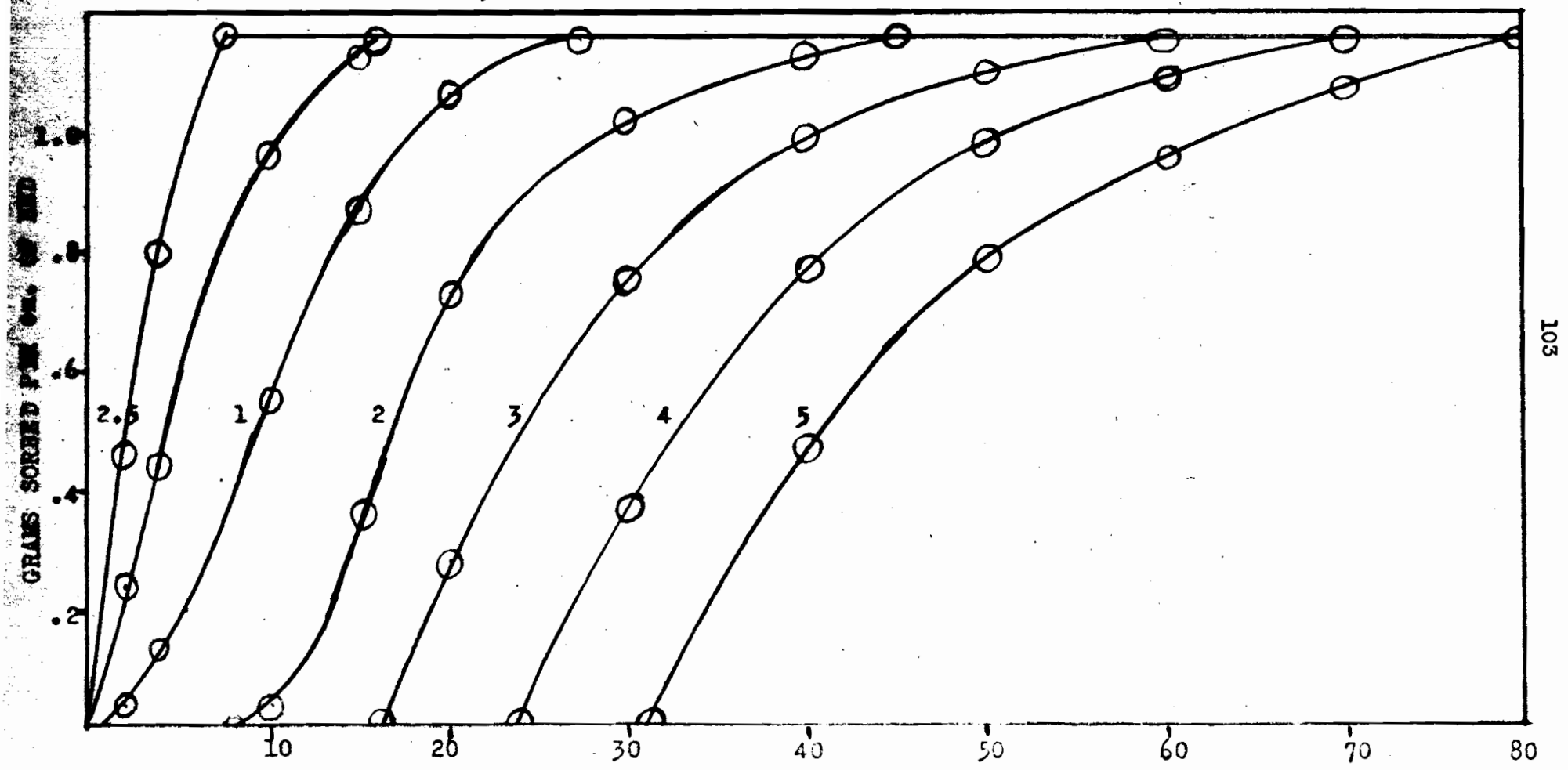

FIGURE 72.

where x is the weight of gas sorbed in time t, and W_s is the equilibrium weight of the gas sorbed, and b is a constant. This relation is identical to that given by Syrkin and Kondraschow (22).

There is another relation between the weight of gas sorbed and time at constant bed depth. This is shown in figure 73 where the logarithm of the weight of gas sorbed is plotted against the reciprocal of the time of passage for different depths in the bed. The data give straight lines which intersect at a point. This point does not seem to have any particular significance.

It is possible, however, to write an equation for these curves

$$x = We^{-L/t}$$

where W is a constant relating to the equilibrium weight of the gas sorbed, and L a constant for any given bed length.

(b) Concentration Gradient of the gas stream in the charcoal cell.

From figure 49, the concentration gradients shown in figure 74 were drawn. Figure 49 gave the concentration of the gases leaving each centimeter layer and entering the next centimeter layer. The values obtained by erecting verticals at times 4, 10, 15 etc were plotted against the corresponding bed depth on figure 74. As before in figure 70, the saturation times were plotted along the maximum concentration and the service times along zero concentration.

The gradients obtained are very similar to those obtained for the amount of the gas sorbed on the charcoal. These gradients agree with those postulated by Danby et al as shown in figure 2, and thus verifies the application of their equations for the concentration of the gases in equilibrium with the charcoal bed.

The initial exponential curves follow the relation postulated by Danby et al

$$C = C_o e^{-kN_o l/L}$$

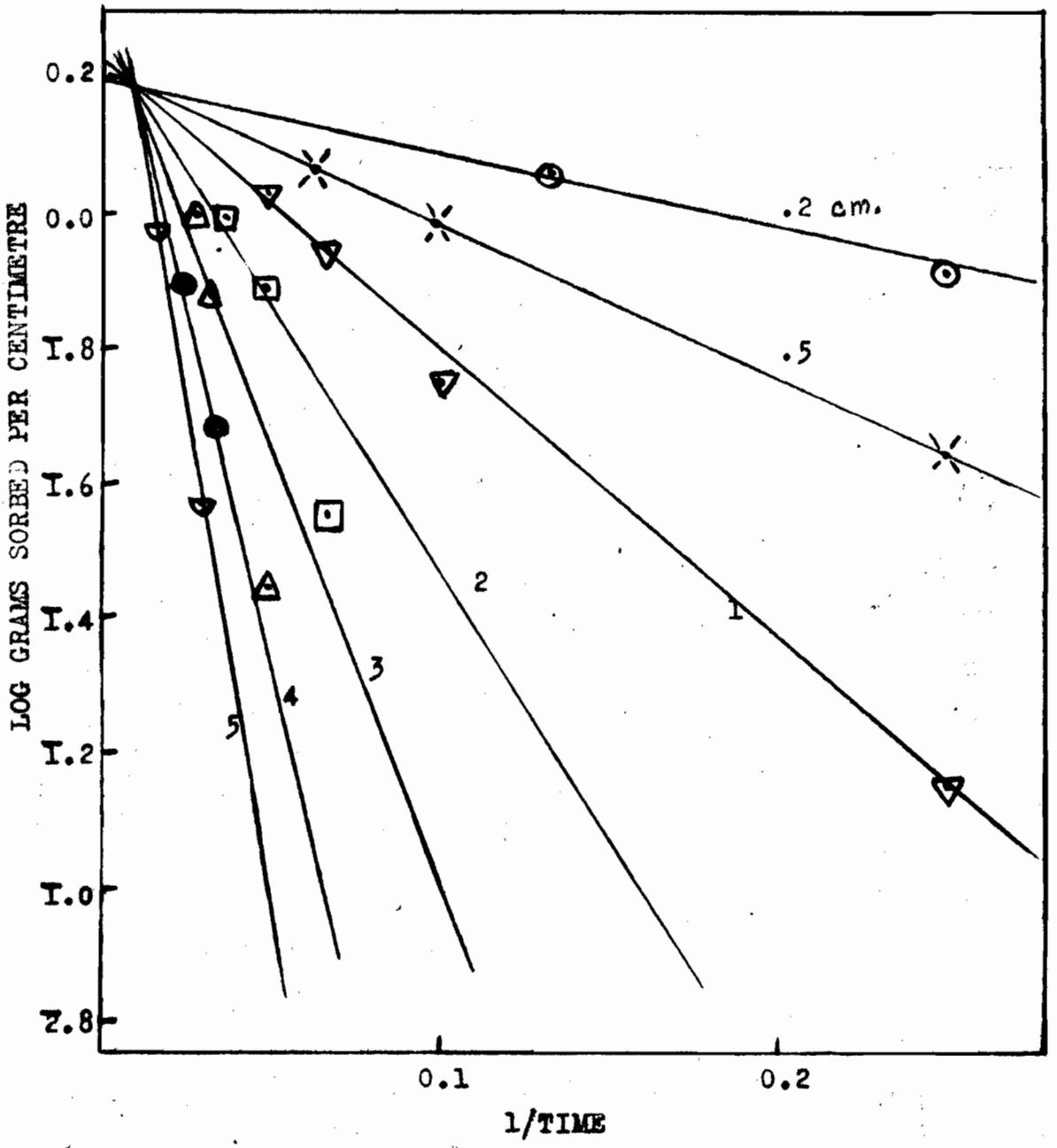
0.2
0.0
1.8
1.6
1.4
1.2
1.0
2.8
LOG GRAMS SORBED PER CENTIMETRE
.2 cm.
.5
1
2
3
4
5
0.1
0.2
1/TIME

FIGURE 73.

CONCENTRATION GRADIENTS IN GAS STREAM

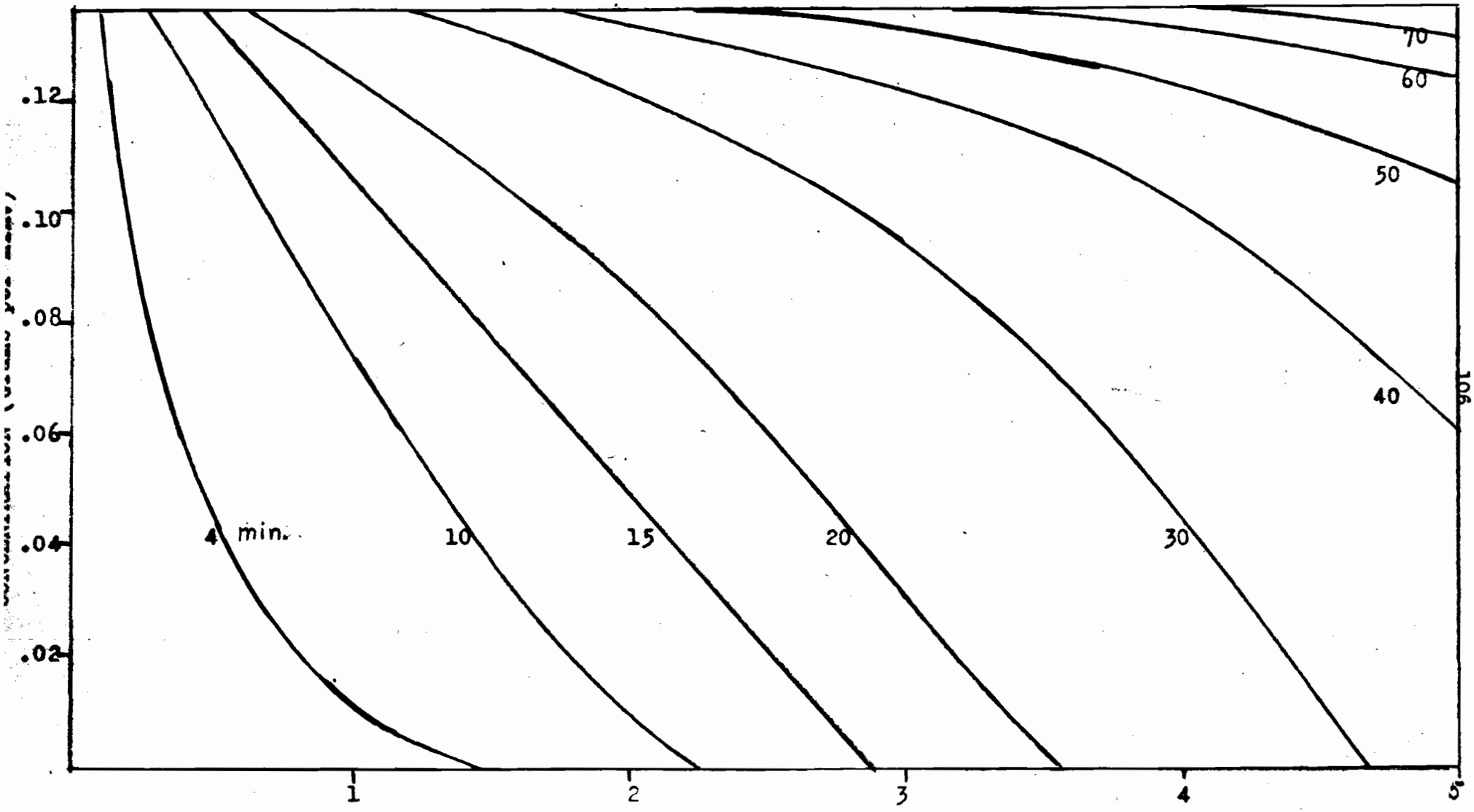

FIGURE 74

when very few of the active centers have been used up. The gradients then change over to their final shape which follows the equation

$$c = \frac{c_o}{e^{-kc_oT}\left(e^{kN_o l/L} - 1\right) + 1}$$

as given by their detailed theory.

The increase in the length of the working layer with time is given in table 24. The values given are those measured from the curves on figures 70 and 74.

The curve of this relation shown in figure 75 indicates that in a five centimeter bed the concentration gradient has not been completely established. The final length of the working layer would appear to be about 4.8 centimeters and would be established at about 60 minutes.

Table 24

Length of Working Layer

Time (mins.)	Working Layer (cms.)
2	1.20
4	1.36
10	1.98
15	2.45
20	2.89
30	3.64

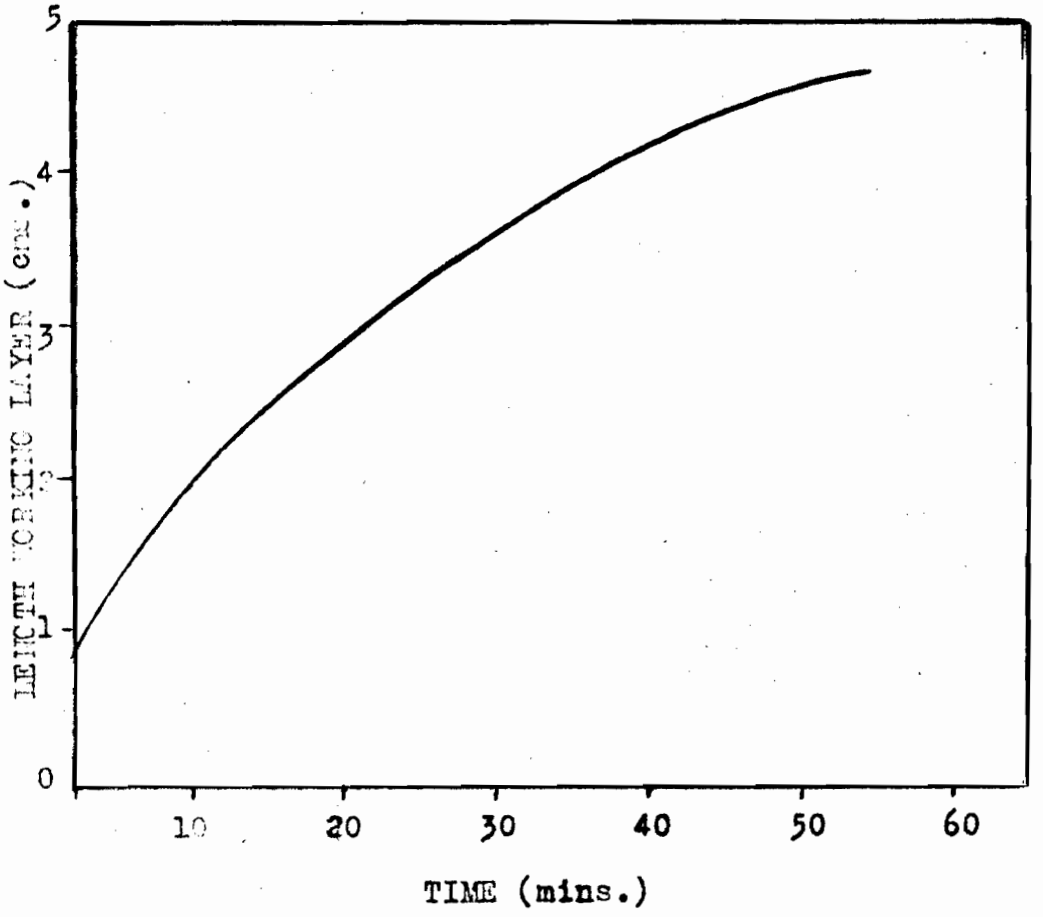

LENGTH OF WORKING LAYER AT VARIOUS TIMES

FIGURE 75

6. Temperature Data

The temperature rise in the centre of the second and fourth centimeter layers, from the bottom of the charcoal bed, were measured as a function of time. The data is recorded in table 25. The temperature rise time curves are similar in shape to those for ammonia (see figure 35) and so are not shown here. With the positions used in the butane experiments, the maximum temperature rise recorded by them were approximately equal if they were both further than one centimeter from the top of the bed.

The maximum temperature rise was found to be mainly dependent on the rate at which the butane was supplied. A linear relation was obtained between them (figure 76). Since these were taken in a four centimeter bed, the top thermocouple T_1 was only half a centimeter from the surface of the charcoal, and recorded a lower temperature than T_2 due to the cooling effect of the gas stream.

Increase in the air flowrate causes a linear decrease in the maximum temperature attained as shown in figure 77.

From the temperature rises recorded in the 1, 2, 3, 4 and 5 centimeter bed at constant concentration and flowrate, the temperature rise through a 5 centimeter bed can be found. This is shown in figure 78. The maximum temperature attained is constant through the bed except at the top centimeter layer, due to the cooling of the air stream, and probably at the bottom centimeter layer as was found for ammonia.

The times at which these maximum temperatures were attained are plotted in figures 79 and 80. These were found to decrease rapidly with increase in butane and air flowrates, apparently to a minimum value.

Table 25

Temperature Data

Height (cms.)	Air Rate	Butane Rate	T_1 °C	t_1 (mins.)	°C T_2	t_2 (mins.)
4.08	3130	53	18	6	23	17
1.94	3020	53			16	4
5.61	1590	53	30	14	29	30
4.09	1530	53	25	7	29	21
2.96	1520	53			27.5	15
2.13	1530	53			24	9
1.19	1520	53				
3.96	500	53	29.5	13	33	27.5
3.95	0	71	36.5	13.5	39	24
4.12	0	53	32	20	36	37
4.00	3020	71	23	5	28	12
3.70	3020	30	10	11	12	27
2.18	3020	30			10.5	8
4.23	3045	24	9.5	18	10	24
4.16	3040	9	1.7	25	3	90
2.12	3000	9			4	24
1.27	3020	9				
4.01	1500	30	16.5	12	16.5	33
2.09	1500	30			6	8
3.99	1403	30	11.5	13.5	12	34
3.88	151	2.7			0	

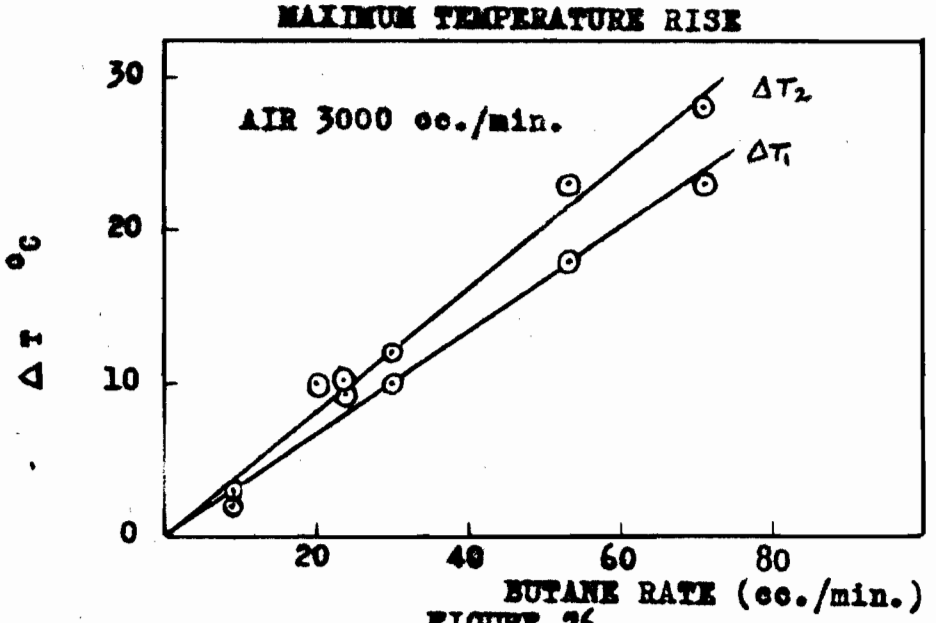

FIGURE 76.
EFFECT OF BUTANE RATE

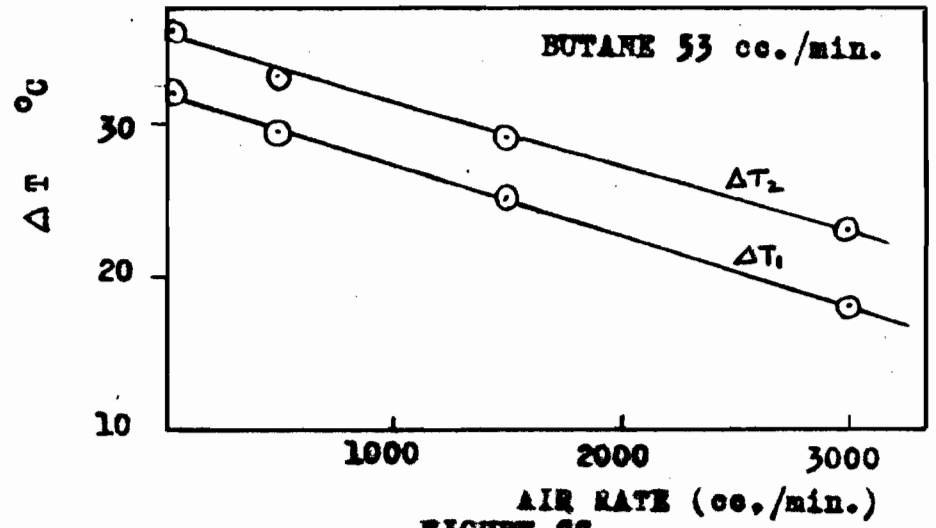

FIGURE 77.
EFFECT OF AIR RATE

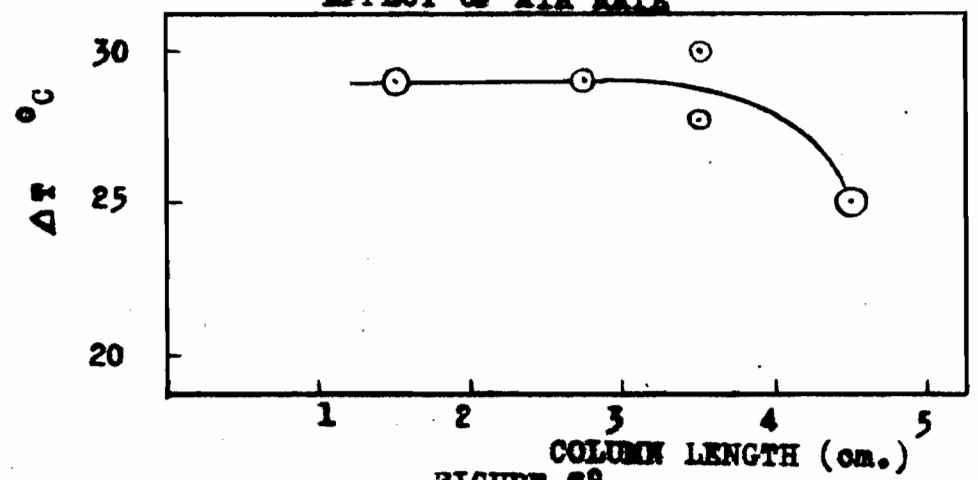

FIGURE 78.
TEMPERATURE ALONG THE BED

TIME OF
MAXIMUM TEMPERATURE RISE

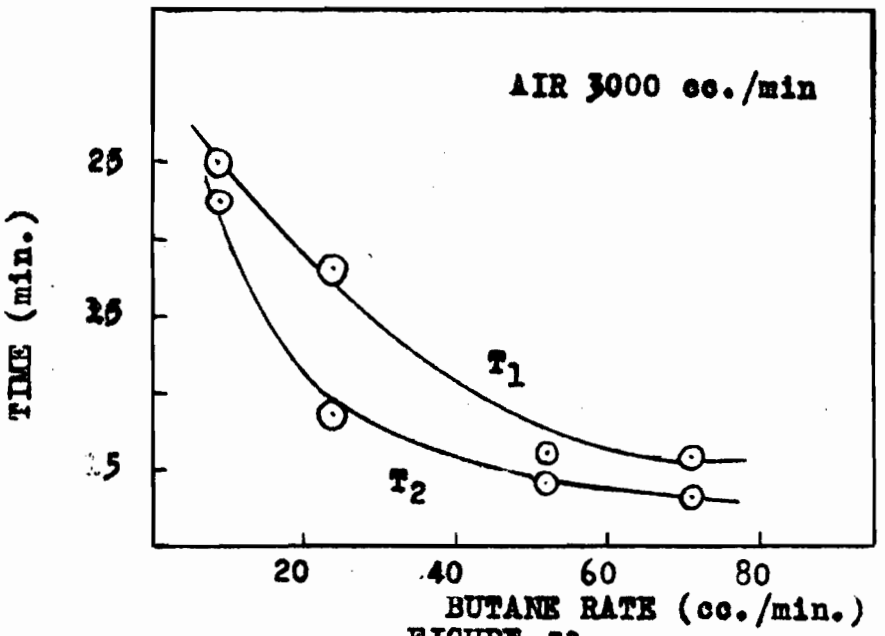

FIGURE 79
EFFECT OF BUTANE RATE

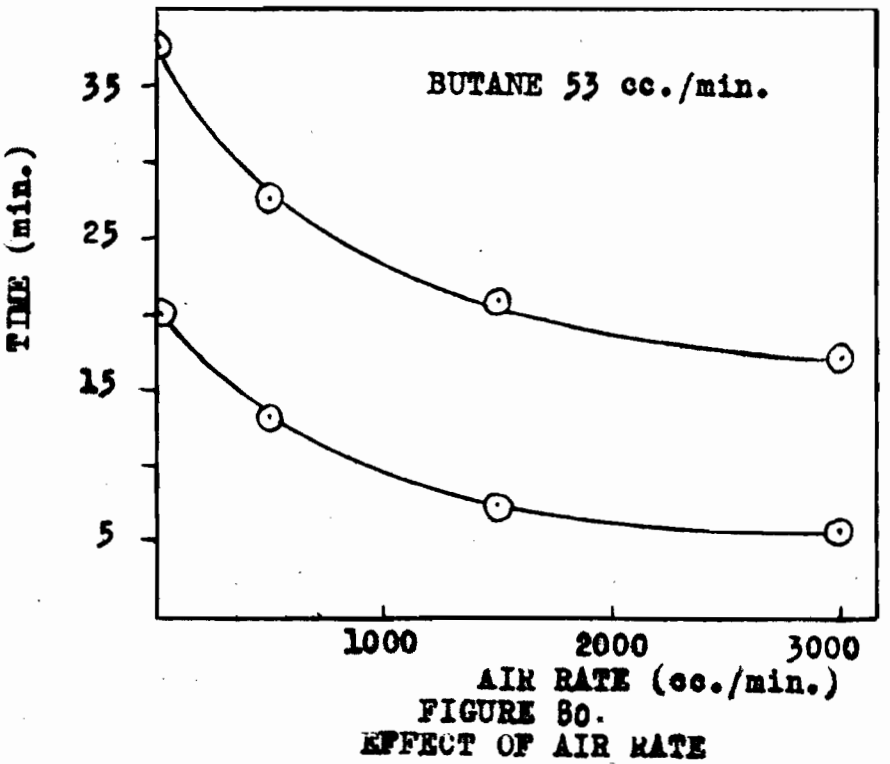

FIGURE 80.
EFFECT OF AIR RATE

C. Desorption Studies

As mentioned in the discussion of the analytical results for both ammonia and butane, the rate of increase in weight of the charcoal over the linear portion of the weight-time curve did not correspond to the total amount of gas admitted to the cell, yet no sorbate appeared in the effluent stream. It was thought that this might perhaps be due to competition for active centers between the sorbate and the air. The charcoal is saturated with oxygen and nitrogen before any sorbate is admitted. These molecules would be displaced, at least in part, from the charcoal surface by ammonia or butane molecules. This would result in a weight being recorded which would be less than the actual amount of butane or ammonia taken up by the charcoal, by the amount of oxygen and nitrogen displaced.

To confirm this behaviour, and to investigate the reversibility of the sorption, studies on the desorption of both ammonia and butane were carried out as previously described. For the first two runs the charcoal was allowed to come to equilibrium with a stream of pure ammonia. It was desorbed using air streams of 100 cc. and 500 cc. per minute and no ammonia flow. The results are given in table 26 and figure 81. The desportion occurs very rapidly at first and then the rate gradually decreases to zero. The desorption does not, however, follow a logarithmic relation with time. Not all of the ammonia is desorbed at the equilibrium, 0.2 grams are left, and this apparently does not vary with the air velocity though the bed for the amount is the same for desorption by both 100 and 500 cc. per minute of air. The initial rate of desorption is more rapid with the greater velocity of the desorbing stream.

Two runs were also carried out using charcoal saturated as above, but these were desorbed using gas streams of 200 cc. per minute air rate and 60 cc. per minute ammonia rate; and with a stream of 300 cc. per

Table 26

Desorption Studies

Sorption Conditions		Equilibrium Weight gms.	Desorption conditions		Desorp. Equil'm. Weight gms.
Air cc./min.	Sorbate cc./min.		Air cc./min.	Sorbate cc./min.	
		A. Ammonia			
0	60	2.16	100	0	0.20
0	60	2.16	500	0	0.20
0	60	2.16	200	60	0.79
0	60	2.16	300	60	0.79
200	60	0.67	200	0	0.09
300	60	0.59	300	0	0.05
		B. Butane			
0	53	6.26	3000	0	(0.40)

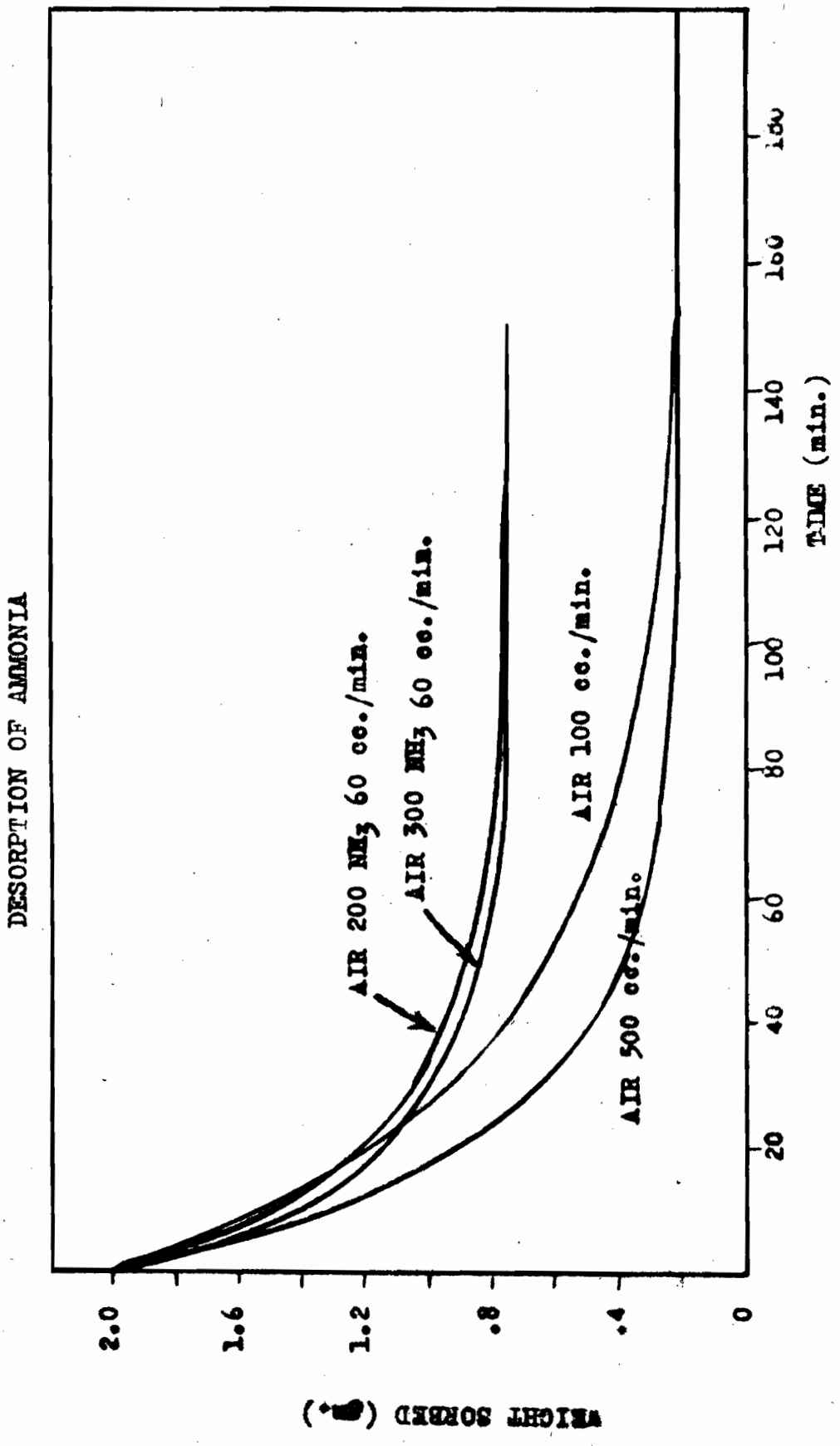
DESORPTION OF AMMONIA
AIR 200 NH3 60 cc./min.
AIR 300 NH3 60 cc./min.
AIR 100 cc./min.
AIR 500 cc./min.
WEIGHT SORBED (g.)
TIME (min.)
0
.4
.8
1.2
1.6
2.0
20
40
60
80
100
120
140
160
180

FIGURE 81.

minute of air and 60 cc. per minute of ammonia. The equilibrium weights for sorption using these conditions are 0.67 gms and 0.59 grams respectively. The equilibrium desorption weight was 0.79 grams in both of the above cases. These are also shown on figure 81. Here again sorption was more rapid initially with the faster air stream.

Starting with charcoal which was in equilibrium with ammonia and air streams of 60 and 200 cc. per minute, and 60 and 300 cc. per minute and desorbing by cutting off the ammonia supply give the desorption curves shown in figure 82. In these cases only 0.09 and 0.05 grams of ammonia remained on the charcoal at equilibrium.

Figure 83 shows a typical desorption of butane. The charcoal was saturated using pure butane, and desorbed, using an air stream of 3000 cc. per minute, from 6.26 grams to 0.40 grams of butane after 30 hours, but had not yet reached equilibrium. It appeared probable that, given sufficient time, the butane would be completely desorbed.

The indications are that for ammonia the sorption is not completely reversible, but that the sorption is reversible for butane. This would indicate that there is at least in part a different mechanism of sorption for butane and ammonia.

Figure 84 shows the differential desorption curves of volume desorbed per minute plotted against time. The lower curve was calculated from the loss in weight of the charcoal by graphical differentiation similar to that done for sorption; the upper curve is calculated from the analysis of the effluent gases. This indicates that more sorbate was detected in the exit gases than appears to be desorbed from the charcoal from its loss in weight. The deviation between the two curves is quite large at first but gradually decreases to zero. When the logarithm of this deviation is plotted against time, a linear curve is obtained (figure 85)

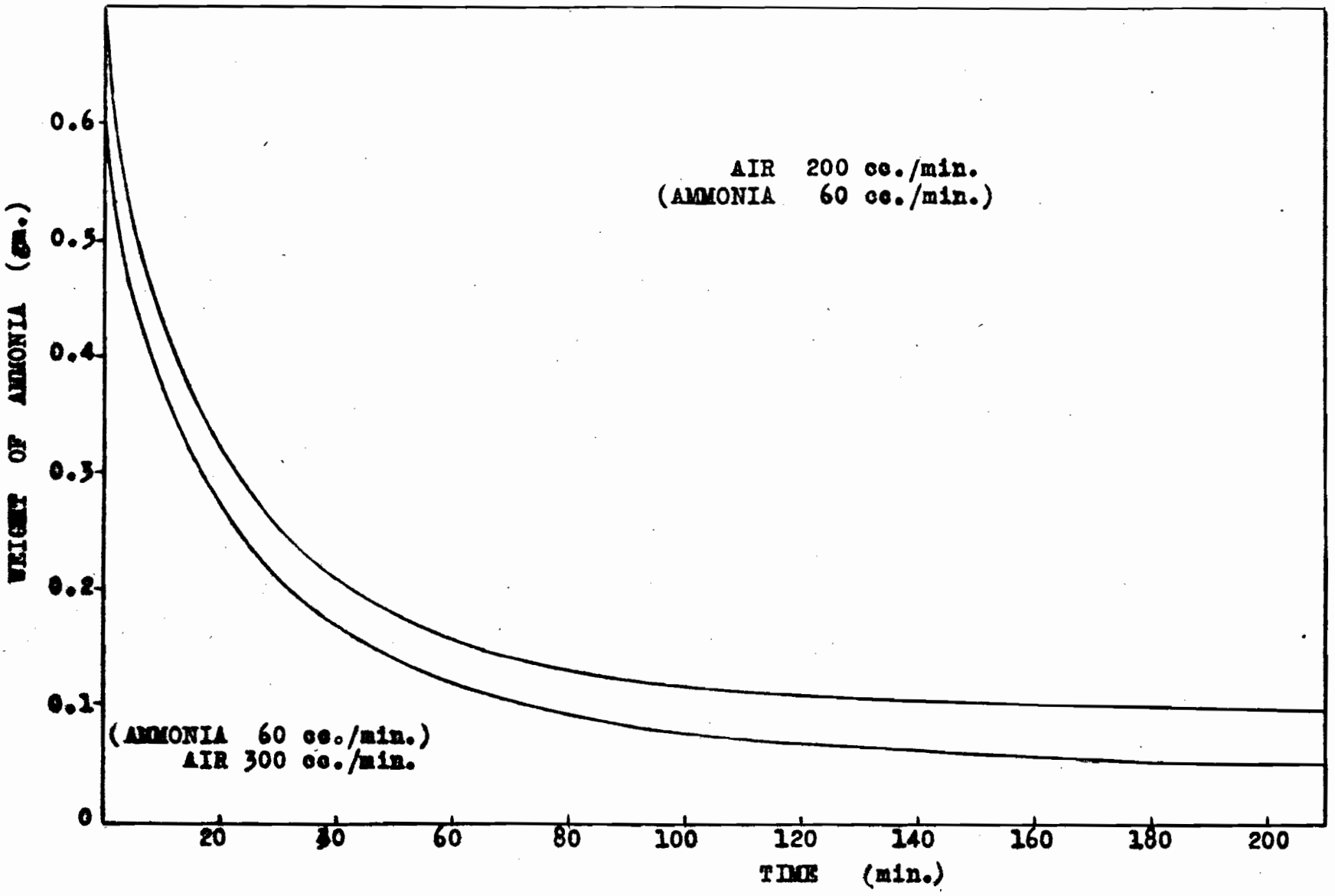

DESORPTION OF AMMONIA

FIGURE 82.

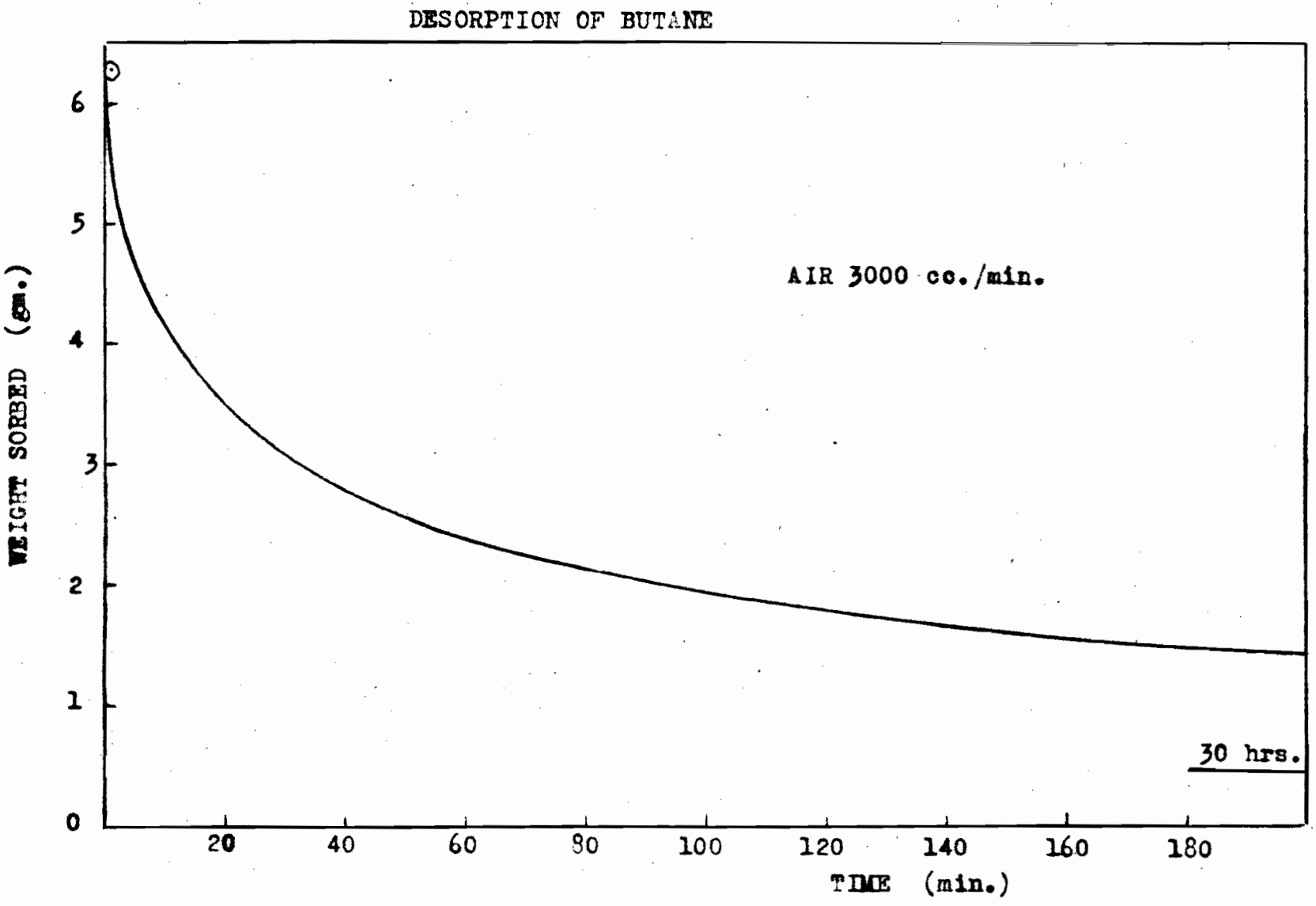
DESORPTION OF BUTANE
WEIGHT SORBED (gm.)
0
1
2
3
4
5
6
AIR 3000 cc./min.
30 hrs.
20
40
60
80
100
120
140
160
180
TIME (min.)

FIGURE 83.

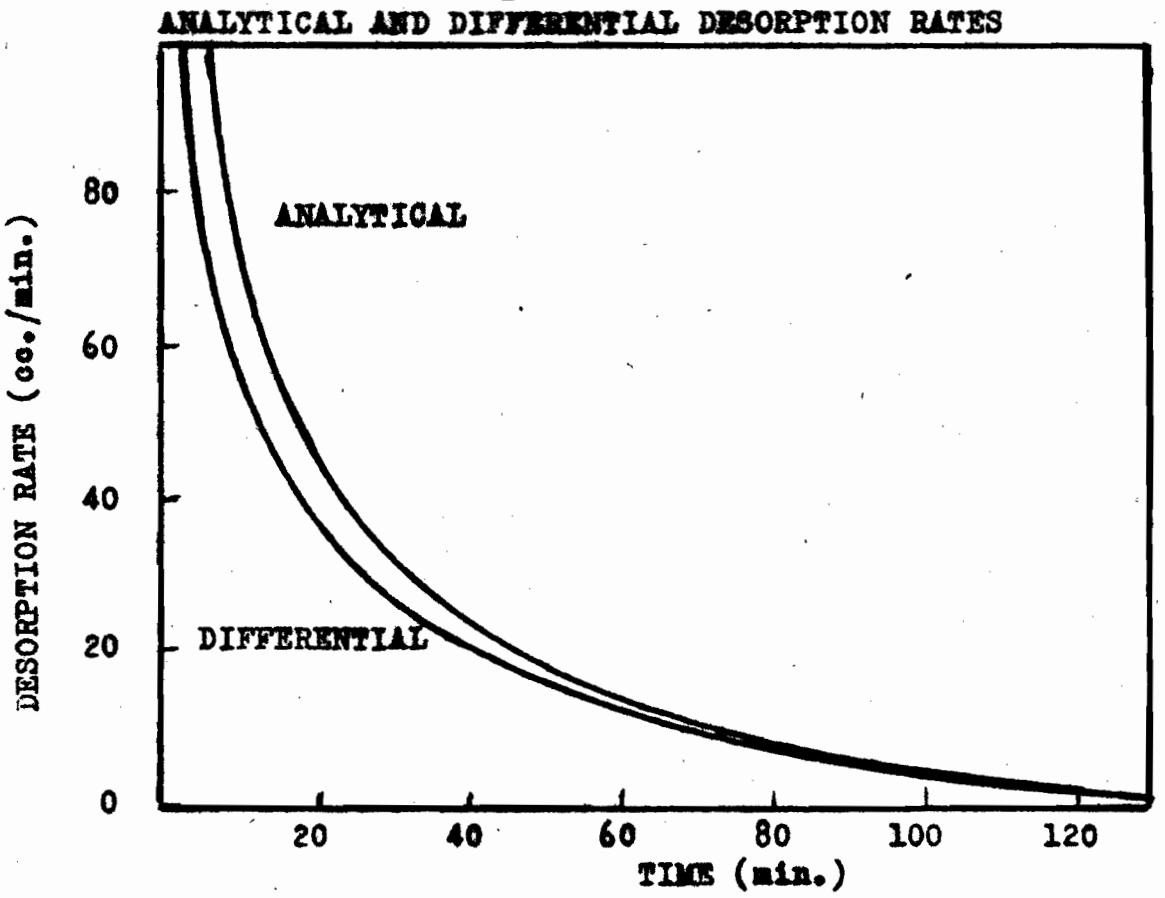

FIGURE 84.

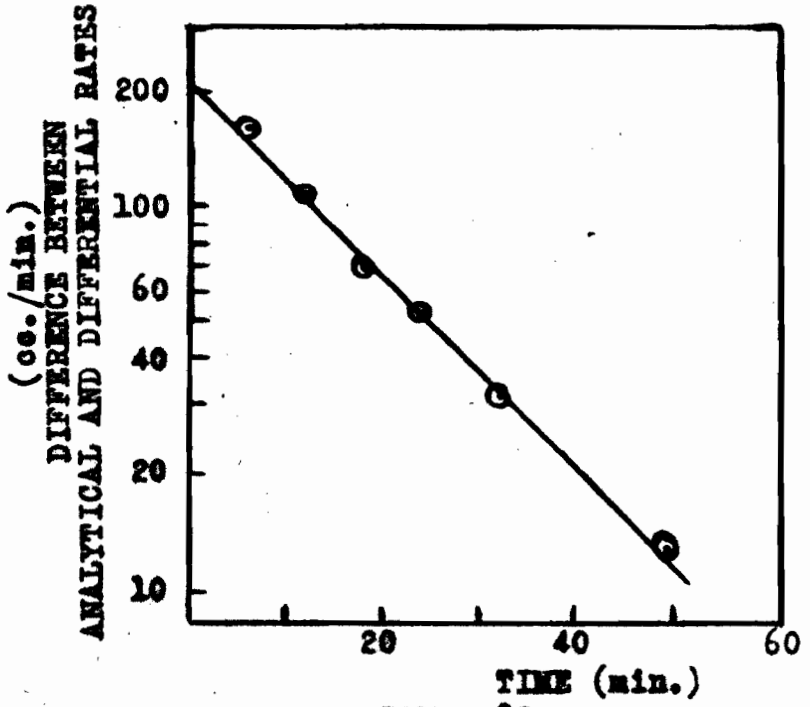

FIGURE 85.

except during the very first and very last stages of the desorption. If it is assumed that during sorption, air is displaced from the charcoal by sorbate molecules, and during desorption, sorbate is displaced from the charcoal by molecules of oxygen and nitrogen, then these deviations between sorption weight and analytical data are readily explained. It may be noted that the analytical methods were sufficiently accurate to justify this explanation.

Berl and Andress (24) have noted this displacement of sorbed air from charcoal by the vapors of several organic compounds and have determined the amount of air displaced.

DISCUSSION.

A study of the dynamic sorption of ammonia and butane has been made over the concentration range of 5 parts per thousand up, and 3 to 100 parts per thousand respectively. In this work an apparatus which permitted the sorption to be followed as a function of time over a wide range of conditions of sorbate concentration and flowrate, was used. In addition, with this apparatus it was possible to obtain temperature data and to analyse the effluent gas stream.

The apparatus was found to be very convenient for an accurate study of such sorption data as sorption capacity, service time, escaping concentration, dead length, sorption gradients in both the charcoal bed and the gas stream, and temperature rise in various sections of the charcoal bed. This type of apparatus has the advantage of measuring the sorption as a function of time rather than of bed length as in a segmented cell. This results in a considerable saving of time as less runs are required for a complete study of any particular sorbate.

It seems advantageous to follow the sorption beyond the service time of any bed for, as pointed out by Mecklenberg (13), the escaping gases are in fact those in equilibrium with the working layer of the charcoal. From the analysis of the effluent stream from various bed lengths, the sorption gradients in the gas phase throughout the bed can be determined.

The accuracy of this apparatus may be increased by the use of a light cell of plastic material, and a more sensitive balance. Such modifications would permit studies to be made of gases which are more difficult to sorb, and also allow the use of shorter bed lengths.

The studies of the sorption of ammonia and butane appear to in-

dicate a difference in the mechanism of sorption of the two gases. On a weight basis, butane is sorbed to a greater extent than ammonia, but on a volume basis, more ammonia is sorbed. For a four centimeter bed, using a stream of pure sorbate, 6.26 grams of butane were sorbed, but only 2.92 grams of ammonia. On a volume basis, 146 cc. of ammonia and 89.2 cc. of butane were sorbed per gram of charcoal.

The equilibrium sorption weights for ammonia were found to be expressed closely by the Langmuir and Freundlich isotherms over the range 50 - 760 mm. Hg partial pressure. The equations determined were

$$x/m = \frac{0.278\ P}{1 + 0.000555\ P}$$

and

$$x/m = 1.06\ P^{\frac{1}{1.31}}$$

The isotherm over this range of pressures, does not show a maximum amount sorbed as the partial pressure is increased. Below 50 mm. Hg the isotherm fell off quite rapidly to the origin. Butane, on the other hand, did not follow an isotherm of this type at all closely over the same range of partial pressures. The amount sorbed increased very rapidly at low partial pressures, but sloped off more gradually than either isotherm predicts, to a maximum value.

The desorption of the two gases using pure air was different. Ammonia was not removed completely from the charcoal when equilibrium had been established between the desorbing stream and the charcoal, while butane desorption indicated that complete removal was possible. Ammonia sorption thus appears to be reversible to a limited extent, and the remaining gas is bound to the charcoal quite firmly. Butane however appears to be sorbed in a completely reversible manner.

The relation between service time and sorbate rate at constant air flow is different for the two gases. The variation of service time with

ammonia rate shows a straight line relation between the logarithm of the service time and the rate. With butane sorption, a straight line relation was obtained between the logarithm of the service time and the logarithm of the butane rate. This difference is possibly due to the difference in the sorptive capacity of charcoal for the two gases as shown by their sorption isotherms.

These differences indicate some difference in the mechanisms of sorption in the two cases. The butane sorption seems to be a molecular sorption, in which the forces binding the gas to the charcoal are not very great, and the sorption is easily reversible. The ammonia sorption, however, appears to be a combination of molecular sorption and chemisorption. The sorption is reversible to some extent indicating some molecular sorption, but there is a residual quantity of ammonia which cannot be desorbed by reducing the partial pressure of the ammonia in the gases above the charcoal. This indicates that chemisorption is occuring in which the ammonia is held by co-volent bonds between the sorbate and the charcoal, a binding which is more difficult to break, making the sorption not completely reversible.

The theories of sorption as developed by Danby et al and Mecklenberg were based on entirely different considerations. Mecklenberg assumed sorption to occur by capillary condensation, while Danby et al postulated the existence of active centers each of which were capable of dealing with a certain number of molecules of sorbate. The theory of Danby et al assumed that the sorption was the rate controlling step, while Mecklenberg assumed the process to be expressible by the Nernst formula for heterogeneous reactions which is dependent on the diffusion rate. Their predictions however, are similar for the relations of the sorption data in terms of the experimental variables.

From the relations in both theories, the concentration of the gas decreases exponentially with distance along the bed from the initial concentration of the entering gases, and increases exponentially with time, so that there is a working layer established when the sorbate is being removed. The relations between the sorption data such as sorption capacity, service time, escaping concentration, dead length, and sorption gradients as derived by both theories has been previously discussed.

In general, the results of the investigations presented herein are in good agreement with the theories of sorption, as expressed by these two authors, and with data for other gases as found by other investigators.

It was found that the logarithm of the escaping concentration gave a linear relation with time during the early stages of breakdown, but deviated as the escaping concentration increased as was predicted by Danby et al. At the higher concentrations, a linear relation was obtained between the logarithm of the escaping concentration, and the reciprocal of the time.

The service time gives a linear relation with column length over the ranges investigated. A linear relation was also found between the service time and the reciprocal of the flowrate at constant concentration. There appears to be a slight disagreement with the theories concerning the relation between service time and initial concentration at low concentrations. The theories predict c_o times T equals a constant. This was found to be true except at low ammonia concentrations when the product falls off as concentration is decreased. This appears to be due to the decreased sorption capacity at very low concentrations, neither theories take this fact into account in their relations.

It was found that the linear relation predicted between dead length and the logarithm of the initial concentrations did not hold below 7 mm. partial pressure of butane. In this region, a linear relation was found

between the dead length and the initial concentration. This again appears to be due to the decreased sorption capacity at very low concentrations.

The sorption gradients obtained agree well with those predicted by Danby et al in their detailed theory, and found by Shilow et al and explained by Mecklenberg. The gradients differ in shape in the first sections of the bed from those in the later since initially the charcoal is completely unsaturated, but the final shape is gradually built up which then moves along the bed at a constant velocity. The length of the working layer thus increases also to a constant value. Mecklenberg explained the change in shape of the gradients as due to the variation in capillary size and the slow migration from the outer into the inner capillaries. Another factor which is suggested by this investigation is that of the temperature rise, which lengthens the working layer by reducing the sorption capacity when the stream first passes through the bed, allowing the sorbate to penetrate further before being completely sorbed. Thus the sorption continues near the end of the gradients as the charcoal in this region is cooled to the temperature of the gas stream.

The investigations reported in this work indicate that the sorption of ammonia and butane agrees with the theories of dynamic sorption with very little modification. They also indicate that the apparatus used is adequate to obtain a thorough investigation of the dynamic sorption of gases. The apparatus could be adopted quite well for the study of gases more pertinent to the present international conflict.

BIBLIOGRAPHY

(1) Pearce, J. A. Ph.D. Thesis McGill University (1941)

(2) Langmuir, I. J. Am. Chem. Soc., 40, 1384 (1918)

(3) Williams, A. M. Proc. Roy. Soc. (London) A 96, 287, 298 (1919)

(4) Henry, D. C. Phil. Mag., 44, 689 (1922)

(5) Homfray, I. F. Z. physik. Chem. 74, 129 (1910)

(6) Titoff, A. Z. physik. Chem. 74, 641 (1910)

(7) Lamb, A. B. and Coolidge, A. S. J. Am. Chem. Soc. 42, 1146 (1920)

(8) McBain, J. W. The Sorption of Gases and Vapours by Solids, George Routledge and Sons (1932)

(9) Gregg, S. J. The Adsorption of Gases by Solids. Methuen and Co. (1934)

(10) Taylor, H. S. J. Am. Chem. Soc. 5298 (1930) 578 (1931)

(11) Polanyi, M. Trans. Faraday Soc. 28, 318 (1932)

(12) Mecklenberg, W. Z. Elektrochem. 31, 485 (1925)

(13) Mecklenberg, W. Kolloid - Z. 52, 88 (1930)

(14) Danby, C. J., Davoud, J. G., Everett, D. H., Hinshelwood, C. N. and Lodge, R. M. Some Aspects of the Physical Chemistry of the Respirator (1941)

(15) Engel Z. ges. Schiess - U. Spreng - stoffwesen 24, 451, 495 (1929)

(16) Schilow, N., Lepin, L. and Wosnessensky, S. Kolloid - Z. 49, 288 (1929)

(17) Dubinin, Parshin and Pupuirev J. Russ. Phys.-Chem. Soc. 62, 1947 (1930)

(18) Izmailov, and Sigalovskaya Trav. inst. chim. Charkow 1, 133 (1935)

(19) Ruff, W. Von Wasser 11, 251 (1936)

(20) Dubinin J. Russ. Phys.-Chem. Soc. 62, 683 (1930)

(21) Allmand Final Summary Report from University of London, (1941)

(22) Syrkin, J. K. and Kondraschow, A. J. Kolloid - Z. 56, 295 (1932)

(23) Arnell, J. C. War Research Reports, McGill University (1921)

(24) Berl, E. and Andress, K. Z. angew. Chem. 34, 377 (1921)

THE REACTION OF HYDROGEN ATOMS WITH PROPYLENE

(In collaboration with B. S. Rabinovitch)

TABLE OF CONTENTS

INTRODUCTION

The reaction of hydrogen atoms with hydrocarbons has been confined to the saturated paraffins and to ethylene. The reaction of propylene with hydrogen atoms produced by the Wood-Bonhoeffer method appeared as the next logical reaction to investigate for it would increase the data of olefin reactions and also, since the characteristics of propylene are intermediate between those of saturated and unsaturated hydrocarbons, would 'tie in' the reactions of olefins with those of saturates.

The Kinetics of Unimolecular Reactions

The contribution of van't Hoff (1) in establishing his law for the temperature dependence of the velocity constant

$$k = Be^{-E/RT}$$

from general thermodynamical considerations, and the later realization of the kinetic meaning of this law by Arrhenius, (2) was essentially the basis of modern chemical kinetics. Arrhenius showed that not all the molecules enter the reaction but only those which have an energy greater than a critical value E called the 'activation energy'. This is the most important dynamical constant characterizing the reacting substance.

In 1918, Lewis (3) made a further modification of Arrhenius' rate law by stating that the rate of a reaction could be represented by the total number of collisions, Z, multiplied by the Maxwell distribution function for the number of molecules with energies above E; i. e.

$$\text{Rate} = Ze^{-E/Rt}$$

The question of activation of unimolecular reactions became important for, according to this theory, at the limit of low pressures, no reaction could take place. To solve this Perrin (4) suggested that the cause of reaction was in the action of radiation upon the molecules. This theory received much support by Lewis (3), Trantz (5) and others but was abandoned when Daniels (6) proved radiation was of negligible effect in a conclusive experiment.

This Lewis equation can easily be solved since Z may be calculated by use of molecular diameters, and E can be determined

from the variation of the specific reaction rate with temperature.

Since the rate of unimolecular reaction is proportional to the concentration of the reacting gas, it was apparent that collisions alone could not be the complete explanation. The constant of the Arrhenius equation was then related to the vibration frequency ν of one of the bonds of the reacting molecule.

$$k = \nu e^{-E/RT}$$

This alone is not a full explanation of the way that a molecule acquires its activation energy. Lindemann (7) explained the peculiarities of unimolecular reactions by suggesting that a reacting molecule acquires its activation energy as a result of a collision, but that there is a time lag before the molecule decomposes. If the period of time between activation and collision is large in comparison to the time between successive collisions, the reaction is kinetically first order even though two molecules are involved in collision. The equation for this is

$$\text{normal molecules} \underset{\text{collision}}{\overset{\text{collision}}{\rightleftharpoons}} \text{Activated molecules} \xrightarrow{} \text{products of reaction}$$

As the pressure is decreased, the rate is independent of pressure until at very low pressures a "critical" pressure is reached where the rate falls off. At this pressure the time between collisions of normal molecules is comparable to the time lag and so the stationary concentration of activated molecules is diminished by their removal by chemical transformation.

This theory was elaborated by Hinshelwood (8) who assumed that the rate of reaction was independent of the energy as long as it exceed-

ed the necessary activation energy. Rice and Ramsperger (9) treated this theory mathematically and suggested that the energy must collect in a single bond for a reaction to take place. Thus the activation energy is a measure of the bond strengths.

Kassel (10) later modified this by stating that the rate was not independent of the amount of energy in excess of E, but a function of this amount. Kassel here treated mathematically the relation between the rate of reaction and the number of quanta which must be located in a particular bond to react,

$$k_{\infty} = Ae^{-mh\nu/kT}$$

where A is a measure of the frequency with which the energy of the molecule is redistributed among the various oscillators, ν, the frequency of the oscillators (here assumed equal) and k, the Boltzmann constant.

Chain Mechanisms

The chain theory of chemical reactions arose from two principal sources; the investigation of the hydrogen-chlorine reaction by Bodenstein in 1913 and from a paper by Christiansen and Kramers in 1923.

Bodenstein (11, 12, 13) in an investigation of the photochemical reaction between hydrogen and chlorine showed that the Einstein law was not even approximately obeyed. The rate of reaction was many times greater than calculated. To explain this he suggested that the absorption of the light quanta by the chlorine molecule resulted in an activated molecule, which reacted with hydrogen producing two molecules of hydrogen chloride, one of which was activated. This activated molecule of hydrogen chloride would then activate another chlorine molecule, thus continuing the chain, i. e.

$$Cl_2 + h\nu \longrightarrow Cl_2^*$$

$$Cl_2^* + H_2 \longrightarrow HCl^* + HCl$$

$$HCl^* + Cl_2 \longrightarrow Cl_2^* + HCl \text{ etc.}$$

Nernst (14) two years later proposed an "atom chain" whereby the light split the chlorine molecule into two atoms which would then start a chain according to

$$Cl_2 + h\nu \longrightarrow 2Cl$$

$$Cl + H_2 \longrightarrow HCl + H$$

$$H + Cl_2 \longrightarrow HCl + Cl \text{ etc.}$$

The other approach to the chain theory was by Christiansen and Kramer (15) who attempted for the first time to apply the chain conception to thermal reactions. The kind of chain suggested was one in which the energy of activation, and the heat liberated were handed on from the products to fresh molecules of reaction. This theory has been further advanced by Christiansen (16) in 1928 and Semenoff (17) in 1932.

Although the energy chain theory is accepted today with some reservations, the real impulse to a chain mechanism was the Rice free radical theory. The thermal reactions were easily explained on the basis of atoms and radical chain carriers.

Paneth and Hofeditz (18) in 1929 and Paneth and Lautsch (19) in 1930 found that they could produce, by pyrolytic reactions, organic radicals that could be detected by their combination with mirrors of mercury or tellurium. With this proof of free radical existance, and with further work done by himself and co-workers, F. O. Rice (20, 21) formulated free radical mechanisms for many reactions. Rice and Herzfeld (22) with arbitrary assumption of activation energies showed that propagation of radical chains should be possible.

Rice postulated that the primary step in the hydrocarbon decomp-

osition was a unimolecular reaction and consisted of a split into free radicals. On the basis of the activation energies required for the possible methods of this splitting, the most probable break can be determined. The activation energies determined then for these reactions should be a measure of the strength of the ruptured bonds.

The strengths of a number of bonds calculated by Pauling (23) from the experimental values of heats of combustion and formation of the gaseous molecules are as follows: (values given by Hückel (24) are also presented)

	Pauling	Hückel
C - H (Hydrocarbons)	100 K.cal.	101 K.cal.
C - C (Hydrocarbons)	82.5 K.cal.	71 K.cal.
C = C (Hydrocarbons)	145 K.cal.	125 K.cal.
C ≡ C (Hydrocarbons)	200 K.cal.	166 K.cal.

As the strength of the C - H bond is considerably stronger than that of the C - C bond, one can conclude that the primary break would be a C - C bond and not a C - H or a double or triple bond. But substitution and structure also have a marked effect on the bond strengths. There is probably only a small difference in strength between the primary, secondary and tertiary C - H bonds in saturated hydrocarbons (25) but the presence of a double or triple bond in the molecule has a pronounced effect upon the adjacent bonds. The bonds in the alpha position to the double bond are much stronger than normal, whereas those in the beta position are much weaker (21,26); e. g., for propylene and 1 - butene

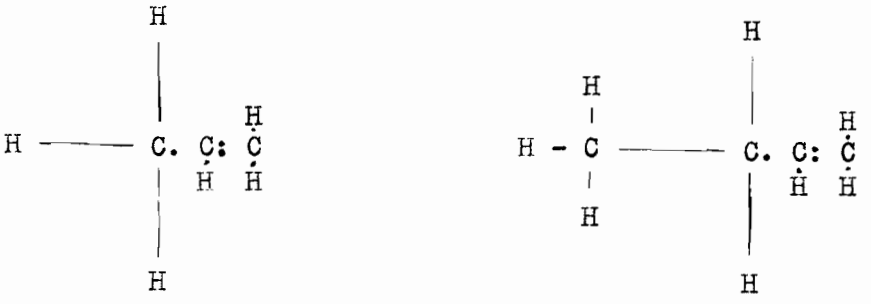

——— weak bonds — normal bonds . strong bonds

Rice assumes that a beta C - H bond in an olefin is at least 6 K.cal less than that of a primary C - H bond in a paraffin hydrocarbon, and that, on the other hand, the strength of the bond holding the alpha hydrogen atom is increased by approximately the same amount. The alpha C - C bond strength is increased in a corresponding ratio. From these assumptions we see that in any reaction between a free radical and an olefinic molecule, the beta hydrogen atoms will be attacked almost exclusively, unless of course association takes place.

A typical Rice mechanism for a saturated hydrocarbon is shown by the following decomposition of propane. The primary reactions would be

P_1 $\qquad C_3H_8 \longrightarrow CH_3 + CH_3CH_2$

followed by the secondary reactions

S_1 $\qquad C_3H_8 + CH_3CH_2 \longrightarrow C_2H_6 + CH_3CH_2CH_2$ or

S_2 $\qquad C_3H_8 + CH_3CH_2 \longrightarrow C_2H_6 + CH_3CHCH_3$

Then A_1 $\qquad C_3H_8 + R \longrightarrow RH - CH_3CH_2CH_2$

$\longrightarrow RH - C_2H_4 - CH_3$

A_2 $\qquad C_3H_8 + R \longrightarrow RH - CH_3CHCH_3$

where R = CH_3 or H

This mechanism assumes that reactions S_1 and S_2 have activation energies less than P_1. The main products of the reaction are governed by the chain mechanism A_1 and A_2 and consist therefore of methane and ethylene in equal amounts, and of hydrogen and propylene, also in equal amounts. Since there are six primary and two secondary hydrogen atoms (which are twice as reactive as the primary) the ratio of A_1 to A_2 would be as 6:4, and the quantitative result would be

$$6\ C_3H_8 \longrightarrow 6\ CH_4 + 6C_2H_4$$

$$4\ C_3H_8 \longrightarrow 4\ C_3H_6 + 4\ H_2$$

Rice and Hersfeld (27) devised a mechanism to explain why the experimental activation energy is less than that required for a C - C split and why, although the reaction is a series of complex steps, the overall mechanism is first order. By making suitable choice of activation energies of the individual steps, they were able to get the overall activation energy to agree with the experimental value. For molecules that contain only one kind of hydrogen atom (and which therefore have only one chain cycle) the only important reactions are those involving the primary rupture of the molecule, the two reactions of the chain cycle, and the final collision of the chain carriers to produce one or more molecules. These may be represented as

		E (K.cal)
(1) $M_1 \longrightarrow R_1 + M_2$	k_1E_1	80
(2) $R_1 + M_1 \longrightarrow R_1H + R_2$	k_2E_2	15
(3) $R_2 \longrightarrow R_1 + M_3$	k_3E_3	38
(4) $R_1 + R_2 \longrightarrow M_4$	k_4E_4	8

A molecule M_1 decomposes into a radical R_1 and a smaller molecule. Radical R_1 then takes off a hydrogen atom from another reactant molecule M_1 forming the molecule R_1H and radical R_2 which in turn decomposes into R_3 and M_3. The chain process (3) and (4) is finally terminated by collision of R_1 and R_2 forming M_4.

Setting up the rate equations we have

$$\frac{dR_1}{dt} = 0 = k_1M_1 - k_2R_1M_1 + k_3R_2 - k_4R_1R_2$$

$$\frac{dR_2}{dt} = 0 = R_2R_1M_1 - K_3R_2 - K_4R_1R_2$$

Solving for R_1 and R_2 we get

$$\frac{-dM_1}{dt} = K_1M_1 + k_2R_1M_1 = k_1M_1\left(1 + \frac{k_2\sqrt{\frac{k_1k_3}{2k_2k_4}}}{k_1}\right)$$

$$= k_1M_1\left(1 + \sqrt{\frac{K_2k_3}{2k_1k_4}}\right) \sim M_1\sqrt{\frac{k_1k_2k_2}{2k_4}}$$

i. e., it follows a unimolecular law. The overall rate of reaction is determined by two factors, the rate of primary reaction (k_1M_1) and that of the chain reaction ($k_2R_1M_1$); the ratio K_2R_1/ k_1 of these two rates gives the length of the chain. Also

E overall = 1/2 (E_1 + E_2 + E_3 + E_4) = 62.5 Kcal. which is well below the strength of the C - C bond.

If the chain terminating step had been

$$2R_1 \rightarrow M_5$$

then the rate would be proportional to the 1.5 power of the concentration of M_1. If the chain had terminated by

$$2R_2 \rightarrow M_6$$

then the rate would be proportional to the 0.5 power of the concentration of M_1. Thus it is necessary to assume that

$$R_1 + R_2 \rightarrow M_4$$

is much faster than the other two possible recombinations to predict a first order rate.

The Rice mechanism for propylene decomposition is as follows:

P_1 $\quad C_3H_6 \rightarrow CH_3- + CH_2 = CH-$

S_1 $\quad C_3H_6 + - CH_3 \rightarrow CH_4 + \dot{C}H_2\dot{C}H\dot{C}H_2$

S_2 $\quad C_3H_6 + CH_2 = CH- \rightarrow C_2H_4 + \dot{C}H_2\dot{C}H\dot{C}H_2$

The chief gaseous products are thus methane and ethylene. There is no chain reaction because the allyl group simply regenerates itself and forms propylene when either of the end carbon atoms takes a hydrogen atom from a propylene molecule, or if the middle carbon adds a hydrogen atom. It either isomerizes to propylene or finally forms propane according to

S_3 $\quad C_3H_6 + \dot{C}H_2CH\dot{C}H_2 \rightarrow \dot{C}H_2CH_2\dot{C}H_2 + \dot{C}H_2\dot{C}HCH_2$

S_4 $\quad C_3H_6 + \dot{C}H_2CH_2\dot{C}H_2 \rightarrow CH_3CH_2\dot{C}H_2 + \dot{C}H_2\dot{C}HCH_2$

S_5 $\quad C_3H_6 + CH_3CH_2\dot{C}H_2 \rightarrow C_3H_8 + \dot{C}H_2\dot{C}HCH_2$

Each allyl radical that becomes propane is replaced by three other allyl radicals. These eventually combine with each other to form diallyl which subsequently decomposes to form liquid products. The overall decomposition should be

$$3C_3H_6 \longrightarrow CH_4 + CH_2 = CH_2 + CH_2 = CHCH_2CH = CH_2 .$$

The amount of propane formed would be small.

Support for the free radical theory was immediate with several chain decompositions being induced by the introduction of free radicals (28, 29, 30).

Staveley and Hinshelwood (31) and others (32, 33) obtained further evidence for this mechanism with the discovery that large amounts of added nitric oxide catalyzed reactions, and small amounts acted as an inhibitor. They assume that maximum inhibition corresponds to complete suppression of the chains. On this basis they calculated the chain lengths of most reactions, in which inhibition was found, to be from two to fifteen which is too small to agree with the Rice-Herzfeld mechanism but is direct evidence for the presence of chains. Recent work (34, 35) indic-

ates that there may be a few long chains rather than a large number of short ones.

The Rice-Herzfeld theory has received much support but the specific mechanisms for a number of reactions do not agree with those originally suggested. It appears that the theory is in part correct but that its present form is too broad and incomplete.

The two main methods of investigating further the elementary reactions of the hydrocarbons are by photochemical and atomic reactions.

With hydrocarbons the photochemical reaction is usually a photosensitized reaction rather than photodecomposition since they are transparent down to the extreme ultra-violet. The photosensitization is done either with hydrogen present to produce a known concentration of hydrogen atoms which react, or the excited vapor can transfer its energy by direct collision with the hydrocarbon molecule. Mercury photosensitization (36, 37) is the most common, using the Hg (6^3P_1) level. Other metals have been used, however, as sensitizers to vary the energy available in the sensitizing atom. Cadmium (38,39) using the 5^3P_1 and the 5^1P_1 lines, and zinc (40) using the 4^3P_1 and the 4^1P_1 lines have been used.

Jungers and Taylor (41) used the sodium D- doublet but they found that although ethylene quenched the radiation, no reaction occurred.

The other main method is the production of the active species by an electrical discharge. Either the hydrocarbon gas is itself subjected to the discharge, which results in almost every possible atom or radical being produced, thus making it impossible to obtain much information about specific chemical reactions; or the products from a discharge are mixed with another substance. Hydrogen, oxygen, nitrogen and other gases

have been used to produce atoms which are then removed and mixed with the reacting substance.

In this investigation the latter method was employed, using hydrogen atoms, as produced by the Wood-Bonhoeffer method, as the active species. Wood (42) showed that hydrogen atoms could be pumped out of a hydrogen discharge tube for considerable distance before they recombined. Bonhoeffer (20, 21) modified Wood's apparatus and made extensive investigations with atomic hydrogen. In this type of apparatus a pressure of about 0.1 to 1 mm. is used with a very high rate of flow, about 3 meters per second.

Atomic Reactions of the Simple Hydrocarbons

Methane

The reaction $H + CH_4 \longrightarrow CH_3 + H_2$ (1)

was investigated first by Bonhoeffer and Harteck (44) and later by von Wartenberg and Schultze (45) and Chadwell and Titani (46) who found that methane was very inert.

Geib and Harteck (47) investigated the reaction up to 183°C but got no apparent reaction and concluded that the activation energy was at least 17 K.cal. They ruled out the suggestion that radicals were formed but that the reaction

$$CH_3 + H \longrightarrow CH_4$$

was so rapid that other reactions could not occur on the grounds that it was unlikely that no other secondary reactions of the methyl radical could occur, and also that the H atoms concentration was not altered by the presence of methane. This latter argument could be explained by assuming that the activation energy of the reverse reaction

$$CH_3 + H_2 \rightarrow CH_4 + H \qquad (2)$$

was low and that the H atom concentration was maintained in this way. Estimations of the activation energy range between 8 to 23 K. cal (48, 49), but it is probably between 15 to 20 K.cals.

Further evidence that reaction (1) has an activation energy greater than 11 K.cal was obtained by Geib and Steacie (50) who investigated the reaction of deuterium atoms with methane up to 100°C using the Wood-Bonhoeffer method. There was no detectable exchange. Their investigation indicated that the reaction was probably

$$CH_4 + D \rightarrow CH_3D + H$$

Steacie (51) further investigated this reaction up to 500°C and obtained an activation energy of 12.9 $\pm$ 2 K.cal.

Farkas (52) in investigating the thermal exchange reaction between deutirium and methane at temperatures around 1000°K concluded that the thermal reaction proceeds by an atomic mechanism with an activation energy for the exchange of about 11 to 12 K.cals.

Later studies have given the value of the activation energy for the exchange to be between 11.7 and 15.6 K.cals. (49, 53, 54, 55, 56), with the evidence pointing to about 15 K.cals. There is a difference of opinion as to whether the primary reaction concurred is

$$D + CH_4 \rightarrow CH_3D + H$$

or

$$D + CH_4 \rightarrow CH_3 + HD$$

The latter reaction seems more plausible.

Gorin, Kauzman, Walter and Eyring (57) calculate for the reaction

$$H + CH_4 \rightarrow CH_4 + H$$

an activation energy of 37 K.cals. which would rule out this reaction in favour of

$$H + CH_4 \rightarrow CH_3 + H_2$$

for which they calculate an activation energy of 9.5 K.cals.

From this it appears methane is fairly stable in H atoms and does not react until a temperature over 180°C is reached.

The reverse reaction

$$CH_3 + H_2 \rightarrow H + CH_4$$

occurs to some extent around 200°C with an activation energy of between 8 to 23 K.cals.

Ethane

Bonhoeffer and Harteck (44) and von Wartenberg and Schultze (45) first investigated the reaction of hydrogen atoms and ethane. They reported the ethane unchanged, though they lost gas which might have been methane. Chadwell and Titani (46) reported methane and ethylene formed in this reaction. Kemula (58) found methane in the reaction of ethane with hydrogen atoms produced by mercury photosensitization.

Steacie and Phillips (53) investigated the reaction of deuterium atoms with ethane using the Wood-Bonhoeffer technique and obtained a value of 6.3 K.cals. for the exchange reaction. They concluded the likely mechanism was

$$C_2H_6 + D \longrightarrow C_2H_5 + H\,D \qquad (1)$$

$$C_2H_5 + D \longrightarrow C_2H_5D \qquad (2)$$

Trenner, Morikawa and Taylor (56) reinvestigated this reaction and obtained 10 - 20% ethane decomposition to methane which was 50% deuterized. They state that at room temperature the main reaction is

$$C_2H_6 + D \longrightarrow CH_3D + CH_3 \qquad 7.2 \text{ K.cals.} \quad (3)$$

and that above 100°C reaction (1) also occurs.

Steacie (59) on reinvestigating the reaction also found methane at room temperature.

The reaction of ethane with hydrogen atoms has been investigated qualitatively by photosensitization with mercury by several workers (58, 60). Steacie and Phillips (61) investigated this reaction in a flow system and found that hydrogen was consumed and methane, propane and butane formed. The mechanism they suggest is in accordance with equations (1) and (3).

The reverse reaction

$$C_2H_5 + H_2 \longrightarrow C_2H_6 + H$$

has been investigated by Leermakers (62) and others (63, 64) and the opinion is that this reaction does occur to some extent at temperatures above 160°C, with activation energy between 9 - 15 K.cals.

Propane

Taylor and Hill (60) by mercury photosensitization found that propane reacts somewhat faster with hydrogen atoms than does ethane, but more slowly than butane.

Trenner, Morikawa and Taylor (56) made two runs with propane and deuterium atoms produced by the Wood-Bonhoeffer method and found that the products were methane and ethane which were highly deuterized and propane which was not deuterized.

Steacie and Parlee (65) investigated the reaction of hydrogen atoms and propane using the Wood-Bonhoeffer method. They found methane almost exclusively at lower temperatures, at 100°C ethane started to form while at 250°C there was more ethane than methane. At some higher temperatures some ethylene was also formed. They obtained a value of 10 ± 2 K. Cals. for the activation energy of the primary step.

That the primary step is

$$H + C_3H_8 \longrightarrow C_3H_7 + H_2$$

was established definitely by Steacie and Dewar (66) who found only hydrogen and hexane as products of the reaction of hydrogen atoms produced by mercury photosensitization with propane.

by the mercury photosensitization and by the discharge tube methods. Geib and Harteck (69) found that hydrogen atoms and ethylene formed ethane at liquid air temperature which indicates a very low activation energy (less than 5 K. cals.)

The reaction was first studied by mercury photosensitization by Taylor and Marshall (70) who found that there was a steady drop in pressure, presumably owing to the formation of ethane. The rate was high, suggesting chain reaction.

Olsen and Meyers (71) using the same method found the initial slope of the pressure curve showed that the initial rate was proportional to the square of the hydrogen atom pressure and so the reaction was not simply

$$C_2H_4 + H_2 \longrightarrow C_2H_6$$

In a later paper (72) they reported the products as follows: witha high initial concentration of ethylene, hydrogen 39 cms. and ethylene 25 cms., the relative amounts of products were methane .018, ethane 1, propane .64 and butane .42; with a lower concentration of ethylene, hydrogen 40 cms. and ethylene 2 cms., the products were methane .22, ethane 1, propane .04 and butane .0008. The mechanism for the primary processes is

$$Hg^{*} + H_2 \rightarrow 2H + Hg$$

$$Hg^{*} + C_2H_4 \rightarrow C_2H_2 + H_2 + Hg$$

and

$$Hg^{*} + C_2H_4 \rightarrow {}_2C_2H_2 + Hg$$

The last of these is impossible since the C = C bond strength is above 112 K. cals. The main secondary reactions they postulate are

$$C_2H_4 + 2H \longrightarrow C_2H_6$$

$$CH_2 + 2H \longrightarrow CH_4$$

and at higher ethylene concentrations

$$CH_2 + C_2H_4 + 2H \rightarrow C_3H_8$$

$$C_2H_4 + C_2H_x^{*} + yH \rightarrow C_4H_{10}$$

Later though, Stewart and Olsen (73) point out that the above analysis cannot be taken too seriously since secondary chemical reactions may occur in the ion stream of the mass spectograph used for analysis.

Bates and Taylor (74) in a mercury photosensitized system of ethylene and hydrogen found that polymerization accompanied the ethane formation. The mechanism advanced was

$$C_2H_4 + Hg^{*} \rightarrow C_2H_2 + H_2 + Hg$$

$$H + C_2H_4 \rightarrow C_2H_5$$

and

$$H + (C_2H_2)_n \rightarrow (C_2H_2)_nH$$

The work of W. H. Johns (75) showed that free ethyl groups liberated in ethylene form high boiling hydrocarbons.

$$C_2H_5 + C_2H_4 \rightarrow C_4H_9$$

This latter reaction is suggested as the mechanism for the polymerization.

Taylor and Hill (37, 60) in a more thorough investigation found that when hydrogen was in large excess the product was mainly ethane; but with relatively more ethylene higher hydrocarbons were formed. They concluded that the main step was

$$H + C_2H_4 \rightarrow C_2H_5$$

Jungers and Taylor (76) in a similar investigation with C_2H_4 and C_2D_4 found that when the hydrogen was in a large excess, the products were mainly butane which disagreed with Taylor and Hill. They suggest this difference was due to the deposit of polymer in Taylor and Hill's apparatus. Jungers and Taylor found that when the hydrogen-ethylene ratio

was greater than three, the rate of reaction was independent of the ethylene concentration, indicating the primary process was

$$H_2 + Hg(^3P_1) \rightarrow HgH + H$$

$$\text{or} \rightarrow Hg\ (^1S_o) + 2H \qquad (1)$$

The next step is

$$H + C_2H_4 \rightarrow C_2H_5 \qquad (2)$$

Since little ethane is formed, the reactions

$$H + C_2H_5 \rightarrow C_2H_6 \qquad (3)$$

and

$$H_2 + C_2H_5 \rightarrow C_2H_6 + H \qquad (4)$$

do not appear to occur. The absence of (4) is explained on the high activation energy required for it, and of (3) is apparently due to reaction (2) removing all the H atoms. Butane formation is explained by

$$2\ C_2H_5 \rightarrow C_4H_{10}$$

Moore and Taylor (77) obtained results similar to Jungers and Taylor.

The other products found are explained by reaction (4) increasing at higher temperatures and also

$$C_4H_9 \rightarrow CH_3 + C_3H_6$$

and

$$C_4H_9 \rightarrow C_2H_4 + C_2H_5$$

For the reaction

$$C_2H_5 \rightarrow C_2H_4 + H$$

Bawn (78) calculates the activation energy to be approximately 49 K. cals.

Propylene

Moore and Taylor (77) made a single run on the mercury photosensitized hydrogenation of propylene. They obtained as products 2% methane, 1% ethane, 26% propane, 5% butane, 2% pentane and 64% hexane. This

indicates the main reactions as

$$H + C_3H_8 \longrightarrow C_3H_7$$

$$2C_3H_7 \longrightarrow C_6H_{14}$$

$$H + C_3H_7 \longrightarrow C_3H_8$$

$$2C_3H_7 \longrightarrow C_3H_6 + C_3H_8$$

Indications are that the activation energy for the primary step is low as in the case of the analagous reaction of ethylene. More propane was formed from propylene than was ethane from ethylene under similar conditions. This may be due to the greater importance of the disproportionation reaction for the propyl radical than for the ethyl radical. This may indicate that the isopropyl radical is formed in the primary step rather than the propyl radical, for Norrish (quoted in Pearson and Glazebrook (79)) found propane and propylene in the photolysis of di-isopropyl ketone; but none of these products in the photolysis of di-n-propyl ketone.

Moore and Taylor (77) also made a single run on butylene under the same conditions and obtained results similar to those reported for propylene.

EXPERIMENTAL

The experiments were carried out in a Wood-Bonhoeffer type apparatus as shown in figure 1. Hydrogen atoms, produced in the discharge tube, were mixed with propylene in the reaction vessel and the products pumped off through a trapping system.

The hydrogen from cylinder A was admitted to the apparatus through the purifying system. It was passed over platinized asbestos in a quartz tube B electrically heated to 500° C which removed any oxygen present. Any impurities present were taken out by the silica gel trap C, immersed in liquid air. The hydrogen was then passed over water in the trap S. This water vapour was added to poison the walls of the discharge tube and reaction vessel thus minimizing the recombination of atomic hydrogen.

Any tendency to build up pressure greater than atmospheric was counteracted by means of a mercury blow-off valve at the base of the manometer tube M_1. Small fluctuations in the pressure were smoothed out by the ballast bulb V_1. The purified hydrogen at atmospheric pressure diffused through the calibrated flowmeter into the discharge tube.

The propylene used was prepared by the dehydration of isopropyl alcohol with phosphoric acid according to the method of Ashdown, Harris and Armstrong (80). The di-isopropyl ether formed at the same time was removed by repeated distillation of the propylene between two traps. Impurities could not be detected in the final material by the analytical methods employed in this study.

The propylene was distilled into the storage volume V_2 which had been thoroughly evacuated beforehand. In making a run, some propylene was expanded into V_3 through the scratched stopcock N. From thereit diffused through the capillary flowmeter and passed into the reaction

vessel from below. By suitable adjustment of the valve N, any desired pressure head could be maintained in V_3, and thus the propylene flow could be altered at will. Knowing the volume of the storage bulbs V_2 and V_3, and the pressure before and after each run, the total flow of propylene during the run could be calculated.

The hydrogen atoms were formed in the high voltage discharge tube D. This consisted of a pyrex tube, 2.5 cm. in diameter, to which were sealed side tubes containing aluminium electrodes E. The leads to the electrodes were heavy platinum wires which passed into the compartments through tightly sealed thickwalled capillary tubing. A 5000 ohm resistance was connected in series with the discharge and 2500 volts applied across the two. The current was supplied by a transformer operating on 220 volts and was maintained at 200 milliamperes by a rheostat in the mains.

To reduce atomic recombination prior to reaction with propylene to a minimum, the outlet of the discharge tube was sealed directly to the reaction chamber R. The pyrex reaction chamber R had a diameter of 7 cm. and a length of 24 cm. It was surrounded by a close-fitting electric furnace F. Two tubes entered the reaction vessel from below, one of these, T, was a thermocouple well, the other served as the inlet for the propylene.

The products of the reaction were pumped out through trap C_3 which was immersed in liquid air. This removed all the propylene, as well as butane, propane, ethylene, and most of the ethane that might be present. The remainder passed through the diffusion pump P and through the silica gel trap C_4 which was kept at liquid air temperature and which would remove any ethane, all the methane and some hydrogen. Unabsorbed hydrogen passed out through the hyvac pump to the atmosphere.

The diffusion pump P had a potential speed of 20 litres per second. It was backed by the hyvac pump and maintained a vacuum of 0.35 mm. under operating conditions. The diameter of all tubing in the pumping and trapping system was about 2 cm. and all stopcocks were of corresponding large bore.

The hydrogen atom concentration in the reaction vessel for each working temperature was measured with the Wrede diffusion gauge W. This was of the usual type (81) and consisted of a capillary tube with a very small orifice situated in the reaction vessel, and an arrangement of stopcocks by means of which the inside or outside of the orifice could be connected to a Pirani gauge at will.

The instrument is based on the different rates of diffusion of atoms and molecules through the small orifice whose diameter is small relative to the mean free path of hydrogen. Atoms diffusing through the orifice recombine on the walls of the capillary tube to form molecules. Thus the pressure inside the orifice is due to molecular hydrogen alone. Hence a pressure gradient is set up between the inside and outside of the orifice. This pressure gradient could be measured on the Pirani gauge. Thus, knowing P_1 the pressure inside, and P_2 the pressure outside, the percentage H atoms is given by

$$\frac{100\ (P_1 - P_2)}{P\ (1 - 0.5\ 2)}$$

The atom concentration determinations could not be made during a run since the presence of propylene molecules would interfere with the above relation. Consequently measurements were made under the same conditions as the run, but with no propylene present. The difference in pressure due to the absence of propylene was very small since the ratio of H_2: C_3H_8 was high throughout all the runs.

The Pirani gauge was first calibrated against the McLeod gauge before it was used. The gauge was kept immersed in ice water. With the discharge operating, the inside of the orifice was connected to the gauge and the resistance due to the pressure was measured by means of a Wheatstone Bridge arrangement. Switching over to the outside, a similar series of readings was taken. This was repeated several times, alternating between the inside and the outside. From the measured resistance, in each case, the corresponding pressure in mm. could be obtained from the calibration curve. The percent atom concentration was determined by substituting these values for P_1 and P_2 in the above equation.

It was necessary to correct for an accompanying thermal effect by making a series of blank measurements with the discharge off, at each operating temperature.

The procedure of a typical run was as follows. The apparatus was first evacuated and the reaction vessel was brought to the desired temperature by adjusting the current through the furnace F. The platinized asbestos in B was heated to 500° C and liquid air was put around trap C_1. The hydrogen tank was opened slightly and hydrogen admitted to the discharge tube.

The discharge was turned on and the discharge current allowed to settle down for about five minutes while the hydrogen was pumped through the apparatus. Traps C_3 and C_4 were then immersed in liquid air, and the pressures and temperature of the propylene in the storage volumes were observed. The propylene flow was then turned on and the time noted. The flow was kept constant by maintaining a certain definite pressure head in V_3. This was accomplished by expanding gas from V_3 through the scratched

stopcock N so that the right arm of the absolute manometer M_2 was kept reasonably constant. The flow ratio of hydrogen to propylene was about 45:1, except in the last run when the flow was in the ratio of 18:1. About 350 c.c. of propylene were allowed to flow through the apparatus during a run, which lasted about 75 minutes. The propylene flow was shut off and the pressures and temperature in the storage volumes again noted. The flow of hydrogen was allowed to continue for about five minutes to flush out all products. It was then cut off, and the stopcock on the traps C_3 and C_4 were closed.

The products were removed from the apparatus to a gas holder through O by means of a Toepler pump. The products from both traps were combined. The silica gel trap was heated to 70° C while the products were being removed.

The products were analysed in a low temperature fractional distillation apparatus of the Podbielniak type. The propane-propylene fraction was analysed on a Burrell gas analysis apparatus. Other fractions were also tested for unsaturation but none was found. The presence of acetylene in the ethane fraction was qualitatively tested for using a silver nitrate solution.

RESULTS

Table 1 shows the experimental conditions and the results of the analysis of the products. The percent decomposition of propylene is given and the mol percent of the products. In all the runs there was less than 0.5% "C_4" hydrocarbon formed. In run 11, only a trace of "C_3" hydrocarbon was found.

The percent reaction in the last six runs was much greater than it was in the first four runs. This was probably due to an increased atom concentration in the last runs. Since the atom concentration was determined only for these last runs, all the calculations of collision yields and activation energies were made using the percent decompositions found from runs 5 to 10 inclusive.

In table 2 the products are expressed as mols per mol of propylene decomposed which makes the results independent of the percent decomposition. Here it is possible to compare all the runs since it is probable that the relative proportions of the products would not be greatly affected by the small change in atom concentration necessary to account for the change in the percent decomposition.

Table 3 presents the average values of the products expressed as mol per mol of propylene decomposed for each temperature.

Table 1

Experimental Conditions and Reaction Products

Press. of all runs - 0.35 mm. of Hg.

Run No.	Temperature °C	Propylene Flow Mols / sec. X 10^{-6}	Hydrogen Flow Mols / sec. X 10^{-5}	Atom Concentration Percent	% reaction of C_3H_6	Products Mol percent			
						CH_4	C_2H_6	C_3H_8	C_3H_6
1	30	4.50	1.96		34.0	12.1	18.9	11.3	57.7
10	30	4.50	1.96	14.0	44.1	17.4	23.5	12.1	47.0
2	100	4.50	1.96		31.1	13.3	19.1	7.9	59.7
3	100	4.50	1.96		32.9	14.5	18.7	9.0	57.7
9	100	4.50	1.96	12.2	41.6	16.0	24.5	10.8	48.7
4	170	4.50	1.96		29.1	11.0	18.6	7.9	62.5
5	170	4.50	1.96	10.1	39.0	13.1	23.5	11.2	52.2
8	170	4.50	1.96	10.1	39.1	14.0	22.6	11.4	52.0
6	250	4.50	1.96	8.3	39.5	15.3	22.6	11.1	51.0
7	250	4.50	1.96	8.3	38.1	16.1	21.2	10.5	52.2
11	54	1.10	1.96	14.0	100	65.3	34.7	Trace	Trace

Table 2

Run No.	Temperature °C	Reaction Products Mol / mol C_3H_6 decomposed.			
		CH_4	C_2H_6	C_3H_8	"C_4"
1	30	0.41	0.64	0.38	0.01
10	30	0.47	0.64	0.33	0.01
2	100	0.49	0.71	0.29	0.01
3	100	0.52	0.66	0.32	0.01
9	100	0.46	0.71	0.31	0.01
4	170	0.43	0.73	0.31	0.01
5	170	0.39	0.70	0.34	0.01
8	170	0.42	0.68	0.34	0.01
6	250	0.46	0.68	0.33	0.01
7	250	0.47	0.65	0.32	0.01
11	54	1.43	0.76	trace	trace

Table 3

Temperature °C	Percent Decomposition	Reaction Products Mol / mol C_3H_6 decomposed			
		CH_4	C_2H_6	C_3H_8	"C_4"
30	14.0	0.44	0.64	0.35	0.01
100	12.2	0.49	0.69	0.31	0.01
170	10.1	0.41	0.70	0.33	0.01
250	8.3	0.46	0.67	0.33	0.01
54[x]	100	1.43	0.76	trace	trace

x Slow propylene flow rate.

Calculation of Collision Yields and Activation Energies.

The total flow rate of gas during a run could be calculated from the flow rates of hydrogen and propylene, and knowing the atom concentration the total flow rate could be corrected for the hydrogen atom formation.

The reaction time (in seconds), for any run was calculated by dividing the capacity of the reaction vessel (920 c. c.) in mols at each operating temperature, by the corrected flow rate (in mols / sec.)

Then knowing the fraction of hydrogen atoms present, and the total pressure, the partial pressure (P_H) of hydrogen atoms during the run was calculated (in mm.,) Knowing Avogadro's number, and the capacity of the reaction vessel, the number of atoms of hydrogen per c. c. (N_H), could be calculated in terms of a constant times P_H/T, T being the absolute temperature of the run.

The number of collisions per second with hydrogen atoms undergone by a propylene molecule is given by the relation (82,83):

$$Z_{C_3H_6H} = 2\sqrt{2\pi} \left(\frac{d_H + d_{C_3H_6}}{2} \right)^2 \left(\frac{M_H + M_{C_3H_6}}{M_H M_{C_3H_6}} \times RT \right)^{1/2} \times N_H$$

where d_H = diameter in cm of the hydrogen atom (2.14×10^{-8}). (83)

$d_{C_3H_6}$ = diameter in cm. of the propylene molecule (4.10×10^{-8}) (84)

M_H = atomic weight of hydrogen, $M_{C_3H_6}$ = molecular weight of propylene.

R = gas law constant in ergs/mol/°C. (8.313×10^7).

T = absolute temperature of the run.

N_H = number of hydrogen atoms per c. c.

Taking into account all the constant values in the above expression, and substituting the proper values, it reduces to the following

$$Z_{C_3H_6,H} = 3.10 \times 10^8 \cdot P_H / T^{1/2}$$

Multiplying this value by the reaction time gave the number of collisions with hydrogen atoms undergone by a propylene molecule in the reaction time. Dividing the percent decomposition by this, gave the collision yield for the run (the number of molecules of propylene decomposed per collision of a propylene molecule with a hydrogen atom).

From the relation

$$\text{collision yield} = Ae^{-E/RT}$$

the activation energy E was calculated, assuming for the steric factor, A, a value of 0.1 in this case

$$E = 2.303 \times 1.987 \times T \times \log \frac{0.1}{\text{collision yield}}$$

The results of these calculations are shown in table 4.

Table 4

Temp. °C	Total Flow Corrected for Presence of atoms (mol/sec x 10^{-5})	Reaction time (sec.)	Hydrogen Atoms Partial Pressure (mm.)	$Z_{C_3H_6,H}$ X Reaction Time X 10^5	% Reaction	Collision Yield X 10^{-7}	K(K.cal.) A = 0.1
Over-all reaction							
30	2.56	.668	.0404	4.81	.441	9.18	7.0
100	2.54	.547	.0352	3.09	.416	16.3	8.3
170	2.52	.465	.0290	2.01	.391	19.5	9.6
250	2.50	.393	.0238	1.33	.388	29.2	10.8

DISCUSSION

Over the temperature range, 35° to 250°C, the products of the reaction do not seem to vary greatly. They depend upon the flowrate of the propylene to a great extent. At ordinary flowrates, 4.5×10^{-6} mols per second, the products consist of methane, ethane, propane, traces of C_4 hydrocarbons, and unchanged propylene; at slow flowrates, they consist of methane and ethane only, with traces of C_3 hydrocarbon and C_4 hydrocarbon. The extent of reaction between 35° and 250° does not vary greatly, but does tend to decrease with increase in temperature, probably due to the decreased hydrogen atoms at higher temperatures.

These facts indicate that the activation for this reaction must be very low, probably less than 5 K.cal. The activation energy reported for the reaction of the methyl radical with propylene is 3.1 K.cal. However this latter is assumed to be the activation energy for the reaction

$$CH_3 + C_3H_6 \longrightarrow CH_4 + C_3H_5$$

For the reaction

$$H + C_2H_4 \longrightarrow C_2H_5$$

the activation energy has been variously taken as between 5 and 14 K.cals. (69,78,86), but the more probable value is 5 K.cals.

Thus the activation energy found in this investigation, 8.5 ± 1.5 K.cal. appears much too high. This energy is probably the activation energy of a secondary reaction which is the rate controlling reaction. The primary reaction appears unlikely to be the controlling factor.

It is also possible that the steric factor assumed, 0.1, is too high, and that a lower factor might be more appropriate. A steric factor of 0.01 would give an activation energy of about 5 K.cals.

Another factor might be that there was not sufficient hydrogen atoms

present to react with all the propylene, that is, that the hydrogen atoms were "cleaned up" as is postulated by Jungers and Taylor for ethylene (76), and therefore the percentage reaction should be 100% instead of 40% as was indicated. This would lower the calculated activation energy by about 2 K.cals.

The increase in activation energy with temperature is probably only apparent. Similar increases have been observed with other hydrogen atom reactions. The explanation for this increase here is likely due to the fact that even though the temperature was varied, the rate of the primary step was constant which would make the variation in the temperature be reflected in the activation energy.

Mechanism of the Reaction

From the information at hand it is difficult to postulate a mechanism that covers all the products. The investigation of the reaction of hydrogen atoms with ethylene at varying flowrates would considerably aid in determining the mechanism for this reaction.

The primary step of the reaction of hydrogen atoms with propylene could be

$$H + C_3H_6 \longrightarrow C_3H_7 \qquad 1(a)$$

$$H + C_3H_6 \longrightarrow C_3H_5 + H_2 \qquad 1(b)$$

or

$$H + C_3H_6 \longrightarrow CH_4 + C_2H_3 \qquad 1(c)$$

Reactions 1(a) and 1(b) both have an activation energy of about 5 K.cals., however, the results of Moore and Taylor (77) and a comparison with the ethylene reaction indicates 1(a) to be more likely. Also, since no ethylene was found in the products it is unlikely that dehydrogenation was the first step. Reaction 1(c) is unlikely to occur despite the

presence fo the weakened C - C bond because the energy required for this would be much greater than that required for the first two equations. Thus it seems likely that reaction 1(a) is the primary reaction.

Secondary reactions such as the following might occur

$$H + C_3H_7 \longrightarrow C_2H_5 + CH_3$$

$$2C_3H_7 \longrightarrow C_3H_8 + C_3H_6$$

$$H + C_2H_5 \longrightarrow 2CH_3$$

$$2CH_3 \longrightarrow C_2H_6$$

$$2C_2H_5 \longrightarrow C_2H_6 + C_2H_4$$

$$H + CH_3 \longrightarrow CH_4$$

$$H + C_2H_4 \longrightarrow C_2H_5$$

At high temperatures,

$$H_2 + CH_3 \longrightarrow CH_4 + H$$

$$H_2 + C_2H_5 \longrightarrow C_2H_6 + H$$

$$H + C_2H_5 \longrightarrow C_2H_6$$

can occur.

The obvious objection to such a mechanism as sketched above is the lack of hydrogen atoms at room temperature to take part in all the reactions. To explain this, one must assume radical reactions with propylene and with other radicals which immediately complicates the issue beyond explanation. The above mechanism with further enlargement might be sufficient to explain the reaction at high temperatures.

This mechanism could explain the results at the low flow when there are sufficient hydrogen atoms present.

$$H + C_3H_6 \longrightarrow C_3H_7$$

$$H + C_3H_7 \longrightarrow C_2H_5 + CH_3$$

$$H + C_2H_5 \longrightarrow 2CH_3$$

$$2CH_3 \longrightarrow C_2H_6$$

and

$$H + CH_3 \longrightarrow CH_4$$

These account for all the products.

A mechanism based on the formation of complexes such as $CH_3 - H - H$ as postulated by Gorin, Kauzmann, Walter and Eyring (57), and presented in the reactions of methyl radicals by H.A. Taylor et. al. (87,88), explains quite well the reaction products.

$$H + C_3H_6 \longrightarrow C_3H_7$$

$$H + C_3H_7 \longrightarrow C_2H_5 + CH_3$$

$$C_3H_7 + H_2 \longrightarrow C_3H_9$$

$$C_3H_9 + C_3H_7 \longrightarrow 2C_3H_8$$

$$C_2H_5 + H_2 \longrightarrow C_2H_7$$

$$C_2H_7 + C_2H_5 \longrightarrow 2C_2H_6$$

$$2CH_3 \longrightarrow C_2H_6$$

$$CH_3 + H_2 \longrightarrow CH_5$$

$$CH_5 + CH_3 \longrightarrow 2CH_4$$

Other reactions are possible that would probably occur to a smaller extent, such as

$$CH_3 + C_2H_5 \longrightarrow C_3H_8$$

$$2C_2H_5 \longrightarrow C_4H_{10}$$

and

$$CH_3 + C_3H_7 \longrightarrow C_4H_{10}$$

The absence of propane in the slow flow rate could be explained as due to the higher concentration of hydrogen atoms per propylene molecule, which would favor the reaction

$$H + C_3H_7 \longrightarrow C_2H_5 + CH_3$$

The reaction

$$H_2 + C_3H_7 \longrightarrow C_3H_9$$

would only occur when there was a shortage of hydrogen atoms.

A third possibility exists for a mechanism. For this it is necessary to postulate that, when hydrogen atoms react with propylene, a very reactive propyl radical is formed. Kistiachowsky et al (89) states that the hydrogenation of propylene

$$H_2 + C_3H_6 \longrightarrow C_3H_8$$

frees 30 K.cal. of energy, 15 K.cal. per hydrogen atom. If a similar amount of energy is available in the reaction with propylene, then a propyl radical containing this extra 15 K.cal. of energy, might be formed. If such an "active" radical were formed, a simple mechanism would result. These "active" radicals could undergo, at room temperature, reactions that are only possible at high temperatures for normal radicals. The following processes could occur, explaining all the products.

$$H + C_3H_6 \longrightarrow C_3H_7^*$$

$$C_3H_7^* + H \longrightarrow C_2H_5^* + CH_3^*$$

$$C_2H_5^* + H_2 \longrightarrow C_2H_6 + H$$

$$CH_3^* + H_2 \longrightarrow CH_4 + H$$

$$2CH_3^* + m \longrightarrow C_2H_6$$

and

$$C_3H_7^* + H_2 \longrightarrow C_3H_8 + H$$

The explanation for the lack of the formation of propane in the case of the slow flow, could be similar to the reason outlined in the preceding theory; that

$$C_3H_7^* + H_2 \longrightarrow C_3H_8 + H$$

only occurs when there are insufficient hydrogen atoms present. In the reaction of

$$C_3H_7^* + H \longrightarrow C_2H_5^* + CH_3^*$$

it seems unlikely that both radicals produced would be "active", but the one that was not active could undergo the normal reactions that have

been presented in the first mechanism since now there would be sufficient hydrogen atoms with which they could react.

Before such a mechanism as this can be postulated, further investigation is necessary, but the possibility of such an "active" radical cannot be overlooked.

Conclusions

The general conclusions that may be reached are that the activation energy of the hydrogen atom reaction with propylene is low, and that the rate of the reaction is independent of temperature. The products of the reaction indicate that a complicated mechanism is necessary, or that complexes or "active" radicals are formed. Before any final conclusions can be drawn, the further investigation of propylene at varying flowrates, and the investigation of the reaction of hydrogen atoms with ethylene is necessary.

Bibliography

(1) van't Hoff, Etudes de dynamique chimique, 1884

(2) Arrhenius S. Z. physik. Chem. 4, 226 (1889)

(3) Lewis, W. C. McC. J. Chem. Soc. 113, 471 (1918)

(4) Perrin, J. Ann. phys. (9) 11, 1 (1919)

(5) Trautz, M. Z. anorg. Chem. 102, 81 (1918)

(6) Daniels, J. quoted in Chem. Rev. 5, 62 (1928)

(7) Lindemann, F. A. Trans. Faraday Soc. 17, 598 (1927)

(8) Hinshelwood, C. N. Proc. Roy. Soc. (London) A113, 230 (1927)

(9) Rice, O. K. and Ramsperger, H. C. J. Am. Chem. Soc. 49, 1617 (1927)

(10) Kassel, L. S. J. Physik. Chem. 32, 225 (1928)

(11) Bodenstein, M. and Dux Z. physik. Chem. 85, 297 (1913)

(12) Bodenstein, M. Z. physik Chem. 85, 329 (1913)

(13) Bodenstein, M. Z. Elektrochem. 22, 53 (1916)

(14) Nernst, W. Z. Elektrochem. 24, 335 (1918)

(15) Christiansen, J. A. and Kramers, H. A. Z. physik. Chem. 104, 151 (1923)

(16) Christiansen, J. S. Trans. Faraday Soc. 24, 596 (1928)

(17) Semenoff, N. Trans. Faraday Soc. 28, 818 (1932)

(18) Paneth, F. A. and Hofeditz Ber. 62, 1335 (1929)

(19) Paneth, F. A. and Lautsch, W. Nature 125, 564 (1930)

(20) Rice, F. O. J. Am. Chem. Soc. 55, 3035 (1933)

(21) Rice, F. O. and Rice, O. K. Aliphatic Free Radicals, Johns Hopkins Press, Baltimore (1935)

(22) Rice, F. O. and Herzfeld, K. F. J. Am. Chem. Soc. 56, 284 (1934)

(23) Pauling, L. J. Am. Chem. Soc. 54, 3570 (1932)

(24) Hückel, E. Theoretische Grundlagen der organischen Chimie, Vol. II p. 203 Akademische Verlagsgesellschaft, (1931)

(25) Brackett, Proc. Nat. Acad. Sci. 14, 857 (1928)

(26) Hurd, C. O. Ind. Eng. Chem. 26, 50 (1934)

(27) Rice, F. O. and Herzfeld, K. F. J. Am. Chem. Soc. 56, 284 (1934)

(28) Frey, F. E. Ind. Eng. Chem. 26, 198 (1934)

(29) Allen, A. O. and Sickman, D. V. J. Am. Chem. Soc. 56, 2031 (1934)

(30) Leermakers, J. A. J. Am. Chem. Soc. 56, 1899 (1934)

(31) Staveley, L. A. K. and Hinshelwood, C. N. Proc. Roy. Soc. (London) A 154, 335 (1936)
Nature 137, 29 (1936)
J. Chem. Soc. 1936, 812

(32) Echols, L. S. and Pease, R. W. J. Am. Chem. Soc. 59, 766 (1937)

(33) Fletcher, C. J. M. and Rollefson, G. K. J. Am. Chem. Soc. 58, 2129, 2135 (1936)

(34) Staveley, L. A. K. and Hinshelwood, C. N. Proc. Roy. Soc. (London) A 159, 192 (1937)

(35) Staveley, L. A. K. and Hinshelwood, C. N. J. Chem. Soc. 1937, 1568

(36) Taylor, H. S., Morikawa, K. and Benedict, W. S. J. Am. Chem. Soc. 57, 383 (1935)

(37) Taylor, H. S. and Hill, D. G. J. Am. Chem. Soc. 51, 2922 (1929)

(38) Steacie, E. W. R. and LeRoy, D. Private communication

(39) Bates, J. R. and Taylor, H. S. J. Am. Chem. Soc. 50, 771 (1928)

(40) Steacie, E. W. R. and Habeeb, H. Private communication

(41) Jungers, J. C. and Taylor, H. S. J. Chem. Phys. 4, 94 (1936)

(42) Wood, R. W. Proc. Roy. Soc. (London) A 104, 1 (1923)

(43) Bonhoeffer, K. F. Z. physik. Chem. 113, 199 (1924)
116, 391 (1925)

(44) Bonhoeffer, K. F. and Harteck, P. Z. physik. Chem. 139, 64 (1928)

(45) Wartenberg, H. v. and Schultze, G. Z. physik. Chem. B 2, 1 (1929)

(46) Chadwell, H. M. and Titani, T. J. Am. Chem. Soc. 55, 1363 (1933)

(47) Geib, K. H. and Harteck, P. Z. physik. Chem. A 170, 1 (1934)

(48) Hartel, H. v. and Polanyi, M. Z. physik. Chem. B 11, 97 (1930)

(49) Sickman, O. V. and Rice, O. K. J. Chem. Phys. 4, 608 (1936)

(50) Geib, K. H. and Steacie, E. W. R. Z. physik. Chem. B 29, 215 (1935)
Trans. Roy. Soc. (Canada) III, 29, 91 (1935)

(51) Steacie, E. W. R. Can. J. Research B 15, 264 (1937)

(52) Farkas, A. J. Chem. Soc. 1936, 36

(53) Steacie, E. W. R. and Phillips, N. W. F. J. Chem. Phys. 4, 461 (1936)

(54) Farkas, A. and Melville, H. W. Proc. Roy. Soc. (London) A 157, 625 (1936)

(55) Morikawa, K., Benedict, W. S. and Taylor, H. S. J. Chem. Phys. 5, 212 (1937)

(56) Trenner, N. R., Morikawa, K. and Taylor, H. S. J. Chem. Phys. 5, 203 (1937)

(57) Gorin, E., Kauzmann, W., Walter, J. and Eyring, H. J. Chem. Phys. 7, 633 (1939)

(58) Kemula, W. Roczniki Chem. 10, 273 (1930)

(59) Steacie, E. W. R. J. Chem. Phys. 6, 37 (1938)

(60) Taylor, H. S. and Hill, D. G. Z. physik. Chem. B 2, 449 (1929)

(61) Steacie, E. W. R. and Phillips, N. W. F. J. Chem. Phys. 6, 179 (1938)

Can. J. Research 16, 303 (1938)

(62) Leermakers, J. A. J. Am. Chem. Soc. 55, 4508 (1933)

(63) Geddes, R. L. and Mack, E. Jr. J. Am. Chem. Soc. 52, 4372 (1930)

(64) Moore, W. J. Jr. and Taylor, H. S. J. Chem. Phys. 8, 396 (1940)

(65) Steacie, E. W. R. and Parlee, N. A. D. Trans. Faraday Soc. 35, 854 (1939)

Can. J. Research B 17, 371 (1939)

(66) Steacie, E. W. R. and Dewar, D. J. J. Chem. Phys. 8, 571 (1940)

(67) Steacie, E. W. R. and Brown, E. A. J. Chem. Phys. 8, 734 (1940)

(68) Klemenc, A. and Patat, F. Z. physik. Chem. B 3, 289 (1929)

(69) Geib, K. H. and Harteck, P. Ber. 66, 1815 (1932)

(70) Taylor, H. S. and Marshall J. Phys. Chem. 29, 1140 (1925)

(71) Olsen, A. R. and Meyers, C. H. J. Am. Chem. Soc. 48, 389 (1926)

(72) Olsen, A. R. and Meyers, C. H. J. Am. Chem. Soc. 49, 3131 (1927)

(73) Stewart, H. R. and Olsen, A. R. J. Am. Chem. Soc. 53, 1236 (1931)

(74) Bates, J. R. and Taylor, H. S. J. Am. Chem. Soc. 49, 2438 (1927)

(75) Jones, W. H. unpublished, mentioned in Proc. Am. Phil. Soc. 65, 96 (1926)

(76) Jungers, J. C. and Taylor, H. S. J. Chem. Phys. 6, 325 (1938)

(77) Moore, W. J. Jr. and Taylor, H. S. J. Chem. Phys. 8, 504 (1940)

(78) Bawn, C. E. H. Trans. Faraday Soc. 34, 598 (1938)

(79) Pearson, T. G. and Glazebrook, H. H. J. Chem. Soc. 1936, 1777

(80) Ashdown, A. H., Harris, L. and Armstrong, R. T. J. Am. Chem. Soc. 58, 850 (1936)

(81) Wrede, J. Z. Instrumentenkde 48, 201 (1928)

(82) Herzfeld, K. F. Kinetische Theorie der Wärme, Braunschweig, (1925)

(83) Bonehoeffer, K. F. and Harteck, P. Photochemie, Leipzig, (1933)

(84) Titani, T. Bull. Chem. Soc. Japan 5, 98,108 (1930)

(85) Taylor, H. S. and Smith, H. A. J. Chem. Phys. 8, 543 (1940)

(86) Rice, F. O. and Herzfeld, K. F. J. Chem. Phys. 7, 771 (1939)

(87) Taylor, H. A. and Burton, M. J. Chem. Phys. 7, 675 (1939)

(88) Taylor, H. A. and Flowers, R. G. J. Chem. Phys. 10, 110 (1942)

(89) Kistiakowsky, G. B., Ruhoff, J. R., Smith, H. A. and Vaughan, W. E. J. Am. Chem. Soc. 57, 876 (1935)

SUMMARY AND CONTRIBUTION TO KNOWLEDGE

A

The Pro-knock Activity of Various Compounds

Quantitative data of the pro-knock effectiveness of various compounds were obtained in an effort to determine whether such compounds might be used in military tactics to render automotive equipment inactive. Techniques were developed for the quantitative addition of gaseous, liquid, and solid compounds to the air intake of an engine, and the standard knock testing procedure was adapted for testing pro-knocks. The relative pro-knock activities of several elements and radicals were classified and the former related to their position in Mendeléef's periodic table. From these data, compounds of the type

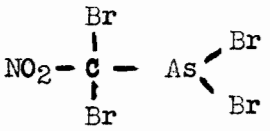

were predicted to have great pro-knock activity. The best pro-knock found in this work was dichloro-methyl arsine which required 3.8 p. p. m. to give an octane decrease of 10 in a leaded fuel.

B

Dynamic Sorption of Ammonia and Butane on Charcoal.

The dynamic sorption of ammonia and of butane was studied using an apparatus which followed the sorption by weight as a function of time, and permitted the temperature rise and analysis of effluent gases over a wide range of sorbate concentrations and flowrates.

The data obtained were applied to the theories of Danby et al and of Mecklenberg and were found to be essentially in good agreement.

The Reaction of Hydrogen Atoms with Propylene.

The reaction of propylene with hydrogen atoms was studied for the temperature range 30 to 250°C. The products obtained were methane, ethane, propane, and traces of C_4 hydrocarbons. About forty percent conversion was obtained. Temperature had little effect on either the relative proportion of products or on the extent of conversion. When the flowrate was reduced to one quarter of its original value, propylene was completely converted to methane, ethane and traces of C_3 and C_4 hydrocarbons. The activation energy of the overall reaction was 8.5 - 1.5 K. cal. calculated for a steric factor of 0.1.

There appears to be a difference in the mechanism of the reaction of unsaturated paraffins and saturated paraffins. Several possible mechanisms are suggested but no definite conclusion can be postulated with the evidence at hand.